# Tissue Engineered Small Diameter Vascular Graft made of Electrospun Scaffold and Adipose Derived Stem Cells: Fabrication and Functional Evaluation

**NEELIMA T**

**Ph.D. THESIS**

**2020**

**SREE CHITRA TIRUNAL INSTITUTE FOR MEDICAL SCIENCES AND TECHNOLOGY**

**THIRUVANANTHAPURAM, INDIA**

# Tissue Engineered Small Diameter Vascular Graft made of Electrospun Scaffold and Adipose Derived Stem Cells: Fabrication and Functional Evaluation

A THESIS PRESENTED BY

**NEELIMA T**

TO

SREE CHITRA TIRUNAL INSTITUTE FOR MEDICAL
SCIENCES AND TECHNOLOGY
THIRUVANANTHAPURAM
INDIA

IN PARTIAL FULFILMENT OF THE REQUIREMENTS
FOR THE AWARD OF
**DOCTOR OF PHILOSOPHY**

**2020**

# DECLARATION

I, **Neelima T**, hereby certify that I had personally carried out the work depicted in the thesis entitled, ***"Tissue Engineered Small Diameter Vascular Graft made of Electrospun Scaffold and Adipose Derived Stem Cells: Fabrication and Functional Evaluation",*** except where due acknowledgment has been made in the text. No part of the thesis has been submitted for the award of any other degree or diploma prior to this date.

Thiruvananthapuram **Neelima T**

05/10/2020 Reg. No: PhD/2013/08

# CERTIFICATE BY RESEARCH GUIDE

**SREE CHITRA TIRUNAL INSTITUTE FOR MEDICAL SCIENCES & TECHNOLOGY**
Thiruvananthapuram – 695011, INDIA
(An Institute of National Importance under Govt. of India)
Phone-(91)0471-2520242/262 Fax-(91)0471-2341814
Email: prabha@sctimst.ac.in Web site – www.sctimst.ac.in

**Dr. Prabha D Nair**
Scientist G (Senior Grade)
Division of Tissue Engineering and Regeneration Technologies
Department of Applied Biology
BMT Wing
SCTIMST
Thiruvananthapuram

This is to certify that **Ms. Neelima T**, in the Division of Tissue Engineering and Regeneration Technologies of this Institute has fulfilled the requirements prescribed for the Ph.D. degree of the Sree Chitra Tirunal Institute for Medical Sciences and Technology, Thiruvananthapuram. The thesis entitled, **"*Tissue Engineered Small Diameter Vascular Graft made of Electrospun Scaffold and Adipose Derived Stem Cells: Fabrication and Functional Evaluation*"** was carried out under my direct supervision. No part of the thesis was submitted for the award of any degree or diploma prior to this date.

* Clearance was obtained from the Institutional Ethics Committee/ Institutional Animal Ethics Committee / The Committee for the purpose of Control and Supervision of Experiments on Animals (CPCSEA) / Research ethics committee, Edinburgh for carrying out the study.

Thiruvananthapuram
05/10/2020

**Dr. Prabha D Nair**
Research supervisor

The thesis entitled

***"Tissue Engineered Small Diameter Vascular Graft made of Electrospun Scaffold and Adipose Derived Stem Cells: Fabrication and Functional Evaluation"***

Submitted by

**Neelima T**

for the degree of

**Doctor of Philosophy**

Of

**SREE CHITRA TIRUNAL INSTITUTE**
**FOR MEDICAL SCIENCES AND TECHNOLOGY,**
**THIRUVANANTHAPURAM, INDIA**

is evaluated and approved by

.....
Dr. Prabha D Nair
(Research Supervisor)

Dr.Prabha D. Nair
Scientist G (Senior Grade)

.....
Examiner
**Professor Rama Shanker Verma**
प्रोफेसर रमा शंकर वर्मा
Department of Biotechnology
जैव-प्रौद्योगिकी विभाग
Indian Institute of Technology Madras
भारतीय प्रौद्योगिकी संस्थान मद्रास
Chennai - 600 036 / चेन्नै - ६०० ०३६

# ACKNOWLEDGEMENT

*With heartfelt sense of gratitude, I take this opportunity with immense pleasure to thank all those who contributed for the success of this study.*

*I would like to express my heartfelt gratitude and respect to my supervisor Dr. Prabha D Nair, Scientist G (SG), Division of Tissue Engineering and Regeneration Technologies, BMT wing, SCTIMST, for her relentless effort and encouragement to me throughout the course of the research. Her guidance, critical evaluations and confidence have helped me to evolve in scientific field. My words are not enough to thank her for being there for me at all points during the course of my study.*

*I am grateful to Prof. Mark Bradley, School of Chemistry, University of Edinburgh, UK for hosting me as his student for the Commonwealth Split-Site Scholarship 2016-2017. His valuable supervision of research work has helped me to achieve new dimension of present research study. I am thankful to Prof. Bruno Peault, MRC-Scottish Centre of Regenerative Medicine, University of Edinburgh for associating with my research and supervision on my project during my period at University of Edinburgh.*

*I thank members of the doctoral advisory committee, Dr. A. Maya Nandakumar, Division of Microbial Technology, Dr. Roy Joseph, Division of Polymeric Medical Devices and Dr. Srinivas Gopala, Biochemistry SCTIMST for their timely suggestions, critical comments which encouraged me to improve my projects and the quality of the research projects for the PhD thesis.*

*I thank SCTIMST - Institute Fellowship for the fellowship provided during my doctoral studies. I thank Commonwealth Commission, UK for selecting me as Commonwealth Scholar 2016-2017 for the Commonwealth split-site fellowship which helped to conduct a part of my thesis at University of Edinburgh, UK. I thank*

*Department Of Science And Technology, India, Department of Biotechnology, India and Commonwealth commission, UK for the travel support for attending conferences at Canada and UK.*

*I am thankful to the Director, SCTIMST and The Head, BMT Wing for the support provided during the course of work. I would also like to thank former Head, BMT Wing Dr. C.P. Sharma for guiding me during the course of my joining at the Institute. Also sincere thanks to the Dean, the Associate Dean, the Deputy Registrar and staff of Division of Academic Affairs for their timely assistance.*

*I express my sincere gratitude to Dr. Unnikrishnan M, former Cardiovascular Thoracic Surgeon, Cardiovascular Thoracic surgery Department, SCTIMST for playing a major role in developing the vascular graft and helping in surgical implantation of the same. I also thank Dr. P.R. Umashankar, Dr. Sachin J Shenoy and staff of Division of In vivo models and device testing for their fruitful in puts during developing the graft , surgical implantation and after surgery assistance. I thank Dr. Harikrishnan V.S and staff of Division of Laboratory Animal Science for helping during small animal surgical procedures.*

*I thank Mr. C.V. Muraleedharan and Mr. Rajeev A for their help in mechanical testing, Mr. Willi Paul, FADDS for Confocal Raman microscopic evaluation. Dr. Sabareeshwaran A, Ms. Sulekha Baby, Ms. Sandhya and Ms. Gayathry of Histopathology Division for pathological evaluation and PCR machine. Mr. Nishad K.V, of Bio ceramics laboratory for SEM, E-SEM. Dr. Lissy. K. Krishnan, Dr. Anugya Bhat, Ms. Priyanka, Mr. Anilkumar, TRU for hemocopatibility studies. Dr. Kalliyana Krishnan K, Ms. Lakshmi, Dr. Renjith P Nair, Dental products lab for micro CT experiments. Mr. Renjith Kartha, TRU for FACS analysis, Mr. Ramesh Babu and staff of Precision fabrication for electrospinning accessories. Dr. Rekha M.R and staff of BST for nanodrop and shaker incubator. Dr. K. Srinivasan, Mr. Hari, Ms. Shanthikrishna A of Polymer analysis lab for their help in FT-IR and GPC.*

*I immensely thank the staff of Rajiv Gandhi Centre for Biotechnology, Trivandrum for giving access to Confocal laser scanning microscope, FACS, PCR machine.*

*I acknowledge each and every person at University of Edinburgh, UK for supporting my research and joyful stay there. I especially thank Dr. Hua Dong, Dr. Seshasailam Venkateshwaran, Dr. Nusrat Khan, Dr. Jin Geng, Dr. Matthew Owens for their timely inputs to my research. I thank Professor Anthony Callanan, Mr. Tim Burton for helping in mechanical testing. Dr. Adriana Taveres and Mr. Carlos for micro CT experiments. I would like to thank my fellow lab mates and friends who helped to have a pleasant atmosphere at the University of Edinburgh.*

*I deeply acknowledge my lab members at Division of Tissue Engineering and Regeneration Technologies. Dr. Neethu Mohan, Dr. Dhanya Gangadharan for teaching me the basics of cell culture experiments. Dr. Dhanesh V, Ms. Geetha K for electrospinning and polymer synthesis. Dr. Dhanasooraj D for the basics in molecular technologies. Dr. Lynda V Thomas for her support. My fellow mates Ms. Jijo Wilson J, Mr. Rahul V.G, Dr. Babitha S, Dr. Shiny Velayudhan, Dr. Neena Aloshyius, Dr. Bindu P Nair, Dr. Prakash S.P for their friendship and support. Ms. Nimi N for technical help. Dr. V.P. Sivadas, Dr. Amrita Natarajan, Ms. Shyna and Ms. Karishma for their support.*

*Cheers to all my friends and well-wishers at SCTIMST and The University of Edinburgh. Thanks to staff of various administrative, accounts, store & purchase, housekeeping departments and library of the Institute and fellow students in the campus. I thank all those beautiful laboratory animals.*

*I thank my family.*

# TABLE OF CONTENTS

**Declaration**……. **i**

**Certificate of Guide** ……. **ii**

**Approval of thesis**…….. **iii**

**Acknowledgements**…….. **iv**

**List of figures**…… **xv**

**List of tables**……... **xviii**

**Abbreviations**…… **xix**

**Annotations**…… **xxii**

**Synopsis**…….. **xxiii**

**CHAPTER 1 – INTRODUCTION**…….. **1**

1.1. Background…….. 1

1.2. Underlying Pathology of Blood Vessel Diseases-Atherosclerosis…….. 3

1.3. The Blood Vessel……. 3

1.4. The process of Atherosclerosis…… 5

1.5. Medical Management of Blood Vessel Diseases……..… 6

1.6. Tissue Engineering……..…. 9

1.7. Vascular Tissue Engineering…….. 10

1.8. Definition of the problem…… 11

1.9. Hypothesis……... 11

1.10. Objectives…….. 12

1.11. Significance of the Study…… 16

**CHAPTER 2 – REVIEW OF LITERATURE**…… **17**

2.1. Strategies for vascular tissue engineering…… 17

2.2. Scaffolds in Vascular Regeneration……. 19

2.2.1. Extracellular Matrix of the Blood Vessel…….. 20
2.2.2. Natural Polymer Based Vascular Grafts…… 22
2.2.3 Synthetic Polymerised based Vascular Grafts…… 23
2.2.4. Hybrid natural – synthetic scaffold based vascular grafts……. 24
2.3. Fabrication of vascular graft - Electrospinning…… 25
2.4. Cell source and vascular regeneration…….. 28
2.5. Animal models for evaluation of vascular graft……. 32

**CHAPTER 3 – MATERIALS AND METHODS…… 35**
**SECTION 1 - SCAFFOLD FABRICATION AND CHARACTERISATION……... 35**
3.1. **Part I-** Synthesis, Fabrication and Characterisation of Gelatin-vinyl acetate/Poly-ε-caprolactone scaffold…….. 35
3.1.1. Synthesis of Gelatin-vinyl acetate……. 35
3.1.2. Characterisation of Gelatin-vinyl acetate…… 36
3.1.2.1. Fourier transform Infrared Spectroscopy……. 36
3.1.2.2. TNBS Assay……... 36
3.1.2.3. Gel permeation Chromatography……... 36
3.1.3. Fabrication of Gelatin-vinyl acetate/Poly-ε-Caprolactone scaffold….. 37
3.1.3.1 Dual Source Co-electrospinning…….. 37
3.1.3.2. Scaffold Cross-linking…… 38
3.1.4. Characterisation of Electrospun scaffold 39
3.1.4.1. TNBS Assay…….. 39
3.1.4.2. FT-IR Spectroscopy……... 40
3.1.4.3. Fibre Morphology- Scanning Electron Microscopy…….. 40
3.1.4.4. Water Contact Angle……. 40
3.15. Fabrication of Tubular Vascular Graft……... 41
3.1.5.1. Morphology of Tubular Scaffold…… 41
3.1.5.2. Porosity of scaffold-Micro-CT……... 41
3.1.5.3. Media Uptake ability…….. 42
3.1.5.4. Degradation Assay…….. 42

3.1.5.5. Mechanical Properties…… 42

3.2. **Part II**- Synthesis, Fabrication and Characterisation of Poly (ethyl methacrylate-co-di ethyl amino ethyl acrylate, 8g7) scaffold……. 43
3.2.1. Synthesis of 8g7…… 43
3.2.1.1. Gel Permeation Chromatography…….. 44
3.2.1.2. FT-IR Spectroscopy……... 45
3.2.2. Fabrication 8g7 tubular scaffold by electrospinning……. 45
3.2.2.1. Scanning electron Microscopy……... 46
3.2.2.2. Water Contact Angle…….. 46
3.2.2.3. Water uptake ability……... 46
3.2.2.4. Micro-CT…… 47
3.2.2.5. Mechanical properties…… 47

**SECTION II- *IN VITRO* CELL BASED STUDIES…….. 48**
3.3 **Part I**- Differentiation of adipose derived mesenchymal stem cells to smooth muscle cells on Gelatin-vinyl acetate/Poly-ε-caprolactone scaffold.. 48
3.3.1 Isolation of rabbit adipose derived mesenchymal stem cells……. 48
3.3.1.1. Population doubling time……... 49
3.3.1.2. Morphology of rabbit adipose stem cells…….. 49
3.3.1.3. FACS analysis and Immunofluorescence staining…… 50
3.3.1.4. Multilineage differentiation of rabbit stem cells…… 51
3.3.2. Isolation of Sheep adipose derived mesenchymal stem cells - Isolation and characterisation of sheep stem cells…….. 51
3.4. Cell-Material Interaction - Rabbit and Sheep stem cells with Gelatin-vinyl acetate/Poly-ε-caprolactone scaffold……. 53
3.4.1. Direct Contact Assay…… 53
3.4.2. MTT Assay…… 53
3.4.3. Cell seeding on tubular scaffold…… 54
3.4.4. Cell viability on scaffold……... 54
3.4.5. Confocal Raman analysis of cell seeded scaffold……. 55

3.5. Differentiation of rabbit and sheep stem cells to smooth muscle cells on scaffold……... 55
3.5.1. Quantitative Real time PCR…….. 56
3.5.2. Immunostaining of SMC markers……. 57
3.5.3. Estimation of extracellular matrix proteins…….. 58
3.6. *In vitro* hemocompatibility of gelatin-vinyl acetate/poly-ε-caprolactone scaffold…… 58
3.6.1. Percentage haemolysis.…….. 59
3.6.2. Haematology…….. 59

3.7. **Part II**- Co-culture of Perivascular cells and endothelial cells on 8g7 scaffold……..... 60
3.7.1. Isolation of human adipose derived perivascular cells and endothelial cells and FACS sorting ……... 61
3.7.2. Cell seeding on 8g7 scaffold……. 64
3.7.3. Cell-Material Interactions, Cell viability …….. 64
3.7.4. MTT Assay…… 64
3.7.5. Scanning electron microscopy……... 65
3.7.6. Actin immuno- staining on scaffold…….. 65
3.8. Co-culture on scaffold…….. 66
3.8.1. Angiogenesis assay…….. 67

**SECTION III– *IN VIVO* EVALUATION OF GELATIN-VINYL ACETATE/POLY-ε-CAPROLACTONE SCAFFOLD**…… **67**
3.9. **Part I** – *In vivo* evaluation in rabbit model…….. 67
3.9.1. Surgical replacement of rabbit common carotid artery with graft…… 68
3.9.2. Angiographic Evaluation……... 69
3.9.3. Gross observation…….. 69
3.9.4. Histopathological evaluations……... 70

3.10. **Part II** – *In vivo* evaluation in sheep model…… 70

3.10.1. Surgical replacement of sheep common carotid artery…… 71
3.10.2. Angiographic evaluation……. 72
3.10.3. Gross observation…… 72
3.10.4. Environmental scanning electron microscopy……. 73
3.10.5. Histopathological evaluations……. 73
3.10.6. Picrosirius red staining of Collagen…… 73
3.10.7. Verhoeff's - Van Geison elastin staining…… 74
3.10.8. Immunofluorescence staining……. 74
3.10.9. Total collagen and Elastin estimation……. 75
3.11. Statistical Analysis……. 75

**CHAPTER 4 – RESULTS…… 77**
**SECTION I – SCAFFOLD FABRICATION AND CHARACTERISATION…….. 77**
4.1 **Part I** – Synthesis, Fabrication and Characterisation of Gelatin-vinyl acetate/Poly-ε-caprolactone scaffold…….. 77
4.1.1. Synthesis of Gelatin-vinyl acetate……. 77
4.1.2. Characterisation of gelatin-vinyl acetate…….. 79
4.1.2.1. FT-IR Spectroscopy and TNBS Assay…….. 79
4.1.2.2. Gel permeation chromatography…… 79
4.1.3. Fabrication of Gelatin-vinyl acetate/Poly-ε-caprolactone scaffold…... 80
4.1.3.1. Dual source electrospinning…….. 80
4.1.4. Characterisation of electrospun scaffold……. 82
4.1.4.1. TNBS Assay…….. 82
4.1.4.2. FT-IR Spectroscopy…….. 82
4.1.4.3. Scanning electron microscopy…… 83
4.1.4.4. Water contact angle…… 84
4.1.5. Fabrication of tubular scaffold for vascular graft…….. 85
4.1.5.1. Morphology of tubular graft…….. 85
4.1.5.2. Porosity - Micro-CT analysis……. 89
4.1.5.3. Media uptake and degradation assay…….. 90

4.1.5.4. Mechanical properties of grafts…….. 91

4.2. **Part II** – Synthesis, fabrication and characterisation of poly (ethyl methacrylate-co-di ethyl amino ethyl acrylate) scaffold……. 92
4.2.1. Synthesis and gel permeation chromatography of 8g7……. 92
4.2.1.1. FT-IR spectroscopy…… 93
4.2.2. Fabrication of poly (ethyl methacrylate-co-di ethyl amino ethyl acrylate) tubular scaffold by electrospinning and characterisation……. 94
4.2.2.1. Water contact angle and water uptake ability of tubular scaffold….. 99
4.2.2.2. Micro-CT analysis of tubular scaffold…… 99
4.2.2.3. Mechanical properties…… 100

**SECTION II – *IN VITRO* CELL BASED STUDIES……. 100**
4.3. **Part I** – Differentiation of adipose derived mesenchymal stem cells to smooth muscle cells on gelatin-vinyl acetate/poly-ε-caprolactone scaffold…… 100
4.3.1. Isolation, characterisation of rabbit adipose derived mesenchymal stem cells……. 100
4.3.2. Isolation, characterisation of sheep adipose derived mesenchymal stem cells…..... 102
4.4. Cell – Material Interaction…… 105
4.4.1. Direct contact assay and MTT Assay…… 105
4.4.2. Cell viability assessment…… 107
4.4.3. Confocal Raman spectroscopic studies…… 109
4.5. Differentiation of mesenchymal stem cells to smooth muscle cell on scaffold – rabbit…… 111
4.5.1. Quantitative Real Time PCR and Immunosttaining……. 112
4.5.2. Estimation of extracellular matrix proteins…… 114
4.6. Differentiation of mesenchymal stem cells to smooth muscle cell on scaffold – sheep, RT-PCR and Immuno-staining…… 115
4.7. *In vitro* hemocompatibility of the scaffold…… 117

4.8. **Part II** – Co-culture of perivascular stem cells and endothelial cells on poly (ethyl methacrylate-co-di ethyl amino ethyl acrylate) scaffold…….. 118
4.8.1. Isolation of human adipose derived perivascular stem cells, endothelial cells..... 118
4.8.2. Cell compatibility of scaffold – Live / dead assay and SEM…… 120
4.8.3. MTT assay…… 121
4.8.4. β-actin and immunostaining of cell markers on the seeded scaffold… 122
4.9. Co-culture of perivascular cells with endothelial cells on scaffold…….. 124
4.9.1. Angiogenesis assay…….. 125

**SECTION III – *IN VIVO* EVALUATION OF GELTIN-VINYL ACETATE / POLY-ε-CAPROLACTONE ELECTROSPUN SCAFFOLD, G3P1**…… **126**
4.10. **Part I** – *In vivo* evaluation in rabbit model…… 126
4.10.1. Surgical replacement of rabbit common carotid artery with G3P1 scaffold cellularised with differentiated smooth muscle cells……. 126
4.10.2. Gross observation of the implant…… 127
4.10.3. Histopathological evaluations……. 128

4.11. **Part II** – *In vivo* evaluation in sheep model…….. 130
4.11.1. Surgical procedure: vascular graft implantation in sheep common carotid artery…… 130
4.11.2. Gross observation of the implant……. 132
4.11.3. Environmental scanning electron microscopy of the implant……. 133
4.11.4. Histopathological evaluation of the implant…… 134
4.11.5. Picrosirius red staining of collagen fibers……... 138
4.11.6. Verhoeff's -Van Geison staining for elastin fibers…….. 139
4.11.7. Immunofluorescence staining……. 139
4.11.8. Total collagen and elastin estimation……. 140

**CHAPTER 5 – DISCUSSION……. 143**
5.1. Synthesis, fabrication and characterisation of gelatin-vinyl acetate/poly-ε-caprolactone scaffold……... 144
5.2. Differentiation adipose derived mesenchymal stem cells to smooth muscle cells on Gelatin-vinyl acetate/PCL (G3P1) tubular scaffold……. 149
5.3. Synthesis, fabrication and characterisation of poly (ethyl methacrylate-co-di ethyl amino ethyl acrylate) tubular scaffold by electrospinning and characterisation…… 152
5.4. Co-culture study……... 156
5.5. *In vivo* evaluation of Gelatin-vinyl acetate / Poly-ε-caprolactone electrospun scaffold in Lapine and Ovine models…….. 158
5.6. Limitations…….. 161

**CHAPTER 6 – SUMMARY AND CONCLUSION…… 163**
6.1. Summary…….. 163
6.2. Conclusion…… 166
6.3. Future perspectives…….. 166

**BIBLIOGRAPHY……. 167**
**LIST OF PUBLICATIONS……. 185**

# LIST OF FIGURES


| | | |
|---|---|---|
| 1 | Non-communicable disease statistics…….. | 2 |
| 2 | Major types of artery – Elastic and muscular tri-layer structure……. | 5 |
| 3 | Progression of atherosclerosis……. | 6 |
| 4 | Treatment modalities of Cardiovascular diseases…… | 7 |
| 5 | The concept of tissue engineering……... | 10 |
| 6 | Graphical representation of Outside-in strategy…….. | 13 |
| 7 | Graphical representation of Inside-out strategy……. | 13 |
| 8 | Fabrication strategies of Vascular tissue engineering……. | 18 |
| 9 | Blood vessel extracellular matrix…… | 20 |
| 10 | Electrospinning set-up……. | 27 |
| 11 | Tissue engineered vascular graft, role of perivascular cells…… | 29 |
| 12 | Phenotypic plasticity of smooth muscle cells…….. | 30 |
| 13 | Adipose derived stem cells…….. | 31 |
| 14 | TGF-β1 signaling……. | 32 |
| 15 | Scheme 1: Synthesis of Gelatin-vinyl acetate……. | 78 |
| 16 | FT-IR and TNBS assay Gelatin-vinyl acetate……. | 79 |
| 17 | FT-IR of Gelatin-vinyl acetate/ PCL scaffold combinations…… | 83 |
| 18 | Scanning electron microscopy, fiber diameter of combinations…….. | 84 |
| 19 | Morphology of G3P1 – 3 mm…….. | 86 |
| 20 | Fiber diameter of G3P1 – 3 mm…… | 87 |
| 21 | Morphology of G3P1 – 5 mm…… | 88 |
| 22 | Fiber diameter of G3P1 – 5 mm…… | 88 |
| 23 | Micro-CT analysis of G3P1 – 3 mm/5 mm…… | 89 |
| 24 | Swelling and Degradation percentage……. | 90 |
| 25 | Mechanical properties of G3P1 – 3 mm/5 mm…… | 91 |
| 26 | Scheme 2: Synthesis of 8g7……. | 93 |
| 27 | FT-IR of 8g7…… | 93 |
| 28 | SEM -Effect of concentration of 8g7 on electrospinning…… | 95 |

| | | |
|---|---|---|
| 29 | SEM - Effect of flow rate of 8g7 on electrospinning……... | 96 |
| 30 | Bright field microscope and SEM - Effect of applied voltage of 8g7 on electrospinning…… | 97 |
| 31 | Morphology of 8g7 graft…….. | 98 |
| 32 | Water contact angle……. | 99 |
| 33 | Micro-CT of 8g7…….. | 99 |
| 34 | Characterization of Rabbit adipose MSCs…….. | 101 |
| 35 | Tri-lineage differentiation…… | 102 |
| 36 | Characterization of Sheep adipose MSCs…… | 103 |
| 37 | Tri-lineage differentiation…… | 104 |
| 38 | Direct contact assay, MTT Assay-Rabbit…… | 106 |
| 39 | Direct contact assay, MTT Assay-Sheep…… | 107 |
| 40 | Live/Dead assay, Depth profile, E-SEM-Rabbit……. | 108 |
| 41 | Live/Dead assay, Depth profile, E-SEM-Sheep ……. | 109 |
| 42 | Confocal Raman spectra analysis-Rabbit…… | 110 |
| 43 | Confocal Raman spectra analysis-Sheep…… | 111 |
| 44 | Scheme 3: Smooth muscle cell differentiation…… | 112 |
| 45 | Gene expression profile- Rabbit…….. | 113 |
| 46 | Confocal laser scanning immunofluorescence image-Rabbit…….. | 114 |
| 47 | Extracellular matrix gene expression and estimation…….. | 115 |
| 48 | Gene expression profile- Sheep……... | 116 |
| 49 | Confocal laser scanning immunofluorescence image-Sheep…….. | 116 |
| 50 | Platelet adhesion assay……. | 117 |
| 51 | Flow cytometry of human adipose tissue digest…….. | 119 |
| 52 | Phase contrast images of cells……. | 119 |
| 53 | Immunofluorescence of perivascular cells…….. | 120 |
| 54 | Live/dead assay, SEM on 8g7 Scaffold…….. | 121 |
| 55 | MTT Assay…….. | 122 |
| 56 | Actin and cell markers immunofluorescence on cells on 8g7 scaffold | 123 |
| 57 | Co-culture - Confocal microscope image……. | 124 |
| 58 | Angiogenesis assay | 125 |

| | | |
|---|---|---|
| 59 | Vascular graft Implantation in rabbit…….. | 126 |
| 60 | Angiographic evaluation of rabbit…….. | 127 |
| 61 | Gross observation, H& E gross staining-Rabbit…….. | 128 |
| 62 | Histopathological observations-Rabbit…… | 129 |
| 63 | Vascular graft Implantation in sheep…….. | 131 |
| 64 | Sheep recovered……... | 131 |
| 65 | Angiographic evaluation of sheep…….. | 132 |
| 66 | Gross observation-sheep……...…….. | 133 |
| 67 | E-SEM of explant-sheep…….. | 134 |
| 68 | Histopathological observations-sheep...…….. | 135 |
| 69 | Histopathological observations patent graft-sheep...…….. | 137 |
| 70 | Picrosirius red staining…… | 138 |
| 71 | Verhoeff's -Van Geison staining…….. | 139 |
| 72 | Immunofluorescence staining…….. | 140 |
| 73 | Total collagen estimation……. | 141 |
| 74 | Total elastin estimation…… | 141 |

# LIST OF TABLES


| | | |
|---|---|---|
| 1 | Summary of electrospinning parameters……. | 38 |
| 2 | Combinations of scaffold fabricated…… | 39 |
| 3 | Reaction conditions of 8g7 polymer synthesis…… | 44 |
| 4 | Details of PCR primers…… | 57 |
| 5 | Antibody panel used for cell isolation……. | 62 |
| 6 | Gel permeation chromatography - Gelatin-vinyl acetate……. | 80 |
| 7 | Standardized electrospinning parameters…… | 81 |
| 8 | Sample code and scaffold ratio…… | 82 |
| 9 | Water contact angle……. | 85 |
| 10 | Gross morphology of G3P1 – 3 mm vascular graft…… | 86 |
| 11 | Gross morphology of G3P1 – 5 mm vascular graft…… | 86 |
| 12 | Mechanical properties of G3P1 graft…….. | 92 |
| 13 | Gel permeation chromatography - 8g7……...……. | 93 |
| 14 | Effect of solvent on electrospinning 8g7……. | 94 |
| 15 | Summary of electrospinning parameters of 8g7…….. | 98 |
| 16 | *In vitro* hemocompatibility of G3P1 scaffold…….. | 117 |

# ABBREVIATIONS

| | |
|---|---|
| 2D | : 2- Dimensional |
| 3D | : 3- Dimensional |
| ACD | : Acid Citrate Dextrose |
| ADMSC | : Adult Mesenchymal Stem Cells |
| ANOVA | : Analysis of Variance |
| ASMA | : Alpha Smooth Muscle Actin |
| bFGF | : basic Fibroblast Growth Factor |
| BSA | : Bovine Serum Albumin |
| CABG | : Coronary artery bypass grafting |
| cDNA | : Complimentary Deoxy ribo Nucleic Acid |
| CD | : Cluster of Differentiation |
| CPCSEA | : Committee for the Purpose and Control of Supervision of Experiments on Animals |
| CVDs | : Cardiovascular diseases |
| DAPI | : 4,5-diamidino-2-phenylindole |
| DMEM-HG | : Dulbecco's Modified Eagle Medium-High Glucose |
| DMF | : Dimethyl formamide |
| dNTPs | : Deoxy Nucleotides triphosphate |
| DPX | : Distyrene, a plasticizer and Xylene |
| ECs | : Endothelial Cells |
| ECM | : Extracellular matrix |
| EDTA | : Ethylene Diamine Tetra Acetic Acid |
| EGM-2 | : Endothelial growth media - 2 |
| EGF | : Epidermal growth factor |
| E-SEM | : Environmental Scanning Electron Microscopy |
| EtCO2 | : End-tidal Carbon dioxide |
| FACS | : Fluorescent activated cell sorting |
| FBS/FCS | : Foetal Bovine/calf Serum |
| FITC | : Fluorescein isothiocyanate |

| | |
|---|---|
| FT-IR | : Fourier Transform-Infrared spectroscopy |
| GAPDH | : Glyceraldehyde-3-phosphate Dehydrogenase |
| GPC | : Gel permeation chromatography |
| GV | : Gelatin-vinyl acetate |
| H&E | : Haematoxylin and Eosin |
| Hb | : Haemoglobin |
| IEC | : Institutional Ethics Committee |
| IAEC | : Institutional Animal Ethics Committee |
| IC-SCRT | : Institutional Committee for Stem Cells Research and Therapy |
| IMA | : Internal Mammary artery |
| MSC | : Mesenchymal Stem Cell |
| Micro-CT | : Micro-Computed Tomography |
| NCDs | : Non communicable diseases |
| NG2 | : Neural glial factor-2 |
| Na Cl | : Sodium Chloride |
| PBMNC | : Peripheral blood mononuclear cells |
| PBS | : Phosphate Buffered Saline |
| PCR | : Polymerase Chain reaction |
| PCL | : Poly-ε-caprolactone |
| PDGF | : Platelet derived growth factor |
| PE | : Phycoerythrin |
| PEUU | : Poly-ester Urethane urea |
| PDI | : Poly Dispersity Index |
| PRP | : Platelet Rich Plasma |
| PVSc | : Perivascular cells |
| RAMSC | : Rabbit Adipose derived Mesenchymal Stem cells |
| RBC | : Red blood Cells |
| RPM | : Revolutions per minute |
| RNA | : Ribonucleic acid |
| RT-PCR | : Reverse Transcriptase-Polymerase Chain Reaction |
| RT | : Room Temperature |

| | |
|---|---|
| SD | : Standard deviation |
| ShMSCs | : Sheep Mesenchymal Stem Cells |
| SMMHC | : Smooth Muscle Myosin Heavy chain |
| SV | : Saphenous vein |
| TCPS | : Tissue Culture polystyrene |
| TEVG | : Tissue Engineered Vascular Graft |
| TGF | : Transforming Growth Factor |
| THF | : Tetrahydrofuran |
| UV | : Ultra violet |
| VEGF | : Vascular Endothelial Growth Factor |
| vWF | : von Wilde Brand Factor |

## ANNOTATIONS

| | |
|---|---|
| % | : Percentage |
| $^0$ C | : Degree Celsius |
| < | : Less Than |
| > | : Greater than |
| α | : Alpha |
| β | : Beta |
| ε | : Epsilon |
| μg | : Microgram |
| μl | : Microlitre |
| μm | : Micrometre |
| μM | : Micromolar |
| a.u | : Arbitrary Unit |
| cm | : centimetre |
| g | : gram |
| kDa | : Kilo Dalton |
| kg | : Kilogram |
| kV | : Kilovolt |
| mg | : Milligram |
| M | : Molar |
| ml | : Millilitre |
| Mn | : Number average molecular weight |
| Mw | : Weight average molecular weight |
| Mv | : Viscosity average molecular weight |
| mM | : Millimole |
| N | : Normal |
| nM | : Nanomole |
| nm | : nanometre |
| (w/w) | : Weight/weight |
| (w/v) | : Weight/volume |
| (v/v) | : Volume/vol |

# SYNOPSIS

Cardiovascular diseases contribute to more than fifty percentage of death and disability caused due to non-communicable diseases worldwide. The death causing cardiovascular diseases like coronary artery disease and cerebrovascular disease is caused by atherosclerotic narrowing of the lumen of these vessels which are small diameter (< 6 mm internal diameter) in nature. The invasive treatment options of blood vessel associated diseases include vessel replacement or bypass grafting. Even though the golden choice of replacement is patient's autologous vessel like saphenous vein or internal mammary artery, there is a lack of availability of these vessels due to donor site morbidity and second time harvest is not possible. Moreover, the vein graft patency decreases drastically over years. The synthetic grafts much prevalent in large vessel replacements is not applicable in small diameter scenario due to thrombotic complications. Tissue engineered small diameter vascular graft thus offers a promising approach to address this unmet clinical need. Vascular tissue engineering follows the basic triad principle – cells, scaffold and biomechanical cues.

Taking in to consideration the blood vessel architecture - Cell and extracellular matrix distribution and its dynamic nature, engineering a small diameter graft is highly challenging. It is very relevant for the success of tissue engineered graft to be assembled based on dimensions of patient's vessel and with cells derived from same patient. This forms the basis of personalized blood vessel regeneration. Tissue engineered graft based on direct scaffolding method and adipose derived mesenchymal stem cells postulates to be superior strategy towards this. Based on this it has been

hypothesized that tissue engineered small diameter vascular graft developed from electrospun scaffold and adipose derived mesenchymal stem cells were expected to have superior functional efficiency.

The thesis has been divided into six chapters. The chapter I gives general introduction that provides the awareness of the study topic - Vascular tissue engineering and its relevance in clinical scenario. The chapter on introduction also covers the details of architectural needs of blood vessel and underlying cause of blood vessel pathology. The chapter II extensively surveys the current literature that highlights approaches towards blood vessel fabrication and its evaluation, if any. The chapter also pinpoints the current limitation that has to be addressed for conception of functional graft with regeneration capabilities. The chapter ends with description of major objectives proposed for proving the hypothesis. Generally, the experimental design is based on two strategies commonly encompassing the idea of cell and scaffold-based tissue engineered small diameter vascular conduit. The first one adopted is outside in strategy were an electrospun scaffold is fabricated and autologous adipose derived mesenchymal stem cells were differentiated to smooth muscle cells. This graft is evaluated for its *in vivo* endothelisation and patency in order to address the influence of cellularisation of graft. In the second or inside out strategy, endothelial cell friendly scaffold material is chosen, and adipose derived perivascular stem cells are co-cultured with endothelial cells for evaluating its angiogenic capability *in vitro.*

The major objectives include:

i. Synthesis of polymer and fabrication of the same into tubular scaffold by electrospinning. Physicochemical and mechanical characterization of fabricated scaffold for its suitability to be used as vascular graft.
ii. Isolation and characterization of adipose derived mesenchymal stem cells and endothelial cells. Evaluation of biocompatibility and blood compatibility of scaffold.
iii. Differentiation of adipose derived mesenchymal stem cells to smooth muscle cells on scaffold and characterizing for contractile nature. Establishing co-culture of adipose derived perivascular cells and endothelial cells on scaffold and evaluating the angiogenic potential.
iv. *In vivo* implantation of smooth muscle cells differentiated scaffold in Lapine and Ovine model with emphasis on endothelisation, patency and regeneration.

The third chapter elaborates the materials and methods embraced in order to achieve the objectives. The whole chapter is divided into three major sections and each section divided into two parts. The Section I describes the scaffold fabrication. Generally electrospinning technique is adopted for scaffold fabrication. The part I of this part describes the synthesis and fabrication of gelatin-vinyl acetate-Poly-ε-caprolactone dual source co electrospun scaffold. This includes synthesis of gelatin vinyl acetate, characterization of polymer. Standardization of co-electrospinning of polymers to obtain grafts of diameter-3mm and 5mm respectively. The tubular grafts were characterized for its porous nature, swelling, degradation and mechanical

robustness. The part II describes the synthesis and characterization of acrylate-based polymer for vessel creation. This polymer is further fabricated to tubular dimensions and characterized for its physicochemical properties as described above.

The section II of comprises the *in vitro* cell based study, which is again divided into two part based on the choice of scaffold material. The part I includes the isolation and *in vitro* characterization of adipose derived mesenchymal stem cells from Lapine and Ovine animal models. This also includes the biocompatibility studies of respective cells with tubular gelatin-vinyl acetate - Poly-ε-caprolactone scaffold. The cells are also differentiated to smooth muscle lineage on scaffold using TGF-β1 mediated protocol. The differentiated smooth muscle cells on scaffold is characterized for it contractile nature based on marker expression through PCR and immuno-staining. The blood compatibility of the scaffold is also described here. The part II comprises of isolation and characterization of human adipose derived perivascular stem cells-Adventitial cells and pericytes along with endothelial cells. A co-culture system is established of these respective cells with endothelial cells after initial biocompatibility evaluation. Angiogenesis assay from co-cultured cell secretome is analysed for functional efficiency of the cellularised graft.

The section III describes the *in vivo* functional evaluation of the fabricated gelatin-vinyl acetate-Poly-ε-caprolactone vessel graft with adipose derived smooth muscle cells. The part I includes the implantation protocol adopted for implantation of the graft (3 mm) in common carotid artery interposition replacement in Lapine model. The angiographic and histopathological evaluation were done after explanting. The part II comprises of the evaluation the same graft in Ovine carotid artery replacement

model with unseeded scaffold control for 3 months. The angiographic, histopathological and immunohistochemical analysis of explant is carried out for patency evaluation, endothelization and regeneration of graft.

The chapter four describes the major findings obtained. The chapter is again divided into three sections and each section into two parts in accordance with the methodologies adopted. The patent nature of gelatin-vinyl acetate-Poly-ε-caprolactone vessel graft with adipose derived smooth muscle cells in ovine model is the highlight of the result section.

The chapter five includes the discussion of the results and correlation of the same with proposed hypothesis. The chapter also points towards the relevance of current strategy for generation of tissue engineered vascular graft. The related studies in the same compared and contrasted. Current limitations of the present study are indicated here.

In chapter six, the research work is summarized, and major conclusions were drawn. The future perspectives are also stated. The thesis ends with bibliography, list of publications and other research outputs.

# CHAPTER 1
# INTRODUCTION

## 1.1 BACKGROUND

Cardiovascular diseases (CVDs) are a group of diseases the affect heart and blood vessels. Vascular diseases being a subgroup of CVD includes vascular diseases of brain and other diseases of blood vessels (Heart Disease and Stroke Statistics—2019 Update: A Report from the American Heart Association.). Normally. The heart, a muscular organ pumps blood that carries oxygen to different parts of the body. Blood vessels takes up the pumped blood and with their own physiological mechanisms deliver blood to different organs. The blood vessels also pump back the blood towards heart for oxygenation from the organs. Heart muscle acquire its own oxygenated blood by the coordinated activity of coronary arteries. Similar to heart other major organ of human body, the brain, receives its own blood supply with the help two major arteries running along the sides of the neck- carotid artery. A lack of blood supply to these two major organs even for few seconds can lead to death or disability. As a consequence of disease associated with these blood vessels, CVDs remains to date as the leading cause of death in the world (WHO - Global atlas on cardiovascular disease prevention and control, 2011).

Blood vessel associated can prove to fatal to less severe. The death causing diseases include ischemic heart disease or coronary artery disease (e.g. myocardial infarction), cerebrovascular disease (stroke), diseases effecting aorta or other arteries (e.g. hypertension, peripheral vascular diseases). The other diseases include congenital heart disease, rheumatic heart diseases, cardiac myopathies and cardiac arrhythmias. Among most of the fatal CVDs, the underlying disease progress is due to narrowing or blockage of blood vessels due to atherosclerosis (Heart Disease and Stroke Statistics—2019 Update: A Report from the American Heart Association).

Among the non-communicable diseases (NCDs), CVDs claim more deaths (48 %) every year than any other diseases like cancer, diabetes mellitus or other respiratory disorders, Figure: 1.1.

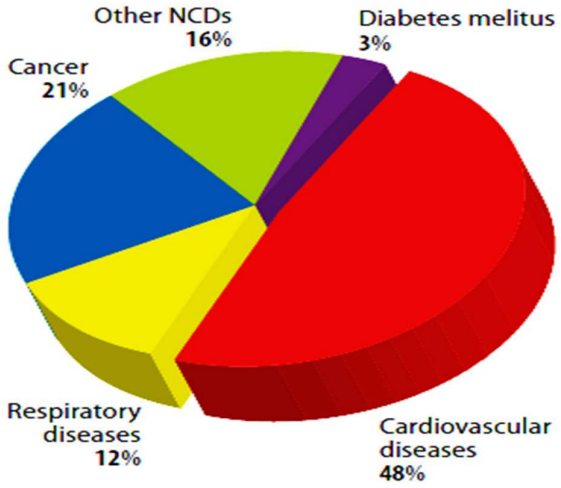


**Figure 1.1: Non-communicable disease statistics**

Recent statistical report confirms that CVDs account for more than 17.6 million deaths per year in 2016 and it is expected to reach a number of 23.6 million death by 2030. Among the CVDs coronary heart diseases was the major cause (43.2%), of deaths, followed by stroke (16.9%), high blood pressure (9.8%), diseases of arteries (3%) and other CVDs (17.7%) (Heart Disease and Stroke Statistics — 2019 Update: A Report from the American Heart Association). Moreover, CVD caused for 14% of total health expenditure and medical costs of CVD are expected to increase to $749 billion in 2035. The scenario prevalent in India concerned of CVDs are no different compared to the world. The global burden of CVDs is mainly pronounced in low- and middle-income countries like India mainly due to population explosion, pollution and age-related factors (Prabhakaran et al., 2018). It was estimated that, in 2016 62.5 million deaths had happened due to CVDs in India. Ischemic heart disease and stroke account for 15% to 205 of all deaths (Prabhakaran 2018). There is a state wise differences in CVD associated morbidity and mortality with highest of heart disease prevalent in Punjab and highest of stoke in West Bengal. Taking in account of all these, the United nations declaration of Non communicable diseases, the World health organization set the global goal to reduce risk of CVDs by 2025 and reduce the premature mortality burden from NCDs by one third by 2030 (Prabhakaran et al., 2018).

## 1.2 UNDERLYING PATHOLOGY OF BLOOD VESSEL DISEASES – ATHEROSCLEROSIS

The disease process that result in damage of blood vessel is known as atherosclerosis. Atherosclerosis is a complex pathological disease progression process of blood vessels which takes years to develop. In this, fatty material or cholesterol are deposited inside lumen of medium-and large-size arteries. These deposits or plaques causes the inner surface of blood vessel to become irregular and narrow, hindering the smooth blood flow through it. This leads to lack of blood reaching the desired organ. Moreover, these plaques can rupture to form blood clot (thrombus). If thrombus occurs in coronary artery it leads to heart attack or if it is in carotid or brain associated artery, it leads to stroke. For understanding the process of atherosclerosis, we need to deeply understand the anatomy, physiology and even the microstructure of blood vessel (Sakakura et al., 2013).

## 1.3 THE BLOOD VESSEL

Blood vessels are organized structures, which are able to autonomously regulate blood flow, which helps to provide oxygen support, nutrients and efficient waste removal from tissues. In human beings, blood vessel forms a closed circulatory system (Eble and Niland, 2009). Artery carries blood away from heart. It branches further to small vessels arteriole and then eventually into capillaries. Nutrient and waste exchange happen at capillaries which then combines with venules, then to vein and finally joins the heart. There also two types of circulation - systemic and pulmonary. In the systemic circuit, arteries carry blood rich in oxygen which is delivered to tissue and deoxygenated blood from tissues reaches heart through vein. In pulmonary circuit, arteries caries blood without oxygen exclusively to lungs for oxygenation, which is then transported back to heart by veins. Basic ultra-structure of arteries and veins remains same, but walls of arteries are much thicker in order to withstand the higher pressure experienced during blood flow. The major death causing blood vessel diseases are associated with conditions that affect arteries. Arteries exhibit a tri-layered architecture, called tunics, namely from the inner most layer to outer, these are the tunica intima, the tunica media, and the tunica externa. The tunica intima consists of epithelial cell line with its connective tissue. Intima contains specialized simple squamous epithelial cell, the endothelium. The entire

vascular tree is lined by endothelium and it's the site were blood contact with its vessel. Damage to endothelium, exposes the blood to its basement membrane of collagen and forms basis initiation of cascade of effects that leads to vessel damage. The basal lamina of endothelium connects the cells to its underlying areolar connective tissue. The connective tissue contains collagenous and elastic fibers. In medium and large sized arteries have internal elastic lamina that delineates intima with the next layer of blood vessel, the tunica media. The lamina allows the vessel to stretch and permeable with opening that allows exchange of small molecules between tunics. The tunica media is the middle layer of blood vessel and its thicker I arteries than veins (Tennant and McGeachie, 1990). It consists of concentric layers of smooth muscle cells embed connective tissue made of collagenous and elastic fibers. The vessel dynamics is mainly provided by this layer were contraction or relaxation of smooth muscle cells maintains the lumen diameter and there by causes temporal pressure variation that allow smooth blood flow. The vasoconstriction or vasodilation is under direct control of Nervi vasorum, the small nerves of blood vessels and also local hormonal or chemical control. The medial layer also regulates the overall health of blood vessel by exchanging small molecules with endothelium and by providing a suitable niche for endothelium to survive. Based on medial thickness, arteries can be divided either into elastic or muscular artery (Figure 1.2). The elastic arteries or conducting arteries are those near to heart. It can be differentiated from muscular artery as in shows relatively higher amount of collagen and elastin bundles in the tunica media (Alberts et al., 2002).These arteries respond critically to pressure changes and exhibit Windkessel effect, which helps the artery to maintain a constant pressure despite the nature of pulsating blood flow through passive contraction after expansion of the artery. Usually large diameter arteries like aorta, pulmonary artery (internal diameter <10mm) are considered elastic, small diameter arteries like common carotid artery, coronary artery also falls under elastic nature (internal diameter <6mm). The muscular artery or distributing artery, on the other hand are medium size arteries that originated from elastic arteries and examples are the splenic, radial, femoral arteries. The muscular artery has smooth muscle layer allowing for involuntary control of vessel caliber. It is important to note that any damage to these elastic arteries due to atherosclerosis cause potential vessel imbalances that impairs the function of vascular system.

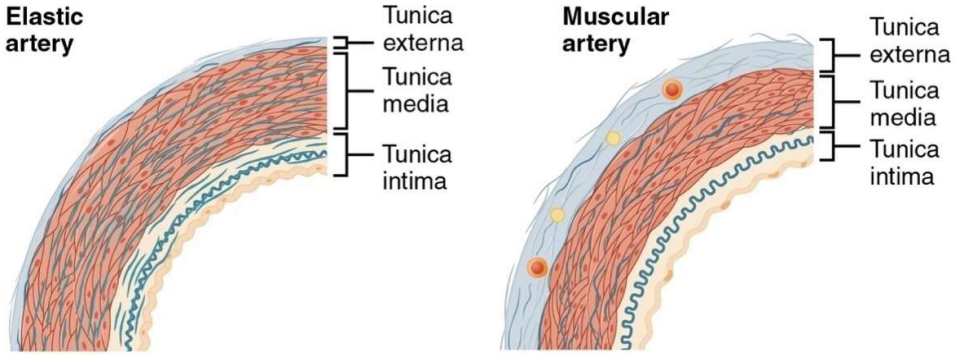


**Figure 1.2: Major types of artery - Elastic and Muscular and the tri-layered structure.**

The outermost layer of artery, the Tunic externa (Tunica adventitia) is sheath of connective tissue consisting of collagenous fibers which blends directly with the surrounding connective tissue. The layer has distribution of adventitial cells which has stem cell like properties. The adventitial layer places the blood vessel intact in position and thus helps no disruption in internal blood flow. Blood vessels are nourished with its own supply of blood vessel, vaso vasorum, which are small capillaries which have endothelial cell tubes in close contact with pericytes (20.1 Structure and Function of Blood Vessels | Anatomy & Physiology).

## 1.4 THE PROCESS OF ATHEROSCLEROSIS

Atherosclerosis progression or atherogenesis is a combined interaction between various risk factors, the cells of artery wall, blood and its components in response to molecular interaction between these. When arterial endothelium encounters a potential risk factor from a diverse range as dyslipidemia, hypertension induced vasoconstrictor hormones, glycoxidation associating hyperglycemia, pro-inflammatory cytokines or any other external factors like bacterial products, pollutants, theses specialized cells express adhesion molecules that attracts blood leucocytes to attach to inner region of arterial wall. The leucocytes-mononuclear phagocytes and T lymphocytes-communicate with endothelial and smooth muscle cells, and as a response to this, the smooth muscle cells migrate from media into intima (Scott, 2004). These cells proliferate and produce rich extracellular matrix. As the lesion progress, calcification occurs at the site. In addition to this, the death of lipid-containing macrophages leads to extracellular matrix deposition

of tissue factor (TF) in the intima and form the lipid rich "necrotic" core of atherosclerotic plaque. Disrupted plaque leads to thrombosis in several ways, either the extracellular matrix of the plaque can initiate platelet activation when contact with collage. The tissue factor produced by macrophages and SMCs activates coagulation cascade. The activated platelets entrapped fibrin makes the classic white arterial thrombus which leads to decrease or block in lumen diameter and there by disrupting the blood flow, Figure: 1.3. (Libby Peter and Theroux Pierre, 2005)

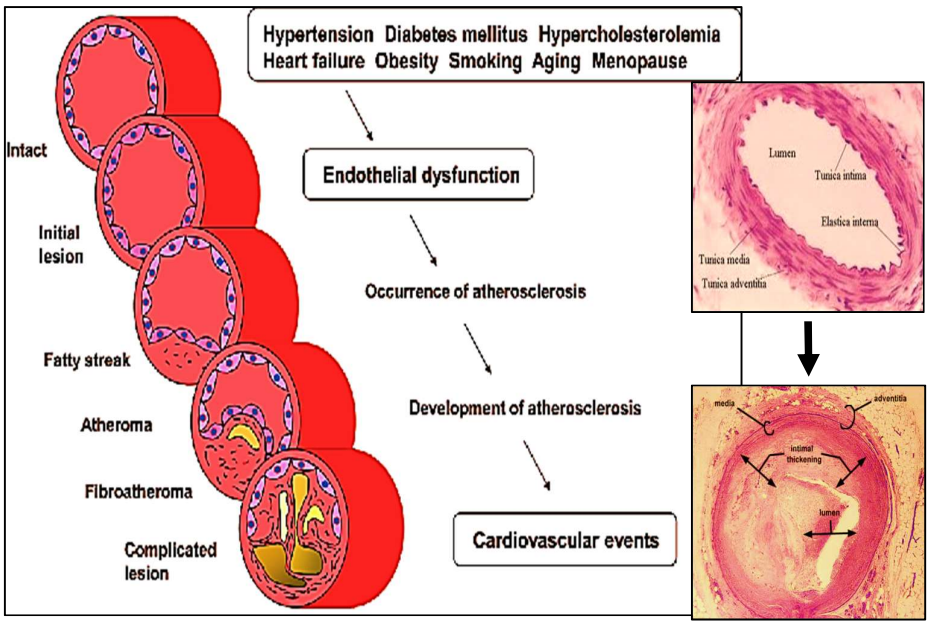


**Figure 1.3: Progression of atherosclerosis (Adapted from (Higashi, 2015), in set histology of artery before after atherosclerotic narrowing).**

## 1.5 MEDICAL MANAGEMENT OF BLOOD VESSEL DISEASE

As CVDs remains as the prime cause of death worldwide, the medical management of the diseases are undergoing immense research for past many decades. Treatment modalities of blood vessel associated diseases span from improving the dietary and lifestyle of the patients, administering pharmaceutical and/or even surgical interventions. A commitment to follow healthy lifestyle prevents CVDs to associate with behavioral risks. Depending upon the disease severity and current stage, a practitioner could advice a patient to eat healthy foods, exercise regularly, reduce

weight, reduce stress and quit smoking. However, during advanced stages if disease or in the case of genetic predisposition factors, drugs can be advised. The panel of drugs include cholesterol-modifying medications, beta blockers, calcium channel blockers, angiotensin-converting enzyme inhibitors and angiotensin II receptor blockers, anti-platelet agents, anti-thrombotic agents etc., all these include the non-invasive options for treatment of CVDs (Bergheanu et al., 2017).

However, when required, vascular surgery may be opted and it includes procedures which are minimally invasive like angioplasty, stent insertion, atherectomy etc., to widen a stenosed blood vessel or to remove the plaque deposited, Figure: 1.4 A. Alternative to these endovascular percutaneous interventions, when a vessel is completely obstructed or the blood flow is extremely narrow, a vascular replacement surgery has to be performed. In the vascular replacement surgery or bypass surgery, a portion of blocked blood vessel area is either bypassed or completely replaced with vascular grafts. Vascular graft-based surgeries for treating CVDs is very promising as this is the optimal choice for patients that require long-term revascularization solutions. The life expectancy of CVD patient could be enhanced by grafting. In bypass grafting, especially in coronary artery bypass grafting, a surgeon replaces or bypass a blocked vessel with a conduit selected from patients' own body, Figure: 1.4 B.

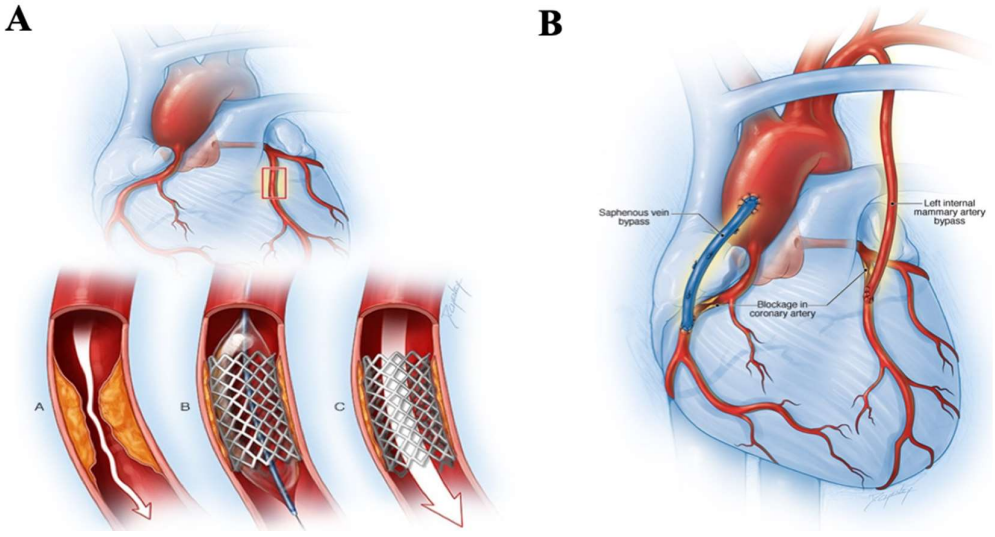


**Figure 1.4: Treatment modalities of CVDs. (A) Coronary stenting. (B) Coronary bypass grafting (Adapted from Mayo clinic research organization).**

To the date, the much-favored replacement graft favored is patients' autologous arteries or veins. These autologous blood vessels become the golden standard in terms of vascular graft procedures, however there are some limitations for these biologically originating vascular conduits. The use of arteries like internal thoracic artery (Left internal mammary artery, LIMA) or radial artery is associated to their extremely superior patency owing to arterial similarity, it is saphenous vein (SV) that is constantly used for bypass grafting. This is because arteries are very limited in availability and mostly harvesting an artery cause much serious donor site complications than harvesting a vein. Vein grafts, despite being a popular choice for bypass grafting, the patency of this not so appreciable (Prapas et al., 2014). There is detrimental decrease in the patency of vein autologous grafts used both for CABG and femoropopliteal bypass grafting showing a failure percentage of almost 50% over 10 years. There is other complication, as similar to arterial grafts have limited availability when intended to harvest second time and also extraction causes donor site morbidity in general (Ruß et al., 2009).

Synthetic blood vessel replacement is much pronounced in the case of large diameter vessel replacement like that of aorta, were internal diameter is almost 10mm or more. Grafts made of Dacron, ePTFE performs extremely satisfactorily even in long term application in these larger vessels (>8 mm internal diameter). The patency is around 90 % with extremely low failure rate in aortoiliac substitutes. However, in the scenario of small (< 6 mm internal diameter) or even medium (6 – 8 mm internal diameter), these synthetic grafts failed to meet the standards. Vascular graft failures in small diameter vessel replacement are commonly associated with thrombosis related complications, intimal hyperplasia, graft atherosclerosis or infections. Thrombosis occurs as a result of lack of well-defined endothelial cell lining to the graft, which leads to adherence of blood proteins and thereby activating the clotting cascade (Pashneh-Tala et al., 2016). The intimal hyperplasia, however, is initiated by smooth muscle migration and their extensive intimal proliferation. This could occur around the anastomosis between graft and native vessel if there is vessel diameter mismatch, lack of endothelization, suture line stress, hemodynamic factors or any other graft related trauma. Graft atherosclerosis occurs may be years after implantation and it is not immediate cause of failure. There are many limitations faced at this point in vessel

grafting and an optimal choice is still an unmet need. This has led to search of new researches in this field and with the emergence of tissue engineering concept it is expected to solve the scarcity (Hansen et al., 1995).

## 1.6 TISSUE ENGINEERING

The limitations of current blood vessel replacement conduits, the application of concepts of tissue engineering to the field of vascular biology provides a potential solution in the future to save the life of patients by vascular surgery. Tissue engineering as conceptualized today is "an interdisciplinary scientific field that applies the principles of engineering and life sciences towards the development of biological substitutes that restore, maintain to improve tissue function or as a whole organ (Langer and Vacanti, 1993). It utilizes the interplay between the scaffolds, cells and other biomechanical cues and forms the basic tissue engineering triad (O'Brien, 2011). The idea of tissue engineering has progressed so far within recent years that, the engineering of tissue has been adopting strategies of personalization. This forms the basis of personalized tissue engineering, where dimension and make of scaffold matches the patients' organ dimensions and cellularization depends solely on cells originated from patient, Figure: 1.5. In terms of blood vessel engineering, the idea of personalized tissue engineering is highly relevant.

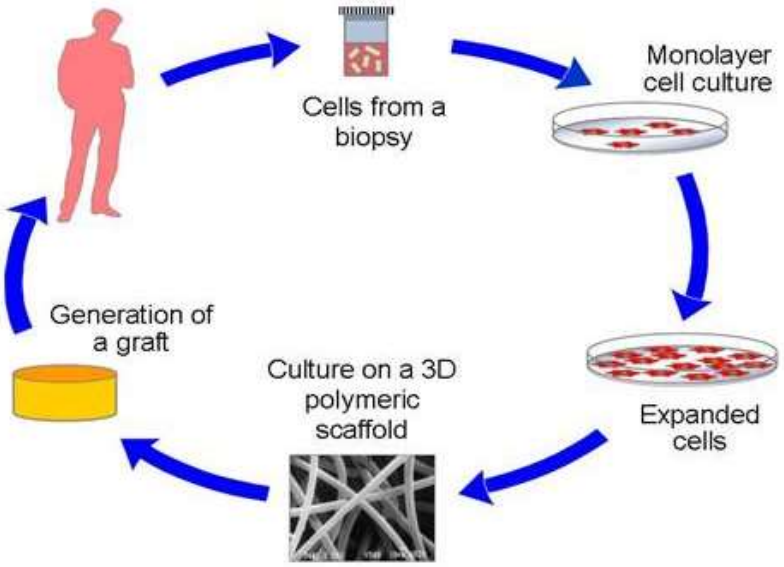


**Figure 1.5: The concept of tissue engineering**

## 1.7 VASCULAR TISSUE ENGINEERING

A tissue engineered vascular graft (TEVG) with the ability to regenerate and repair in vivo has clear advantage for vascular surgery and would be highly beneficial in the scenario of small diameter blood vessel engineering. Vascular tissue engineering could be generally defined as 'Generation of tubular conduits that incorporate the functionality of tri-layered artery, withstand physiological stresses and promote integration in host tissue without mounting immunologic rejection'. A TEVG should satisfy a number of design standards for being placed as an integral part of vascular network (Song et al., 2018a). The primary importance of the graft is to support smooth flow of blood as this is a direct blood contacting device. The graft should not be self-thrombotic, cytotoxic or illicit negative immunological response, such as chronic inflammation, complement cascade activation or adaptive immune system triggering (Dhulekar and Simionescu, 2018). Moreover, it should possess adequate properties to withstand the physiological stresses experienced during blood flow. It must be able to keep in control the pressure variation without being aneurysmal in nature. It should also possess suitable compliance with native vessel and no stresses at anastomosis that induce undesirable flow patterns. Apart from this from a medical device point of view, a graft

should be suitable for implantation with ease without kinking and should have ability to be handled and sutured. It should be able to mass produced in desirable dimensions (length, diameter etc.,), stored and quality controlled. Moreover, it should be economical and easily available (Chang and Niklason, 2017a).

## 1.8 DEFINITON OF THE PROBLEM

Tissue engineered small diameter vascular graft has various advantages as a replacement option in vascular reconstructive surgery. However, the concept of small diameter blood vessel engineering is still in its infancy as a myriad of factors should interplay for its successful application. Moreover, it has to be specifically personalised towards the vessel requirement of each patient. In order to achieve this, the problem defined in the present study, is to engineer a small diameter vascular graft based on autologous cell source on suitable polymeric scaffold and to evaluate its functional efficacy in animal model.

Autologous cells, such as adipose tissue derived mesenchymal stem cells or vascular cells differentiated from these cells have various scientific and ethical advantages. The properties of polymeric scaffolds could be fine-tuned in order to achieve the properties desirable for vascular graft. In this current background, the study hypothesis was developed in order to address the problems or requirements as stated above for successful generation of tissue engineered small diameter vascular graft.

## 1.9 HYPOTHESIS

Tissue engineered small diameter arterial graft fabricated by autologous adipose tissue derived mesenchymal stem cells on electrospun tubular scaffold is expected to have superior functional efficiency. In order to test the hypothesis, two strategies of cell-scaffold based tissue engineering has been studied. The outside-in strategy of analysing the effect of adipose stem cell derived perivascular smooth muscle cell seeded tubular scaffold for its functional efficiency *in vivo* specifically on patency, endothelisation and regeneration capacity. The other strategy, is inside-out strategy where an endothelial cell friendly scaffold was selected and co-cultures with adipose tissue derived perivascular

stem cells like adventitial cells and pericytes respectively with endothelial cells were established. The functional efficiency of this concept is defined in terms of its angiogenic potential *in vitro*.

## 1.10 OBJECTIVES

To experimentally prove, the above stated hypothesis, the study progresses based on four well defined objectives. The objectives were further subdivided and are as follows:

1. Scaffold fabrication
    - To synthesis and characterise polymers suitable for scaffold fabrication.
    - To fabricate tubular vascular grafts of small diameter with the synthesised polymers and/or its combinations with other polymers by electrospinning.
    - To characterise the properties of fabricated vascular grafts- physico-chemical, mechanical, biocompatibility and hemocompatibility.

2. Cell source
    - To isolate autologous adipose tissue derived mesenchymal stem cells, perivascular stem cells-adventitial cells, pericytes and to isolate endothelial cells.
    - To characterise adipose derived cells, perivascular stem cells-adventitial cells, pericytes and endothelial cells for their potential to be used for stem cell based tissue engineered vascular graft.

3. Vascular tissue engineering strategy
    - To establish the outside-in strategy, adipose derived mesenchymal stem cells are differentiated to vascular smooth muscle cell lineage on electrospun polymeric scaffold, Figure: 1.6.
    - To characterise the differentiated cells on scaffold for its contractile nature based on gene expression, extracellular matrix deposition.

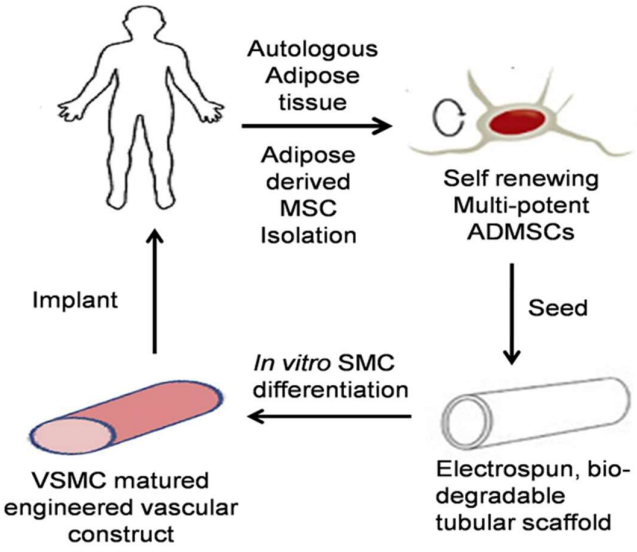


**Figure 1.6: Graphical representation of Outside-in strategy**

- To establish the inside-out strategy, adipose derived perivascular stem cell-adventitial cell and pericytes are co-cultured respectively with endothelial cells on electrospun polymeric scaffold, Figure: 1.7.
- To characterise the cells, standardise co-culture and to analyse the *in vitro* angiogenic potential of each co-culture system on scaffold.

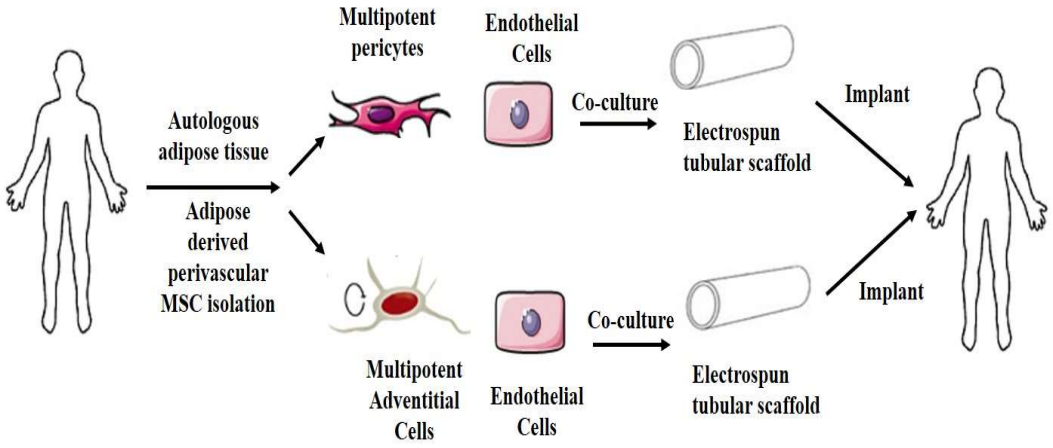


**Figure 1.7: Graphical representation of Inside-out strategy**

4. *In vivo* evaluation of the graft.

- To evaluate the functional efficiency of vascular graft fabricated based on outside-in strategy, which is smooth muscle cells cellularised electrospun tubular scaffold graft, the grafts were implanted in Lapine and ovine animal models as common carotid artery interposition graft.
- To evaluate the patency of graft by angiography.
- To evaluate the regeneration potential of the graft in terms of endothelisation, extracellular matrix deposition, neo-vascularisation.

The experimental design was made based on objectives and chapters in the thesis are as follows. The Chapter 1: Introduction, where the concepts are introduced and hypothesis was framed. The Chapter 2: Literature review, which screens the major findings in the field of small diameter vascular tissue engineering from past studies published, with emphasis on objectives under study. The Chapter 3: Material and methods, thoroughly presents the major methodology used to achieve the objectives. This chapter is divided into three sections and each section into two parts. The part I of section I and section II describes the methodology adopted to achieve the outside-in strategy of vascular graft fabrication. In this a natural-synthetic polymeric hybrid scaffold is fabricated by dual source co-electrospinning and differentiation of adipose derived smooth muscle cells on the scaffold is established.

The part II of section I and section II described the methodology adopted to achieve the inside-out strategy, the co-culture based development of vascular graft, where a synthetic endothelial friendly polymer is synthesised and fabricated to form tubular scaffold. Co-culture of perivascular stem cells with endothelial cells were studied.

The section III describes the *in vivo* evaluation of graft fabricated based on smooth muscle cells and co-electrospinning and has two parts, Part I describes *in vivo* evaluation in Lapine model, part II describes *in vivo* evaluation in Ovine model.

The Chapter 4: Results, the major results obtained are furnished and pattern of conveyance is similar to that as described in Chapter 3.

The Chapter 5: Discussion. Thoroughly analyse and critically evaluate the major results obtained.

Chapter 6: Summary and conclusion. The chapter summarises all major achievements and conclude the major milestones and limitations of the present study.

## 1.11 SIGNIFICANCE OF THE STUDY

The study signifies the relevance of tissue engineered small diameter vascular grafts, its fabrication strategies and functional efficiency. The graft developed based on cell-scaffold tissue engineering concept is expected to perform better in terms of its patency, angiogenic potential and regeneration capacity. The graft fabricated by electrospinning of polymers and adipose derived cells has shown to support positively the vascular cells and helps in in vivo regeneration. The approach and findings have the potential to be extrapolated in the future to solve the unmet clinical need of small diameter vascular graft. Our long term goal is to achieve tissue engineered small diameter vascular graft that has its ability to grow, remodel and repair *in vivo*

# CHAPTER 2
# REVIEW OF LITERATURE

## 2.1 STRATEGIES FOR VASCULAR TISSUE ENGINEERING

Cardiovascular disease complications associated with blood vessel damage due to atherosclerotic progression and thrombotic complications remains as the leading cause death and disability worldwide (Wang et al., 2016). To date, there is an insistent demand for suitable blood vessel replacement graft especially in the context of small diameter blood vessel replacement. Several strategies were applied by the researchers all over the world in order to meet the rising need of vascular graft, but an ideal tissue engineered graft still remains as a "holy grail" in the field of cardiovascular tissue engineering. Most of the current literature analysis shows that there are several short comings associated with designing and fabrication of a suitable arterial replacement. The history of engineering small diameter arterial blood vessels date backs to 1986 when first tissue engineered vascular graft (TEVG) was constructed by collagen coating of thin Dacron mesh and seeding bovine endothelial and smooth muscle cells. Even though the idea was a breakthrough, the success of this graft was limited due its extremely poor mechanical properties (Weinberg and Bell, 1986). In order to engineer a vascular conduit, a tubular structure has to be initially created and vascular cells has to be arranged on the tube so that they mimic and perform similar to that of native blood vessel, also the final vascular tubes should possess all the desirable properties ranging from anti-thrombotic nature to mechanical strength successful tissue engineered small diameter vascular graft.

The generation of tubular structure involve mainly three methods which may or may not involve the use of biomaterial. These are cell-sheet rolling or molding the material in tubular molds (tissue engineering by self-assembly), xenogeneic vessel source like that of decellularized vessels from animals or direct scaffold technique. The tubular structures created could either be used as cellularised or acellularized graft with or without vascular cell seeding, Figure: 2.1 (Song et al., 2018b).

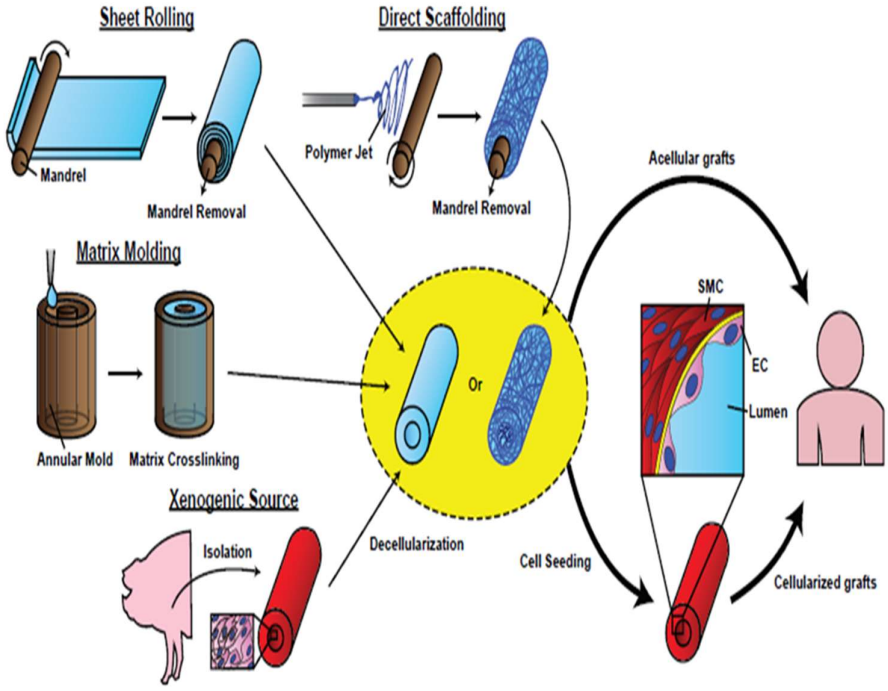


**Figure 2.1: Fabrication strategies of tissue engineered small diameter vascular graft (Adapted from HH Song et al., 2018)**

The tissue engineering by self-assembly method does not rely on scaffold or any other support for creating tubular structures. The foremost clinical trial of TEVG in the case of small diameter vessel replacement was sheet-based tissue engineering in which autologous fibroblasts and endothelial cell sheets were layered on tubular mandrel with emphasis on production of large amount of extracellular matrix by these cells (Peck et al., 2012). In this clinical study as hemodialysis access, however only 4/10 grafts were patent over 20 months. In another study, TEVG was created by wrapping sheets of cultured smooth muscle cells around tubular mandrel which was then followed by fibroblast layer. This was cultured in a bioreactor conditions and endothelial cells were seeded in the lumen. However, the disadvantage of this study was it took almost more than a month to develop the desired structure of the graft (L'Heureux et al., 1998; L'Heureux and McAllister, 2008). Recently a study was reported in which an annular mold was used to generate a graft made of cells. The graft was implanted in lamb model (Syedain et al., 2016). Despite many studies, there are many limitations for this method.

The primary drawback of this method is the extended time required to culture cells and lack of attaining desired mechanical integrity even after that.

The process of decellularization involves the complete removal of immunogenic cellular and other proteinaceous materials from native vessel while preserving the extracellular matrix. Chemical agents like detergents, acids/bases or enzymes and physical methods like abrasions or pressure are used for decellularizing tissues. Mostly blood vessel, ureter or small intestine submucosa of animal or human cadaver origin are used for generation of tissue engineered graft. The advantage of this method is the natural extracellular matrix of the tissue is kept intact which may further help in attaining mechanical properties or aid in easy recellularization. There are many commercially available decellularized grafts- Synergraft 100 (Bibevski et al., 2017), ProCol (Schmidli et al., 2004), Artegraft (Lindsey et al., 2018). These xenogeneic origin graft have lot of limitations including fatal immunological reactions even though decellularization reduces the antigenicity of graft, complete exclusion of foreign agents is difficult to accomplish. Graft geometry, lack of mechanical reliability, ethical concerns and cost also limits the usage of decellularized grafts (Shirakigawa and Ijima, 2017).

## 2.2 SCAFFOLDS IN VASCULAR REGENERATION

When considering the disadvantages of above methods to generate vascular graft, the direct scaffolding method using biomaterial-based scaffold has various advantages. Vascular cells when cultured *in vitro* are not able to self-organise themselves into tubular structures. Therefore, support of scaffold helps them to arrange themselves very similar to native blood vessel. Tissue engineered small diameter vascular grafts could be made from a range of biomaterials either natural, synthetic or even hybrid and fabrication technology vary from casting to electrospinning or bio-printing. The properties of scaffold could hence be fine-tuned so that it exactly matches with characteristics of extracellular matrix of the blood vessel (Thottappillil and Nair, 2015).

### 2.2.1 EXTRACELLULAR MATRIX OF THE BLOOD VESSEL

The sophisticated extracellular matrix of the blood vessel attributes in a large way to the functional efficacy of the vessel. The ECM could act as scaffold that maintains the architecture of blood vessel which in turn determines the function. The mechanical properties associated with the blood flow is mainly controlled by the extracellular matrix proteins of the blood vessel. There is very intricate network of collagens and elastin fibres with their associated protein that regulate the contraction-relaxation cycles of blood flow and pressure variations. The ECM acts as a storage reservoir of many small molecules like growth factors, micro-vesicles that remarkably contribute to the proliferation and maturation of vascular cells. Blood vessel regeneration during injury, healing and graft remodelling is also highly controlled by the extracellular matrix (Eble and Niland, 2009b). Hence designing a scaffold that mimic the native vessel ECM is highly challenging. It should thus possess several physicochemical properties that makes it ideal for blood vessel engineering, moreover it should also facilitate graft remodelling.

The major protein of blood vessel extracellular matrix is collagen and elastin fibrils along with other proteoglycans, Figure: 2.2.

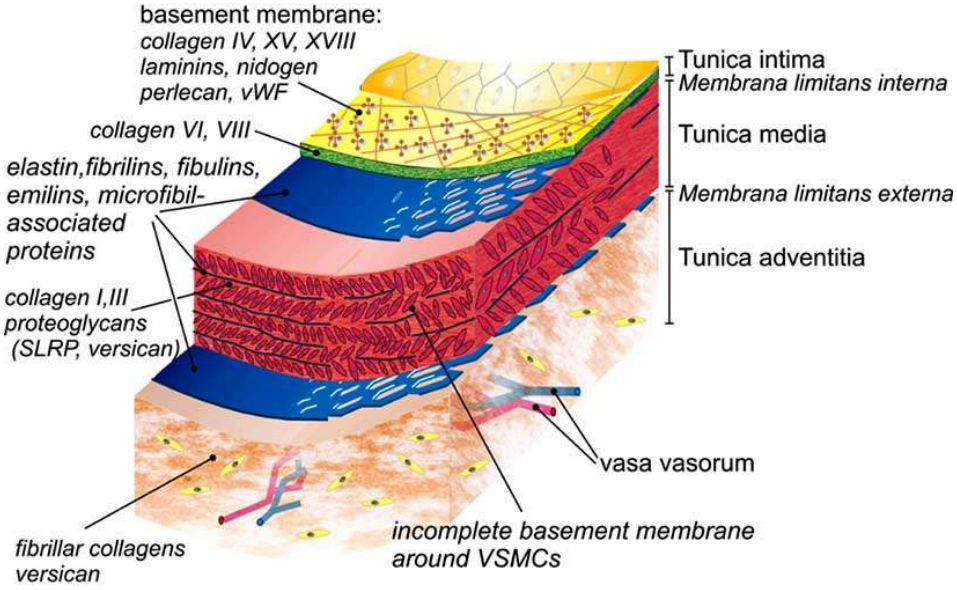


**Figure 2.2: Blood vessel extracellular matrix components (Adapted from Eble and Niland, Extracellular matrix of Blood vessel, 2009).**

Blood vessel consists of three layers and ECM protein distribution in each layer is highly diverse. The tunica intima media is the endothelial layer that resides on basement membranes. The main component of the basement membrane is collagen type IV which forms a peculiar two-dimensional network interconnected by their 7S and NC domains. This crosslinked structure contributes majorly to the mechanical stability of the membrane. Other types of collagen are type XV and XVIII which mediate the basement membrane stabilisation to underlying medial connective tissue (Kühn, 1995; Marneros and Olsen, 2005; Pöschl et al., 2004). Other proteins laminins are needed for organisation of basement membrane (Smyth et al., 1999) and nidogens connects laminins and collagen IV (Ho et al., 2008). Yet another integral component of basement membrane are perlcans (Zhou et al., 2004) and secreted protein acidic and rich in cysteine (SPARC or osteonectin) (Phan et al., 2007). Both these molecules seem to associate with growth factors like Fibroblast growth factor, VEGF, platelet derived growth factors and modulate angiogenesis. The von Willebrand factor (vWF) is also present which binds to platelets and blood clotting factor VIII (Elzorkany et al., 2018). During endothelial dysfunction, exposure of blood to collagen and vWF triggers platelet activation. Endothelial cells are anchored to basement membrane through integrin and syndecan connections (Echtermeyer et al., 2001; Wallez and Huber, 2008).

The tunica media of the blood vessel has highly variable ECM with difference in elastic and muscular arteries. Elastin forms a major component of media and are arranged in concentric layer within which vascular smooth muscle cells reside. The elastin is secreted by smooth muscle cells as tropoelastin and several elastin moieties are cross-linked to form a network by lysyl oxidases. The major structural role of blood vessel elastin is to maintain its dimensions during blood flow. The resilience of blood vessels during pulsatile flow is due to the ability of elastin fibres to stretch to a length 220% of its original length and recoil to the original state without any deformation (Mithieux and Weiss, 2005). It is also reported that elastin regulates smooth muscle cell proliferation (Brooke et al., 2003), additionally the fibrillin and fibulin protein linkers that connects elastin lamellae also participate in TGF-β signalling (Rifkin, 2005). Due to the immense role played by elastin in blood vessel structure maintenance and cell regulation, it is an inevitable component of creating a tissue engineered graft. Elastin deposition or

elastogenesis is marker of matured graft and its regeneration ability (Patel et al., 2006). The collagen also forms a major part of tunica media especially type I and III. Collagen fibrils are interspersed within elastin network and does not recoil; however, collagen limits the extent to which elastin could deform. There are internal and external elastic lamellae that delineates media from adventitia and intima. Other types of collagen seen are collagen VI and VIII (Myllyharju and Kivirikko, 2004). The tunica adventitia extracellular matrix consists of fibrillar collagens and versican (Wight and Merrilees, 2004).

### 2.2.2 NATURAL POLYMER BASED VASCULAR GRAFTS

Natural polymer based vascular grafts have been extensively reported. The advantages of a natural biomolecule-based graft are that they exhibit appreciable biocompatibility or lack of toxicity. The binding sequences mimicking similar to that of natural ECM molecules, the vascular cells find natural scaffolds a better place to attach and function. Fibrin based scaffolds were used in different studies where smooth muscle cells were seeded and SMCs maintained their contractile phenotype (Yao et al., 2008). In another study, dermal fibroblasts were seed on fibrin-based graft and matured in a bioreactor condition. Despite of the advantages, both these scaffolds failed to meet the mechanical properties comparable to that of native vessel (Syedain et al., 2011). In another report silk fibroin was used by electrospinning, irrespective of good degradation behaviour, the graft did not exhibit appreciable mechanical strength. In another strategy of gel spinning of silk fibroin and graft was implanted in rats (Lovett et al., 2010). There was patency up to four weeks and vascular remodelling, however, further follow up data were not available. Hyaluronan based material (hyaff-II) implanted in porcine model, showed remodelling with only 7/10 graft occlusion (Zavan et al., 2008). Recombinant tropoelastin based vascular grafts by electrospinning showed excellent attachment of bone marrow endothelial outgrowth cells *in vitro* (Jordan et al., 2007). In another study, murine SMCs were seeded on knitted chitosan tube coated with gelatin which showed appreciable burst pressure of 4000mmHg (Zhang et al., 2006). Collagen based scaffold has added advantage of being similar to the ECM of blood vessel. However, the major drawbacks include lack of mechanical strength, immunogenicity and high cost. In a study where collagen gel encapsulated with porcine SMCs and ECs were used, the burst

pressure obtained was very low (Boccafoschi et al., 2007). Freeze dried collagen and elastin tubes were seeded with umbilical SMCs under mechanical stimulation for improved tensile strength (Engbers-Buijtenhuijs et al., 2006).

### 2.2.3 SYNTHETIC POLYMER BASED VASCULAR GRAFTS

Synthetic vascular grafts have added advantages than natural ones as these shows improved mechanical properties, tuneable fabrication strategies and even slower degradation rates. However, the disadvantages of this lack of cell compatibility and regeneration capability. In a study, Poly glycolic acid mesh tubes seeded with porcine or human vascular cells in a bioreactor were implanted in baboons which showed patency up to four weeks. This was later, decellularized and implanted in baboons to obtain patency for six months. In another report where Poly ester urethane urea (PEUU) grafts were seeded with stem cells or pericytes, implantation in murine model showed patency for 8 weeks (Nieponice et al., 2008a). Poly glycerol sebacic acid (PGS) and Poly-ε-caprolactone (PCL) based scaffold were patent up to 90 days in rat aorta and the scaffold was acellular. There are several studies using PCL based vascular graft, while many of these studies claims grafts showed patency in small animal model, there was no follow up studies in either (Hiob et al., 2016). In one study PCL grafts were electrospun on to a 2mm mandrel. The graft had excellent mechanical properties however, when implanted in rat until six months but after that a clear regression and calcification was observed. These were acellular grafts. In another report, heparin was immobilised on PGS tube and further wrapped with PCL layer. These grafts when implanted in rat for three months showed no aneurysm or stenosis, and there was formation of confluent endothelial lining. Poly (l-lactide-*co*-ε-caprolactone) grafts were implanted in rat abdominal aorta for12 months by which the graft remodelled with pulsation and mechanical properties (Zhu et al., 2018). In one study co-electrospun PCL/PU nanofibrous grafts were fabricated which showed that the graft compliance was increased to 43% by altering the percentage to 90% and *in vivo* evaluation showed foreign-body granulomatous reaction (Jirofti et al., 2018).

There are endless studies in the field of scaffold development for vascular tissue engineering using both natural and synthetic scaffold. To date, an ideal biomaterial that

meet the properties for making a successful graft has not yet been obtained. Comparing and contrasting the properties of synthetic and natural vascular graft, the natural polymer-based scaffolds could provide remodelling characteristics even when cultured *in vitro* with vascular cells due to their excellent cell compatibility. But these scaffolds in most studies has failed to meet the mechanical standards. Some natural polymers also exhibit antigenicity and requirement of extensive cross-linking. Synthetic polymers on the other hand has tuneable mechanical properties but does not show appreciable biological performances. While the natural polymers show the tendency to degrade faster *in vivo*. The synthetic polymers like PCL has slower degradation profile which will give sufficient room for vessel regeneration.

### 2.2.4 HYBRID NATURAL - SYNTHETIC SCAFFOLD BASED VASCULAR GRAFTS

Considering the advantages and disadvantages of both synthetic and natural polymers have led researchers to develop hybrid scaffold-based system through various reinforcing methods of two different biomaterials. The resulting combinatorial biomaterial scaffold system may possess properties attributed by the parent polymers and usually an improved functional behaviour is expected. Synthetic polymers are either coated with one or more natural polymers to improve its cell conducive properties. In one of the studies, co-polymers of L-lactide and D-lactide knitted structure was coated with fibrin gel and SMCs which was then co-cultured wit ECs and fibroblasts. Six months follow up in sheep however showed stenosis and there was no indication of mechanical properties of the graft (Koch et al., 2010). In another case, PCL/PLA electrospun tubes were coated with collagen and seeded with aortic endothelial cells in bioreactor conditions. This was further implanted in rabbit for seven weeks without endothelial cells (acellular) there was no blood leakage and no cell infiltration (He et al., 2009).A blend of PCL/Collagen type I/elastin which were electrospun in three concentric layers, with each layer differing in composition, showed burst pressure of 3000mmHg, but no studies related to scaffold cell compatibility was reported (McClure et al., 2010). In another study, a collagen micro sponge and tube made of Poly lactic acid and poly-glycolic acid fabricated by air jet spinning seeded with umbilical vein endothelial cells were implanted in dogs. After 1 year, the grafts were patent showing no signs of

aneurysms, endothelisation and deposition of elastin (Yokota et al., 2008). Our group has reported seeding of rat aortic SMCs on gelatin modified with vinyl acetate under pulsatile conditions. The SMCs were contractile in nature and there was elastin deposition (Thomas and Nair, 2012). RGD peptide sequences were immobilised on PCL grafts and 2mm grafts were implanted in rabbit carotid artery. The grafts showed patency and endothelisation (Zheng et al., 2012a). A cell free nanofiber PCL/chitosan scaffolds showed excellent regeneration without neo-tissue formation and stenosis in sheep model (Fukunishi et al., 2017).A heparin loaded PCL/gelatin graft was fabricated by electrospinning and it was shown to regulate the proliferation of smooth muscle cells and helps in endothelisation (Horakova et al., 2018). In another recent study, a graft was generated by different electrospun layers of porcine gelatin/ PCL and human tropoelastin/PCL and was well characterised and a computer assisted design optimisation scheme was deduced in order to fabricate grafts based on target geometry and compliance (Tamimi et al., 2019).The list of biomaterials used to fabricate blood vessel is considerable. The hybrid scaffolds incorporating the properties two or more polymeric materials is the recent development in this field and is considered as smart biomaterials for vascular tissue regeneration. This helps to substantiate the mechanical, degradation and other tuneable properties of a synthetic material. Also, the cell compatible nature and biomechanical niche provided by the natural polymer part (Catto et al., 2014). Despite of several studies, there is a still an immense search for the “perfect graft” that meets biomimetic criterion (Carrabba and Madeddu, 2018; Pashneh-Tala et al., 2016).

## 2.3 FABRICATION OF VASCULAR GRAFT - ELECTROSPINNING

The tubular shape of vascular graft can be achieved through various fabrication strategies. The selection of most suitable fabrication strategy for a given biomaterial is extremely important for the success of vascular graft. Traditional methods of polymer fabrication like freeze drying, mould casting, salt leaching could be used for development of graft and there are various reports on this. However, in order to fine tune the properties of biomaterials, these methods often fail. There is no ultra-structural similarity of the grafts fabricated through these processes similar to native ECM. Other properties like porosity, mechanical strength is never optimal for the grafts fabricated by these strategies. Other techniques like 3D bio-printing are still in infancy in terms of vascular

tissue engineering. For fabrication of microvascular tissue 3D bioprinting has been extensively used. A study indicated using poly(propylene fumarate) 3D printed by digital light stereo lithography, acellular graft performance in sheep vena cava for six months, even though the graft was patent and supported vessel regeneration, the implant chosen was of large diameter (Melchiorri et al., 2016).In another study, controlled nitric oxide release was obtained from Polyethylene glycol-PCL-S-nitroso-N-Acetyl-D-Penicillamine based 3D printed scaffold which had antibacterial and platelet inhibiting properties (Kabirian et al., 2019). However, 3D printing has not yet proved to be advantageous than any other fabrication strategy in the field of vascular tissue engineering.

Electrospinning is a versatile process that allows fabrication of grafts. The process allows fine tuning of graft properties. The ECM of blood vessel is fibrous in nature under microscope, and electrospun scaffold could mimic this ultra-structural feature. Moreover, the ease of methodology allows to combine different polymeric biomaterials into a single scaffold. A precise control over scaffold micro-architecture, gross dimension, biocompatibility and mechanical properties are made possible by altering combinatorial parameters of electrospinning process. Also, the process provides suitable niche for vascular that facilitates tissue regeneration and host integration. The basic set up of electrospinning apparatus is extremely simple. The polymer solution is loaded into a blunt needle syringe and mounted on to a pump that allows the controlled extrusion of polymer. Polymer under influence of high voltage and its intrinsic viscoelastic properties can be drawn into a cone shape, called the Taylor cone. When the provided voltage exceeds threshold of surface forces, a narrow polymeric jet is initiated which get deposited on an oppositely charged collector. The solvent system of polymer solution evaporates on its way to the collector, Figure: 2.3. The basic set up of the electrospinning could be modified in many ways to produced aligned or non-aligned fibres, multi-layered grafts, hybrid tri-component grafts, grafts showing sustained release of biomolecules, cell-based electrospinning. The electrospinning parameters like solution viscosity, conductivity, flow rate, applied voltage, tip to collector distance, temperature and relative humidity affect the fibre diameter (Hasan et al., 2014a). However, data in the literature in this regard is highly variable and cannot be easily generalised.

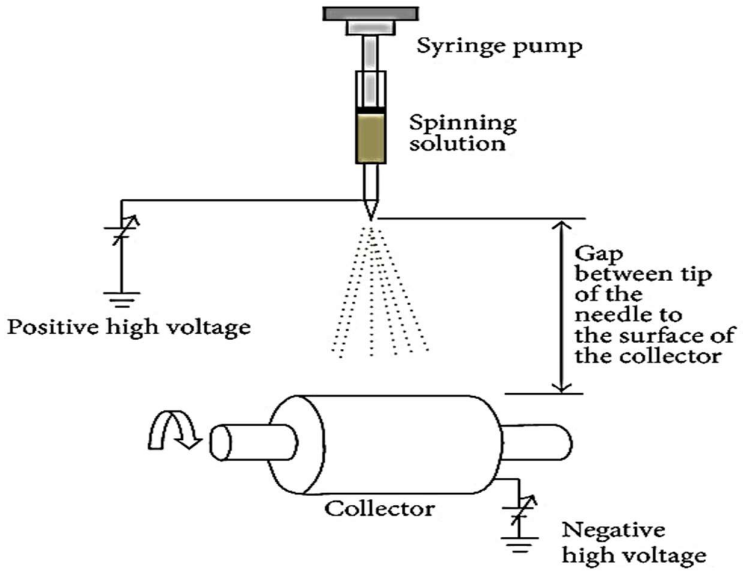


**Figure 2.3: Basic electrospinning set up with rotating cylindrical mandrel as the collector**

The advantage of hybrid scaffold made of two or more different polymers is immense in the field of vascular tissue engineering. Dual source co-electrospinning process facilitate the fabrication of hybrid scaffold as it offers the feasibility of electrospinning two polymeric solutions. The physico-chemical and biological characteristics could be modulated by selectively choosing the polymers. The overall properties of the hybrid scaffold will also be novel (Torricelli et al., 2014). In one study grafts were fabricated from co-electrospinning PCL, gelatin and polyvinyl alcohol and then immobilising with heparin. The graft exhibited high cell infiltration and *in vivo* results showed enhanced endothelial cell proliferation and was antithrombogenic (Han et al., 2011). In another study, grafts were fabricated by co-electrospun composite of PCL/Polyurethane and was implanted in rat and sheep models. There was no evidence of aneurysm, thrombogenesis and intimal hyperplasia (Pan et al., 2017). Once a suitable biomaterial is identified and fabricated into tubular structures, cellularising the biomaterial is expected to enhance the success rate of tissue engineered small diameter vascular graft.

## 2.4 CELL SOURCE AND VASCULAR REGENERATION

A cellularised vascular graft usually demonstrated better functional behaviour in terms of patency and regeneration *in vivo*. Taking into consideration of the different types of cells of blood vessels – Perivascular cells like smooth muscle cell, pericytes and adventitial cell and endothelial cells, various strategies were employed to cellullarise the graft. Different cell source, types and combinations were actively investigated for optimal performance of graft. Among the cells, endothelial cell lining is the direct blood contacting surface and well-established endothelium is a sign of graft regeneration and thereby success of the graft. A smooth EC luminal lining is not the only requirement to recapitulate the structural and physiological features of native vessel. Sources of endothelial cells for vascular tissue engineering include umbilical vein, saphenous or radial vein, adipose tissue microvascular and blood progenitors. Vascular graft regeneration can be achieved through many strategies like seeding endothelial cells on to grafts prior to implantation, modifying the surface chemistry of grafts to capture circulating endothelial cells or progenitors, perivascular cell based niche creation and endothelisation (Zou et al., 2016).The perivascular cells and especially smooth muscle cells maintain the functionality of the graft. These cells are an excellent choice for repopulating blood vessel graft due to same anatomical location, improve vessel stability by maintaining the blood pressure, increased elastin secretion which maintains the vessel mechanics, and decreased leakage. Moreover, perivascular cells and endothelial crosstalk through the release of small molecules is so crucial in maintaining mature phenotypes of both these cells. This helps in increased maturation, proliferation and migration of endothelial cells on the graft (Avolio et al., 2017). Perivascular cells thus help in maintaining a suitable niche for endothelial cell survival and/or helps in homing of endothelial cell to graft during *in vivo* implantation, Figure: 2.4.

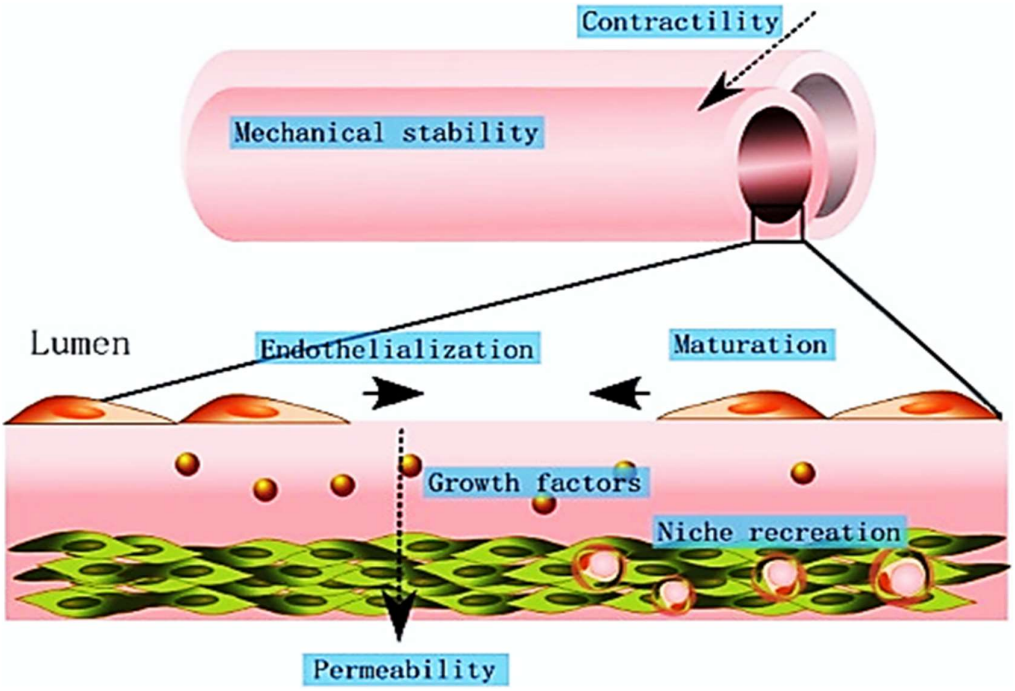


**Figure 2.4: Tissue engineered vascular graft and role of perivascular cells (Adapted from Avolio *et al*, 2017).**

The role of smooth muscle cells in generation of tissue engineered vascular grafts is much appreciated in many studies. A recent study indicated that an electrospun gelatin/PCL scaffold loaded with TGF-β2 helps in modulation of SMC migration and maturation for vascular tissue engineering (Ardila et al., 2019). In another study, tecophilic based scaffold was coated with fibronectin and gelatin, in which gelatin adsorbed graft showed decreased proliferation of smooth muscle cells (Vatankhah et al., 2017). Stiffness based aligned electrospun fibers of poly (l-lactide-co-caprolactone)/poly (l-lactic acid) in shell-core tubular graft promoted contractile phenotype of smooth muscle cells. The matrix rigidity influences the phenotype of smooth muscle cells (Yi et al., 2019) and contractile phenotype is always preferred. Smooth muscle cells express different markers and exhibit phenotypic plasticity. In mature vessel, the SMCs are quiescent, contractile in nature and produces elastin, Figure: 2.5 (Rzucidlo et al., 2007).

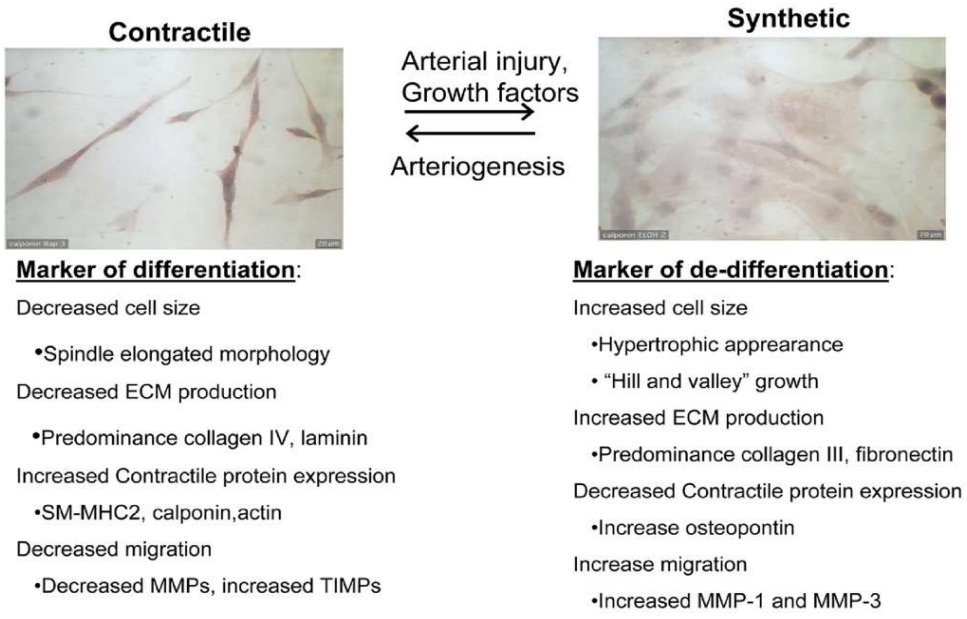


**Figure 2.5 Phenotypic plasticity of smooth muscle cells and major characteristics (Adapted from Rzucidlo et al, 2007)**

Pericytes are another important perivascular cell that interacts directly with endothelial cells in capillary and helps the formation of vaso vasorum of blood vessels. These cells show progenitor cell characteristics with restricted proliferation which thereby reduces the risk of tumorigenesis. Even though their use as cell for vascular graft fabrication-based studies are limited, pericyte based grafts are impressive investigational route for vascular graft regeneration. In a study human pericyte seeded PEUU scaffold when implanted in rats showed excellent regeneration of graft (He et al., 2010). It is reported that pericytes regulate endothelial cell maintenance in terms of proliferation, migration and maturation by secreting a plethora of growth factors. Such events in vascular graft scenario has direct effect on graft remodeling (Chen Yikuan et al., 2013). There is also immunomodulatory effect for pericytes which helps in graft regeneration. In another study, saphenous vein pericytes were seeded on to peptide functionalized PCL grafts. This was co-cultured with endothelial cells and was observed that scaffold with pericytes enhanced endothelial cell density and pro-angiogenic growth factor retention on the scaffold (Campagnolo et al., 2016). Adventitial cells also show stem cell nature and has potential to contribute to blood vessel regeneration. In a study, adventitial stem

cells which were seeded on mouse vein graft showed excellent neointima formation (Chen Yikuan et al., 2013).

Despite of the advantage of terminal vascular cells for blood vessel engineering, there is no suitable source to obtain these cells. The extraction of these cells from blood vessels is usually associated with donor site morbidity. Also, the number of cells obtained is very less from autologous vessels so that it increases time for expansion in culture. These disadvantages have led to the investigation of suitable cell source and various stem cell sources are explored for generation of vascular graft (Zou et al., 2016). Among the various sources, adipose tissue derived stem cell has been a suitable source for isolation of adult stem cells. Like any other stem cells, adipose derived stem cells show fibroblast morphology, multipotent and proliferation capacity. Also, isolation of these cells is associated with less ethical liabilities. The basis of autologous cell-based tissue engineering or personalized tissue engineering is the ability of adipose derived stem cells to provide optimal performance when seeded on scaffolds (Gimble Jeffrey M. et al., 2007). The adipose tissue can be extracted from patients with lesser discomfort so as to isolate cells from them. The microvasculature of the adipose tissue is also a source of perivascular cells and endothelial cells, Figure: 2.6 (Lerman et al., 2016; Pashneh-Tala et al., 2016).

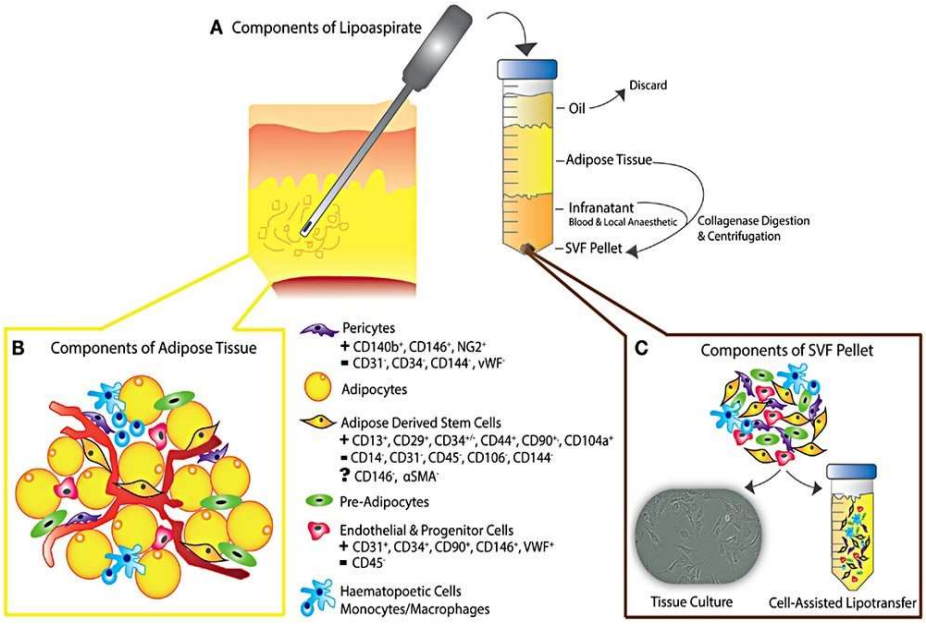


**Figure 2.6: Isolation of adipose derived stem cell showing the different cell types isolated (Adapted from Dold et al., 2012)**

Adipose derived stem cells can be differentiated to smooth muscle and endothelial cell lineage. The differentiation of adipose stem cells to smooth muscle cells is facilitated by growth factors like bone morphogenetic protein, Transforming growth factor beta, thrombin, Sphingosine phosphate, Figure:2.7 (Guo and Chen, 2012a).

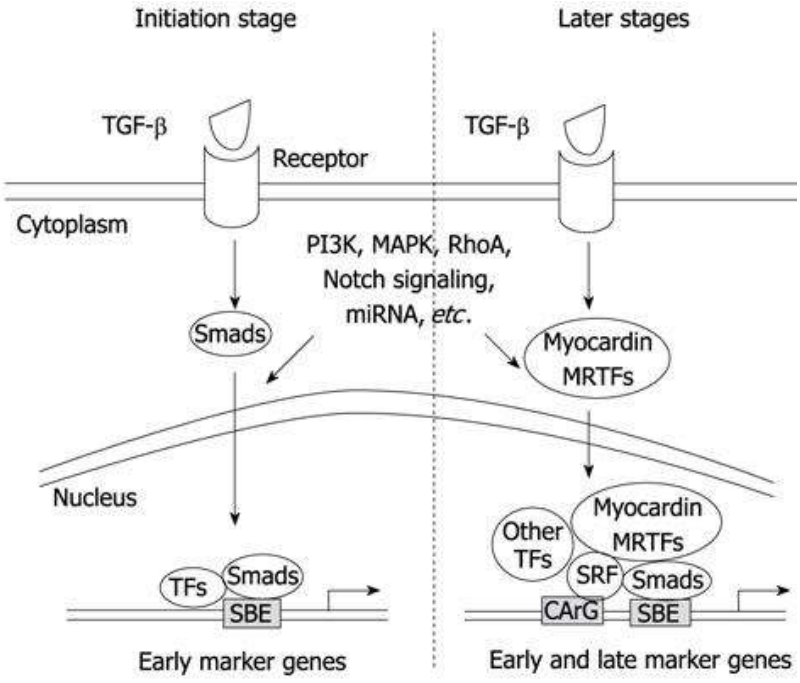


**Figure 2.7 Differentiation of smooth muscle cells from stem cells -TGF-β Signaling (Adapted from Guo, 2012)**

## 2.5 ANIMAL MODELS FOR EVALUATION OF VASCULAR GRAFT

Prior to the clinical application of small diameter vascular graft, it is necessary to test its efficacy in a suitable animal model. Even though different animal models are available, defining a single model most suitable for application of graft is not possible. Different aspects of grafts including thrombogenicity, physiological dynamics withstanding ability, mechanical compliance, regeneration ability, implantability, cost-

effectiveness, animal availability has to be kept in mind before considering an animal model. Also, as part of surgical implantation conditions like handling of animal, ease of surgical performance, suitable sites for implantation and monitoring techniques like angiographical evaluation should be feasible.

Among smaller animal models, rats and mice are used despite of their unmatched circulatory profile with that of humans. In most cases, diameter less than 2mm was evaluated in rat models. In one study, macro-porous PCL grafts showed regeneration when implanted in rat abdominal artery for long-term (Wu et al., 2018). Another long-term study was conducted replacing the abdominal aorta of rat PCL based graft with aligned fibers seeded with smooth muscle cells. The graft showed no thrombosis or aneurysm (Li et al., 2018). Rabbit models allows the implantation of 1-4mm diameter grafts. It has blood vessel physiology and thrombogenicity mechanisms comparable to humans however only limited short term studies could be performed in these animals. In one recent study, intestinal mucosa graft (2mm) were coated with heparin and implanted in rabbit carotid artery for two months. Among the different groups, several grafts were patent but not all (Fang et al., 2019). A composite graft of PCL/gelatin fabricated by coaxial electrospinning were implanted as carotid inter position for three months. The graft exhibited anti-thrombogenicity and patency however cell infiltration was minimal (Johnson et al., 2019). In another study, poly (l-lactide-co-caprolactone) grafts were implanted in common carotids of rabbit. After six months, the grafts were patent with endothelial regeneration. However, several grafts failed to be patent due to high degradation rate of the polymeric material (Horakova et al., 2018).

In the case of large animal models like canine, pigs and sheep multiple implantation sites are available. In canine subjects there is reported to be a lack of endothelization which is observed in two other models. Canine thrombogenicity and inflammatory mechanisms differs from humans. Pigs, on the other hand has similar vascular physiology. But immune response and rapid animal maturation leads to unambiguous data. Sheep on the other hand has cardiovascular similarity and thrombogenesis matching to that of humans. Endothelization is also observed to be similar to humans. In one study, polyester was coated with collagen to make a graft which was implanted in sheep carotid artery as bilateral bypass for 161 days. The patency rate

was 92 %. There were localized thrombi. Microscopic observation showed appreciable regeneration and slight narrowing of the lumen (Grus et al., 2018). In another study bone marrow stromal cells were seeded on multilayered graft fabricated by electrospinning of collagen-chitosan with heparin encapsulation. The graft after implantation showed pulsatile blood flow for one month. The diameter was changing at anastomosis and there was slight intimal hyperplasia. Endothelization was poor in acellular graft and the study concluded the relevance of stem cells on polymeric graft enhance regeneration (Madhavan et al., 2018). In a study, a porous graft of polyester based on the self-complementary ureido-pyrimidinone (UPy) quadruple hydrogen-bonding motif absorbable graft was implanted in pulmonary artery for one year. The graft possesses 92 % patency with remodelling and enhanced burst pressure (Brugmans et al., 2019). Despite several studies and few progressing clinical trials, active research is ongoing in the field of small diameter vascular graft generation by tissue engineering for identifying the best options.

# CHAPTER 3
# MATERIAL AND METHODS

## 3. SECTION I – SCAFFOLD FABRICATION AND CHARACTERISATION

### 3.1 PART I – SYNTHESIS, FABRICATION AND CHARACTERISATION OF GELATIN-VINYL ACETATE/POLY-ε-CAPROLACTONE SCAFFOLD

#### 3.1.1 SYNTHESIS OF GELATIN- VINYL ACETATE (GV)

The gelatin-vinyl acetate co-polymer was synthesized according to previously published protocol (Thomas and Nair, 2013). Briefly, Gelatin from Porcine skin (Type A, bloom value 300, Sigma-Aldrich, USA) was dissolved in de-ionized water purged with nitrogen gas at $40^0$C. After the complete dissolution of gelatin, vinyl acetate monomer (Sigma- Aldrich, USA) was added at a weight ratio of 71.5:28.5 with constant stirring at 300 rpm. The free radical co-polymerization was initiated by adding 0.1 % (w/w) of N, N'- azo bis iso butyronitrile (AIBN). The reaction was carried out at $60^0$ C in an inert nitrogen atmosphere with constant stirring at 300 rpm for 4 hours. The synthesized polymer, after cooling, was precipitated with excess volume of acetone and air dried for 24 hours. The precipitated polymer was then subjected to methanol based soxhlet extraction for removing homopolymer for 21 cycles. The graft ratio and grafting efficiency were calculated as given below:

Graft ratio = (Weight if co-polymer / Weight of gelatin) ……Equation 1

Grafting efficiency (%) = [(Weight of co-polymer before extraction) - (weight of co-polymer after extraction) / (Weight of co-polymer before extraction)…….....Equation 2

### 3.1.2 CHARACTERISATION OF GELATIN-VINYL ACETATE

#### 3.1.2.1 FOURIER TRANSFORM -INFRARED SPECTROSCOPY

The polymer was characterized by following methods, the FT-IR spectra of equal weight of samples were collected on Bruker Alpha spectrometer, USA fitted with diamond ATR accessory, at room temperature with a scan range of 4000-500$cm^{-1}$and processed with Opus software.

#### 3.1.2.2 TNBS ASSAY

The percentage of free amine group in gelatin before and after polymerization with vinyl acetate was determined using 2, 4, 6-trinitrobenzenesulfonic acid (TNBS) (Sigma- Aldrich, USA). Each sample, 5 mg of finely powdered gelatin-vinyl acetate and gelatin, was treated with equal volumes of $NaHCO_3$ (Avra, India) solution, 4 % (w/v) and 0.05 % (w/v) TNBS solution freshly prepared for 3 h at $40^0$C. To this thrice the volume of 6N HCl was added and hydrolysed for 30 minutes at $60^0$C. The calibration curve was deduced from glycine (Sigma-Aldrich, USA) standards prepared in $NaHCO_3$ concentration range from 1mg $ml^{-1}$ to 25 mg $ml^{-1}$. TNBS blanks were set and subtracted from sample values. The optical density of the solution was read at 349 nm in ASYS 340m, UK micro plate spectrophotometer. The experiments were done in triplicate.

#### 3.1.2.3 GEL PERMEATION CHROMATOGRAPHY

Weight average molecular weight distribution of polymer synthesized were obtained by gel permeation chromatography (GPC, Waters GPC systems, USA). Ultra-hydrogel column 2000/ 1000/ 500 were connected in series and mobile phase used was 0.5 M sodium acetate/acetic acid buffer (Merck, USA). Flow rate was 1 ml/minute and sample injection volume were 20 µl (Rheodyne injector, 1 mg $ml^{-1}$). The refractive index detector 2414 was used to detect the sample. Relative calibration standards were dextran standards (Mp: 900000, 48600) and Polyethylene Glycol (Mp: 400).

### 3.1.3 FABRICATION OF GELATIN-VINYL ACETATE/ POLY-ε-CAPROLACTONE SCAFFOLD

#### 3.1.3.1 DUAL SOURCE CO-ELECTROSPINNING OF POLYMERIC SOLUTIONS-STANDARDISATION OF ELECTROSPINNING

In order to incorporate the properties two polymers in a single scaffold, dual source co-electrospinning technique was employed. In this technique fabrication of scaffold was performed by electrospinning two polymeric solutions – Gelatin-vinyl acetate and Poly-ε-caprolactone (PCL), simultaneously on to a single collector. The electrospinning apparatus consisted of a high-voltage power supply that can provide as much as 40 kV, with two electrodes, syringe pumps, and a collector (Holmarc, India). Gelatin-vinyl acetate, 15 % (w/v) was dissolved in solvent system glacial acetic acid: ethyl acetate: water (4:4:2, Merck, USA) and PCL (20 %, Mw: 70,000 to 90,000, Sigma Aldrich, USA) in chloroform: methanol solvent system (7:3, Merck, USA). The solution were loaded into two separate syringes (BD bioscience, India, 10 mL, 21G) and mounted onto two separate syringe pumps. The pumps were placed at the opposite poles of the rotating steel mandrel, which acted as a collector. The collector was rotated at rate of 2000 rpm and had an external diameter of 3 mm (Rabbit implantation studies). For initial standardisation of electrospinning conditions, 3 mm collector were used. Collector of 5mm were used in order to prepare grafts suitable for sheep implantation studies. Different parameters were standardised based on electrospin-ability of solutions, smooth fibre generation and easy retrieve ability of scaffold from mandrel. The scaffold combination were altered based on flow rate of gelatin-vinyl acetate solution. The voltage applied across the electrospinning system was standardised to 10.5 kV. The temperature at which electrospinning was carried out was at room temperature ($<25^0$C), Table: 3.1.

| PARAMETER | GV (15%) | PCL (15%) |
|---|---|---|
| Solvent | Glacial acetic acid : Water : Ethyl acetate (4:2:4) | Chloroform: methanol (7:3) |
| Syringe | 21G | 21G |
| Flow rate | 1-3 ml/hour | 1 ml/hour |
| Tip to collector distance | 10 cm | 8 cm |
| Mandrel speed | 2000 rpm | 2000 rpm |
| Voltage | 10.5 kV | 10.5 kV |

**Table 3.1: Summary of electrospinning parameters**

The flow rate of gelatin-vinyl acetate was optimised between 1- 3 ml per hour, based on production of stable polymeric jet and smooth bead-less fibre production. The PCL flow rate was kept constant at 1ml per hour. The codes were assigned based on this, Table: 3.2. The retrieved scaffold from mandrel was then allowed to air dry at room temperature for 24 hours. The gelatin-vinyl acetate and PCL alone scaffolds were also fabricated with same flow rate as that of hybrid scaffold but with voltage of 13 kV and 8 kV respectively.

| SAMPLE CODE | GELATIN-VINYL ACETATE (G) Flow rate (ml/hour) | PCL (P) Flow rate (ml/hour) | THEORETICAL RATIO (G:P) |
|---|---|---|---|
| G1P1 | 1 | 1 | 50:50 |
| G2P1 | 2 | 1 | 67:33 |
| G3P1 | 3 | 1 | 75:25 |

**Table 3.2: Combinations of the scaffold fabricated**

### 3.1.3.2 CROSSLINKING

The tubular scaffold was washed in sterile ice-cold Phosphate Buffered Saline (Gibco, Fischer Scientific, UK) twice and then treated with 0.5% (v/v) glutaraladehyde (Laboratory rasayan, India) in PBS for 24 hours at room temperature. After the treatment, scaffold was then quenched with 0.1 M Glycine (Sigma-Aldrich, USA) buffered saline for one hour. Further, scaffold was washed in several changes of deionized water and then in 70 % ethanol. Excess solvent was removed by blotting and overnight air drying. For sterilization scaffolds were UV treated and stored aseptically for all cell culture-based studies.

## 3.1.4 CHARACTERISATION OF ELECTROSPUN SCAFFOLD

### 3.1.4.1 TNBS ASSAY - DETERMINATION OF PERCENTAGE GELATIN-VINYL ACETATE IN DUAL ELECTROSPUN SCAFFOLD

The percentage of total gelatin-vinyl acetate present in the dual source co-electrospun scaffold (Uncross-linked) was determined by using TNBS assay. 3mg of scaffold (n=3) was finally minced in to powder like pieces and extracted with $NaHCO_3$ solution containing TNBS. The percentage amine group was estimated against standard calibration plot of glycine. Experimental ratio of gelatin-vinyl acetate to PCL were compared with theoretical ratio.

### 3.1.4.2 FOURIER TRANSFORM INFRARED (FT-IR) SPECTROSCOPY

For chemical group analysis of co-electrospun scaffold, Fourier transform infrared (FTIR) spectra (in ATR mode) of scaffold combinations - G1P1, G2P1,G3P1, PCL were taken using Thermo Nicolet 5700 spectrometer with Diamond ATR Accessory DTGS (Deuterated triglycine sulfate) detector, USA. The scan number was approximately 50 with a resolution of 4 in reflectance mode. The spectra were taken in the frequency range of 4000–400 $cm^{-1}$. The spectra was read using Omnic software and further analysed.

### 3.1.4.3 FIBER MORPHOLOGY ANALYSIS BY SCANNING ELECTRON MICROSCOPE

The microstructure of the scaffold was characterized using scanning electron microscopy (SEM). The tubular electrospun scaffold combinations- G1P1, G3P1, G3P1 were sputter-coated with gold and examined with SEM (JEOL JSM 6390LV, Japan) operated at 15 kV under high vacuum mode. The average fibre diameter was inferred from SEM images using Image J (NIH, USA) software by analysing approximately 25 random fibres from images.

### 3.1.4.4 WATER CONTACT ANGLE

Surface wet ability of G1P1, G2P1, G3P1, GV, PCL scaffold (n=3) were characterized with water contact angle measurement by sessile drop method. 2µL drops of Milli Q purified water placed in Hamilton syringe, were captured on to surface scaffold cut out pasted on to glass slides. The images of the droplet on the scaffolds were visualized through the image analyser (OCA15 plus, Optical Contact Angle System; Data Physics, Germany). Water contact angle of the drops were calculated using SCA 20 software.

### 3.1.5 FABRICATION OF TUBULAR SCAFFOLD FOR VASCULAR GRAFT

The basis of personalised vascular tissue engineering scenario, fabrication of graft that matched the recipient blood vessel dimension is very crucial. Taking this to consideration, for implanting the vascular graft in rabbit and sheep animal models, dimensions of carotid artery of these animals (rabbit internal diameter: 3 mm and sheep internal diameter 5 – 6 mm) were used to fabricate graft. Accordingly rotating mandrel of 3 mm and 5 mm external diameter were chosen for electrospinning. The parameters of dual source co-electrospinning were same as standardised.

Among the different combinations a flow rate of 3 ml/hour gelatin-vinyl acetate and 1 ml/hour PCL (G3P1) were chosen for further fabrication of graft based on physico-chemical properties. Theoretical weight ratio of gelatin-vinyl acetate/PCL were fixed as 75:25 based on individual polymer feed rate (G3P1) which allows incorporation of maximum amount of natural polymer making it cell friendly.

#### 3.1.5.1 MORPHOLOGY OF TUBULAR SCAFFOLD

Gross morphology of tubular scaffold- G3P1 – 3 mm and G3P1 – 5 mm were analysed for its diameter, length, thickness ( Baker thickness micrometre gauge, India), colour and texture. The microstructure of the scaffold sections were analysed under Scanning electron microscope (JOEL, Japan) and from the images random fibers (n=25) were selected to investigate the fibre diameter using Image J software (NIH, USA).

#### 3.1.5.2 POROSITY ANALYSIS

For evaluating the pore size, a portion of tubular scaffold, G3P1 - 3 mm and 5 mm, was cut into 0.5 mm width and 1 cm length. The porous nature was evaluated and imaged using high-resolution Micro-Computed Tomography ($\mu$-CT-40, Scanco Medical, Switzerland). A 3D image was generated exhibiting the porous structure and density. From this the average pore size, pore volume and percentage porosity was determined.

### 3.1.5.3 MEDIA UPTAKE ABILITY

Pre-weighed scaffolds - G3P1 – 3 mm, G3P1 - 5 mm, GV, PCL of dimension of 0.5 cm x1 cm (n=6), were immersed in PBS pH 7.4 in pre weighed containers for known intervals of time. The medium was carefully withdrawn at intervals and excess was blot dried. The wet weight of scaffold was measured at different intervals until the weight equilibrated with time. Percentage swelling was calculated using the following formula.

Swelling percentage = [(final weight-initial weight) X 100] / Initial weight...Equation 3

### 3.1.5.4 DEGRADATION ASSAY

An *in vitro* degradation assay profile of the materials - G3P1 – 3 mm, G3P1 – 5 mm, GV and PCL was determined by immersing the samples in phosphate-buffered saline (PBS) and measuring mass loss with respect to time. The samples were incubated in PBS with 0.1% sodium azide (Sigma-Aldrich, USA) at $37^0$C for 3 months (n=6). The respective samples after each week were removed and dried in oven. The mass loss was calculated by comparing the initial mass (W0) with that at a given time point (Wt).

Mass loss (%) = [(W0 -Wt) / W0] x 100……Equation 4

### 3.1.5.5 MECHANICAL PROPERTIES OF ELECTROSPUN GRAFTS

**Thickness measurement**: The electrospun grafts - G3P1 – 3 mm, G3P1 – 5 mm were cut opened in order to obtain flat sheets. From this 0.5 cm X 0.5 cm square sample cut outs were made to measure the thickness. Each sample were mounted onto Thickness gauge (Baker gauge, India) and thickness were measured (n=6).

**Uniaxial tensile testing**: Blood vessels experience stretch – relaxation cycles both axially and circumferentially. The electrospun tubular scaffolds - G3P1 – 3 mm, G3P1 – 5 mm (n=4) were subjected to mechanical strength analysis using Uniaxial Tensile system (Instron, USA). For axial stretching, 3 cm long scaffold were clamped between the heads of the machine with a study distance of 1.5 cm. The rate of displacement was 5mm/min with force of 100 N. Circumferential tension of gelatin vinyl acetate and PCL

tubes were also analysed. For transverse tensile testing of the tubular graft, 5 mm length, ring samples were cut and fixed between the heads using polyester suture of size 0. For both tests, samples were equilibrated in phosphate buffered saline for $37^0$ C for 10 minutes before beginning of the tests. A displacement rate of 5mm/min and load cell of 100 N were used.

**Burst Pressure**: Theoretically, burst pressure of electrospun scaffold tubes was calculated from tensile strength maximum, by the Laplace law rearrangement considering the tube as thin-walled hollow cylinder under pressure effects; the equation for theoretical estimation of burst pressure is as follows (Gauvin et al., 2011):

Burst Pressure $_{estimated}$ = 2 ([Maximum Tensile strength X Wall thickness]/Internal vessel diameter) ……...…Equation 5

**Suture retention force**: The suture retention force of the electrospun G3P1 tubes were measured according to ISO 7198:2016 Cardiovascular implants and extracorporeal systems -- Vascular prostheses -- Tubular vascular grafts and vascular patches. The 3 cm long scaffolds were pre-equilibrated in PBS bath set at $37^0$ C for 10 minutes. One side of the tubular is clamped into the fixed head of the tensile machine. The other end of the scaffold was pierced with 6/0 prolene suture (Ethicon, India) 2mm down the end and the sutures were clamped in between the movable head of the machine. The movable head was displaced at a rate of 150 mm/minute until the tube slit. The maximum force attained before tearing was recorded (n=3).

## 3.2 PART II - SYNTHESIS, FABRICATION AND CHARACTERISATION OF POLY (ETHYL METHACRYLATE-CO-DI ETHYL AMINO ETHYL ACRYLATE) SCAFFOLD

### 3.2.1 SYNTHESIS OF POLY (ETHYL METHACRYLATE-CO-DI ETHYL AMINO ETHYL ACRYLATE)

Poly (ethyl methacrylate-co-di ethyl amino ethyl acrylate), 8g7 was synthesized by free radical polymerization of ethyl methacrylate (EMA, Sigma-Aldrich, UK) and 2-

(diethyl amino) ethyl acrylate ( DEAEA, Sigma-Aldrich, UK).The polymerization is initiated by using 2, 2'-azobis (2-methylpropionitrile) (AIBN, Sigma-Aldrich, UK).The inhibitors from monomers were removed using acidic alumina column (Sigma-Aldrich, UK). The polymerization was carried under inert nitrogen atmosphere overnight under constant stirring. The reaction conditions were represented in the given in the Table: 3.3.

After termination of reaction, the synthesized polymer was precipitated in a poor solvent hexane with constant stirring in order to obtain solid- rubbery polymer. The polymer obtained was washed in several changes of hexane and dried for four hours at $40^0$C inside the vacuum oven (Pernagallo et al., 2012).

| Polymer | Monomer (moles) | Monomer ratio (mol %) | Initiator (grams) | Solvent (Volume %) |
|---|---|---|---|---|
| 8g7 | EMA: 0.216<br>DEAEA: 0.0915 | 70/30 | 0.062 | Toluene (50) |

**Table 3.3: Reaction conditions for synthesis of Poly (ethyl methacrylate-co-di ethyl amino ethyl acrylate), 8g7**

### 3.2.1.1 DETERMINATION OF MOLECULAR WEIGHT OF POLY (ETHYL METHACRYLATE-CO-DI ETHYL AMINO ETHYL ACRYLATE) BY GEL PERMEATION CHROMATOGRAPHY

Approximately 1 - 3 mg/ml of the synthesized polymer is dissolved in GPC grade N-dimethyl formamide (DMF, Fischer scientific, UK) and filtered using 0.44 µm filter into GPC vials. The eluent used was DMF (flow rate: 1ml/min) and GPC was carried out on PLgel Mixed-C columns (5 µm, 300 X 7.5 mm) for 2 hours at $60^0$ C. The GPC system was calibrated using polystyrene standards. The molecular weight and poly dispersity of different batches of synthesized polymer were collected using the data analysis software of Agilent GPC system, UK).

### 3.2.1.2 FOURIER-TRANSFORM INFRARED SPECTROSCOPY (FT-IR) OF POLY (ETHYL METHACRYLATE-CO-DI ETHYL AMINO ETHYL ACRYLATE)

The chemical signature characterization of the synthesized polymer was confirmed by FT-IR spectroscopy (Bruker Tensor 27 spectrophotometer, USA) of the polymer. The peaks were obtained by IR analysis of the polymer using OPUS software.

### 3.2.2 FABRICATION OF POLY (ETHYL METHACRYLATE-CO-DI ETHYL AMINO ETHYL ACRYLATE) TUBULAR SCAFFOLD BY ELECTROSPINNING AND CHARACTERISATION

The process of electrospinning of the polymer has to be standardized for obtaining a smooth bead free fibres. The initial standardization of each parameter was done on electrospinning onto flat stationary collector and further progression was carried out after microscopic confirmation of collected fibres. The electrospinning set up consisted of high voltage system and syringe pump with grounded collector (Spray base electrospinning, Ireland). A wide range of solvents were screened for the solubility of the polymers from 30 - 80% (w/v). The solvents include ethanol (Merck, UK), methanol (Merck, UK), chloroform (Merck, UK), chloroform : methanol (7:3), N-dimethyl formamide (DMF), Tetrahydrofuran (THF), Dimethyl formamide : chloroform (1:1) Dimethyl formamide : Tetrahydrofuran (1:9 to 9:1). Various solutions in different solutions were analysed for ease of solubility, days required for complete dissolution of the polymer and electrospinning ability with stable jet formation. Similar to this the effect of different voltage and flow rate on fibre deposition and fibre morphology were also standardized. After standardization on flat collector, the parameters were then tested on to tubular rotating collector with mandrel diameter of 5 mm and speed of 2000 rpm. The tip to collector distance was 15 cm and solution was loaded in to 5 ml luer lock syringes fitted with tube and 21G blunt needle (Braun, UK). The mandrel was coated with 7% (w/v) polyvinyl pyrrolidone (Sigma-Aldrich, UK) dissolved in 70% ethanol. The tubes were retrieved by immersing the mandrel in water.

#### 3.2.2.1 SCANNING ELECTRON MICROSCOPY

The ultra-structure of fibre mats produced during standardization of electrospinning parameters and tubular scaffold were investigated by SEM imaging. The air dried electrospun mats and/or scaffolds were affixed on aluminium stubs with carbon tabs and subjected to sputter coating with gold palladium (20 nm). Different areas on both sides of the specimen were scanned under SEM (Carl Zeiss SIGMA HD VP Field Emission SEM Electron Source: Schottky thermal field emitter, Accelerating voltage range: 0.02 to 30 kV, Resolution: 1.9nm at 1 kV, 1 nm at 15 kV, UK).The thickness of the walls of the tubular scaffold were also measured by using specific stub for mounting specimen sideways. The SEM images were investigated using image J (NIH, Image processing software) for fibre diameter calculation by selecting randomly 25 fibres from images (n=3).

#### 3.2.2.2 WATER CONTACT ANGLE

The wet ability of scaffold was analysed using water contact angle (Kraus DS30drop shape analyser, USA). Scaffold sections from tubes were out in the dimension of 5 cm X 0.5 cm and fixed on surface of clean glass slide.18G Hamilton syringe with ultra-pure water was loaded to pendant drop tensiometer and air-water contact angle images were captured at time points like zero second and one minute.

#### 3.2.2.3 WATER UPTAKE ABILITY OF TUBULAR SCAFFOLD

The water or media uptake ability of the scaffold is crucial as the scaffold should be conducive for cell adhesion and proliferation. In order to access the water uptake ability of scaffold, pre-weighed scaffold samples are immersed in Phosphate buffered saline (pH: 7.4) at different time points ranging from one minute to 1 hour. The percentage swelling of the scaffold is calculated as mention above (Equation 3)

### 3.2.2.4 MICRO-CT ANALYSIS OF TUBULAR SCAFFOLD – POROUS NATURE

Porous nature of the scaffold is extremely crucial in terms of cell interaction with scaffold and mechanical properties of the scaffold. Micro-Computed Tomography (Micro-CT, Siemens Health care, USA) provides an option for non-destructive evaluation of scaffold architecture three dimensionally. In order to analyse the porous nature of the electrospun scaffold, 1 cm long scaffold were used. The scaffold was mounted on to custom made holder and examined for its porous structure. The samples (n = 4) were scanned by rotating with respect to X-ray source along various axes and tomographic algorithm-based image slices were generated. These images were reconstructed using the system software. A bin frequency value was created from the 3D reconstruction. The average porosity (Pore volume/specimen volume X 100 %) and pore size (mean pore diameter) were then calculated. The interconnectivity of the pores was also observed from the image generated.

### 3.2.2.5 MECHANICAL PROPERTIES OF TUBULAR SCAFFOLD

The mechanical characterization of a tubular scaffold that is intended to be used as a blood vessel replacement is extremely relevant. In general, the blood vessel experiences hemodynamic forces along its long axis and circumferentially that is around the axes. The blood pumped from heart is forced to move further due to this spatiotemporal attributed by the cell and matrix arrangement. In order to mechanically characterize the fabricated scaffold, it was subjected to mechanical tensile strength-based measurement (Universal tensile machine, Instron, USA). For the measurement of longitudinal tensile strength, scaffold of 3 cm X 0.5 cm rectangular tube cut out was clamped between the heads of tensile machine. A 50 N load cell value was used to pull one head of the machine at a rate of 0.5 mm/minute. The thickness of the scaffold sample was noted before each measurement with Vernier calliper (n = 6). The distance between clamp head before stretching is also adjusted to 1 cm. The scaffolds were stretched until there was fracture. The load and displacement were inferred from the software generated curve (Blue hill). Similar to longitudinal tensile strength, circumferential tensile strength on the ring samples were carried out. 0.5 cm long ring samples of equal wall thickness (n = 6) were mounted between parallel rod-based clamp heads of tensile machine. A 50

N load cell was used to stretch the ring samples until load failure. From the data generated by the software, the ultimate tensile strength, Young's modulus, elongation at break and theoretical burst pressure were calculated as per the equation mentioned in the previous section (Equation 5).

Suture retention force of the scaffold were measured by tensile stretching of the graft sections (n=6) clamped to the machine head by 6-0 prolene sutures. The scaffold samples were initially sutured and ends of the suture were tied on to the clamps. The stretching of the scaffold was performed using load cell of 50 N at mm/minute. The maximum load at failure was noted to be the retention force.

# SECTION II – *IN VITRO* CELL BASED STUDIES

## 3.3 PART I – DIFFERENTIATION OF ADIPOSE DERIVED MESENCHYMAL STEM CELLS TO SMOOTH MUSCLE CELLS ON GELATIN-VINYLACETATE/POLY-ε-CAPROLACTONE SCAFFOLD

### 3.3.1 ISOLATION OF RABBIT ADIPOSE DERIVED MESENCHYMAL STEM CELLS (RAMSCS)

**ETHICAL STATEMENT**

The studies involving animal subjects were conducted as per the ethical guidelines and recommendations concerning the Purpose of Control and Supervision of Experiments on Animals, India and the Institutional Animal Ethics Committee approved form B number: SCT/IAEC-187/JANUARY/2018/89. For conducting stem cell-based research work approval was obtained from Institutional Committee for Stem Cell Research and Therapy under the number: SCT/IC-SCR/21/OCT 2014.

For isolation of subcutaneous adipose tissue from supra-scapular region, New Zealand white rabbits were selected (young adult, either sexes). After anaesthetizing the animal, a 4 cm incision was made in the supra-scapular region. Adipose tissue was surgically isolated and transferred aseptically in Dulbecco's phosphate buffered saline containing 1X antibiotic and antimycotic (Gibco, Thermo Fischer, USA). The tissue is washed in antibiotic containing PBS thrice and minced into small pieces. To this

Collagenase Type II (Gibco, USA) enzyme in the concentration of 0.075 % (w/v) per 2g of initial weight of fat is added in Dulbecco's modified Eagle's Medium High glucose (DMEM-HG) without foetal bovine serum (FBS).The fat tissue pieces is digested in the medium at $37^0$C for 40 minutes and then centrifuged at 2500 rpm for 10 minutes at $4^0$C.The supernatant is removed and pellet containing cells is re suspended in DMEM-HG with 10 % (v/v) FBS (Gibco, USA), 1X AB/AM (Gibco, USA) and plated onto T25 tissue culture grade flask (Nunc, Thermo Fischer Scientific, USA). The flasks were maintained in incubator at $37^0$C with 5% $CO_2$ (Eppendorf, USA). The cells are allowed to attach, and media was changed on every alternate day till confluence. The cells were sub-cultured further using 0.25% Trypsin-EDTA (Gibco, USA). The cell seeding density is fixed at 2 x $10^4$ cells/$cm^2$ of surface area by Trypan blue counting in hemo-cytometer. The morphology of the cells was confirmed by visualizing under phase contrast mode of microscope (Leica Generic, Germany).

### 3.3.1.1 POPULATION DOUBLING TIME

A constant number of cells were plated on to T25 flasks and after 90% confluence, cells were harvested by trypsinisation and counted by Trypan blue dye (Invitrogen, USA) based hemo-cytometer counting. The total time for doubling of mesenchymal stem cells were calculated using the formula:

$$\text{Doubling time} = (T \times \text{Log } 2) / (\text{Log } N_t - \text{Log } N_i) \quad \text{Equation 6}$$

T is the total time period in culture, $N_t$ is the number of cells at time T and $N_i$ is the number of cells initially. The doubling time was calculated from Passage 1 to passage 12. Based on this RAMSCs between the Passage 3 and 6, is only selected for all the further cell culture related experiments.

### 3.3.1.2 MORPHOLOGY OF RAMSCS

The cells were seeded on four well tissue culture plates at a density of 1 X $10^4$ cells/$cm^2$. After reaching 60% confluence, cells are stained for cytoskeletal Actin. Briefly, media is removed from plates and cells are washed gently with PBS twice. The

cells are then fixed with 4% Paraformaldehyde at room temperature for 10 minutes, washed again with PBS. Cells were permeabilised with 50% ice cold methanol (Merck, USA). Phalladoin-Fluorescien iso thiocyanate 488 (Invitrogen, Alexa Fluor 488, USA) were diluted in PBS (1:100) were added to cell monolayer and incubate for 1hour in the dark. The nuclei were counter stained with Hoechst (Sigma-Aldrich, USA). The images were captured by inverted fluorescent microscope with UV filter (Olympus Microsystem BH2, Japan).

### 3.3.1.3 FLOW CYTOMETRY AND IMMUNOFLUORESCENCE STAINING

All procedures followed as per International Society for Cellular Therapy for immune functional assay for mesenchymal stromal cells (Dominici et al., 2006). The mesenchymal stem cell immuno-phenotyping was analysed by Fluorescent assisted cell sorting based on expression of CD markers on cell surface. Cells were grown to confluence in T25 flasks, trypsinised and washed with PBS. Initially cells were fixed with 4% Paraformaldehyde for 10 minutes at room temperature. The cells were then washed and treated with primary unconjugated anti bodies of CD44 (1:100, Abcam, USA), Vimentin (1:100, Abcam, USA) and negative markers CD34/45 (1:50, BD Biosciences, India), incubated for one hour at room temperature. The cells were again washed with PBS and treated with FITC-Conjugated secondary antibodies and incubated for 30 minutes at room temperature. After washing the percentage positivity of cells were analysed by flow cytometry with corresponding isotype controls (BD FACS Cali bur, USA). A minimum of 10,000 cellular events were recorded for each sample. The data obtained was analysed FACS Diva software, USA.

Immunostaining of cells grown in monolayer were also performed. A sub confluent cell layer was washed with PBS and fixed with Paraformaldehyde. The cells were then treated with CD44, CD90 (1:100, Abcam, USA) and CD34/45 antibodies and incubated over night at $4^0$C. The cells are then washed twice with PBS and then treated with FITC-Conjugated secondary antibody (Abcam, 1:50). The cells were then counterstained for nuclei with Hoechst. The images were captured in Olympus microsystem BH2, Japan.

### 3.3.1.4 MULTI-LINEAGE DIFFERENTIATION OF RABBIT MESENCHYMAL STEM CELLS

In order to evaluate the multi-lineage potential of isolated mesenchymal stem cells. The cells were differentiated to adipogenic, osteogenic, chondrogenic lineages by culturing them in respective induction media. Cells were seeded at density of 2 x $10^4$ cells/$cm^2$ in culture plates with adipogenic induction media (DMEM-HG,10% FBS,1X anti biotic-anti mycotic,0.5 µm Isobutyl methyl xanthine, 1 µM dexamethasone, 10 µg/ml Insulin, 200 µM Indomethacin,14 days, Sigma-Aldrich, USA) and osteogenic media (DMEM-HG, 10% FBS, 1X antibiotic-antimycotic, 0.1 µM dexamethasone, 10 mM β-glycerophosphate, 0.2 mM ascorbate-2-phosphate, 21 days). For Chondrogenesis, cell pellet culture method was adopted in 15ml polypropylene tubes by centrifuging 1 x $10^6$ cell per tube. The cell pellet were grown in chondrogenic medium (DMEM-HG, 10% FBS, 1X anti biotic-anti mycotic, 50 µg/ml acorbate-2-phosphate, 100 µg/ml sodium pyruvate, 40 µg/ml Proline, 1.4 mM L-glutamine, 100nM Dexamethasone, 0.1mM non-essential amino acids, 10 ng/ml TGF-β2, 21 days). Cells grown in complete media without additional factors served as the controls. Media were changed every alternate day. After specific time point, Adipogenesis and osteogenesis of the cells were assessed by Oil red O (Sigma-Aldrich, USA) staining for lipid vacuoles and Alizarin red S (Sigma -Aldrich, USA) staining for calcium deposition respectively. The pellet of chondrogenesis is carefully fixed and embedded in tissue freezing media and cryo-sectioned. The sections, 5 µm, were stained with Safranine O for glycosaminoglycans.

### 3.3.2 ISOLATION OF SHEEP ADIPOSE DERIVED MESENCHYMAL STEM CELLS (ShMSCs)

#### ETHICAL STATEMENT

The studies involving animal subjects were conducted as per the ethical guidelines and recommendations concerning the Purpose of Control and Supervision of Experiments on Animals, India and the Institutional Animal Ethics Committee, SCTIMST approved form B number: 71$^{st}$ CPCSEA/25/9/2019 and SCT/IAEC-292/JAUARY/2019/99. For conducting stem cell-based research work approval was

obtained from Institutional Committee for Stem Cell Research and Therapy under the number: SCT/IC-SCR/50/SEPTEMBER/2018

**ANAESTHESIA**

The animals were subjected to whole body general anaesthesia. A combination of Atropine sulphate (0.01 mg/kg body weight), Xylazine (0.3 mg/kg body weight) and Ketamine (7 mg/kg body weight) were used to induce anaesthesia in animals. The sheep were then intubated with a cuffed endotracheal tube (size 9) after administering Propofol bolus (3 mg/kg body weight) intravenously. Ventilation was initiated with a tidal of 10-12 ml/kg body weight to achieve an $EtCO_2$ at 30-35 mm of $H_2O$ under isoflurane maintenance.

**SURGICAL PROCEDURE: ADIPOSE TISSUE COLLECTION**

Under general anaesthesia and standard aseptic precautions, abdominal area was prepared for surgical incision. A 3 cm long incision was made on skin and subcutaneous fat tissue was excised. The tissue was collected in sterile PBS for cell isolation. The surgical wound was closed by suturing with monofilament nylon sutures. The animal was then allowed to recover from anaesthesia. After recovery the animal was monitored daily and wound was dressed routinely. The surgical wound was allowed heal and animal was kept in isolation till then. Later the animal was tagged and housed in general sheep house till implant associated surgery. The subcutaneous adipose tissue collected from sheep was weighed and subjected to Collagenase Type II digestion (Gibco, USA). The protocol adopted was very similar to that used for rabbit mesenchymal stem isolation as mentioned previously. The cells were initially seeded on T25 flasks for propagation. The difference experienced here was cells appeared seven days later to isolation. Population doubling time of the sheep cells were calculated as per the equation 6. For characterisation of cells, the procedures as per International society of stem cell were followed as discussed in previous section similar to rabbit. The difference in case of trilineage differentiation of ShMSCs was in chondrogenic lineage were micro mass culture was adopted. Here, $5 \times 10^5$ cells were spotted in at a single point on tissue culture plate and allowed to grow in chondrogenic media for 21 days. After this, culture was stained with Alician blue stain (Sigma-Aldrich, USA) and photographed.

## 3.4 CELL - MATERIAL INTERACTIONS

### 3.4.1 CYTOTOXICITY STUDIES: DIRECT CONTACT TESTS WITH L929 FIBROBLASTS AND ADIPOSE DERIVED MESENCHYMAL STEM CELLS-RABBIT, SHEEP

The *in vitro* cytotoxicity of UV sterilized scaffold was checked with direct contact of scaffold with mouse fibroblast cells (ISO 10993 - Part 5) and RAMSCs. Briefly, both cells were grown to confluent monolayer in complete media at $37^0$ C, 5% $CO_2$ incubator. Scaffolds in dimension of $1cm^2$ are placed in contact with the cells by carefully placing them on top of the cells. The cells with scaffolds were incubated for 48 hours. After this, cell surrounding the scaffold is examined under phase contrast microscope for response towards the scaffold. The morphological changes, cell death was observed and scored. The nature of the cellular response was compared with positive cytotoxic polyvinyl chloride discs and negative non cytotoxic high-density polyethylene discs.

### 3.4.2 MTT ASSAY

The in direct quantitative evaluation of cytotoxicity of scaffold was assessed by extract method. MTT [3-(4, 5-Dimethylthiazol-2-yl)-2, 5-diphenyltetrazolium bromide, Sigma-Aldrich, USA] assay was performed using isolated RAMSC, ShMSCs and L929 cells. The scaffold extracts of 1 day, 3 days, 7 days and 14 days were collected (3 $cm^2$ /ml of serum free medium). The cells were seeded in 96 well plates and grown till semi-confluence. The medium is then replaced with fresh media consisted of scaffold extract and complete media in ratio of 7:3 (Test media). The L929, RAMSC, ShMSCs cells were incubated in the test media for a period of 24 and 48 hours. As a positive control, DMSO (5 % w/v in PBS) and negative control complete cell culture media was used. After incubation media was removed and cell were gently rinsed out in PBS. 200 µL MTT solution (5 mg/ml in PBS) was added into each well and incubated at $37^0$ C for 4 hours. The MTT solution was then removed and 100µL of DMSO was added in order to dissolve the formazan crystals, incubated for 30 minutes. The optical density was measured at 540 nm (630 nm reference) in plate reader (ASYS Hitech GmBH, 340M, USA). Blanks were also set, and percentage cell viability was calculated as

Percentage Cell viability = [(Absorbance of test) - (Absorbance of blank)/ (Absorbance of control) - (Absorbance of blank)] x 100……Equation 7

The data was compared with controls and untreated group viability was set as 100%. All the values are represented in mean ± standard deviation of experiment triplicates.

### 3.4.3 CELL SEEDING ON TUBULAR SCAFFOLD

Cells were seeded on dry tubular scaffolds at seeding density of 2 x $10^4$ cells/$cm^2$ of external surface area. The total external surface area of the scaffold was calculated using the formula 2πh (R + r); were h is the height of the tube, R is the external radius which includes the thickness of the scaffold and r is internal radius. The cell seeding is done by dividing the total cell suspension in complete media into 100 µl each. On to one side of the scaffold placed in sterile glass petri plate, 10 drops of 10 µl were added length wise and incubated for 30 minutes for cell attachment. Further, the scaffold was rotated again $90^0$ and seeded again. The procedure was repeated four times until the full surface was seeded with cells. The cell seeded scaffold was allowed to float in the media for cellular growth.

### 3.4.4 CELL VIABILITY ASSESSMENT

Viability of RAMSC and ShMSCs cells seeded on tubular scaffolds were assessed by LIVE/DEAD Viability/Cytotoxicity Kit for mammalian cells (L3224, Thermo Fischer, USA). After 3, 7, 14 days of cell growth on scaffold, tubes were cut open and 1$cm^2$ pieces of scaffold was washed carefully with PBS. The procedure for staining was in accordance with manufacture's protocol. Briefly, to prepare the staining solution, 5 µL of Calcein AM (494/517 nm) and 20 µL ethidium homodimer-1 (528/617 nm) was mixed in 10 ml PBS. The solution was added onto cell seeded scaffold and incubated for 15 minutes at $25^0$C. Cytoskeletal organization and spreading of the cells on scaffold on day 14 was visualized by Actin fluorescence by staining with Phalladoin-Alexa Fluor 488 (Invitrogen, USA) after fixing the construct in 4% paraformaldehyde.

After incubation, the constructs were shifted to glass bottom dished in PBS and imaged using confocal laser scanning microscope (Nikon A1Rsi, Japan). The depth profile diagram was also generated from live cell image at day 14 using Nikon software in order to assess the depth of cell penetration into the scaffold.

### 3.4.5 CONFOCAL RAMAN SPECTROSCOPIC STUDIES

RAMSC and ShMSCs seeded G3P1 constructs (Day 3) were subjected to Raman spectroscopic mapping by confocal Raman microscope (Witec Inc. alpha300R, Germany). For the measurements a frequency doubled NdYAG laser: l = 532 nm was used. The excitation light was polarized horizontally (in the x-direction) with respect to the Raman image. All measurements were performed using a SP2300i spectrometer and back illuminated CCD camera DU401A. The cell seeded G3P1 section was investigated using a 20 x Nikon (NA=0.4) objective. The sample was illuminated and focused with top light. The distribution of chemical species on the sample was obtained in Raman spectral imaging mode. In this imaging mode a complete Raman spectrum is recorded (integration time of 0.5s) at every imaging point (120 x 120 points for 50 x 50 $\mu m^2$), leading to a 2D array of Raman spectra. Background subtraction, cosmic ray removal, and averaging a certain region manually, and spectral de-mixing were performed on this 2D array of Raman spectra using Witec Project plus software. The distribution of the Raman spectra over the examined sample area is colour coded based on the characteristic peaks of PCL (blue) and Gelatin-vinyl acetate (yellow), cell cytoplasm(green) and nuclei(red).

## 3.5 DIFFERENTIATION OF MESENCHYMAL STEM CELLS TO SMOOTH MUSCLE CELL ON SCAFFOLD-RABBIT, SHEEP

Rabbit mesenchymal stem cells and Sheep mesenchymal stem cells were subjected to differentiation to smooth muscle cells both on tissue culture polystyrene plates (TCPS) and G3P1 scaffold. The cells were seeded on G3P1 scaffolds as mentioned above and grown in smooth muscle induction media (SMIM) for differentiation. The differentiation media was fixed based on protocols developed by various groups and consisted of two sets of media formulation. The cells after seeding on scaffold and TCPS,

was initially grown for 3 days in normal complete media. On day 3 media was changed into smooth muscle induction media I (SMIM I) consisting DMEM-HG, 3% FBS, IX AB/AM, 10 ng/ml TGF-β1 (Human recombinant, Sigma-Aldrich, USA), 30 μM ascorbic acid-2-phosphate (Sigma-Aldrich, USA), 100 U/ml heparin sodium salt (Sigma-Aldrich, USA) for 7 days. After this again the media composition was changed for another 7 days to smooth muscle induction media II (SMIM II) which was devoid of ascorbic acid and reducing TGF-β1, 5 ng/ml. The media was changed every alternate day.

### 3.5.1 QUANTITATIVE REAL TIME PCR

The expression profile of smooth muscle cell specific genes was quantified by real time PCR reaction. Total RNA was isolated from cells after differentiation using TRizol reagent (Gibco, USA). The concentration and purity of the isolated RNA were analysed using Nano drop spectrophotometer based on absorbance ratio of 260nm/280nm. 1 μg of total RNA was reverse transcribed to cDNA (High capacity cDNA reverse transcription kit, Applied Bio-systems, USA) using random primers and dNTP mix on thermal cycler (Eppendorf Master Cycler, USA) programmed according to manufacturer's protocol.

For real time polymerase chain reaction, 100ng of synthesized cDNA is added into reaction mix containing specific forward and reverse primers. SYBR green master mix (Fast Start Universal SYBR Green Master (ROX), Roche life sciences, Germany) was used to set up the qPCR reaction programme according to the protocol for 40 amplification cycles with an initial activation step at $95^0$ C for 10 minutes (Applied Biosystem Quant Studio 5, USA). The house keeping control was GAPDH and melt curve analysis was done in order to ensure specificity. Fold change was calculated after GAPDH normalization for each set of experiment compared to calibrator without scaffold and induction media, using $2^{-ddCt}$ formula (Schmittgen and Livak, 2008). A minimum of three replicates were done for each group. In the case of differentiation of sheep mesenchymal stem cells to smooth muscle cells, β-Actin was used as the calibration control. The PCR reaction was carried out using the primers, Table: 3.4, and SYBR green master mix (Roche, Germany) according to manufacturer's protocol.

| No | GENE NAME | PRIMER SEQUENCE (FORWARD/REVERSE 5'-3') |
|---|---|---|
| 1 | GAPDH (rabbit) | TCACAATCTTCCAGGAGCCA<br>CACAATGCCGAAGTGGTCGT |
| 2 | TAGLN (sheep/rabbit)<br>(SM22α) | TCACTCCTTGCTGCGAAT<br>GCTCCTCGTCGTACTTCT |
| 3 | CNN3(sheep/rabbit)<br>(Calponin) | AGACCTTCGCAACTGGATT<br>ATGAGTTCGCAGAGGATGAT |
| 4 | Collagen 1A2 (rabbit) | TCTGAAGTCTCTGAACAACCA<br>GTGACCACTGCTCCACTCT |
| 5 | MYH11(sheep/rabbit)<br>(Myosin heavy chain 11) | ACAACTACACATTCCTCTCAAA<br>GCTGCTCCTCTTCACTGA |
| 6 | ACTA2(sheep/rabbit)<br>(Smooth muscle actin) | GTTCCAGCCCTCCTTCAT<br>GAGAGCACATTGTTAGCATAGAG |
| 7 | Elastin(rabbit) | CTTGGAGTTGGTGCTGGT<br>TCCGTATTTCGCTGCCTTA |
| 8 | Collagen type I alpha 2 chain<br>(Sheep) | GCTGGTCAGCCCTGTAGAAG<br>AACATGGTGATCAAGGTGC |
| 9 | Elastin (sheep) | CTTTGGAGTCTGAGAGCACCC<br>CCATCCCTCAAAGTGCTTG |
| 10 | Beta -Actin (Sheep) | CAGTCGGTTGGATCGAGCAT<br>AGAAGGAGGGTGGCTTTTGG |

**Table 3.4: Details of primers used for RT-PCR**

### 3.5.2 IMMUNO-STAINING FOR SMC SPECIFIC MARKERS

Cells after differentiation both on scaffold and TCPS were fixed with 4% paraformaldehyde. The cells were permeabilised 0.05% (v/v) Triton X 100 (Sigma-Aldrich, USA) containing PBS for 10 minutes and blocked with 0.5% (w/v) BSA in PBS. Primary unconjugated antibodies specific to ASMA (Abcam), SM22α (Abcam), and SMMHC (Merck Millipore, USA) were diluted in the ratio of 1:100 in PBS with 2% (w/v) BSA in PBS and incubated overnight at $4^0$C in moist chamber. Secondary

antibodies were added in dilution of 1:50 after washing and incubated at room temperature. The cells are then counter stained with Hoechst (Sigma-Aldrich, USA) and imaged under confocal laser scanning microscope (scaffolds, Nikon A1Rsi, Japan).

### 3.5.3 ESTIMATION OF EXTRACELLULAR MATRIX PROTEINS

The total soluble collagen content of the explant was estimated using Sircol soluble collagen assay kit (Biocolor life sciences assay, UK). Steps were followed according to manufacturer's protocol. Bare G3P1 graft served as blanks for normalizing the value. The collagen standards given in the kit (500 μg/ml of bovine or rat tail collagen type I in 0.5 M acetic acid) were used for plotting the calibration curve. The initial weight of each samples was recorded. Collagen were isolated from tissue samples by using the acid neutralizing agent (0.5 M acetic acid with pepsin) and collagen concentration reagent (Polyethylene glycol with TRIS-HCL buffer pH 7.6). After extraction, the contents were treated with Sircol collagen binding dye. The absorbance was recorded at 555 nm in microplate reader (ASYS plate reader). The concentration of samples (n=4) is elucidated from calibration plot.

For estimation of elastin Fastin Elastin assay kit (Biocolor life science, UK) were employed. According to manufacturer's protocol, elastin in the samples were converted to soluble form of α-elastin by heating the samples with 0.25 M oxalic acid (Laboratory rasayan, India) for 2 hours at $100^0$C. Elastin standards provided were used for plotting calibration curve. The dye used for binding elastin was 5, 10, 15, 20-tetraphenyl-21H, 23H-porphine tetra sulfonate. The absorbance if the samples were measured at 513 nm. The concentration of samples (n=3) were detected from the calibration plot. The expression of extracellular collagen 1 type A 1 and elastin were also analysed by quantitative RT-PCR by protocol described above.

## 3.6 *IN VITRO* HEMOCOMPATIBILITY OF THE SCAFFOLD

Hemocompatibility of fabricated scaffold was analysed in detail as the end application of the scaffold was to be used as tissue engineered vascular graft. All the tests were carried out as per ISO 10993 - 4 based protocols. Human blood was collected from

people with informed consent and by authorized personnel. The blood collection was approved by Institutional Ethics Committee, ECR/189/INST/KL/2013.

### 3.6.1 PERCENTAGE HAEMOLYSIS STUDY

The fabricated scaffold and its effect on lysis of red blood cells on contact with whole blood was analysed through doing haemolysis assay. Blood from human volunteer was collected into containers with Acid citrate dextrose anticoagulant (ACD). Tubular scaffold samples (n=6) of diameter 3 mm and length 1 cm were placed in polystyrene plates containing PBS. The samples were washed by agitation for 5 minutes. After removal of PBS, 1.5 ml of blood was added of which 0.5 ml were drawn out immediately for initial analysis. The remaining blood was agitated with samples at 70 ± 5 rpm for 30 minutes at temperature $35\pm2^0$ C on shaker (Environ Lab-line instruments Inc. USA). As reference, three empty polystyrene tubes were exposed with blood. From the initial blood sample drawn, the total haemoglobin was analysed with an automatic haematology analyser (Symex-K4500). From the 30 minute exposed blood sample, platelet-poor plasma was isolated to access the free haemoglobin released. This was measured for each sample with the help of Diode array Spectrophotometer (Hewlett Packard 8453, Germany). The percentage haemolysis for each sample were calculated by following equation:

Haemolysis (%) = (Free Haemoglobin / Total Haemoglobin) x 100……Equation 8

### 3.6.2 HEMATOLOGY – LEUCOCYTE COUNT, RBC COUNT, PLATELET COUNT AND PLATELET ADHESHION ASSAY

The scaffold samples (n=6) were exposed to whole blood in order to analyze the change in initial and final percentages of leucocytes, RBC and platelet present after exposure. Tubular samples were kept in polystyrene dishes and exposed to 1.5 ml whole blood, 0.5 ml of blood was withdrawn immediately after exposure and rest was agitated with samples at 70 rpm for 30 minutes at $37^0$C in shaker. Polystyrene tubes were used as reference. The blood counts were analysed initially and after 30 minutes exposure to samples using Haematology Analyzer (Symex-K 4500). The equipment calibration was verified with internal quality control. Percentage change of leucocytes, RBC and platelets

were calculated for both initial and final sample and compared with references. Uncertainty of measurement was ± 5%. After treating the scaffold with whole blood for 30 minutes, the scaffold was then washed gently with deionised water twice and fixed with 3.5% glutaraladehyde solution for observation of adhered platelets and RBCs if any under scanning electron microscope (JOEL, Japan).

## 3.7 PART II – CO-CULTURE OF PERIVASCULAR STEM CELLS AND ENDOTHELIAL CELLS ON POLY (ETHYL METHACRYLATE-CO-DI ETHYL AMINO ETHYL ACRYLATE) SCAFFOLD

### 3.7.1 ISOLATION OF HUMAN ADIPOSE DERIVED PERIVASCULAR STEM CELLS AND ENDOTHELIAL CELLS

#### ETHICAL STATEMENT

All procedures for collection and further processing of the adipose tissue samples were performed with permission granted in University of Edinburgh by the South East Scotland Research and Research Ethics Committees. Patient subjects were informed about the tissue collection and written consent was obtained.

The collected tissue is stored in sterile storage containers with PBS (Sigma-Aldrich, UK) constituted with 5% (v/v) Foetal calf serum (FCS, Gibco, UK) at $4^0$ C. The whole fat obtained from abdominoplasty was thoroughly minced into small pieces using a scalpel. The Scarpa's fascial layer was initially removed. The adipose tissue pieces were then combined with PBS (150 ml tissue with 100 ml PBS) and mixed manually for 30s by inverting. 50 ml of the digest was then transferred to 50 ml centrifuge tubes and then centrifuged at 2000 rpm at room temperature for 10 minutes. After centrifugation, the tube will hold a three-phase content of which the middle layer was carefully transferred into a new tube. The upper layer consisted of fat and lower was the blood layer. The middle layer was then mixed with 25 ml of PBS – 2% (v/v) FCS and centrifuged again at 200 rpm for 10 minutes at room temperature. To the stromal vascular fraction (SVF)

pellet, 25 ml digestion solution was added and mixed gently. The digestion media consisted of DMEM-HG (Gibco), 0.5% (w/v) BSA (Sigma-Aldrich), 1 mg/ml Collagenase Type II – S (Sigma-Aldrich), 0.5 mg/ml Collagenase Type IV - S (Sigma-Aldrich). The tubes were then kept for shaking in a water bath set at $37^0$C, 150 rpm, and 45 minutes. After this the tubes were further centrifuged at 2000 rpm, 10 minutes, room temperature. The supernatant was discarded, and the pellet was then suspended in 25ml PBS – 2% (v/v) FCS. Disrupt the pellet by pipetting up and down gently. Larger clumps have to be manually removed by using sterile 3ml Pasteur pipette. Further pass the pellet suspension through the 400 μm strainer (Cambridge Biosciences, UK), then filter further through 100μm and 70μm cell strainers (BD biosciences). The filtrate was then added with excess amount of PBS – 2% (v/v) FCS and centrifuged at 2000 rpm for 10 minutes. The aspirate was then discarded, and pellet was then suspended in 10 ml RBC lysis solution. RBC lysis solution consisted of stock I (8.3g Ammonium chloride in 1-liter distilled water) and stock II (20.59g of Tris Base in 1L distilled water, pH 7.65 adjusted with 1M HCl). The final solution was made by mixing 9 parts of stock I and 1 part of stock II, adjusting the final pH at 7.65 with 1M HCl. Incubate the cell pellet suspension in RBC buffer solution at room temperature for 5 minutes. To this, 20 ml of PBS – 2% (v/v) FCS was added and filtered through 40 μm cell strainer. Further add to the filtered solution with PBS – 2% (v/v) FCS and centrifuge at 1500 rpm for 10 minutes at $4^0$C. The supernatant was then discarded, and pellet was suspended in 5 ml of PBS – 2% (v/v) FCS. The suspension was counted by treating with Trypan blue (Gibco) in automated cell counter (Bio-Rad). The suspended pellet was then subjected to FACS based sorting of cells.

### 3.7.1 FACS SORTING OF CELL SUSPENSION

The cell suspension was immune-stained for antibody panel-based sorting of cells present in the stromal vascular fraction. Prior to sorting, the cell suspension was treated with blocking buffer consisting of PBS, 0.1% BSA, 1X human IgG. The concentration was fixed at 5 x $10^7$ cells/ml. Tubes were prepared as given in the table below, Table: 3.5.

| Tube | Name | Antibody (Dilution) | Cell suspension (µl) |
|---|---|---|---|
| Tube 1 | Unstained | No antibody | 100µl |
| Tube 2 | Unstained | No antibody | 100µl |
| Tube 3 | Full stained | CD146 BV711(1:100)<br>CD34 PE (1:100)<br>CD45 V450(1:400)<br>CD56 V450 (1:100)<br>CD 31 FITC (1:100) | 400µL |
| Tube 4 | Fluorescent minus one CD146 | CD34 PE (1:100)<br>CD45 V450(1:400)<br>CD56 V450 (1:100)<br>CD 31 FITC (1:100) | 100 µl |
| Tube 5 | Fluorescent minus one CD34 | CD146 BV711(1:100)<br>CD45 V450(1:100)<br>CD56 V450 (1:100)<br>CD 31 FITC (1:100) | 100 µl |
| Tube 6 | Fluorescent minus one CD45/CD56 | CD146 BV711(1:100)<br>CD34 PE (1:100)<br>CD 31 FITC (1:100) | 100 µl |
| Tube 7 | Fluorescent minus one CD31 | CD146 BV711(1:100)<br>CD34 PE (1:100)<br>CD45 V450(1:400)<br>CD 56 V450 (1:100) | 100 µl |

**Table 3.5: Antibody panel used for cell isolation**

Compensation beads were also prepared for each antibody by using equal volumes of positive and negative beads in 2% (v/v) FCS. Isotype controls for each antibody was also prepared. The unstained and isotype control were used for compensation. After blocking, each tube with cells were incubated with corresponding antibodies as shown in the table for 20 minutes at $4^0$C. Washing was done after incubation by centrifugation and the stained cells were suspended in DMEM -HG with 20% (v/v) FCS. The cell concentration was maintained at $1x10^7$ cells /ml. Just before sorting, to each tube viability compensator DAPI dye was added (Invitrogen, 1: 10000). Sterile sorting of the cells was carried out in BD LSR Fortessa high-speed cell sorter with special order five-laser (633, 561, 488,405 and 355 nm) using BD Diva v.6.0 software, USA. The rate of sorting was fixed not to exceed 8000 cells/ second through a 100µm nozzle at 23 psi pressure power with four-way sorting precision. Isotype controls were used to counterbalance the spectral overlap and fluorescent minus one control were used to establish definite sorting gates. The forward and side scatter based single cell sorting was initially done followed by exclusion of dead cells and hematopoietic cells based on DAPI and CD45 fluorescence respectively. The endothelial were detected and collected based on $CD31^+$/CD $34^+$ cells in collection tube. The adventitial cells based on $CD34^+$/$CD146^-$ and pericytes based on $CD146^+$/$CD34^-$ were collected in separate collection tubes. Analysis were done using FlowJo software v.10.0. The collection tube contained 3ml of DMEM-HG with 20% (v/v) FCS. The collected cells were then plated to 2% gelatin coated plates with DMEM-HG with 20% (v/v) FCS for adventitial cells and pericytes, EGM-2 (Lonza, UK) for endothelial cells.

The isolated cells were passaged after confluence by trypsinization using 0.25% Trypsin EDTA (Invitrogen, UK). At each passage the perivascular stem cells -Adventitial cells and Pericytes were observed under phase contrast microscope (EVOS M5000 Cell Imaging system, Invitrogen, USA) for its confluence and fibroblastic morphology. Both cells at Passage four were used for further studies. However, the isolated endothelial cells had lesser proliferative capacity and due to time constraints, the further studies were carried out by late endothelial outgrowth cell isolated from peripheral blood and was gifted from Centre for Cardiovascular sciences. These cells were proved to behave as equally to native endothelial cells like Human umbilical vein endothelial cells (Tura et

al., 2013). The cells were between passage 3-6 and showed cobblestone morphology under phase contrast microscope (EVOS).

### 3.7.2 CELL SEEDING ON THE SCAFFOLDS

The scaffolds were initially sterilized by UV treatment. For standardization of cells seeding of each type of cells-Adventitial cell, Pericytes and Endothelial cells, on Poly (ethyl methacrylate-co-di ethyl amino ethyl acrylate) scaffold, 8g7, and the scaffolds were cut out from the tubes and laid flat at the bottom of cell culture dish. In order to prevent the uplifting of scaffold, when media was added, sterile cloning cylinders were fitted firmly on the scaffold and cells were seeded onto scaffold exposed inside cylinder. The cell seeding density of 2 X $10^5$ cells/ $cm^2$ of the scaffold surface was fixed for each cell type. The cells were trypsinised from culture flasks, counted by trypan blue staining before seeding. The cellularization of the scaffold at different time points were visualized by nuclear staining with DAPI.

### 3.7.3 CELL COMPATIBILITY OF SCAFFOLD – LIVE / DEAD ASSAY

Cells were seeded on scaffold and treated with Live / dead assay staining kit (Invitrogen) in order to visually analyze the live cells at day 3 and day 14. Cells after seeding were washed thrice in PBS in order to remove traces of serum protein. Assay was carried out as per manufacture's protocol. The live staining reagent Calcein AM was mixed with dead staining reagent ethidium homodimer in PBS and cell seeded scaffold was incubated in the reagent for 15 minutes at $37^0$C. After the incubation, the cells on scaffold were imaged under confocal laser scanning microscope with z-stacking of different fluorescent planes (Leica microsystem, Germany). The captured images were processed and analysed by ImageJ - FIJI software (NIH, USA).

### 3.7.4 MTT ASSAY

Cells at density 5 x $10^3$ cells were seeded onto scaffold cut out press fitted into the bottom of 96 well plates (Area: 0.8 $cm^2$). After culturing the cells for time periods – 3, 7 and 14 days, the media was removed and 200 µl of 1 mg/ml of filter sterilized MTT solution in PBS (Sigma-Aldrich, UK) was added to each well. As positive control, cells seeded on tissue culture plates were set. Blanks were also set as scaffold without cells.

MTT solution was incubated in the plate for 4 hours in the $CO_2$ incubator. To each well 200 µl of 1 % (v/v) DMSO (Sigma-Aldrich, UK) was added and incubated for 30 minutes with vigorous shaking for 1 hour. After incubation, the solution from each well was pipetted into a fresh 96 well plate. The absorbance was read at 570 nm in plate reader (Biotek synergy, UK). The cell viability was calculated using the equation:

Cell viability (%) = (Absorbance of test – Absorbance of blank) / (Absorbance of control – Absorbance of blank) ……...…….…..……Equation 9

### 3.7.5 SCANNING ELECTRON MICROSCOPY OF CELLS ON SCAFFOLD

The cell seeded scaffold at day 14 was washed initially with PBS and then twice with deionized water. The scaffold was then fixed with 3.5% para formaldehyde overnight. After fixation scaffold was washed gently with deionized water and freeze-dried overnight (Virtis freeze dryer). The freeze-dried samples were carefully mounted onto stubs of Scanning electron microscope with carbon tapes and coated with palladium gold for improved contrast. The samples were the visualized under high voltage SEM (Carl Zeiss Sigma HD, UK).

### 3.7.6 β-ACTIN AND IMMUNOSTAINING OF CELL MARKERS ON THE SEEDED SCAFFOLD

In order to analyze the cell adhesion and spreading of the cells on scaffold, the Actin cytoskeleton of the cells were detected by immunofluorescence-based staining. The identity of each cell on scaffold were also checked by immuno-staining with corresponding cell markers. After 14 days of culture, the cell seeded scaffolds were retrieved carefully, washed gently in PBS twice and fixed with 4% Para formaldehyde solution (Sigma-Aldrich) for 20 minutes at room temperature. The paraformaldehyde was then removed, and scaffolds was washed with PBS containing 0.01% (v/v) Tween 20 (Sigma-Aldrich), PBS-T. In the case of antigens bound in the cytoplasm permeabilization was carried out by treating with 0.5% Triton X 100 (Sigma-Aldrich) in PBS for 10 minutes at room temperature. The Triton X was then discarded and washed twice with PBS-T. Incubated with protein blocker (Invitrogen) for 45 minutes at room temperature. The primary antibody was diluted in antibody diluent (Invitrogen) and

added to cover the scaffold, incubated overnight at $4^0$C. After incubation, the primary antibody was washed away with PBS-T and secondary antibody was applied (1:300 dilution), incubated for 1 hour. The secondary antibody specificity was different for two cell types. The scaffold after washing was then transferred to glass slide and added DAPI fluorescent mounting media (Life technologies) for 10 minutes. A cover glass was carefully placed over scaffold. The images of the scaffold were taken by confocal laser scanning microscope (Leica Microsystem) with corresponding excitation and emission wavelength of secondary antibody by *z*-stacking the retrieved image planes. The images were combined and analysed by using ImageJ-FIJI software (NIH). Immunofluorescence of cells cultured on Tissue culture plates were also carried out in case of adventitial cells and pericytes for stem cell markers following the protocol described as above. The plates were analysed by epi-fluorescence semi-confocal microscope (Carl Zeiss).

## 3.8 CO-CULTURE OF PERIVASCULAR CELLS WITH ENDOTHELIAL CELLS ON SCAFFOLD

In order to standardize the co-culture of perivascular cells – adventitial cells and pericytes respectively with endothelial cells on tubular scaffold, the cells were initially grown to confluence on tissue culture plates. The passage of adventitial cells and pericytes were at P3 while that of endothelial cells were at P2. The cells were cultured till 14 days on scaffold with seeding density of 2 x $10^2$ cells / $cm^2$ taking in consideration of tubular scaffold total surface area. Different ratios of adventitial to endothelial cell (1:1, 1:2, 1:3, 1:4, 1:5) were analysed. In the case of pericytes ratio to endothelial cells (1:1, 1:2, 1:3) were analysed. Double immunofluorescence of markers expressed on both cell types (adventitial/endothelial cell - CD44/CD31, pericytes/endothelial cell - CD146/CD31) were used to analyze each ratio and the final ratio was fixed as adventitial cell to endothelial cells as 1:5 and pericytes to endothelial cells as 1:1. The cell culture medium used was EGM-2 with 10% (v/v) FCS. After 14 days, the scaffold cut outs were fixed and double immunostained for specific marker to confirm the establishment o co-culture. The images were taken under confocal laser scanning microscope and processed with Image J-FIJI software

### 3.8.1 ANGIOGENESIS ASSAY

The tissue culture media collection from the co-culture systems were done as follows. Initially cells were co-cultured for 14 days on scaffold as reported above in EGM-2 media containing 10 % (v/v) FCS (n= 12 for each system). On day 15, the media is removed completely, cells were washed twice with EGM-2 media without serum or any other supplements. The cells were cultured for one day in this media at standard culture conditions. The culture media was then collected and stored at -80$^0$C. The co-culture secretome were analysed by proteome profiler Human angiogenesis Array kit (R&D Systems, ARY007, USA) according to the manufacturer's instruction. The media was then filtered using 0.22μm syringe filter (Merck Millipore) and centrifuged at 500 rpm at 4$^0$ C for 5 minutes. The secretome was added on to antibody bound microarray sheet provided and incubated as per the manufacturer's protocol. The signal was detected immediately after incubation using LiCOR Odyssey Fc detection system, USA exposing each array membrane for 5-10 minutes. The images were captured with LiCOR software and quantified for positive signals (Image Studio Lite software, LiCOR). The pixel intensity of each protein spot was calibrated against average intensity of negative control spots. The final signal intensity of each protein spot was then plotted in order analyse the difference in each co-culture system in terms of promoting angiogenesis.

## SECTION III – *IN VIVO* EVALUATION OF GELTIN-VINYL ACETATE / POLY-ε-CAPROLACTONE ELECTROSPUN SCAFFOLD, G3P1

## 3.9 PART I – *IN VIVO* EVALUATION IN RABBIT MODEL

### ETHICAL STATEMENT

The studies involving animal subjects were conducted as per the ethical guidelines and recommendations concerning the Purpose of Control and Supervision of Experiments on Animals, India and the Institutional Animal Ethics Committee approved form B number: SCT/IAEC-187/JANUARY/2018/89. For conducting stem cell-based research work approval was obtained from Institutional Committee for Stem Cell Research and Therapy under the number: SCT/IC-SCR/ OCT 21/2014.

**ANIMAL WELFARE**

The health status and general well-being of the in-house animals subjected to research-based experimentation were constantly monitored. Animal housing consists of individual well-ventilated cages. Animals were maintained at temperature of 22±5$^0$C, relative humidity of 55±10% and equal 12-hour dark and light cycles. Rabbits were fed with cleaned processed vegetables and drinking *ad libitum*. The health was monitored as per Federation for Animal Science Associations (FELASA) guidelines for parasitology and regularly stamped for infections if any.

### 3.9.1 SURGICAL REPLACEMENT OF RABBIT COMMON CAROTID ARTERY WITH G3P1 SCAFFOLD CELLULARISED WITH DIFFERNTIATED SMOOTH MUSCLE CELLS

**ANESTHESIA AND SURGICAL PROCEDURE**

For implantation studies, the animal model selected was New Zealand white rabbits of either sexes of body weight range of 2.5- 3 kg body weight. The animals chosen were the same animals which had undergone adipose tissue retrieval procedure for stem cells isolation. The implantation was conducted three months after the tissue retrieval considering the full health of the animal. Animals (n=2) were anaesthetized with atropine sulphate, xylazine, midazolam and Ketamine (Anket, Neon lab, India) intramuscularly. Anaesthesia was maintained either with continuous propofol infusion through marginal ear vein and provided with an oxygen mask or by iso-flurane delivery after endotracheal intubation.

The animals anaesthetized with xylazine- midazolam- ketamine combination and was controlled in supine position. The area at the ventral neck was prepared aseptically and a mid-ventral incision shall be made on the neck to expose approximately 1.5 – 2.0 cm of the carotid artery. Heparin 100 IU per kg was administered intravenously and the proximal and distal clamps was applied on the carotid artery 1.5cm apart. Approximately 2 cm long segment of the carotid artery was excised and removed and 3 cm of G3P1 tissue engineered vascular graft was implanted by end to end anastomosis with 6/0 Prolene sutures (Ethicon). Prior to implantation, the scaffold with smooth muscle cells were aseptically transferred to the operation theatre from culture conditions. The grafts

were gently washed with sterile PBS thrice to remove the traces of media. The skin incision was closed in layers. Animals were closely monitored and given antibiotics and analgesics for five postoperative days. The rabbits were given two doses of Low Molecular Weight Heparin at the rate of 1 mg/kg body weight subcutaneously at 12 hours interval. Aspirin was also be administered post operatively at the rate of 2 mg/kg body weight for two weeks. Animals were under daily veterinary inspection and was given intramuscular injections of antibiotics (ceftriaxone) and anti-inflammatory (meloxicam) for 5 days postoperatively. Sutures were removed on seventh post-operative day. Animals were then cared for and fed ad libitum feed and water. The total period of study was two weeks.

### 3.9.2 ANGIOGRAPHIC EVALUATION OF THE IMPLANT

After the implantation period, the rabbits were anaesthetized as described above and terminal angiographic evaluation was carried out in order to access the blood flow through the graft. The contrast dye was injected initially through the same side of the implanted graft by through incision made in thoracic artery and trailing towards the implant site in carotid artery. Further evaluation was also done by injecting the dye through laterally opposite carotid artery. The angiographic images were captured with help of radiation source fitted above the table (GE health care systems, UK).

### 3.9.3 GROSS OBSERVATION OF THE IMPLANT

The animal was euthanized after angiographic evaluation of the implant by administering excess dose of thiopentone sodium. The animal was the shifted to aseptic room and felt the neck for implant. A 5 cm long incision was made carefully along the neck exposing the carotid artery with implant. The graft with surrounding carotid artery was excised. The gross observation of the graft was made with emphasis on structure of graft, its dimensions after implantation and positional change if any. The grafts were then fixed wit 10% (w/v) neutral buffered formalin (NBF) for further histopathological evaluations.

### 3.9.4 HISTOPATHOLOGICAL EVALUATIONS

From the explant, tissue pieces from both proximal, distal anastomosis and mid graft region were taken, processed routinely, embedded in paraffin. Five-micron thick sections were taken by cutting the blocks in microtome. The section was de-paraffinized in xylene and stained with Haematoxylin and Eosin (Sigma-Aldrich, UK). The sections were observed under microscope (Leica Microsystems, Germany) and evaluated for the degree of cellularization, types of cells, extracellular matrix deposition.

## 3.10 PART II – *IN VIVO* EVALUATION IN SHEEP MODEL

### ETHICAL STATEMENT

The studies involving animal subjects were conducted as per the ethical guidelines and recommendations concerning the Purpose of Control and Supervision of Experiments on Animals, India and the Institutional Animal Ethics Committee approved form B number: 71$^{st}$ CPCSEA/25/9/2019, SCT/IAEC-292/JAUARY/2019/99. For conducting stem cell-based research work approval was obtained from Institutional Committee for Stem Cell Research and Therapy under the number: SCT/IC-SCR/50/SEPTEMBER/2018

### ANIMAL WELFARE

In order to make sure the health of large animals. The animals were group housed under natural climatic conditions and closely monitored following the guidelines of CPCSEA. Clinical health of animals was routinely checked by analysing the haematological and biochemical parameters. The sheep were fed on in-house made special feed consisting of crude and roughages. Water was given *ad-libitum*.

### PRE-EXPERIMANTAL EVALUATION OF ANIMAL SUBJECT

Female sheep, adult, 25-45 kg body weight (n=3) were kept under observation right after adipose tissue isolation for a minimum of three months. For implantation of graft, the same sheep were identified with ear tag and conditioned for one month. Body weight, other conditions like illness or pregnancy were avoided. 24 hours prior to surgery,

clinical examination of the animals was carried out for checking any abnormality in the health and behaviour of the animals. The animals were starved for a day prior to surgery and isolated in the post-operative room with assistance.

**ANAESTHESIA**

The animals were subjected to whole body general anaesthesia. A combination of Atropine sulphate (0.01 mg/kg body weight), Xylazine (0.3 mg/kg body weight) and Ketamine (7 mg/kg body weight) were used to induce anaesthesia in animals. The sheep were then intubated with a cuffed endotracheal tube (size 9) after administering Propofol bolus (3 mg/kg body weight) intravenously. Ventilation was initiated with a tidal of 10-12 ml/kg body weight to achieve an $EtCO_2$ at 30 - 35 mm of $H_2O$ under isoflurane maintenance.

### 3.10.1 SURGICAL PROCEDURE: VASCULAR GRAFT IMPLANTATION

The animals study groups (n=3) were selected in such a way to minimise the number of animal subjects. The right and left carotid artery of the same sheep were used to implant cell seeded scaffold (G3P1 + SMC subgroup, n=3) and bare scaffold (G3P1 alone subgroup, n=3).

The G3P1 tubular graft of 5mm internal diameter and 7 cm length cellularised with adipose derived stem cell differentiated smooth muscle cells were prepared for implantation. The animals study groups were selected in such a way to minimise the number of animal subjects. The right and left carotid artery of the same sheep were used to implant cell seeded scaffold and bare scaffold. The implantation was carried on Day 15 after 14-day differentiation of cells. On the day of implantation, the tissue engineered graft and sterile bare graft (unseeded control scaffold alone) were washed in sterile PBS twice just prior to implantation.

Under general anaesthesia and standard aseptic conditions, the sheep ventral neck area was prepared for surgery. Initially side corresponding to cellularised scaffold implantation was prepared. A longitudinal incision was made in the superior border of the jugular grove left or right to jugular vein. The exposed jugular vein is retracted dorsally, and carotid artery was exteriorized. The animal was heparinized, and 5 cm left,

or right carotid artery was excised following clamping using bulldog vascular clamps. Either tissue engineered graft or bare scaffold graft is positioned and sutured in end to end anastomosis fashion to carotid artery using 6/0 prolene suture. After suturing, both the ends, the clamps are slowly removed for blood flow. Any leakage of blood over graft were observed. The surgical wound was then closed in layers and animal was allowed to recover from anaesthesia. The animal was shifted to post-operative care room and allowed to recover. The wound was dressed routinely with antiseptics and antibiotic injections (Strepto-penicillin-meloxicam) were given for seven days. The study period was for 3 months.

### 3.10.2 ANGIOGRAPHIC EVALUATION OF THE IMPLANT

After the implantation period of three months, the sheep were anaesthetized as described above and terminal angiographic evaluation was carried out in order to access the blood flow through the graft. The contrast dye was injected along the catheter path through femoral artery of the sheep. Images of both implants were recorded.

### 3.10.3 GROSS OBSERVATION OF THE IMPLANT

The animal was euthanized after angiographic evaluation of the implant by administering excess dose of thiopentone sodium. The animal was the shifted to aseptic room and felt the neck for implant. A 7 cm long incision was made carefully along the neck exposing the carotid artery with implant. The graft with surrounding carotid artery was excised. The gross observation of the graft was made with emphasis on structure of graft, its dimensions after implantation and positional change if any. The grafts were then fixed wit 10% (w/v) neutral buffered formalin (NBF) for further histopathological evaluations.

### 3.10.4 ENVIRONMENTAL SCANNING ELECTRON MICROSCOPY OF THE IMPLANT

Section from the mid region of the patent implant were subjected to E-SEM imaging. Both luminal and abluminal areas were scanned in order to check the cell distribution and morphology.

### 3.10.5 HISTOPATHOLOGICAL EVALUATION OF THE IMPLANT

Tissue section from proximal, distal and mid graft region were excised, routinely processed and embed in paraffin blocks. Paraffin blocks of native carotid artery and cell seeded G3P1 graft were also made. Sections of five-micron thickness were taken on glass slide with help of microtome (Leica system, Germany). The sections were de-paraffinized in changes of xylene (SDFCL chemicals, India), rehydrated in decreasing percentage of ethanol (Avra, India) and stained with haematoxylin (Electron microscopy systems) and then with eosin (Microscopicals, SDFCL, India). The sections after staining were dehydrated in ethanol, xylene cleared and mounted with cover glass with DPX mountant (Spectrochem, India). The stained sections were observed under light microscope (Leica DM4000, Germany) for cell distribution, neo-vascularization, endothelization and inflammatory responses.

### 3.10.6 PICROSIRIUS RED STAINING OF COLLAGEN FIBERS

As process of remodelling of the implanted graft, collagen fibers will be deposited on the implant. In order to observe this section of implant were subjected to picrosirius based staining of collagen. Under light microscope, the collagen fibers appear red when stained with Sirius red and show bifringence under polarizer microscope. The sections were deparaffinized and rehydrated and stained with Sirius red solution in picric acid (Sigma-Aldrich, USA) for one hour. Nuclei were counter stained with Wiegert's haematoxylin (Sigma-Aldrich, USA) for 10 minutes. The slides were then washed with acidified water (glacial acetic acid in water), dehydrated in ethanol and xylene. The sections were mounted with cover glass with DPX mountant. The sections were observed under light and polarizer microscopes (Leica DM 4000, Germany).

### 3.10.7 VERHOEFF'S -VAN GEISON STAINING FOR ELASTIN FIBERS

The elastin deposition of the implant is a hallmark to confirm the regeneration potential the vascular graft. The deposition of elastin fibers was observed by staining the tissue with Verhoeff's-Van Geison staining protocol. The paraffin-embedded five-micron thick sections were de-paraffinized in xylene and rehydrated in several changes of ethanol gradient and in distilled water. Sections were stained in Verhoeff's solution (5% (w/v), Alcoholic haematoxylins (Electron microscopy systems, India), 10% (w/v) Ferric chloride (SDFCL), 8% (v/v) of Wiegert's Iodine) for one hour until the tissue sections are coloured dark. After washing with water, the sections were differentiated with 2% (v/v) ferric chloride for 2 minutes. Differentiation was stopped with by using several changes of tap water. The slides were treated with 5% (w/v) Sodium thiosulphate (Labrasayan Ltd.). Washed and counterstained with Van Giesons's solution with for 5 minutes. Slides were dehydrated with 95% alcohol and two changes of 100% alcohol. Cleared in xylene and mountant with DPX mountant. The sections were observed under light microscope for the presence of brown-black elastin fibers with blue black nucleus.

### 3.10.8 IMMUNOFLUORESCENCE STAINING

In order to analyse the endothelization in the mid-section of implanted graft, immunofluorescence staining of endothelial cell specific CD31antigen were performed. Also, the distribution of smooth muscle cells on the sections were analysed by α smooth muscle actin staining. Mid sections of patent graft implants were analysed. The paraffin embed section were initially deparaffinized and rehydrated. Antigen retrieval in formalin fixed section were done by treating the sections enzymatically with trypsin solution (0.5% (v/v) Trypsin (Gibco), 1% (w/v) calcium chloride (Analytical rasayan) in distilled water, pH 7.8). Sections were warmed at $37^0$C with trypsin solution inside a humidified chamber for 30 minutes. After treatment the section are washed in PBS containing Tween 20 (PBS-T). The sections were then blocked with 0.5% (w/v) Bovine serum albumin in PBS for 20 minutes at room temperature. The primary unconjugated antibody (CD31 1:200, Abcam and αSMA 1:100, Abcam) were diluted in PBS with 2% ( w/v) BSA and sections were incubated overnight with antibodies at $4^0$C.The slides were then washed with PBS-T and incubated with secondary antibody conjugated with FITC ( 1:500, Abcam) for 1 hour. After incubation the sections were washed and treated with nuclear

staining reagent Hoechst (Sigma-Aldrich) for 10 minutes. Slides were washed and mounted with DPX. The stained slides were visualized under confocal laser scanning microscope with z-stacking (Nikon Air microsystem, Japan).

### 3.10.9 TOTAL COLLAGEN AND ELASTIN ESTIMATION

The total soluble collagen content of the explant was estimated using Sircol soluble collagen assay kit (Biocolor life sciences assay, UK). Steps were followed according to manufacturer's protocol and as described above. The explants, native artery and G3P1 graft prior to implantation were also analysed. Bare G3P1 graft served as blanks for normalizing the value. The concentration of samples (n=4) is elucidated from calibration plot.

For estimation of elastin Fastin Elastin assay kit (Biocolor life science, UK) were employed. The explants, native artery and G3P1 graft prior to implantation were also analysed. According to manufacturer's protocol, elastin in the samples were converted to soluble form of α-elastin by heating the samples with 0.25M oxalic acid (Laboratory rasayan, India) for 2 hours at $100^0$C. The concentration of samples (n=3) were detected from the calibration plot.

## 3.11 STATISTICAL ANALYSIS

All data were represented as mean ± standard deviation. The data were analysed for statistical significance by one-way ANOVA followed by Tukey post-hoc test for more than two testing conditions. The analysis was performed using Vassar stat: website for statistical computation. The significance of the data set was pronounced by P value and were specifically mentioned in each analysis.

# CHAPTER 4
# RESULTS

## SECTION I – SCAFFOLD FABRICATION AND CHARACTERISATION

## 4.1 PART I – SYNTHESIS, FABRICATION AND CHARACTERISATION OF GELATIN-VINYL ACETATE/POLY-ε-CAPROLACTONE SCAFFOLD

### 4.1.1 SYNTHESIS OF GELATIN-VINYL ACETATE (GV)

The synthesis protocol of gelatin-vinyl acetate was earlier reported (Thomas and Nair, 2013). Briefly, gelatin, a natural protein was modified with vinyl acetate by free radical mechanism according the reaction mechanism scheme as given below, Scheme: 1. After reaction gelatin-vinyl acetate (GV) polymer was precipitated, homopolymer removed by Soxhlet extraction, air dried and stored at room temperature. A weight ratio of 71.5:28.5 (Gelatin to vinyl acetate) has been chosen for synthesis as per standardized. The grafting ratio was found to 0.49 with an efficiency of 49.7 ± 0.7%.

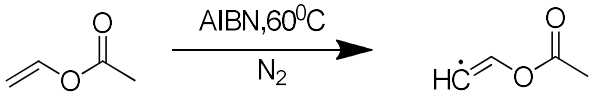


a) Formation of free radicals on vinyl acetate

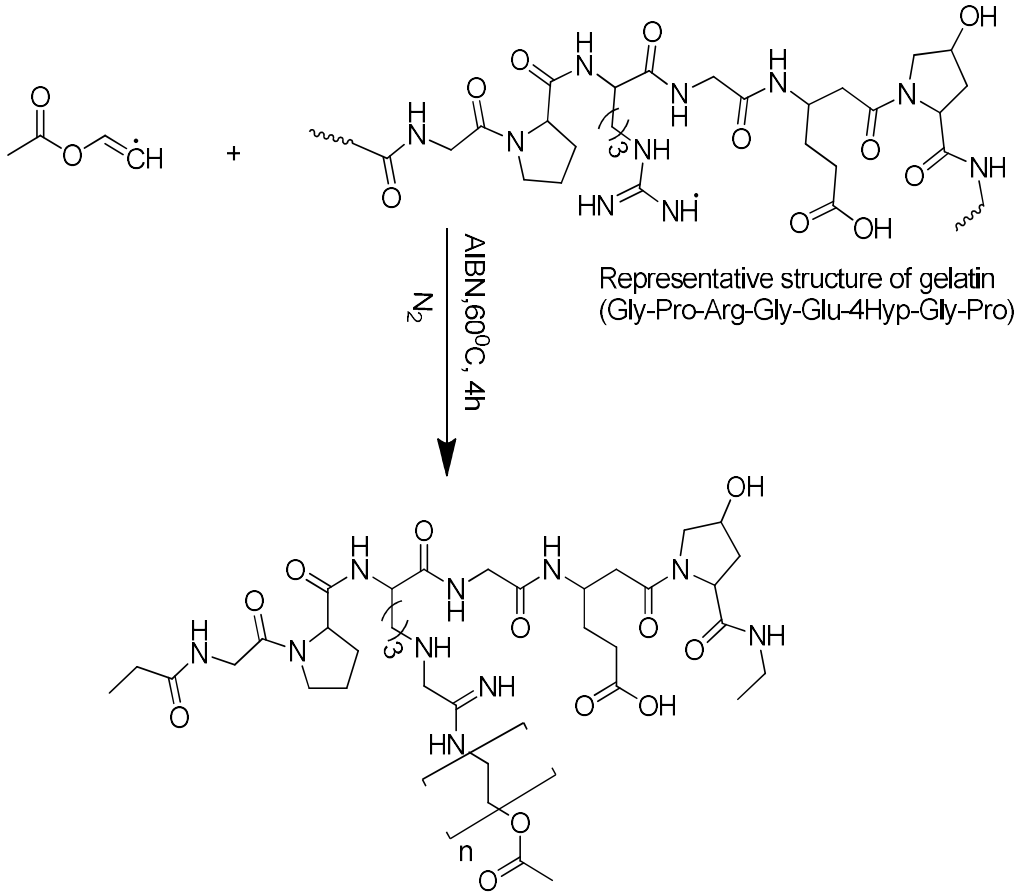


b) Graft polymerization vinyl acetate on gelatin

**Scheme 1: Synthesis of gelatin-vinyl acetate**

### 4.1.2 CHARACTERISATION GELATIN-VINYL ACETATE (GV)

#### 4.1.2.1 FOURIER TRANSFORM - INFRARED SPECTROSCOPY AND TNBS ASSAY

The ATR FTIR of gelatin vinyl acetate in comparison with gelatin, shows the presence peaks of amide I (1641 $cm^{-1}$) and amide II (1536 $cm^{-1}$) and intense C=O stretch at 1754 $cm^{-1}$, which confirm the grafting reaction. The percentage amine group of gelatin is 70 ± 1.2% while gelatin-vinyl acetate is 49±2% which was evaluated through TNBS assay, Figure: 4.1 A, B.

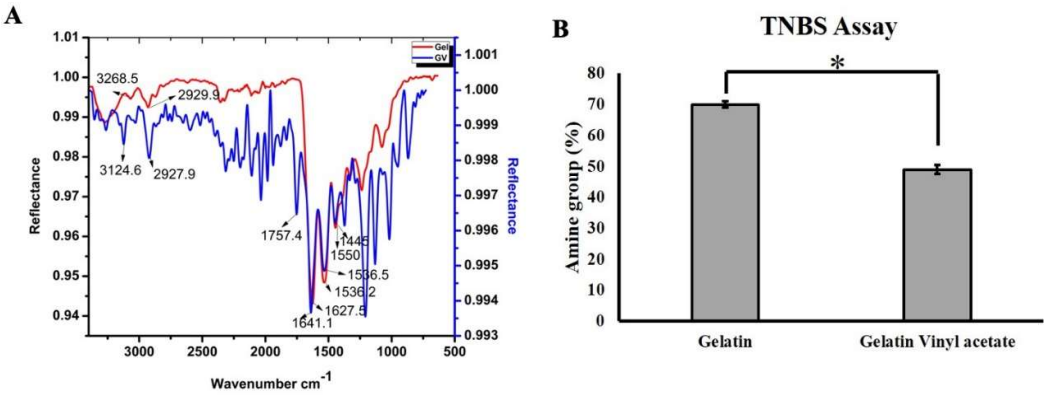


**Figure 4.1: (A) FT-IR Spectra of Gelatin and synthesized Gelatin-vinyl acetate. (B) TNBS Assay of gelatin and gelatin-vinyl acetate (*p<0.01).**

#### 4.1.2.2 GEL PERMEATION CHROMATOGRAPHY

Gel permeation chromatography of gelatin and gelatin vinyl acetate showed an increase in molecular weight and poly dispersity for gelatin vinyl acetate. The weight average molecular weight (Mw) was increased from 47 kDa to 95 kDa. The poly dispersity of gelatin vinyl acetate has also been increased to 2.63. The increase in molecular weight clearly indicate the vinyl acetate has been grafted on to gelatin, Table: 4.1

| Sample Name | Mn | Mw | MP | Poly dispersity |
|---|---|---|---|---|
| Gelatin | 29561 | 47982 | 59525 | 1.62 |
| Gelatin-vinyl acetate | 36172 | 95054 | 39210 | 2.63 |

**Table 4.1: Gel permeation chromatography showing number average (Mn), Weight average (Mw), Viscosity Average (MP) and Poly dispersity of gelatin and gelatin - vinyl acetate**

### 4.1.3 FABRICATION OF GELATIN-VINYL ACETATE/ POLY-ε-CAPROLACTONE SCAFFOLD

#### 4.1.3.1 DUAL SOURCE CO-ELECTROSPINNING OF POLYMERIC SOLUTIONS - STANDARDISATION OF ELECTROSPINNING

The advantage of dual source co-electrospinning is that, this technique allows the incorporation of two or more polymers into a single scaffold system without compromising the individual properties. For standardisation of electrospinning, initially solvent system for gelatin-vinyl acetate was selected. Taking into consideration of greener chemistry and cost, highly fluorinated corrosive solvents like Hexafluoroisopropanol and trifluoro ethanol was avoided. Also, water as solvent system was not favoured as higher percentage of gelatin-vinyl acetate in water showed rapid gelling behaviour at room temperature. Gelatin-vinyl acetate in glacial acetic acid alone showed not so appreciable electrospinning and scaffold retrieve-ability was difficult owing to its sticky nature. A combination of glacial acetic acid and ethyl acetate solvent system for electrospinning of gelatin has been reported, however for gelatin-vinyl acetate has less spin ability in this. In order to make the solvent more miscible, water interface was added between glacial acetic acid and ethyl acetate making it suitable. The solvent showed dissolution of gelatin-vinyl acetate at various percentage with highest at 20% (w/v). The percentage of solution of gelatin-vinyl acetate was fixed at 15% (w/v) below which it did not generate consistent fibres when spun simultaneously with PCL. The solvent system employed for PCL (Chloroform: Methanol, 7:3) was widely used and

weight percentage was fixed based on solubility. The flow rate of gelatin-vinyl acetate electrospinning was fixed between 1ml/hour- 3ml/hour. Any flow rate above or below did not produce stable jet. The fibres of gelatin-vinyl acetate appeared at 6kV while that of PCL appeared at 8.5 kV. However, up to 10 kV fibre jet was highly discontinuous and continuous jet appeared at 10.5 kV till 12 kV, above which there was spitting like phenomenon. The mandrel chosen was made of steel and rotated at speed of 2000 rpm. Tip to collector distance was fixed based on fibre corona diameter so that fibers spread and attach uniformly on to the mandrel. Summary of standardised parameters are given below, Table: 4.2.

| **PARAMETER** | **GV (15%)** | **PCL (15%)** |
|---|---|---|
| Solvent | Glacial acetic acid : Water : Ethyl acetate (4:2:4) | Chloroform: methanol (7:3) |
| Syringe | 21G | 21G |
| Flow rate | 1-3 ml/hour | 1ml/hour |
| Tip to collector distance | 10 cm | 8 cm |
| Mandrel speed | 2000 rpm | 2000 rpm |
| Voltage | 10.5 kV | 10.5 kV |

**Table 4.2: Standardised electrospinning parameters**

### 4.1.4 CHARACTERISATION OF ELECTROSPUN SCAFFOLD

#### 4.1.4.1 TNBS ASSAY - DETERMINATION OF PERCENTAGE GELATIN-VINYL ACETATE IN DUAL ELECTROSPUN SCAFFOLD

The combination of scaffolds fabricated were based on three different flow rates. The samples are name coded accordingly and TNBS assay performed showed the amount of gelatin-vinyl acetate in 3 mg of equal dimension scaffold. Table: 4.3 shows different samples and ratio of gelatin-vinyl acetate to PCL in comparison to calculated theoretical ratio. The ratios were more or less similar to theoretical ratios. Electrospun scaffold composition: Gelatin-vinyl acetate content of the tubular scaffold was estimated to be 71±3% by TNBS assay which approximates to that of theoretical ratio based on feed rate (G:P-3:1 vs. 2.4:1). It is inferred that gelatin-vinyl acetate fibers in the G3P1 scaffold is present in more numbers than PCL fibers

| Sample code | Gelatin-vinyl acetate (G) Flow rate (ml/hour) | PCL Flow rate (P) (ml/hour) | Theoretical ratio (G:P) | Experimental ratio (TNBS ASSAY) |
|---|---|---|---|---|
| G1P1 | 1 | 1 | 50:50 | 55:45 |
| G2P1 | 2 | 1 | 67:33 | 62:38 |
| G3P1 | 3 | 1 | 75:25 | 71:29 |

**Table 4.3: Sample code and ratio of scaffold combinations**

#### 4.1.4.2 FOURIER TRANSFORM INFRA-RED (FT-IR) SPECTROSCOPY

The FT-IR data confirms the presence of two polymers in the scaffold and thus substantiate the feasibility of the technique in creating bi-component scaffold, Figure: 4.2. FT-IR analysis of scaffold showed characteristic combinatorial fingerprints of

gelatin-vinyl acetate (Amide I: 1628cm$^{-1}$and Amide II: 1540cm$^{-1}$) and PCL (C=O stretch at 1722cm$^{-1}$) in all the scaffold combination.

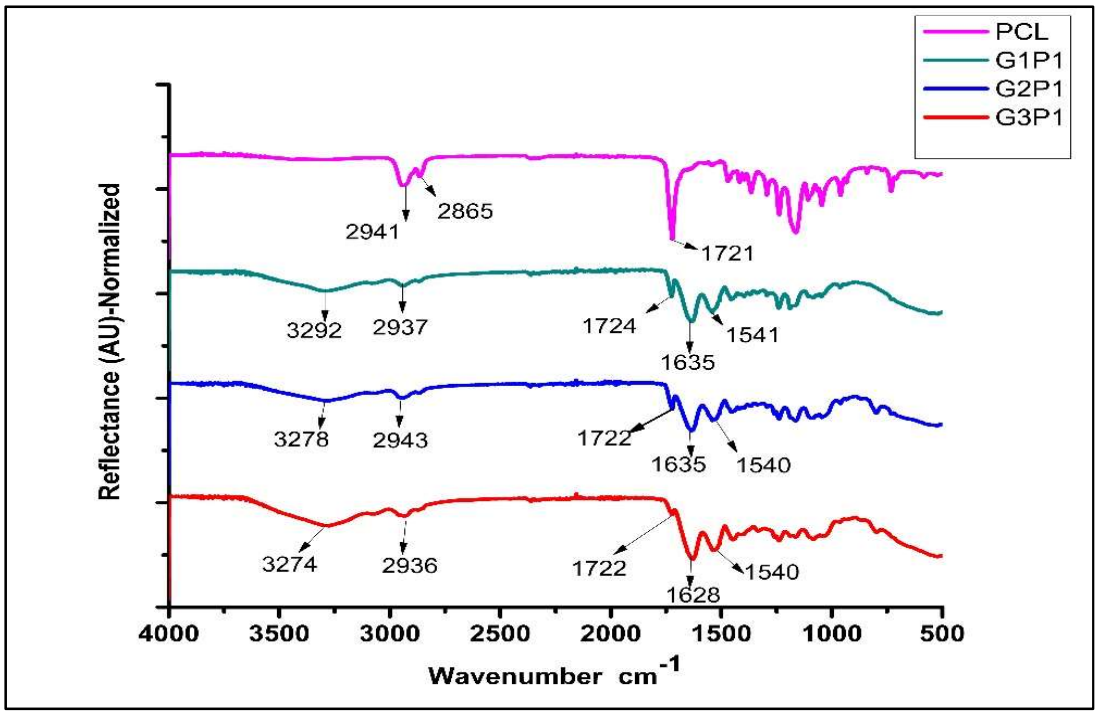


**Figure 4.2: FT-IR Spectra of scaffold combinations**

### 4.1.4.3 FIBER MORPHOLOGY ANALYSIS BY SCANNING ELECTRON MICROSCOPE

The scanning electron microscopic images shows smooth, bead-less fibers of the polymers. Analysis of fibre diameter showed that on increasing the flow rate of gelatin-vinyl acetate, the diameter range decreased from more than 1µm to 0.7 µm. The fibre diameter in the case of G3P1 combination was 0.73 ± 0.03 µm, which was the lowest among the three.

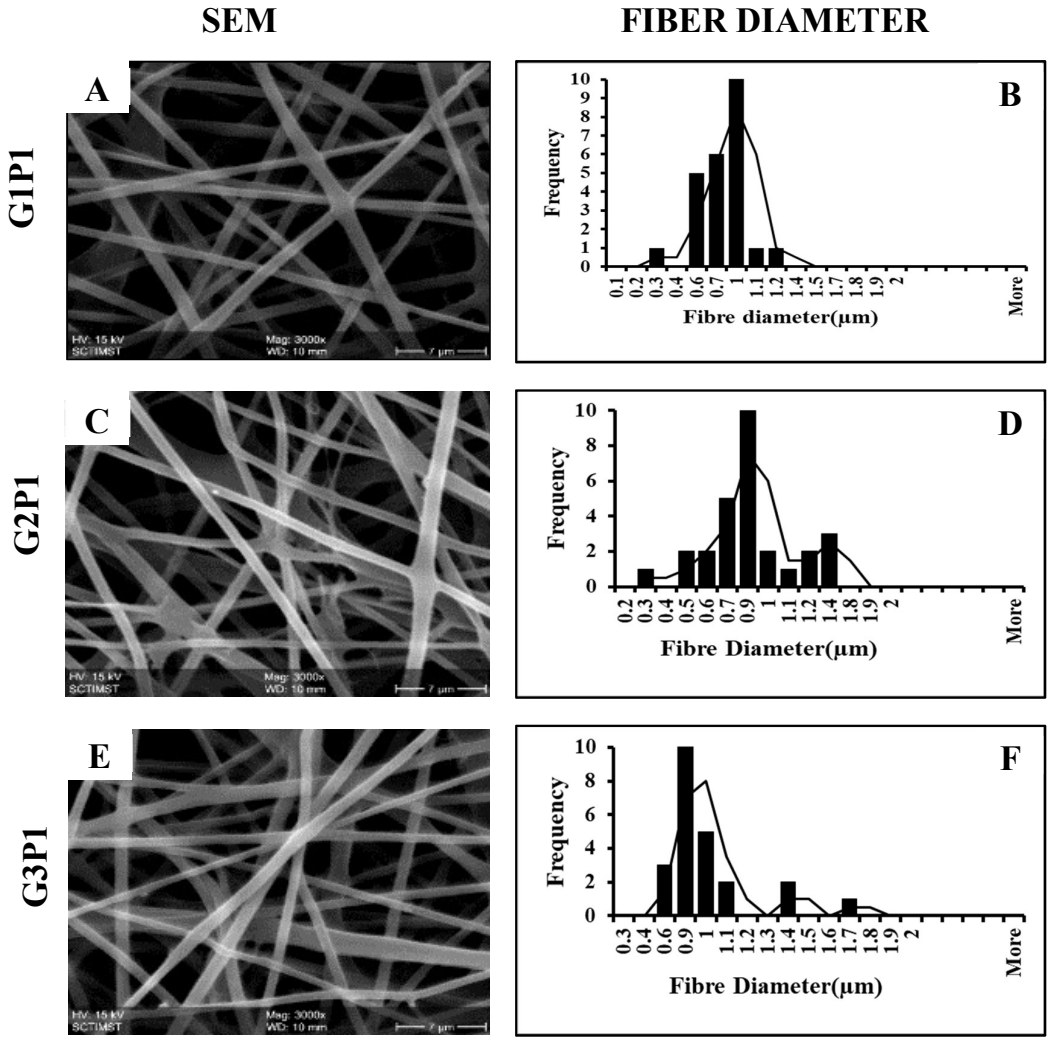


**Figure 4.3: SEM of different scaffold combinations and fibre diameter – G1P1 (A&B), G2P1 (C&D), G3P1 (E&F)**

### 4.1.4.4 WATER CONTACT ANGLE

Surface wet ability of G1P1, G2P1, G3P1, GV, PCL scaffold showed that the combinatorial scaffold wet ability falls between the parent compounds. As the flow rate of gelatin-vinyl acetate increases, the contact angle decreases. While lower flow rate scaffold was more inclined to hydrophobic nature, higher flow rate was to hydrophilic nature. Table: 4.4, summarises the water contact angle values at time 10 seconds.

| Water Contact Angle (10 second) | |
|---|---|
| 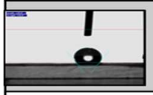 PCL | 120±3 |
|  G1P1 | 99±3 |
|  G2P1 | 88±2 |
|  G3P1 | 74±5 |
|  GV | 55±2 |

**Table 4.4: Water contact angle**

The scaffold combination selected for further fabrication tubular vascular grafts was the one prepared through the flow rate of 3ml/hour of gelatin-vinyl acetate (G3P1). This was selected due to its overall properties and for incorporation of maximum amount of natural polymer to make scaffold more conducive for cell growth. The crosslinking was carried out with 0.5% (v/v) of glutaraldehyde. The scaffolds were sterilised by UV treatment overnight or at least 1 hour by turning each side of the scaffold and stored in sterile containers at room temperature.

## 4.1.5 FABRICATION OF TUBULAR SCAFFOLD FOR VASCULAR GRAFT

The tubular vascular graft was fabricated by dual source electrospinning of gelatin-vinyl acetate (flow rate 3 ml/hour) and PCL (flow rate 1 ml/hour). The mandrel diameter was 3 mm and 5 mm and hence named as G3P1 – 3 mm and G3P1 – 5 mm respectively.

### 4.1.5.1 MORPHOLOGY OF TUBULAR SCAFFOLD

Gross morphology of tubular scaffold- G3P1 - 3 mm, was as summarised in tables given below, Table: 4.5. The white electrospun tube had a thickness of 200 ± 100µm and total length approximately 5 cm. The SEM image shows the fibrous wall of the

scaffold with well interconnected pores and fibre diameter was analysed to be 890 ± 50 nm, Figure: 4.4, 4.5. The gross morphology of G3P1 – 5 mm was again summarised in Table: 4.6, the scaffold has a length of 7 cm and wall thickness of 300 ± 100µm. The fibre diameter was 729 ± 23 nm, Figure: 4.6, 4.7.

| GROSS MORPHOLOGY OF GRAFT G3P1-3mm | |
|---|---|
| Shape | Tubular |
| Colour | White |
| Internal Diameter | 3 mm |
| Wall thickness | 200 ± 100µm |
| Total length | 4 cm |

**Table 4.5: Summary of morphological characteristics of G3P1-3mm graft**

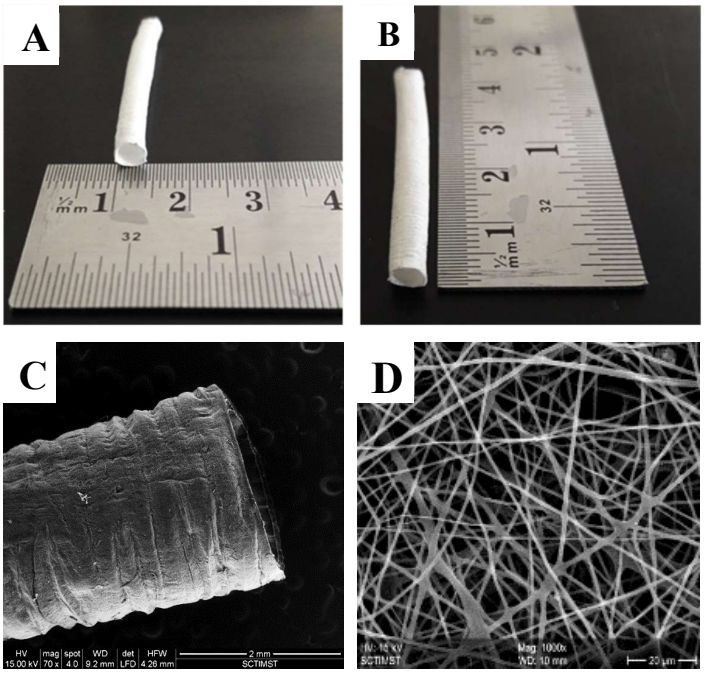


**Figure 4.4: Morphology of G3P1 - 3mm – (A) Diameter (B) Length (C, D) SEM image showing tube, fibres**

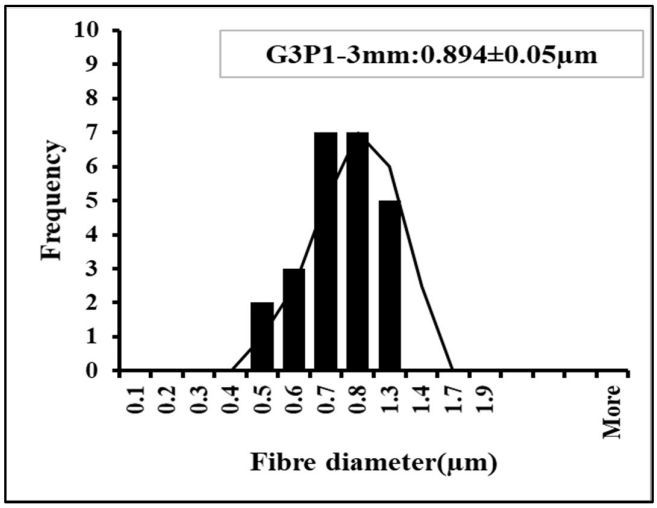


**Figure 4.5: Fibre diameter range of G3P1 – 3 mm (from SEM, figure 4.5 D)**

| GROSS MORPHOLOGY OF GRAFT G3P1-5mm | |
|---|---|
| **Shape** | **Tubular** |
| **Colour** | **White** |
| **Internal Diameter** | **5 mm** |
| **Wall thickness** | **300±100 µm** |
| **Total length** | **~7 cm** |

**Table 4.6: Summary of gross morphology of G3P1 – 5 mm vascular graft**

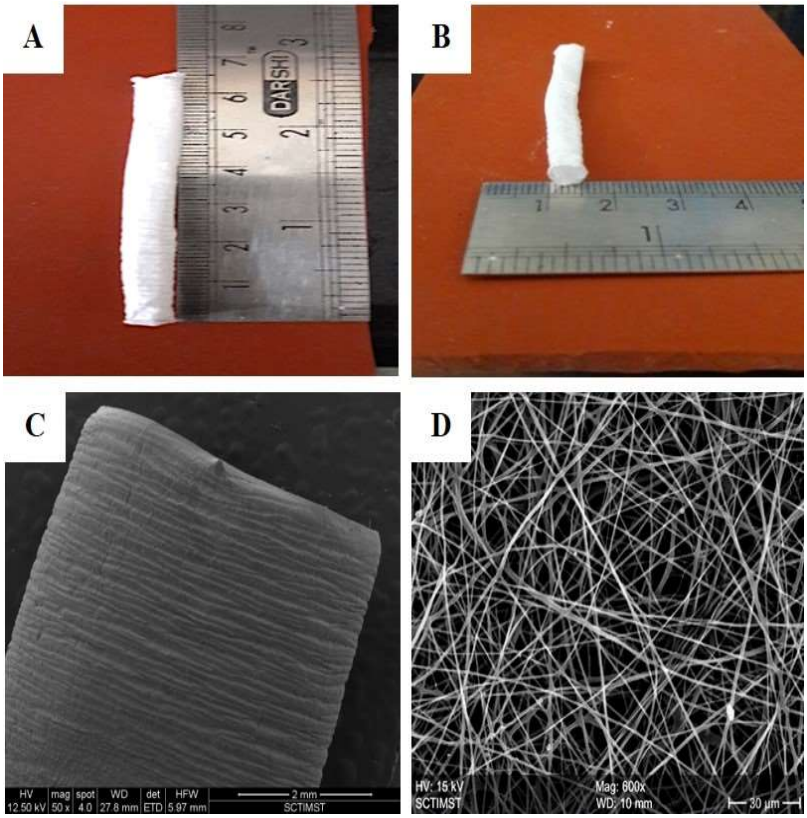


**Figure 4.6: Morphology of G3P1 – 5 mm – (A) Diameter (B) Length (C, D) SEM image showing tube, fibres**

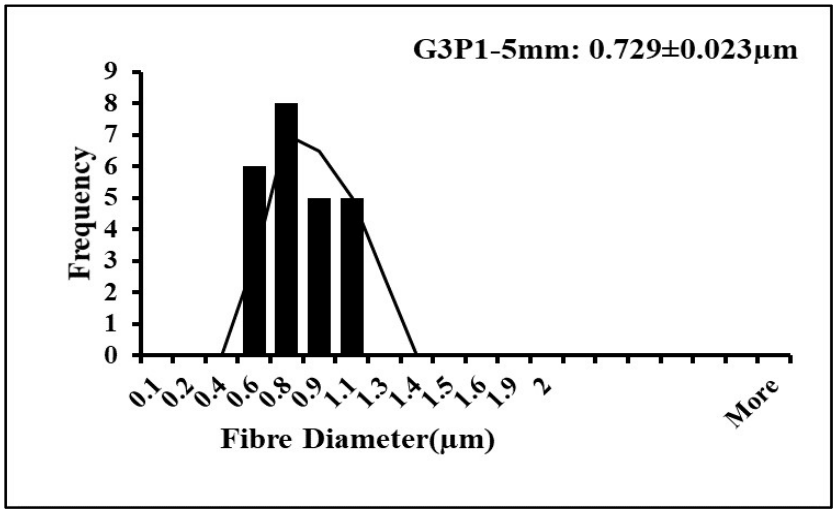


**Figure 4.7: Fibre diameter range of G3P1 - 5 mm (from SEM, figure 4.7 D)**

#### 4.1.5.2 POROSITY ANALYSIS

Micro-CT analysis of scaffold sections (Shown blue inset) showed well interconnected pores, Figure: 4.8. In the case of G3P1 – 3 mm, the pore size was 36 µm (32 %) and for G3P1 – 5 mm, it was 24 µm (41%).

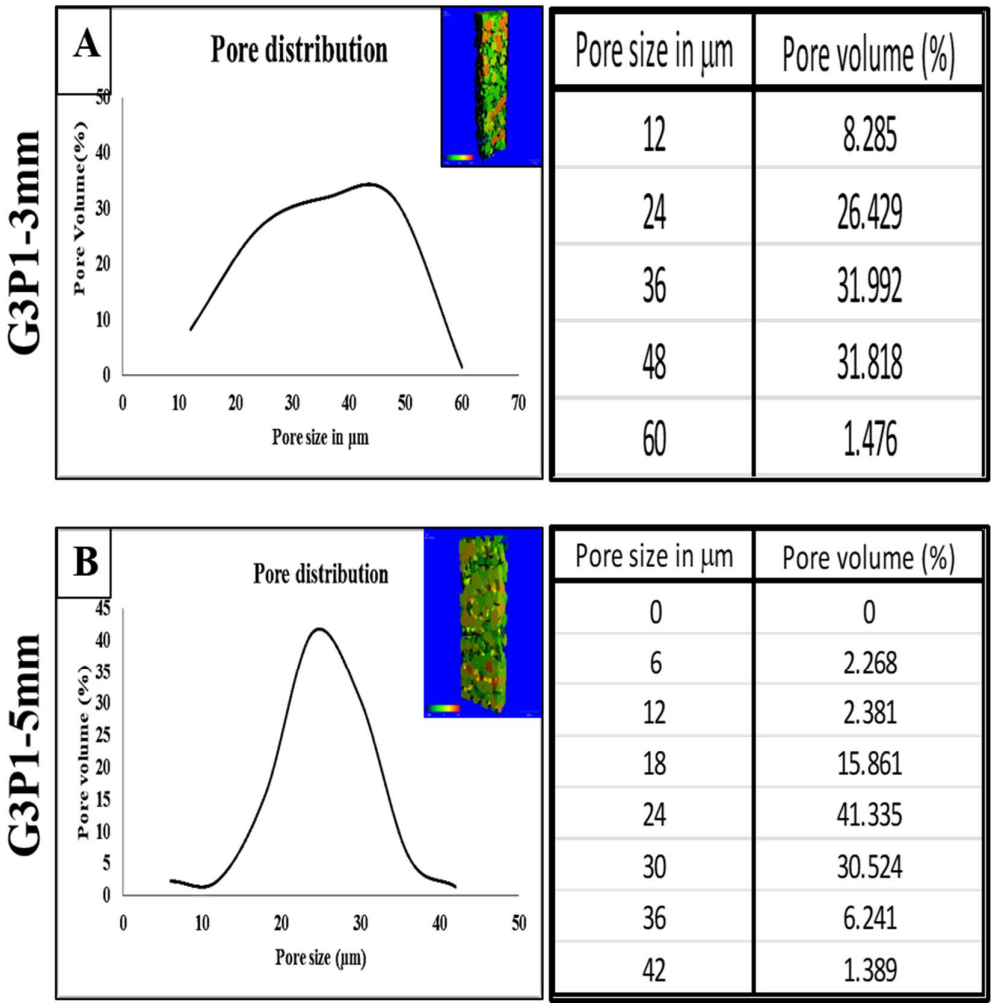


| Pore size in µm | Pore volume (%) |
|---|---|
| 12 | 8.285 |
| 24 | 26.429 |
| 36 | 31.992 |
| 48 | 31.818 |
| 60 | 1.476 |

| Pore size in µm | Pore volume (%) |
|---|---|
| 0 | 0 |
| 6 | 2.268 |
| 12 | 2.381 |
| 18 | 15.861 |
| 24 | 41.335 |
| 30 | 30.524 |
| 36 | 6.241 |
| 42 | 1.389 |

**Figure 4.8: Micro-CT of grafts- (A) G3P1 – 3 mm. (B) G3P1 - 5 mm (Blue Inset - 3D morphometry showing interconnectivity)**

### 4.1.5.3 MEDIA UPTAKE ABILITY AND DEGRADATION ASSAY

Media uptake ability in terms of swelling percentage of G3P1 – 3 mm, G3P1 - 5 mm, GV, PCL in PBS pH 7.4 for 48 hours (2880 minutes) were measured in different time interval. While GV showed increased swelling over time PCL had very little swelling ability. The scaffold of both diameter showed a swelling percentage of 160 ± 43% (G3P1 – 3 mm) and 173 ± 20% (G3P1 – 5 mm) within 15 minutes respectively after which there was no appreciable swelling, Figure: 4.8 A.

The degradation of scaffold over a period of three months (12 weeks) showed much similar results for both grafts as 38 ± 4% (G3P1 – 3 mm) and 42 ± 2% (G3P1 – 5 mm) percentage weight loss respectively, Figure: 4.9 B. PCL showed a little degradation over 3 months while GV degraded more than 70%.

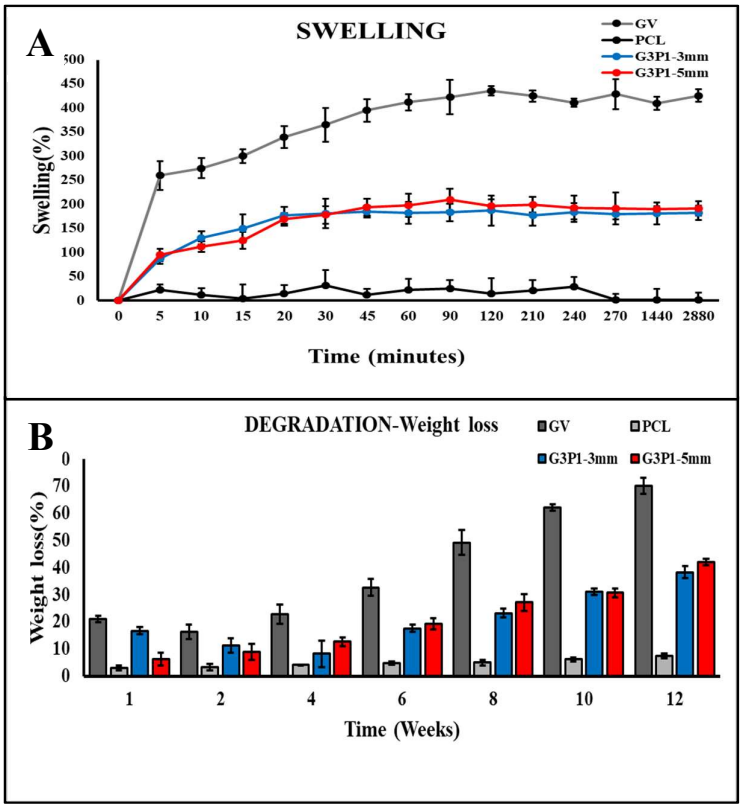


**Figure 4.9: (A) Swelling percentage of scaffolds. (B) Degradation assay.**

#### 4.1.5.4 MECHANICAL PROPERTIES OF ELECTROSPUN GRAFTS

The mechanical properties of both grafts were measured in order to access the robustness of the graft to with stand hemodynamic forces. The percentage elongation, ultimate tensile strength was measured, and Young's modulus was calculated from that. Theoretical burst pressure was also estimated, Figure: 4.10 A to D. The table: 4.7 summarises the values in comparison with properties of saphenous vein (SV) and Internal mammary artery as reported from literature. For both scaffolds, the Young's modulus circumferential (C, Figure: 4.10 A) is in between their parent components – GV – 3 mm and PCL – 3 mm. The suture retention force for G3P1 – 3 mm was 2.3 ± 0.7N and G3P1 – 5 mm was 2.9 N.

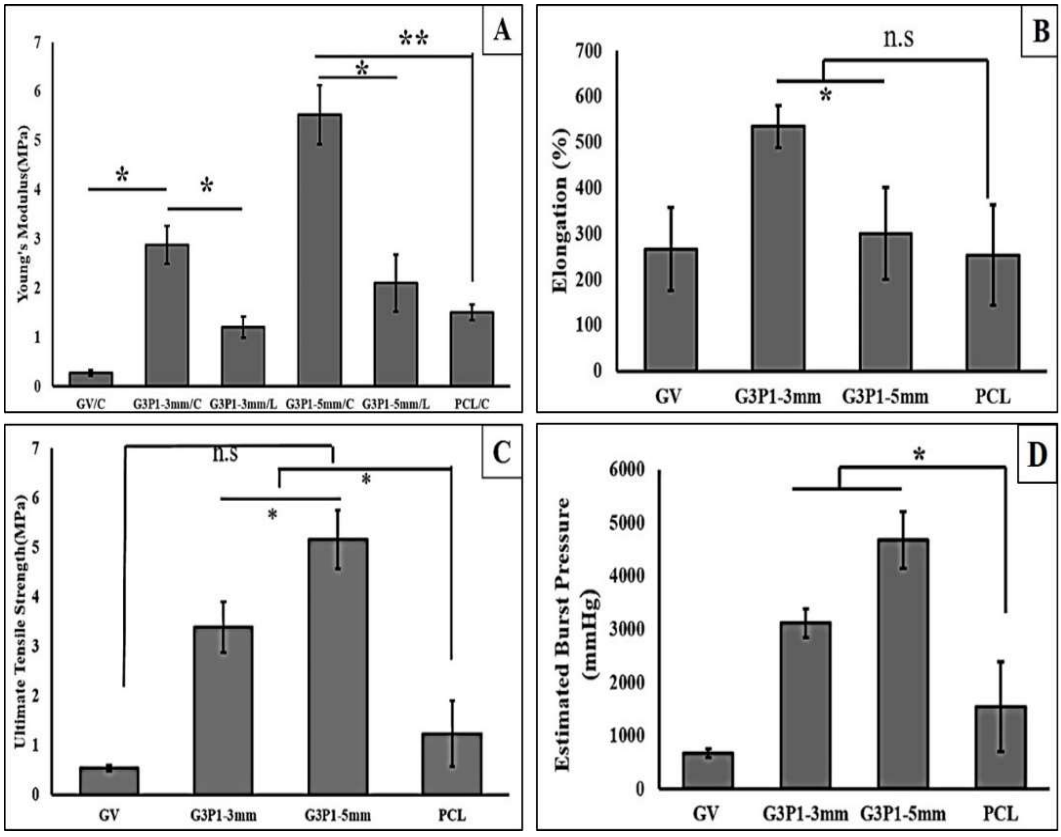


**Figure 4.10: Mechanical properties of tubular scaffolds-GV, G3P1-3mm, G3P1 5mm, PCL – (A) Young's Modulus -C: circumferential, L-longitudinal (*p<0.01, **p<0.001). (B) Percentage elongation (Circumferential n.s: non-significant). (C) Ultimate tensile strength (MPa). (D) Estimated burst pressure (mmHg).**

| Sample | Ultimate tensile stress (MPa) | Percentage elongation | Young's modulus (MPa) | Burst Pressure (mm Hg) | Suture Retention force (N) |
|---|---|---|---|---|---|
| GV | 0.54±0.06 | 266±91 | 0.3±0.06(C) | 675±77 | |
| PCL | 1.2±0.67 | 253±110 | 1.5±0.16 (C) | 3120±270 | |
| G3P1-3mm | 3.38±0.51 | 534±47 | 2.87±0.38(C)<br>1.21±0.27(L) | 4680±540 | 2.3±0.17 |
| G3P1-5mm | 5.15±0.7 | 300±100 | 5.5±0.6(C)<br>2.1±0.6(L) | 1545±840 | 2.9±0.93 |
| IMA | 4.1 | | 7.3(C) | 2000 | |
| SV | 2.25 | | 4.3 | 1680-3900 | |

**Table 4.7: Summary of the mechanical properties of fabricated vascular graft**

## 4.2 PART II - SYNTHESIS, FABRICATION AND CHARACTERISATION OF POLY (ETHYL METHACRYLATE-CO-DI ETHYL AMINO ETHYL ACRYLATE) SCAFFOLD

### 4.2.1 SYNTHESIS OF POLY (ETHYL METHACRYLATE-CO-DI ETHYL AMINO ETHYL ACRYLATE) AND MOLECULAR WEIGHT

Poly (ethyl methacrylate-co-di ethyl amino ethyl acrylate), 8g7 was synthesized by the Scheme 2 given below. The molecular weight (Mw) of the synthesised polymer was found to be consistent within different synthesis batches and was 11kDa with poly dispersity of 3.28, Table: 4.8.

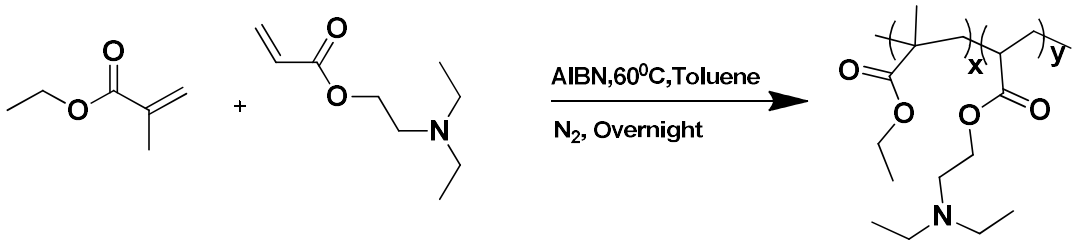


**Scheme 2: Free radical polymerization of Poly (ethyl methacrylate-co-di ethyl amino ethyl acrylate), 8g7**

| Sample | Mn | Mw | Mp | PD |
|---|---|---|---|---|
| 8g7 | 35634 | 116944 | 120949 | 3.28 |

**Table 4.8: Gel permeation chromatographic values of 8g7 Molecular weight**

### 4.2.1.1 FOURIER TRANSFORM INFRARED SPECTROSCOPY (FT-IR) OF POLY (ETHYL METHACRYLATE-CO-DI ETHYL AMINO ETHYL ACRYLATE)

The FT-IR spectra of the synthesised polymer shows its characteristic peaks for -C-H stretch at 2974 $cm^{-1}$, -C=O stretch at 1721 $cm^{-1}$, -C-N at 1141 $cm^{-1}$, Figure: 4.11.

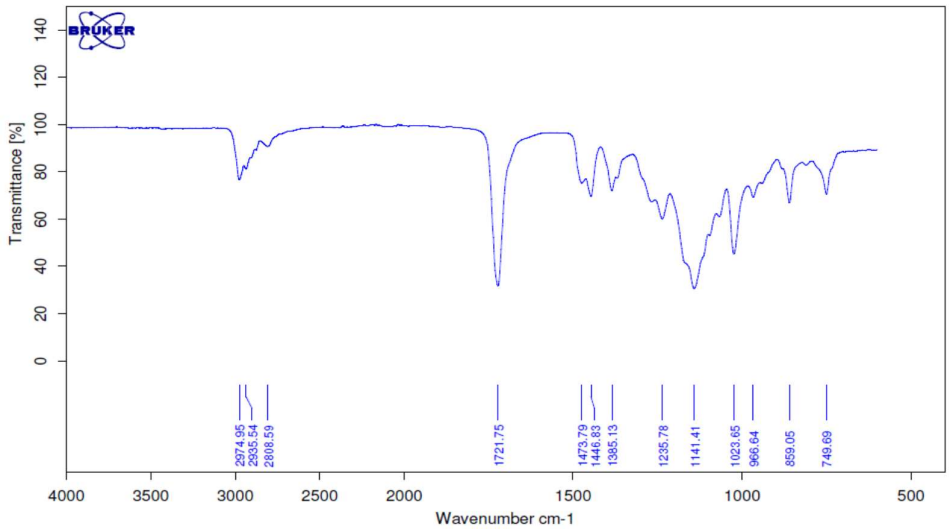


**Figure 4.11: FT-IR spectra of synthesised polymer**

### 4.2.2 FABRICATION OF POLY (ETHYL METHACRYLATE-CO-DI ETHYL AMINO ETHYL ACRYLATE) TUBULAR SCAFFOLD BY ELECTROSPINNING AND CHARACTERISATION

The effect of different solvents on the solubility of the polymer was studied and it was found that the polymer was soluble in solvents like Dimethyl formamide, Tetrahydrofuran, chloroform, methanol, ethanol and their combinations. However, considering the ease of solubility even at higher percentage within short time and stable fibre production, a solvent system of DMF: THF of ratio 9:1, Table: 4.9 were selected.

| SOLVENT | SOLUBILITY OF POLYMER | ELECTROSPINNING ABILITY | FIBRE MORPHOLOGY |
|---|---|---|---|
| Dimethyl formamide | Soluble | Yes | Beaded fibres at low concentration, smooth fibre at high concentrations |
| Tetrahydrofuran | Easily soluble at any weight percentage | No, Electro spraying | No Fibers |
| Chloroform | Easily soluble | No stable jet, dripping | No Fibers |
| Methanol | Soluble | No | |
| Ethanol | Soluble | Yes, intermittent dripping | No fibre consistency, fibre breaking |
| Chloroform : methanol (7:3) | Soluble | No spinning | |
| **DMF : Chloroform (1:1)** | Easily soluble, 4 Days | Yes | Smooth fibre, Mixed fibre diameter |
| DMF:THF (5:5,4:6,3:7,2:8,1:9) | Easily soluble, 1 day | No, Electro spraying | No Fibers |

| | | | |
|---|---|---|---|
| DMF:THF<br><br>(5:5,6:4,7:3,8:2) | Easily soluble,<br><br>1 day | Yes, intermittent ejection of fibers | |
| **DMF:THF(9:1)** | Easily soluble,<br><br>1 day | Yes, stable jet | Smooth bead free fibers |

**Table 4.9: Summarises the effect of solvent system on electrospinning of 8g7**

In the DMF: THF (9:1) solvent system different weight percentages of polymer were subjected to electrospinning. All weight percentages above 30% (w/v) produced fibres. However smooth bead-less fibre production started only at 60% (w/v), Figure: 4.12. With respect to flow rate fibres were initiated form stable jet at 0.3 ml/hour up to 4 ml/hour. At higher flow rate fibers were showing flat morphology, while at flow rate less than 0.5 ml/hour there was unstable fibre production. The flow rate was thus fixed at 0.5 ml/hour, Figure: 4.13.

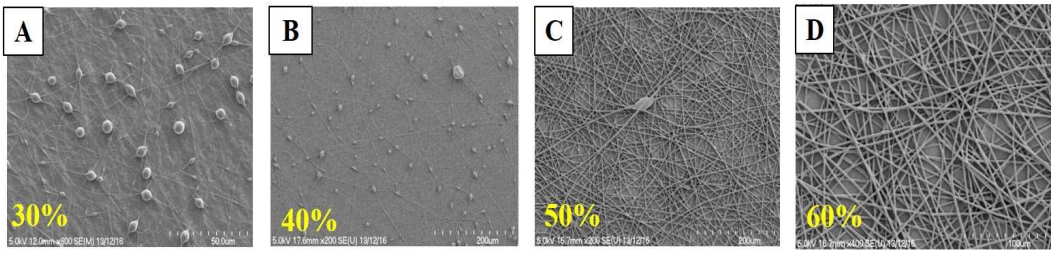


**Figure 4.12: SEM images - Effect of polymer concentration on electrospinning. (A) 30% polymer solution. (B) 40% polymer solution (C) 50% polymer solution (D) 60% polymer solution.**

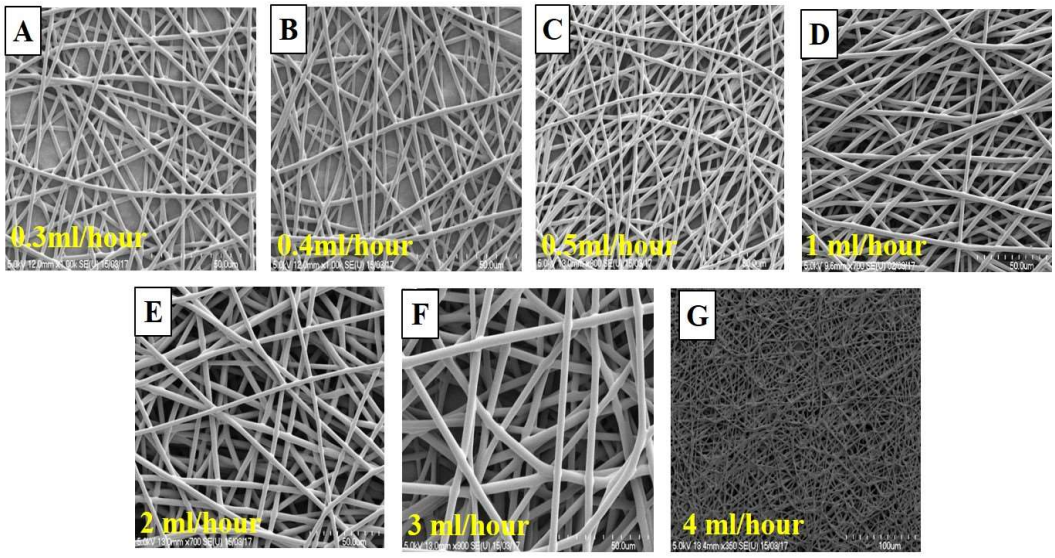


**Figure 4.13: SEM images -Effect of flow rate on electrospinning. (A) 0.3ml/hour. (B) 0.4 ml/hour. (C) 0.5ml/hour (D) 1ml/hour (E) 2ml/hour (F) 3ml/hour (G) 4 ml/hour**

The effect voltage on electrospinning was investigated and it was found that bead-less fibre was produced from 7 kV onwards. Fibre were ribbon like after 14 kV. The spinning was standardised at 10.5kV. Figure: 4.14 A & B (Phase contrast microscopic image), C to K (SEM images).

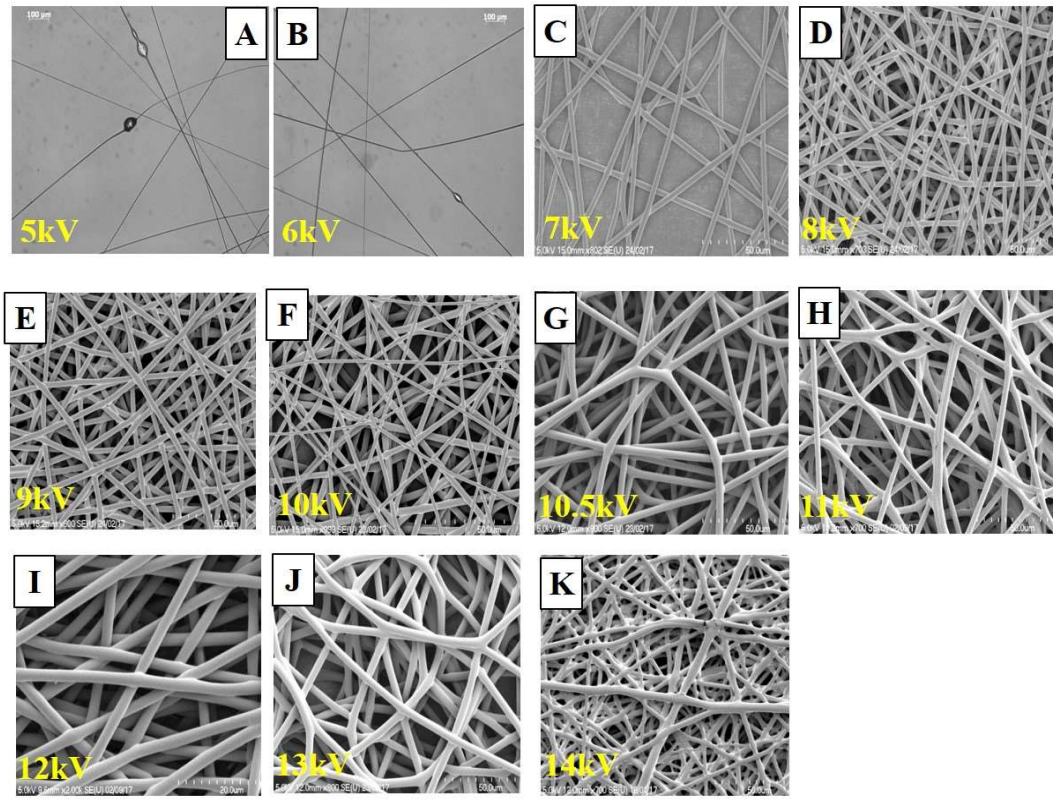


**Figure 4.14: Bright field Microscopic and SEM images -Effect of applied voltage on electrospinning. (A) 5 kV (Bright field). (B) 6 kV (Bright field). (C) 7 kV (D) 8 kV (E) 9 kV (F) 10 kV (G) 10.5 kV (H) 11 kV (I) 12 kV (J) 13 kV (K) 14 kV.**

The electrospinning parameters was summarised as given in the Table: 4.10. A rotating mandrel of 3 mm and 5 mm were used as collector. A white coloured tubular scaffold was produced of thickness 200 µm and length 7 cm for 5 mm diameter. Further characterisation was done with 5 mm tubular scaffolds as the study was indented to be *in vitro* only, so a larger diameter was chosen for ease of handling (8g7 - 5 mm). The SEM images shows the thickness of scaffold and also smooth fibrous wall. The fibre diameter of 8g7 - 5mm was elucidated from SEM and was 4.3 ± 0.1µm, Figure: 4.15.

| PARAMETER | 8g7 (60%) |
|---|---|
| Solvent | DMF:THF (9:1) |
| Syringe | 21G |
| Flow rate | 0.5 ml/Hour |
| Tip to collector distance | 15 cm |
| Mandrel speed (Diameter) | 2000 rpm (3 mm, 5 mm) |
| Voltage | 10 kV |

**Table 4.10: Summary of electrospinning parameters of 8g7**

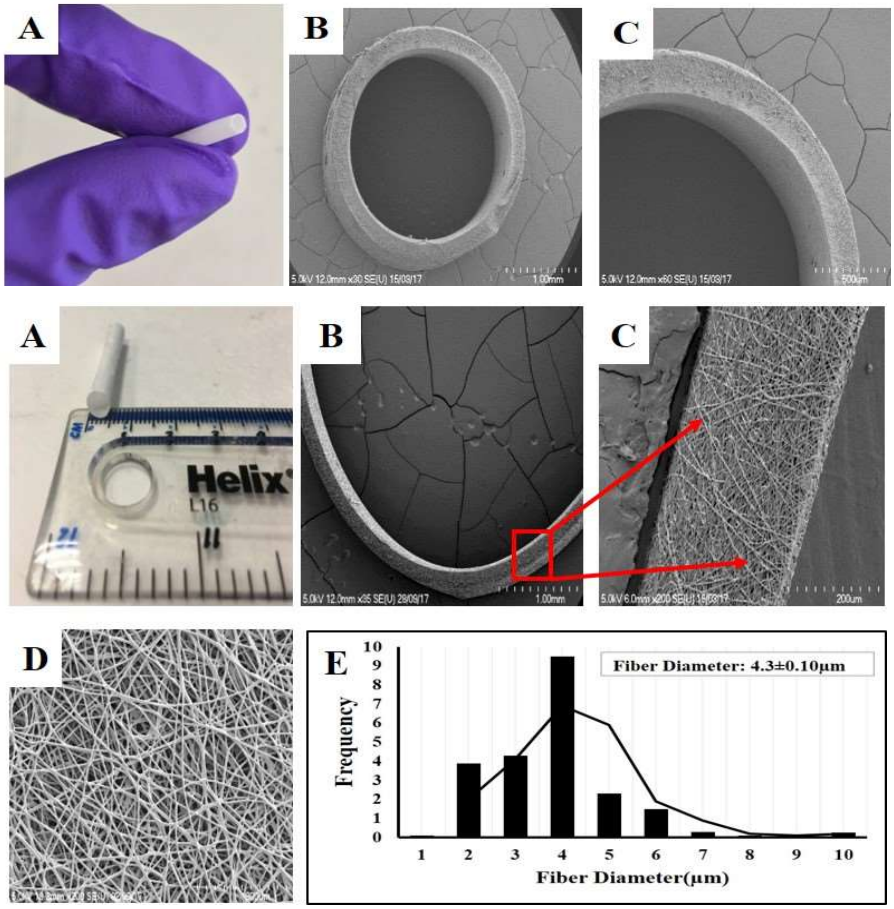


**Figure 4.15: Morphology of 8g7 graft: 8g7 - 3 mm (A) 8g7 – 3 mm. SEM of cross-section of tube. 8g7 - 5 mm (A) 8g7 – 5 mm (B, C) SEM of Cross-section of tube, thickness. (D) SEM of tube wall section and graph showing fibre diameter frequency.**

#### 4.2.2.1 WATER CONTACT ANGLE AND WATER UPTAKE ABILITY OF TUBULAR SCAFFOLD

The water contact angle of the tubular scaffold section was 104 ± $8^0$ making the scaffold to be hydrophobic. However, within 1 minute the water droplet was absorbed by the scaffold, Figure 4.16: A, B. The percentage solubility of the scaffold was calculated to be 56 ± 3 % within 10 minutes which remained more or less constant over time, Figure: 4.16 C.

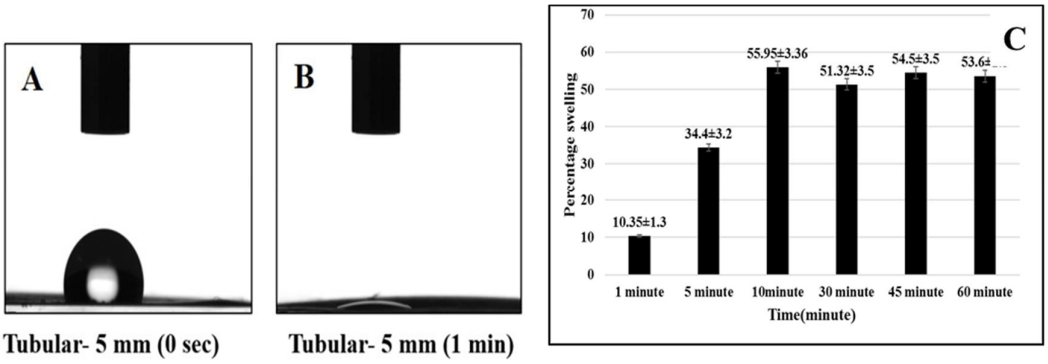


**Figure 4.16: Water Contact angle of 8g7 - 5mm (A) 0 second (B) One minute (C) Percentage swelling of 8g7 – 5 mm.**

#### 4.2.2.2 MICRO-CT ANALYSIS OF TUBULAR SCAFFOLD – POROUS NATURE

It was evident from the SEM images that scaffold was highly porous. The micro-CT analysis showed a scaffold with average pore size of 36 ± 2.3μm with a pore volume percentage of 42 ± 4.34%, Figure: 4.17.

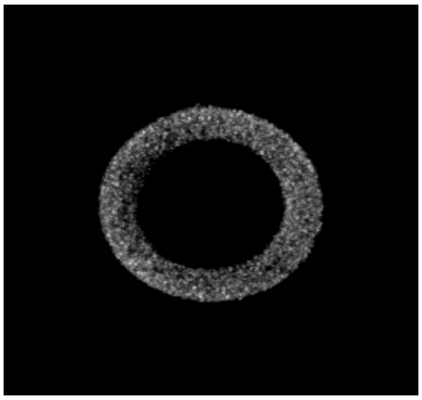

**Figure 4.17: Micro-CT 3D reconstructed image showing porous nature of scaffold (black void shows attenuation of air to white portion of scaffold).**

#### 4.2.2.3 MECHANICAL PROPERTIES OF TUBULAR SCAFFOLD

The scaffold shows Young's modulus of 6.6 ± 1.8 MPa in circumferential direction and 3.64 ± 1.4 MPa in longitudinal direction. The ultimate tensile stress (Circumferential) was 4.93 ± 0.4 MPa. The suture retention force was 2.3 N. The estimated burst pressure was very high compared to native vessels and was 3000 ± 614 mmHg.

## SECTION II – *IN VITRO* CELL BASED STUDIES

### 4.3 PART I – DIFFERENTIATION OF ADIPOSE DERIVED MESENCHYMAL STEM CELLS TO SMOOTH MUSCLE CELLS ON GELATIN-VINYLACETATE/POLY-ε-CAPROLACTONE SCAFFOLD

### 4.3.1 ISOLATION AND CHARACTERISATION OF RABBIT ADIPOSE DERIVED MESENCHYMAL STEM CELLS (RAMSCs)

Rabbit adipose tissue derived mesenchymal stem cells attached and appeared on day 2 on tissue culture plates, Figure: 4.11 A. The cells became confluent within one week. Actin-cytoskeletal staining of cells showed the fibroblastic appearance of plastic adherent cells, Figure: 4.11 B. Population doubling time calculation of cells showed that cells took longer time to divide in initial passage, which decreased till P6 and further increased after that. Thus, for all the studies, cell between passages P3 - P4 was used, Figure: 4.11 C. Immuno-phenotyping of cells based on FACS confirms positivity of stem cell markers - 93% (Vimentin), 68% (CD44), and 0.5% (CD34/CD45), Figure: 4.11 D to G. Immunofluorescence staining also justifies the presence of stem cell markers, Figure: 4.11 H to K, thus proving the 'mesenchymal stem cell nature of the isolated cells.

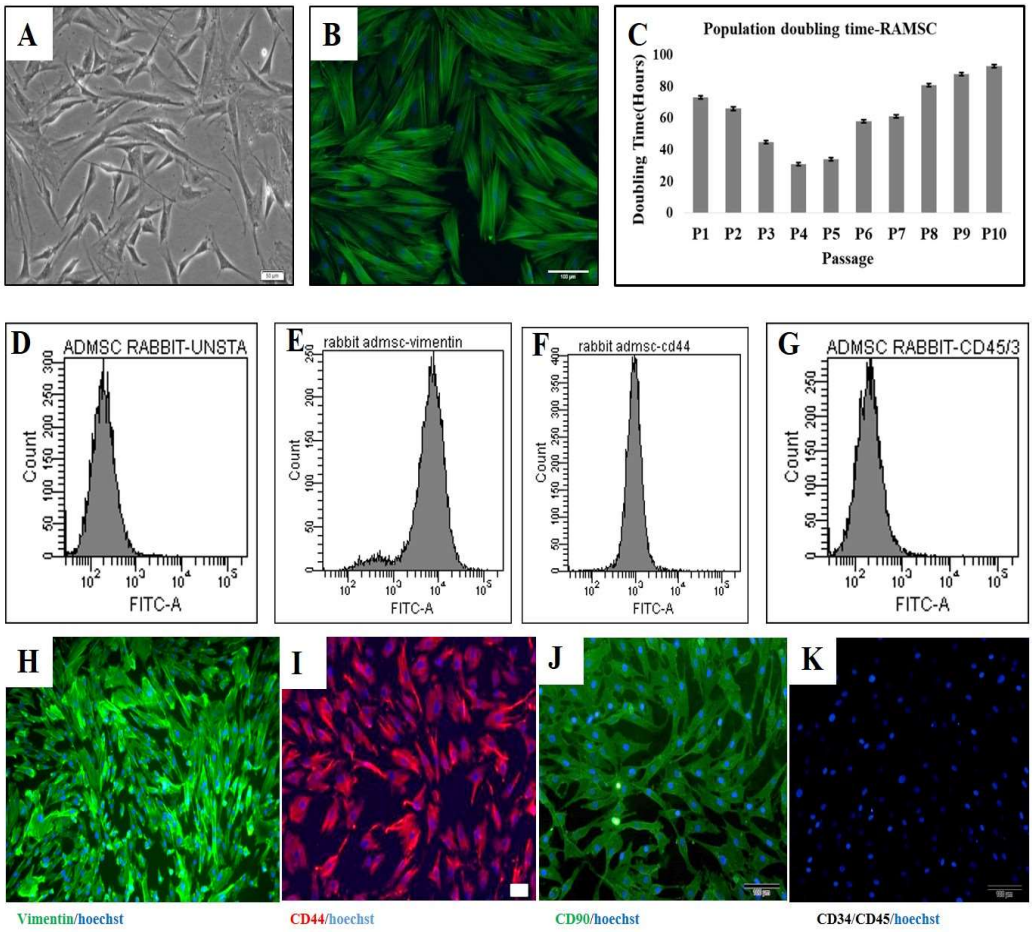


**Figure 4.11: Characterisation of Rabbit Adipose Mesenchymal Stem cells. (A) Cells as appeared on TCPS after isolation (Phase contrast, Scale Bar - 50µm). (B) Actin-Phalladoin staining of isolated cells (Fluorescence, Scale Bar - 100µm), (C) Population doubling time of Cells. (D to G) FACS analysis of markers-Vimentin, CD44, CD34 /45 compared to unstained control. (H to K) Antibody staining of markers Vimentin, CD44, CD90 and CD 34/45, Nuclei stained with Hoechst (Fluorescence, Scale Bar - 100µm).**

Mesenchymal stem cells isolated was subjected to differentiation to adipogenic, osteogenic and chondrogenic lineages by specific differentiation media. After 14 days of differentiation, the adipogenesis was confirmed by Oil red O staining, Figure: 4.12 A, B. Osteogenesis after 21 days was confirmed by Alizarin red S staining for calcium deposition, Figure: 4.12 C, D. The extracellular glycosaminoglycans were stained with Safranine O for confirmation of Chondrogenesis, Figure 4.12 E.

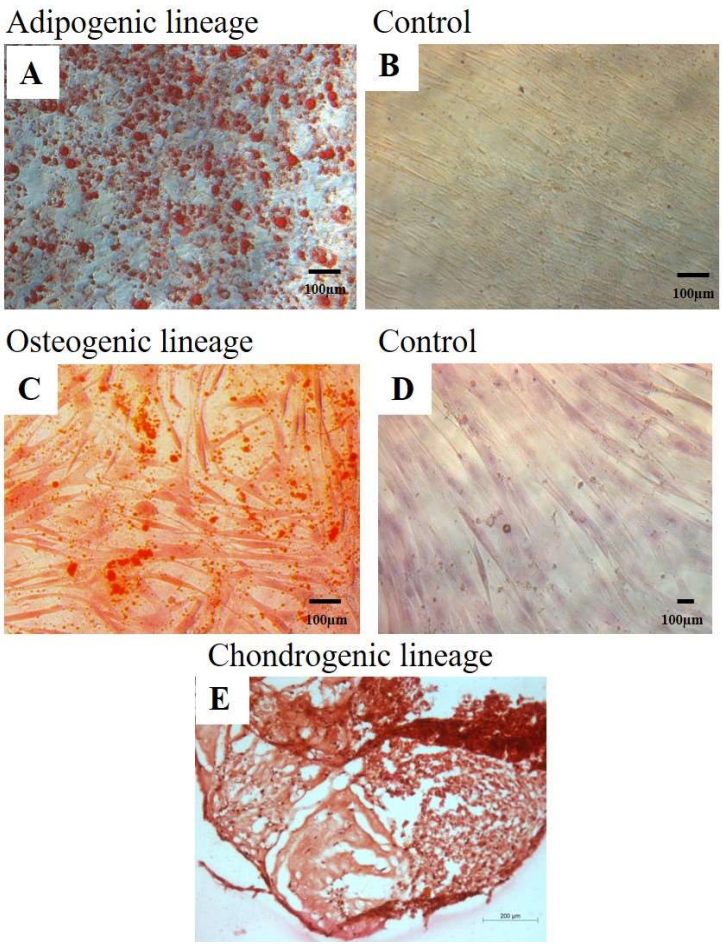


**Figure 4.12: Tri-lineage differentiation of Rabbit mesenchymal Cells. (A, B) Oil red O staining for Adipogenesis and control (Bright field, Scale bar - 100µm). (C, D) Alizarin red S staining for calcium nodules in Osteogenesis and control (Bright field, Scale bar - 100µm). (E) Safranine O staining for chondrogenesis nodule micro-sections (Bright field, Scale bar -200µm).**

### 4.3.2 ISOLATION AND CHARACTERISATION OF SHEEP ADIPOSE DERIVED MESENCHYMAL STEM CELLS (ShMSCs)

Sheep mesenchymal stem cells were isolated by collagenase treatment. The cells appeared on day 7 and became confluent on day 14. They showed fibroblast like appearance on culture plates, Figure: 4.13 A, B. Based on population doubling study cells between passages P3-P6 showed less doubling time and was selected for further *in vitro* studies, Figure: 4.13 C. FACS and immunofluorescence confirmed the stem cell like nature of the isolate cells, Figure: 4.13 D to J.

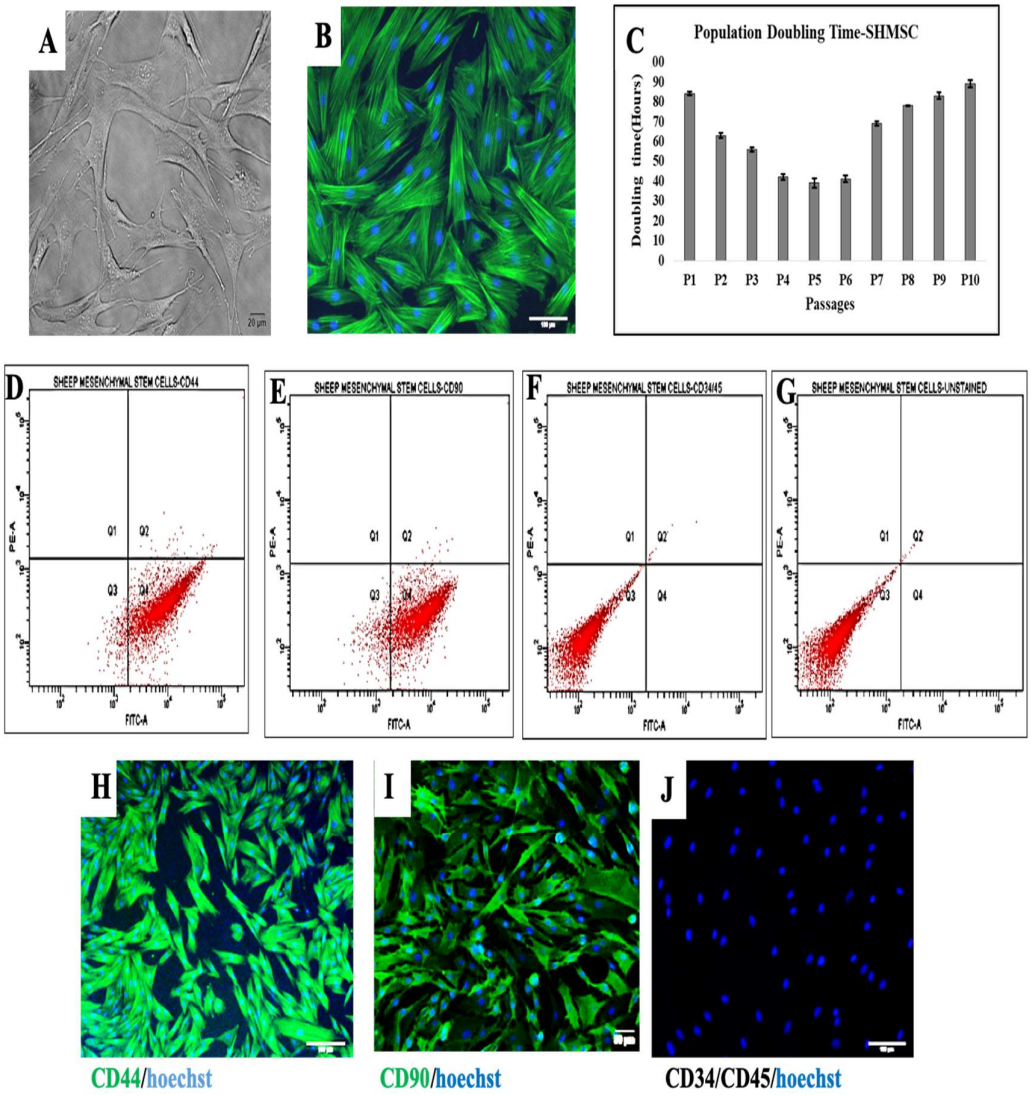


**Figure 4.13: Characterisation of Sheep Adipose Mesenchymal Stem cells. (A) Cells as appeared on TCPS after isolation (Phase contrast, Scale Bar - 20µm). (B) Actin-Phalladoin staining of isolated cells (Fluorescence, Scale Bar - 100µm), (C) Population doubling time of Cells. (D to G) FACS analysis of markers - CD44, CD90, and CD34/45 compared to unstained control. (H to K) Antibody staining of markers Vimentin, CD44, CD90 and CD 34/45, Nuclei stained with Hoechst (Fluorescence, Scale Bar - 100µm).**

Similar to rabbit stem cells, sheep stem cells also showed tri-lineage differentiation. Oil red O stained oil vacuoles confirmed adipogenesis compared to undifferentiated control, Figure: 4.14 A, B. Osteogenic differentiation was stained positive by Alizarin red S staining of deposited calcium nodules, Figure: 4.14 C, D.

Alician blue staining was used to confirm the presence chondrogenic nodules, Figure: 4.14 E, F.

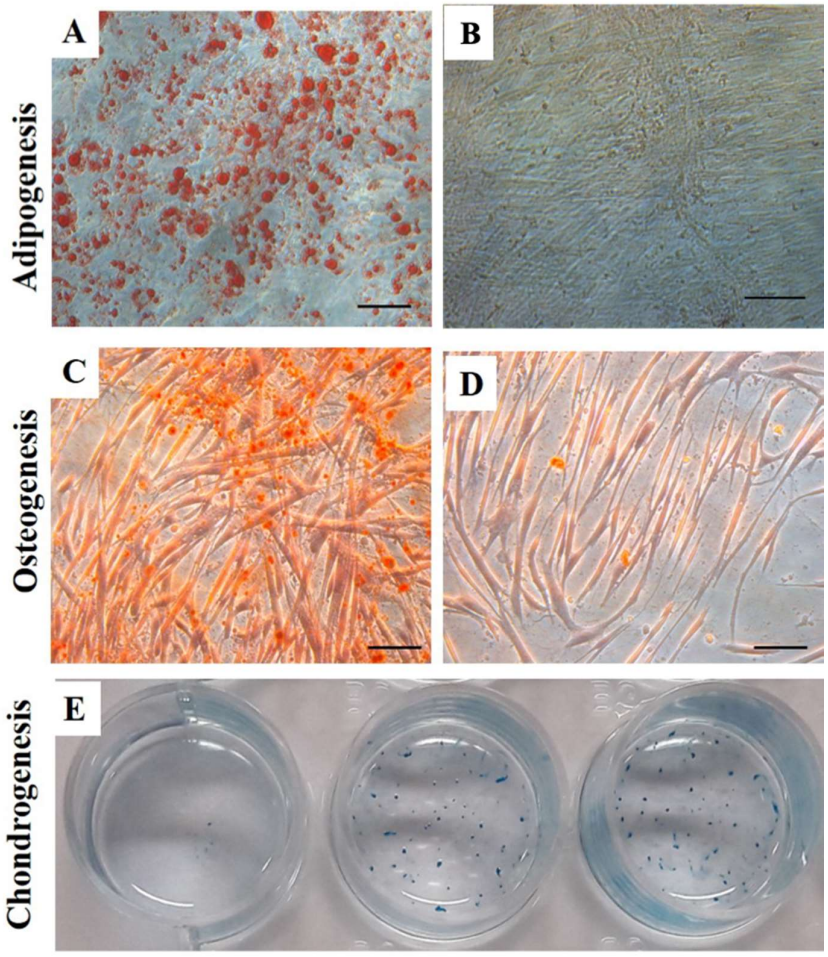


**Figure 4.14. Tri-lineage differentiation of sheep mesenchymal stem cells. (A, B) Oil red O staining for Adipogenesis and control (Bright field, Scale bar - 100µm). (C, D) Alizarin red S staining for calcium nodules in Osteogenesis and control (Bright field, Scale bar - 100µm). (E) Photograph of Alician blue staining for chondrogenesis nodule in micro-mass culture**

## 4.4 CELL - MATERIAL INTERACTIONS

### 4.4.1 CYTOTOXICITY STUDIES: DIRECT CONTACT TESTS AND MTT ASSAY WITH L929 FIBROBLASTS AND ADIPOSE DERIVED MESENCHYMAL STEM CELLS - RABBIT, SHEEP

*In vitro* cytotoxicity assay by direct contact of scaffold with L929 and RAMSC cells shows no morphological change or dead cells when compared to positive and negative controls, Figure: 4.15 A to D. Similarly, Sheep MSCs in contact with scaffold were also showed no signs of toxicity, Figure: 4.16 A to D. The tests were conducted according to ISO 10993 - 5:2009 - Biological evaluation of medical devices - Part 5: Tests for *in vitro* cytotoxicity.

The metabolic activity of both L929 and RAMSC cells were seen to be more than 70% on 24 hour and 48 hours compared to untreated control. The metabolic activity is found to be increased to 80% for RAMSC cells on day 7. The results thus shows that scaffold extract at various time points is non-cytotoxic, Figure: 4.15 E, F. The time points for extract is collected by keeping in mind the differentiation time point of mesenchymal stem cells to smooth muscle cell lineage. However, sheep MSCs showed more than 80 % viability over both 24 hour and 48 hours treatment of scaffold extracts collected at time points day 1, day 3, da y 7, day 14, Figure: 4.16 E.

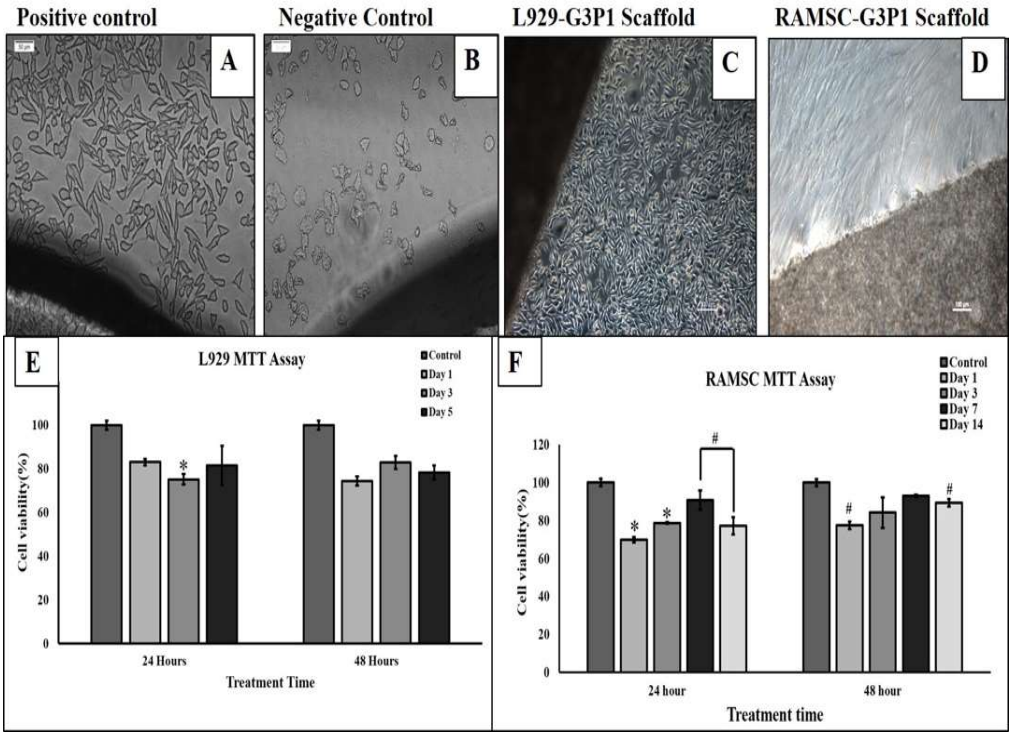


**Fig 4.15. *In vitro* cytotoxicity of G3P1 scaffold, Direct Contact assay, (A) L929 cells contact with positive control (Scale bar - 10µm). (B) L929 cells contact with negative control (Scale bar - 10µm). (C) L929 cells contact with G3P1 scaffold (Scale bar - 100µm). (D) RAMSCs in contact with G3P1 scaffold (Scale bar - 100µm). MTT Assay (E) L929 cells treated with scaffold extract for 24 hour and 48 hours (*p<0.01). (F) RAMSCs treated with scaffold extract for 24 hour and 48 hours (*p<0.01. # p<0.05).**

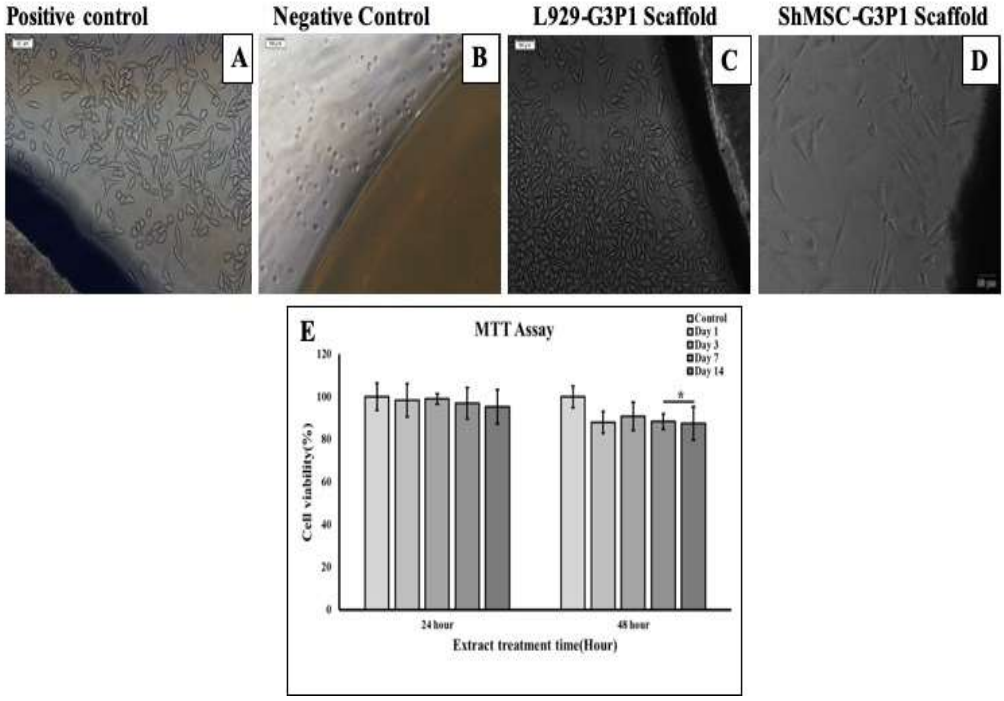


**Figure 4.16. *In vitro* cytotoxicity of G3P1 scaffold, Direct Contact assay, (A) L929 cells contact with positive control (Scale bar - 10µm). (B) L929 cells contact with negative control (Scale bar - 10µm). (C) L929 cells contact with G3P1 scaffold (Scale bar - 100µm). (D) ShMSCs in contact with G3P1 scaffold (Scale bar - 10µm). MTT Assay (E) ShMSCs cells treated with scaffold extract for 24 hour and 48 hours (*p<0.01).**

### 4.4.2 CELL VIABILITY ASSESSMENT

The live/dead cell imaging shows that cells when on the scaffold for different time points like 3, 7 and 14 days were mostly viable, Figure: 4.17 A, B, C. Viable cells emit green fluorescence imparted by Calcein AM when cleaved by cellular esterase. The dead cell takes up ethidium homodimer and emit red fluorescence since their cell membrane was disrupted. The *z* - stacked confocal images of both RAMSCs and ShMSCs, Day 14, Figure: 4.18 A, on scaffold shows more than 95% scaffold was covered by live cells. At day 14, the depth profile of RAMSCs in to the scaffold was analysed by confocal microscope software and it shows that cells penetrate into the scaffold for a depth of about 110µm of scaffold, Figure: 4.17 D.

The cell adhesion and spreading on scaffold detected by actin/nuclear staining. The *z* - stacked image shows that cells spreads on the scaffold and penetrate deep through pores, Figure: 4.17 E, 4.18 B. The ShMSCs actin staining image was used to analyse the depth to which cell penetrates into scaffold and it was observed that ShMSCs migrated up to 35 - 45µm into the scaffold, Figure: 4.18 C. Environmental Scanning electron micrographs also shows the surface of the scaffold covered with MSCs, Figure: 4.17 D, 4.18 D.

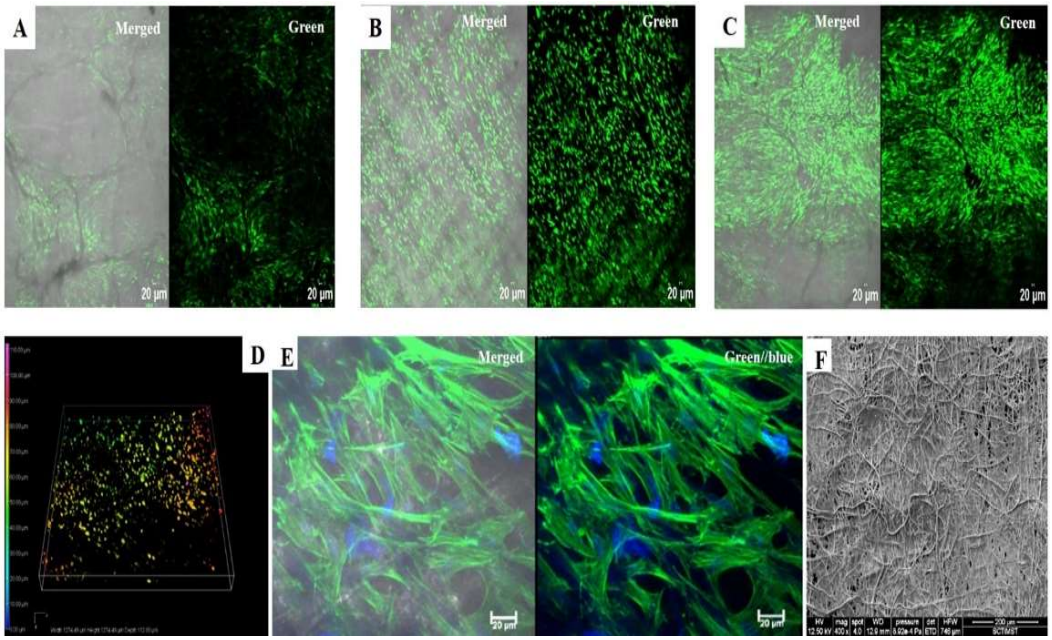


**Figure 4.1.7: Cell Interactions on scaffold. Live /Dead assay of rabbit mesenchymal cells on G3P1 scaffold for day 3(A), day 7 (B), day 14 (C). Live green cells are shown (Confocal *Z*-stacked fluorescence image, Scale bar - 20 µm). (D) Depth profile of cells on scaffold based on live cell (green) fluorescence. (E)Actin-Phalladoin staining of RAMSC on G3P1 - 3mm scaffold, nucleus stained blue (Confocal *Z* - stacked fluorescence image, Scale bar - 20 µm). (E) E-SEM image of section of cells on scaffold (Scale bar - 200 µm).**

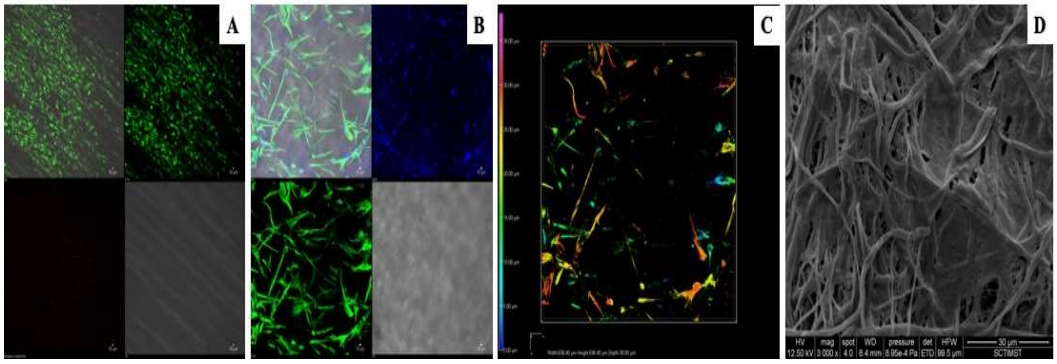


**Figure 4.18: Cell Interactions on scaffold. (A) Live / dead assay of sheep mesenchymal cells on G3P1 – 5 mm scaffold for day 14. Live green cells are shown (Confocal *Z* - stacked fluorescence image, Scale bar - 10 µm). (B) Actin-Phalladoin staining of ShMSC on G3P1 – 5 mm scaffold, nucleus stained blue (Confocal Z-stacked fluorescence image, Scale bar - 10 µm). (C) Depth profile of cells on scaffold based on Actin fluorescence. (D) E-SEM image of section of cells on scaffold (Scale bar - 30 µm).**

### 4.4.3 CONFOCAL RAMAN SPECTROSCOPIC STUDIES

The Raman spectra of the samples - RAMSCs on G3P1 and ShMSCs on G3P1 were acquired by selecting the appropriate areas on the scaffold containing cells. The individual spectra were then analysed for the characteristic components on the scaffold and for the cells. From the spectral plot we can see that the PCL alone showed no characteristic absorptions after 3000 $cm^{-1}$ confirm that the area of scan contains only PCL. The spectra of GV, GVPCL (indicated here for G3P1) and the cell (cytoplasm mainly) have the amine stretch and vibrations which were recorded respectively in the figure. For further analysis we are focusing the characteristic peaks positions in the range from 500 $cm^{-1}$ to 2000 $cm^{-1}$only. The GVPCL (G3P1) area showed the combinations of characteristics peaks of GV and PCL. The new peaks at the amide region (1637 - 1648 $cm^{-1}$) were absent in PCL and cells showed the characteristic protein and DNA stretching vibrations, Figure: 4.18 A to D. This Raman mapping confirms the presence of the individual components (PCL, GV) and their combination (GVPCL / G3P1) as the scaffold which supports the cell growth, Figure: 4.19 A to C.

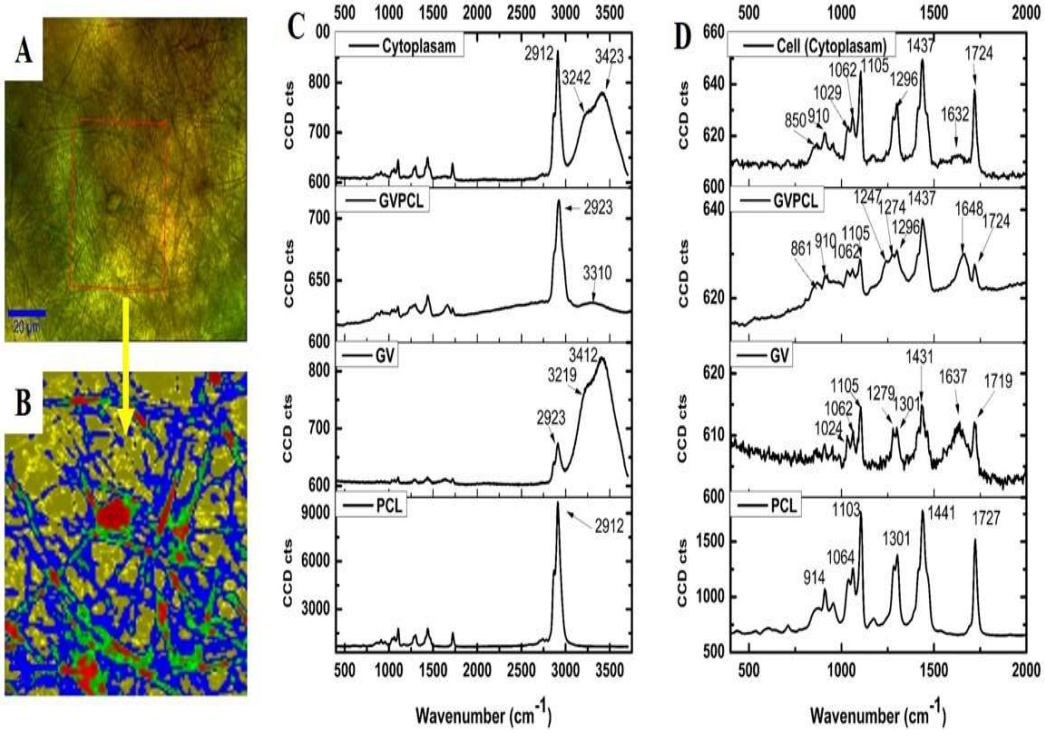


**Figure 4.18. Raman spectra, analysis of RAMSC on G3P1 scaffold (A) Cell seeded scaffold under confocal Raman microscope (Red box: area scanned). (B) Chemically colour coded image of area scanned (Blue: PCL, Yellow: GV, Green: Cytoplasm, Red: Nucleus). (C) Raman Spectra deduced from image. (D) Peak labelled zoomed spectra.**

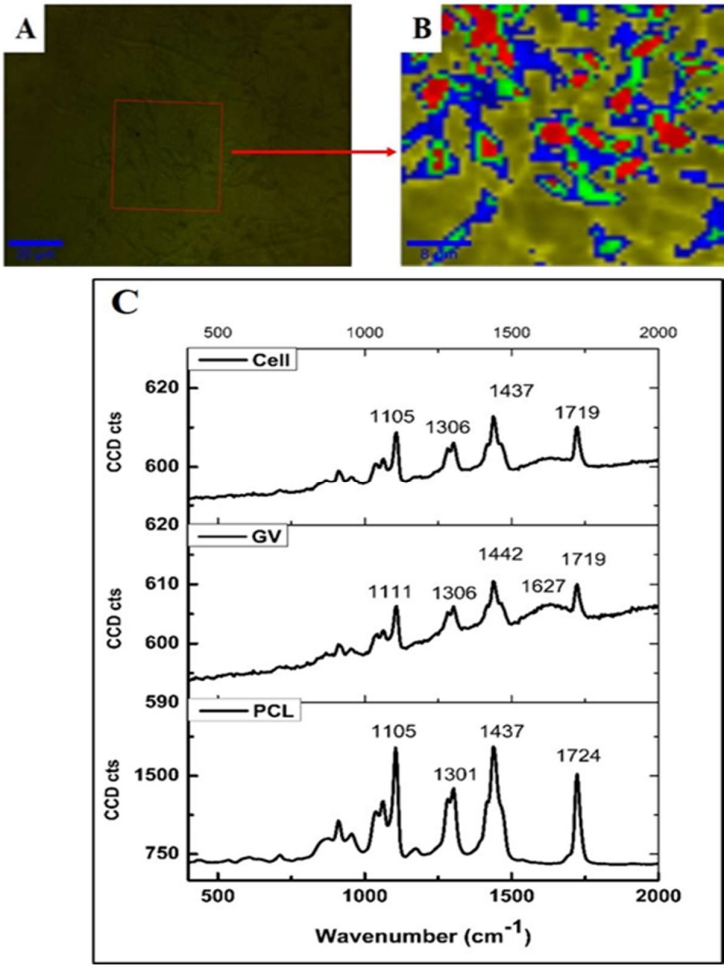


**Figure 4.19. Raman spectra, analysis of ShMSCs on G3P1 scaffold (A) Cell seeded scaffold under confocal Raman microscope (Red box: area scanned). (B) Chemically colour coded image of area scanned (Blue: PCL, Yellow: GV, Green: Cytoplasm, Red: Nucleus). (C) Raman Spectra deduced from image.**

## 4.5 DIFFERENTIATION OF MESENCHYMAL STEM CELLS TO SMOOTH MUSCLE CELL ON SCAFFOLD – RABBIT

Rabbit mesenchymal stem cells and Sheep mesenchymal stem cells were subjected to differentiation to smooth muscle cells both on tissue culture polystyrene plates (TCPS) and G3P1 scaffold. For induction into smooth muscle lineage, TGF-β1 containing biochemical cocktail was used for 14 days, Scheme: 3.

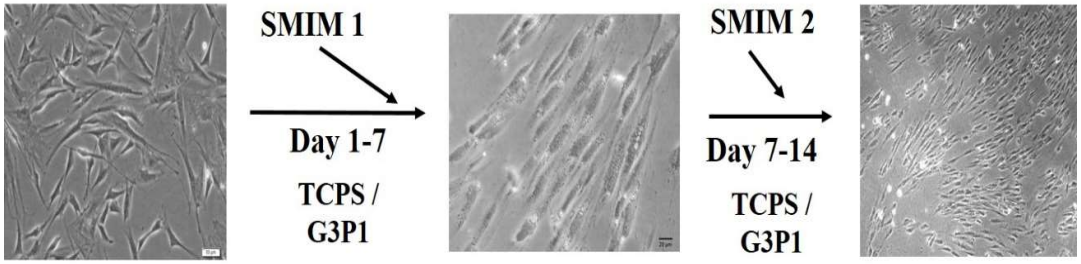


**SMOOTH MUSCLE INDUCTION**

| SMIM 1 | SMIM 2 |
|---|---|
| ➢ DMEM HG<br>➢FBS-3%<br>➢AB/AM-1X<br>➢TGF β(10ng/ml)<br>➢Ascorbic acid(300μM) | ➢DMEM HG<br>➢AB/AM-1X<br>➢TGF β 1(5ng/ml)<br>➢Heparin(100U/ml) |

**Scheme 3: Methodology used for smooth muscle cell induction (RAMSCs on TCPS towards SMCs depicted).**

### 4.5.1 QUANTITATIVE REAL TIME PCR AND IMMUNO-STAINING

In the initial stage of differentiation, TGF-β1 activates Smad pathway and leads to the expression of early marker genes like alpha smooth muscle actin (ASMA), SM22α (Transgelin), Calponin (CNN3) etc., This is in concordance with present protocol that rabbit mesenchymal stem cells seeded on G3P1 scaffold with induction medium shows 33 fold increase in ASMA expression, Figure: 4.20 A, 55 fold increase in transgelin expression, Figure: 4.20 B and 12 fold increase in acidic Calponin (CNN3) compared to cells on TCPS with control medium, Figure: 4.20 C. The expression pattern of SMC genes is under the influence of induction medium on TCPS were also found to be increasing but lesser extent compared to scaffold. In addition to increase in the early and mid-markers of SMCs there is an increase in the expression of late marker myosin heavy chain, MYH11 on G3P1 scaffold, Figure: 4. 20 D. While the expression of the marker is not so pronounced on TCPS which is less than baseline calibrator. The panel of antibody stained for ASMA, SM22α, SMMHC confocal laser scanning microscope also shows the

positivity of cells for early smooth muscle cells markers. SMMHC is the sole markers that is not associated with fibrotic nature of mesenchymal stem cells and expression of the same confirms the contractile nature of differentiated smooth muscle cells, Figure: 4.21 A, B, C.

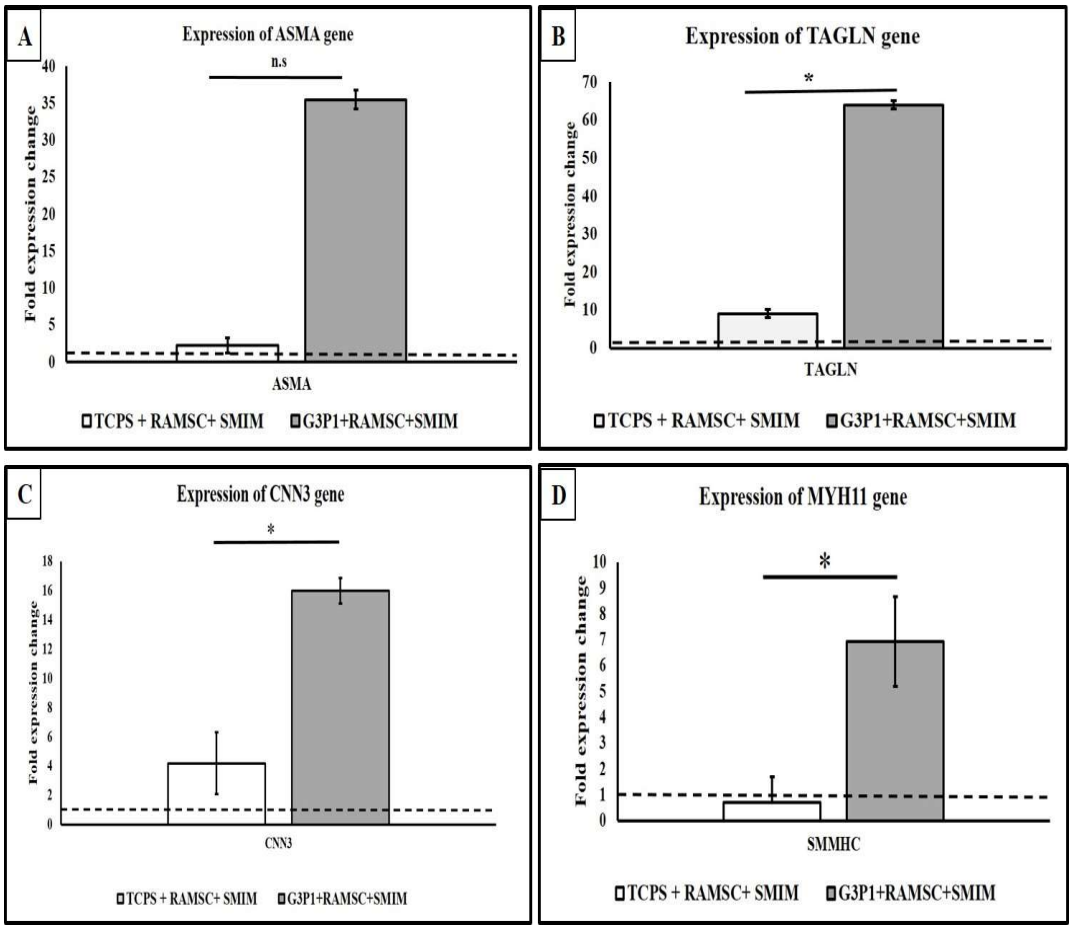


**Figure 4.20: Gene expression profile of differentiated smooth muscle cells on tissue culture plate and G3P1scaffold compared with calibrator (----).(A) Fold change of ASMA gene.(B) Fold change of Transgelin gene.(C) Fold change of Calponin gene.(D) Fold change of SM-MHC gene.(*p<0.01,n.s:non significance).**

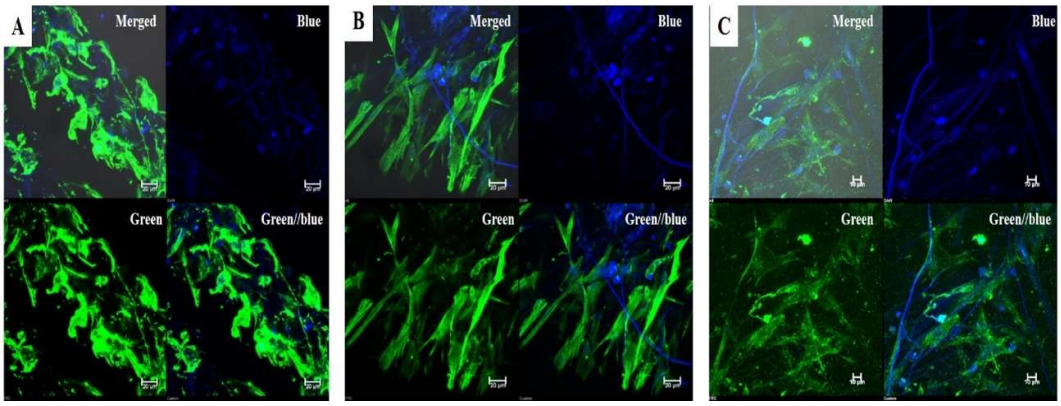


**Figure. 4.21: Confocal laser scanning images of Immunofluorescence (green) of differentiated SMCs on G3P1 scaffold-(A) SM Actin, Scale bar-10µm. (B) SM22α, Scale bar-20µm. (C) SM-MHC Scale bar-10µm. Nuclear Hoechst and Fibers (Blue). (Confocal *Z* - stack fluorescence).**

### 4.5.2 ESTIMATION OF EXTRACELLULAR MATRIX PROTEINS

Blood vessel extracellular matrix plays a crucial role in maintaining the overall physiological function of the vessel. The collagen gene expression profile of SMCs differentiated on G3P1 scaffold shows a 147-fold increase and 42-fold increase on TCPS, Figure: 4.22 A. This enhanced difference indicate that the differentiated cells produce collagen type 1and vascular graft that is conducive for *in vivo* regeneration on its own. Total soluble collagen extracted from scaffold is assayed to be150 µg/mg of wet weight of tissue by Sircol assay. Another relevant component of blood vessel extracellular matrix is elastin. Our results show appreciable up regulation of elastin gene on G3P1 scaffold while it's less than base line on TCPS, Figure: 4.22 B. The total elastin estimation provided an amount of 15 µg/mg wet weight of elastin deposition on scaffold.

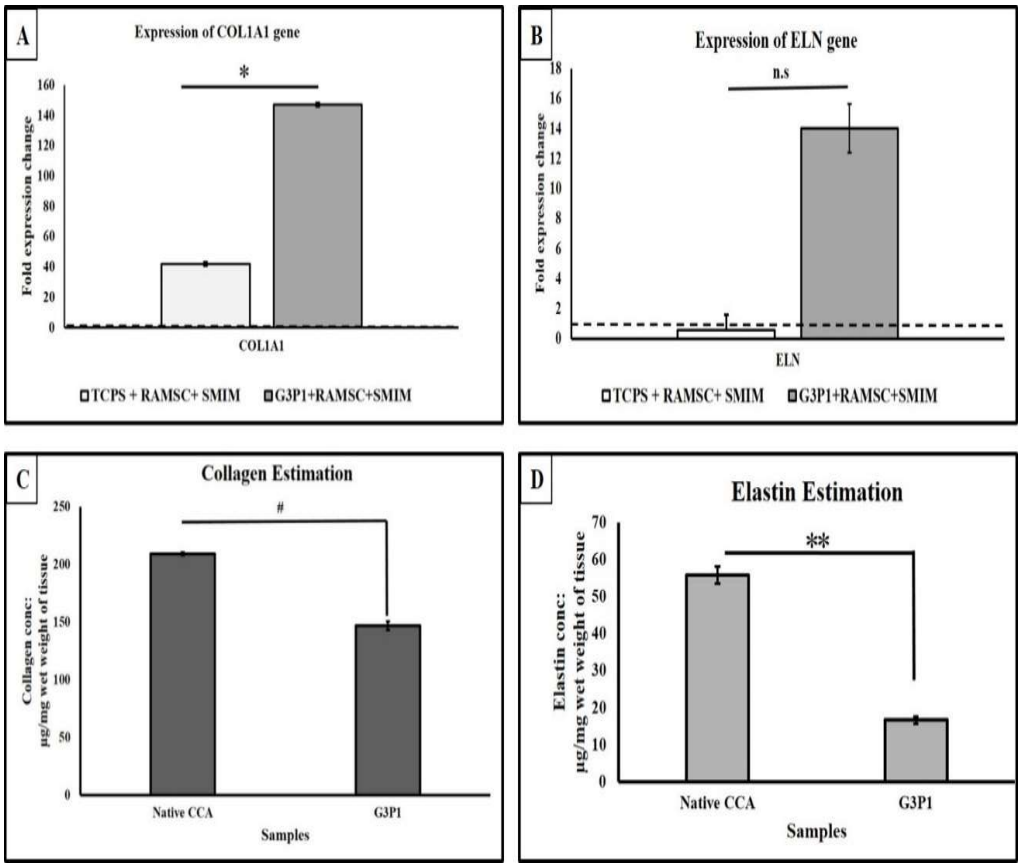


**Figure 4.21. (A) Extracellular matrix gene expression of Collagen. (B) Elastin. (C) Sircol collagen estimation (D) and Fastin Elastin estimation (*P<0.01, #P<0.001, **P<0.0001, n.s: non-significant).**

## 4.6 DIFFERENTIATION OF MESENCHYMAL STEM CELLS TO SMOOTH MUSCLE CELL ON SCAFFOLD – SHEEP

Sheep mesenchymal stem cells seeded on G3P1 scaffold differentiated to smooth muscle cells following the same protocol as mentioned in Scheme 2. Compared to calibrator gene expression, there was an increased expression of ASMA gene both in tissue culture plate and G3P1 scaffold, Figure: 4.22 A. However, the late marker gene SMMHC (Myh 11) showed a two-fold increase in expression on G3P1 scaffold than on culture plate, Figure: 4.22 B. There was increased expression of collagen gene also in culture plate than in G3P1 when cells were differentiated, Figure: 4.22 C. We could justify this as, both ASMA and COL1AI were also markers of proliferative phase of

SMCs, so on plates even though differentiated to smooth muscle lineage, cell will be still in proliferative stage which was less evident on G3P1 scaffold. Immunofluorescence also confirms the differentiation, Figure: 4.23 A to C.

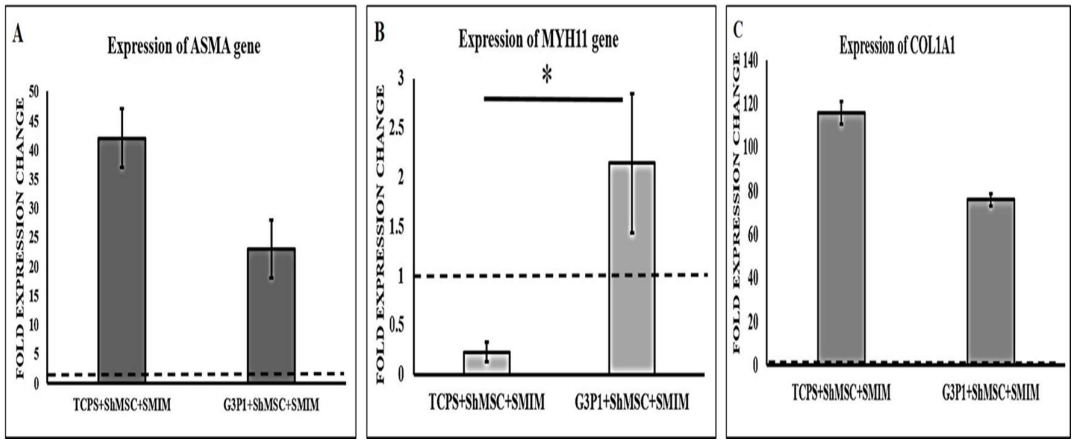


**Figure 4.22: Gene expression profile of differentiated smooth muscle cells on tissue culture plate and G3P1scaffold compared with calibrator (----). (A) Fold change of ASMA gene. (B) Fold change of SMMHC gene. (C) Fold change of Collagen gene. (*p<0.01, n.s: non significance).**

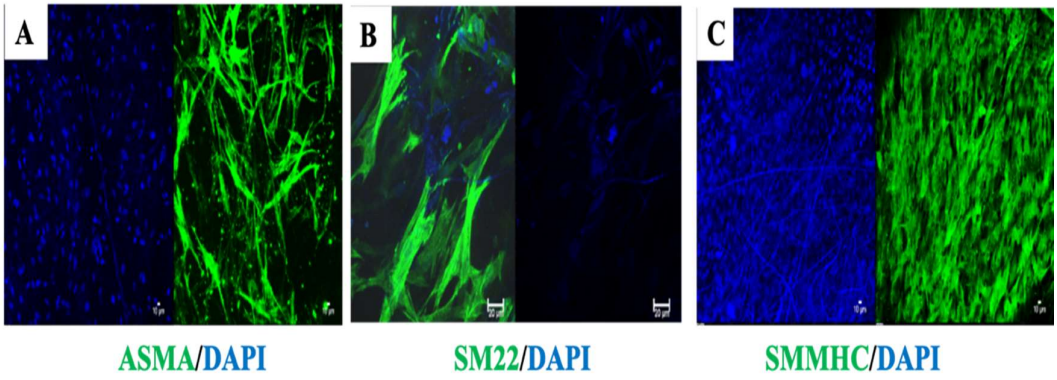


**Figure. 4.23: Confocal laser scanning images of Immunofluorescence (green) of differentiated SMCs on G3P1 scaffold-(A) SM Actin, Scale bar-10µm. (B) SM22α, Scale bar-20µm. (C) SM-MHC Scale bar-10µm. Nuclear Hoechst and Fibers (Blue). (Confocal *Z* stack- Fluorescence).**

## 4.7 *IN VITRO* HEMOCOMPATIBILITY OF THE SCAFFOLD

The blood compatibility of the scaffold was studies as per the ISO standards. It was seen that the values obtained for percentage change in haemolysis, Leucocyte count, RBC count and platelet count were within the limits prescribed for biomaterial interaction with blood. The values obtained were summarised in Table: 4.11 (Acceptable values given in bracket in the table). The platelet adhesion on the scaffold were scanned under SEM and there were less evident platelets adhered to scaffold with sparse RBCs Figure: 4.24. Overall the blood compatibility studies indicate that the blood compatible nature of G3P1 scaffold intended to be used as vascular graft.

| TEST | Percentage change (Acceptable value) |
|---|---|
| Hemolysis | 0.05 ± 0.01% (<0.1 %) |
| White blood cells count | 3.05 ± 0.9% (<5 %) |
| Red blood cells count | 0.68 ± 0.4% (<5 %) |
| Platelet count | 7.13 ± 1.3% (<10%) |

**Table 4.11: *In vitro* hemocompatibility of G3P1 scaffold**

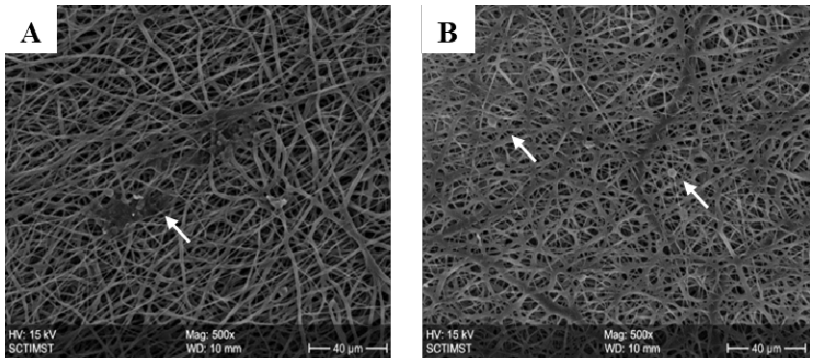


**Figure 4.24: Platelet Adhesion assay. (A, B) G3P1 scaffold showing adhered platelets and RBCs (White arrow).**

## 4.8 PART II – CO-CULTURE OF PERIVASCULAR STEM CELLS AND ENDOTHELIAL CELLS ON POLY (ETHYL METHACRYLATE-CO-DI ETHYL AMINO ETHYL ACRYLATE) SCAFFOLD

### 4.8.1 ISOLATION OF HUMAN ADIPOSE DERIVED PERIVASCULAR STEM CELLS AND ENDOTHELIAL CELLS

After human adipose tissue digestion by collagenases, the flow cytometry mediated identification and isolation of perivascular stem cells namely adventitial cells, pericytes were isolated. Endothelial cells were also isolated. Initially after compensation and gating dead cell population from cell suspension was ruled out. CD45/CD56 single cells were then selected and from this CD34+/CD31+ endothelial cells were collected (16 ± 2%). Later, CD34+/CD146- adventitial cells (37 ± 12%) and CD34-/CD146+ pericytes (19 ± 1.3%) were sorted, Figure: 4.25 A to D. The endothelial cells showed cobble stone morphology and perivascular cells showed fibroblast like morphology, Figure: 4.26 A to C. Perivascular cells between P3 - P5 were used for further experiments. Endothelial cells however showed lesser proliferation capacity after P4 and there was a lack of enough number of cells. The studies were thus carried out by late endothelial outgrowth cells. The group of perivascular cells were a sub population of mesenchymal cells and shows stem cells like properties when cultured *in vitro* which was stained positive for CD44/CD90 and pericyte specific CD146, Figure: 4.27 A to C, on tissue culture plates.

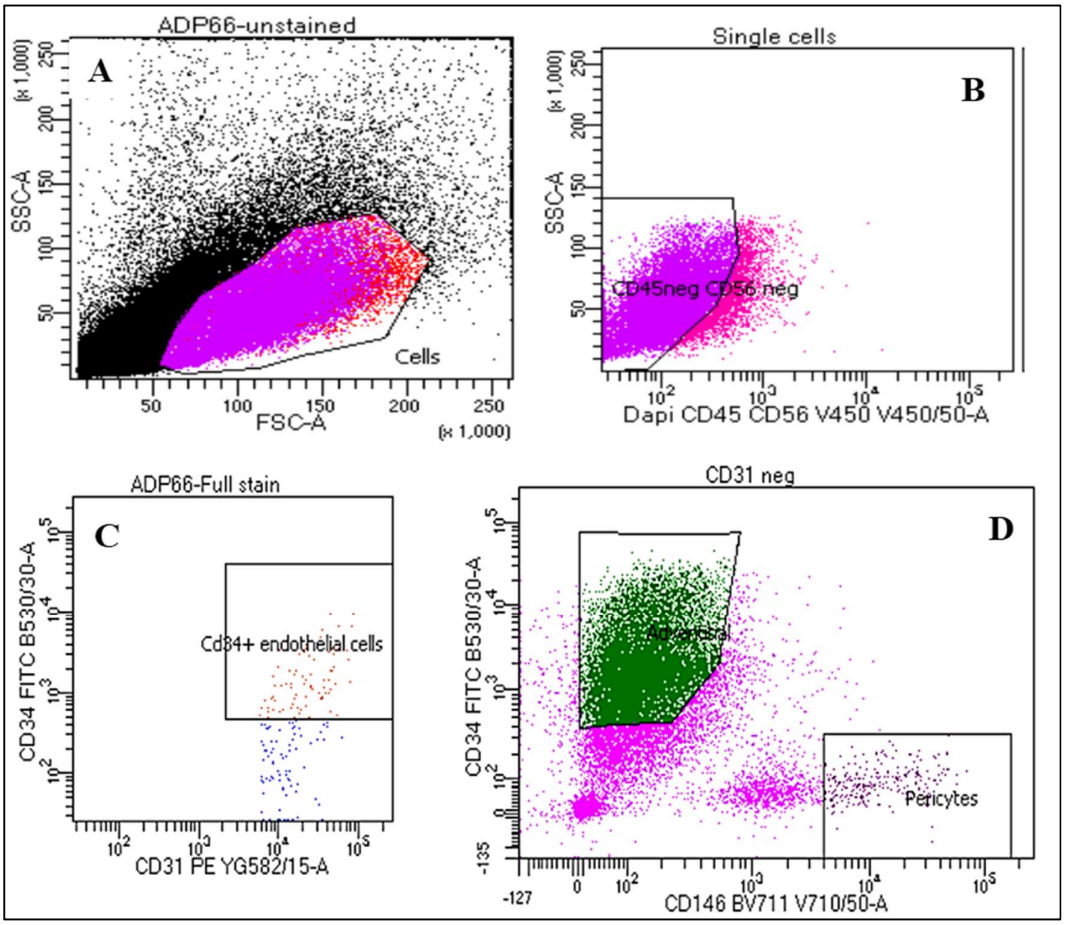


**Figure 4.25: Flow cytometry of adipose tissue digest. (A) Dead cell exclusion by DAPI staining. (B) CD45/CD56 cell selection and exclusion. (C) Isolation of endothelial cells. (D) Isolation of perivascular adventitial cells and pericytes.**

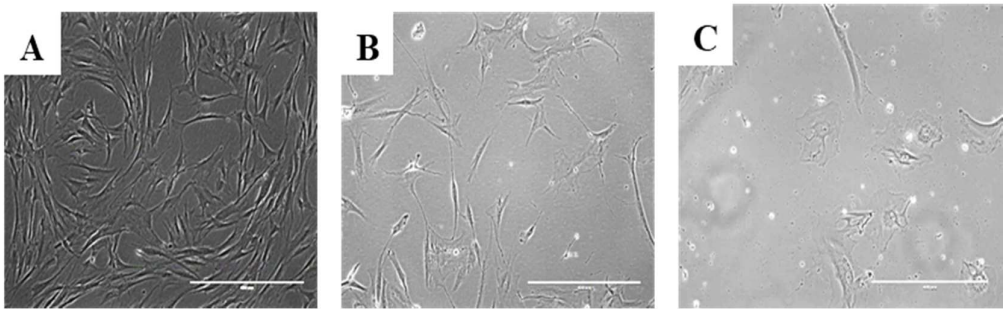


**Figure 4.26: Phase contrast microscopic images of isolated cells of adipose tissue digest. (A) Adventitial cells. (B) D) Isolation of perivascular adventitial cells and pericytes (Scale bar - 20µm).**

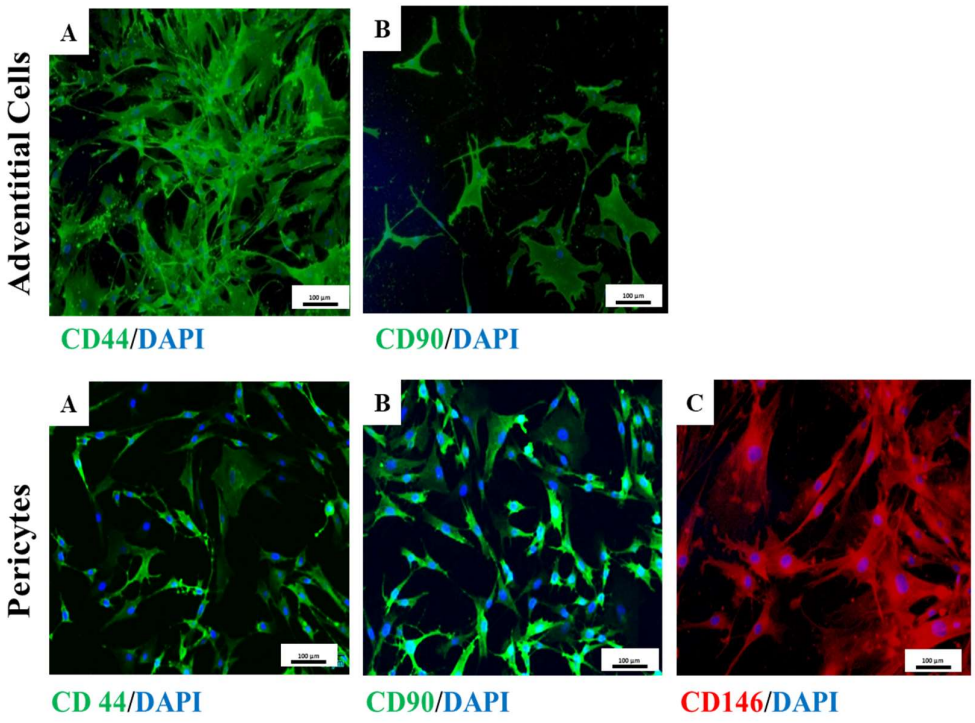


**Figure 4.27: Immunofluorescence of Perivascular Cells - Adventitial cells (A) CD44/DAPI (Scale bar - 100µm). (B) CD90/DAPI (Scale bar - 100µm). Pericytes (A) CD44/DAPI (Scale bar - 100µm). (C) CD90/DAPI (Scale bar - 100µm). (D) CD146/DAPI (Scale bar - 100µm).**

### 4.8.2 CELL COMPATIBILITY OF SCAFFOLD – LIVE / DEAD ASSAY AND SEM

Live / dead assay showed that the cells on scaffold were live at different time points. Live cells emitted green fluorescence compared with dead cells which emitted red fluorescence, Figure: 4.28 A to B panel. The scanning electron microscopic image at day 14 of the three cell types shows that the cell covered almost whole area of the scaffold. However, it was evident that endothelial cell had low proliferation capacity compared to adventitial cell and pericytes on scaffold. This was much similar to what was observed in tissue culture plates, Figure: 4.28 C panel.

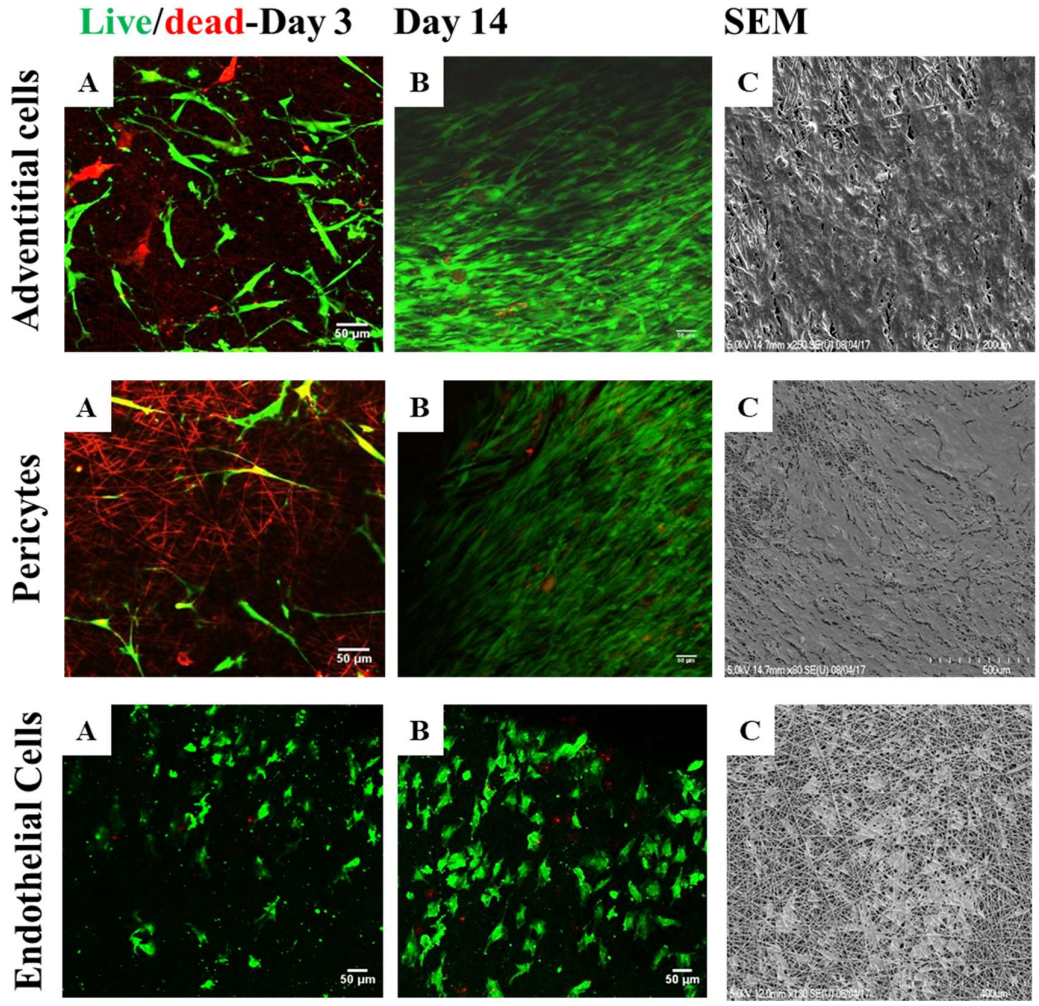


**Figure 4.28: Cell Interactions on 8g7 scaffold. (A) Live /Dead assay of Adventitial cells, pericytes and endothelial cells on Day 3. Live green cells/ dead red cells and fibres are shown (Confocal *Z*-stacked fluorescence image, Scale bar - 50 µm). (B) Live /Dead assay of Adventitial cells, pericytes and endothelial cells on Day 14 (Scale bar - 50 µm). (C) SEM image of cells on scaffold (Scale bar - 200 µm, 500 µm, 400 µm).**

### 4.8.3 MTT ASSAY

Cell viability percentage shows than when adventitial cell grown on 8g7 scaffold at all-time point cell viability was greater than 80%. In the case of pericytes the viability gradually increases over time points and at day 14 it was above 80%. Endothelial cell, at day 3 viability was more than 60% which increases over 80% on day 7 and on day 14

was 78%. Cell viability assay confirms that scaffold was cell growth conducive, Figure: 4.29 A to C.

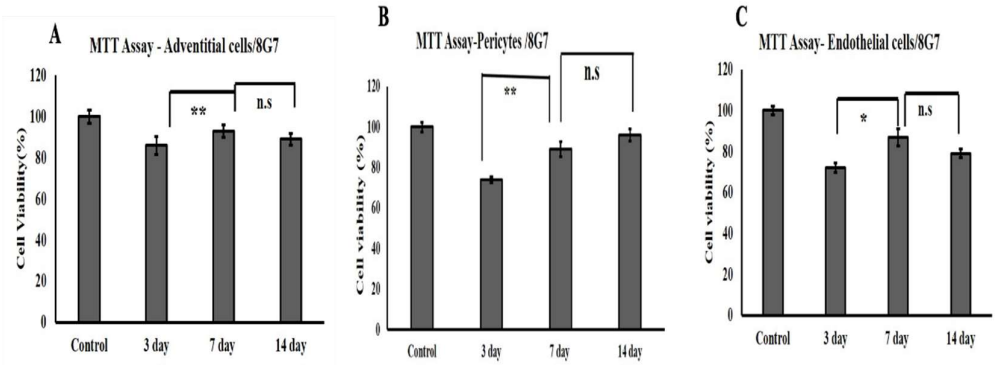


**Figure 4.29: Cell Interactions on 8g7 scaffold. (A) MTT Assay of Adventitial cells. (B) MTT assay of Pericytes. (C) MTT Assay of Endothelial cells. (**p <0.001).**

### 4.8.4 β-ACTIN AND IMMUNOSTAINING OF CELL MARKERS ON THE SEEDED SCAFFOLD

The cell adhesion on 8g7 scaffold was proved by actin-cytoskeletal staining. The adventitial cells, pericytes and endothelial cells exhibited attachment and spreading on the scaffold, Figure 4.30 A, B, C, D. The identity of each cell on scaffold was investigated by immunofluorescence staining. The cells showed positivity with respect to all markers specific to them in a similar fashion of what they exhibit when cultures on tissue culture plates, Figure 4.30 A, B, C, D. These experiments prove that electrospun 8g7 allow attachment, proliferation and marker expression of these cells when cultured on scaffold.

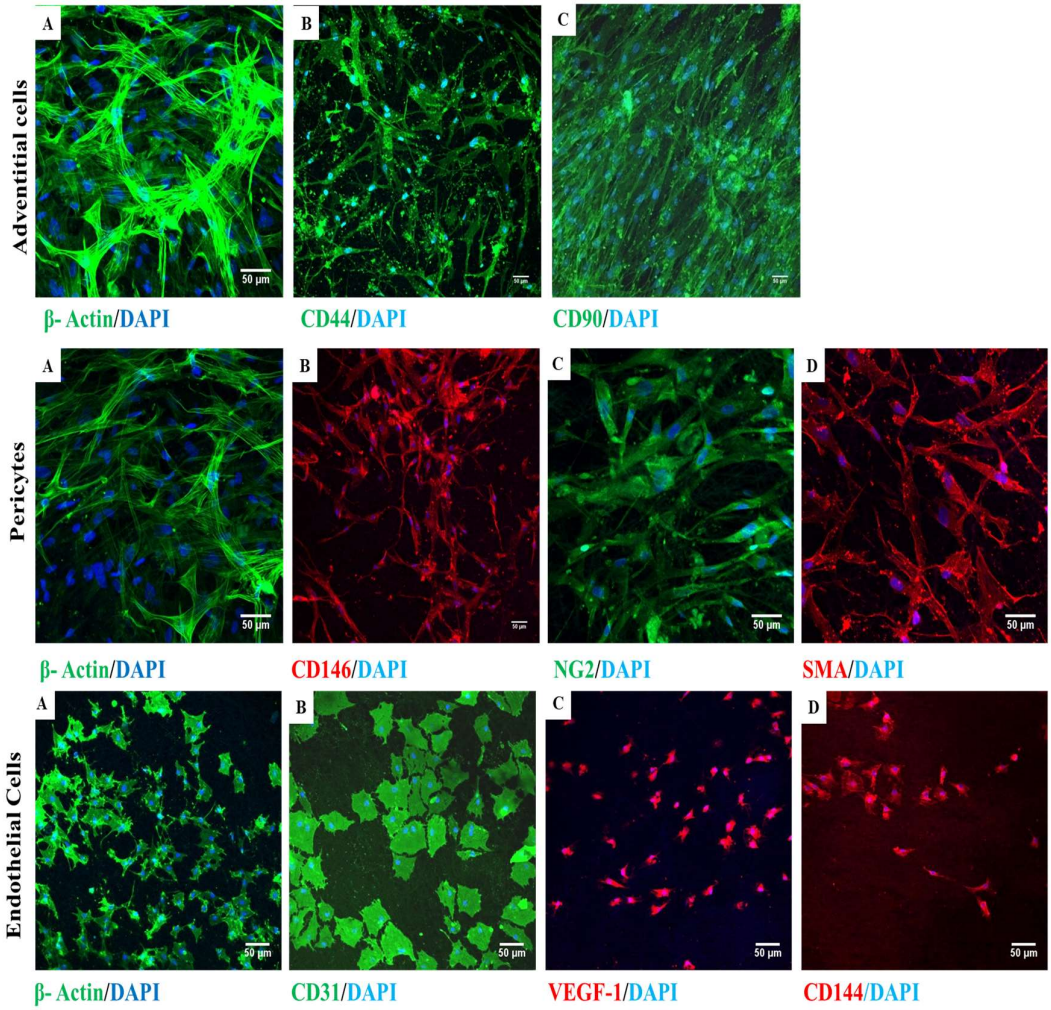


**Figure 4.30: Fluorescence of Perivascular Cells and endothelial cells on 8g7 scaffold – Adventitial cells (A) Actin-phalladoin staining (Scale bar - 50µm). (B) CD44/DAPI (Scale bar - 50µm). (C) CD90/DAPI (Scale bar - 50µm) Pericytes (A) Actin-phalladoin staining (Scale bar - 50µm). (B) CD146/DAPI (Scale bar-50µm). (C) Neural glial factor-2/DAPI (Scale bar - 50µm). (D) Smooth muscle actin/DAPI (Scale bar - 50µm). Endothelial cells (A) Actin-phalladoin staining (Scale bar - 50µm). (B) CD31/DAPI (Scale bar - 20µm). (C) Vascular endothelial growth factor-1/DAPI (Scale bar - 50µm). (D) CD144/DAPI (Scale bar - 50µm).**

## 4.9 CO-CULTURE OF PERIVASCULAR CELLS WITH ENDOTHELIAL CELLS ON SCAFFOLD

Co-culture systems – Adventitial cells: endothelial cells and pericytes: endothelial cells were established on scaffold after standardising different conditions. The media used for co-culture was EGM-2 as this media supported the growth and proliferation of perivascular cells and endothelial cells. The ration of each cell type was fixed by trial and error of different ratios. It was evident from the co-culture that adventitial cells always proliferated faster and outnumbered endothelial cells when cultured in equal or low endothelial cell numbers. The endothelial cells were evident and was able to equalise with adventitial proliferation when the ratio of adventitial to endothelial cells was 1:5. The cells co-cultured at this ratio were characterised by specific markers, Figure: 4.31. At this ratio of 1:5 endothelial cells appeared on day 3 which was observed by double immunofluorescence staining of CD31/CD44. Both cells proliferated and expressed their markers on day 7 and day 14. Pericytes, on the other hand supported endothelial cell growth even in lower ratio. A 1:1 ratio of pericyte to endothelial cells helped both cells to survive and express their markers, Figure 4.31 A, B, C at different time points.

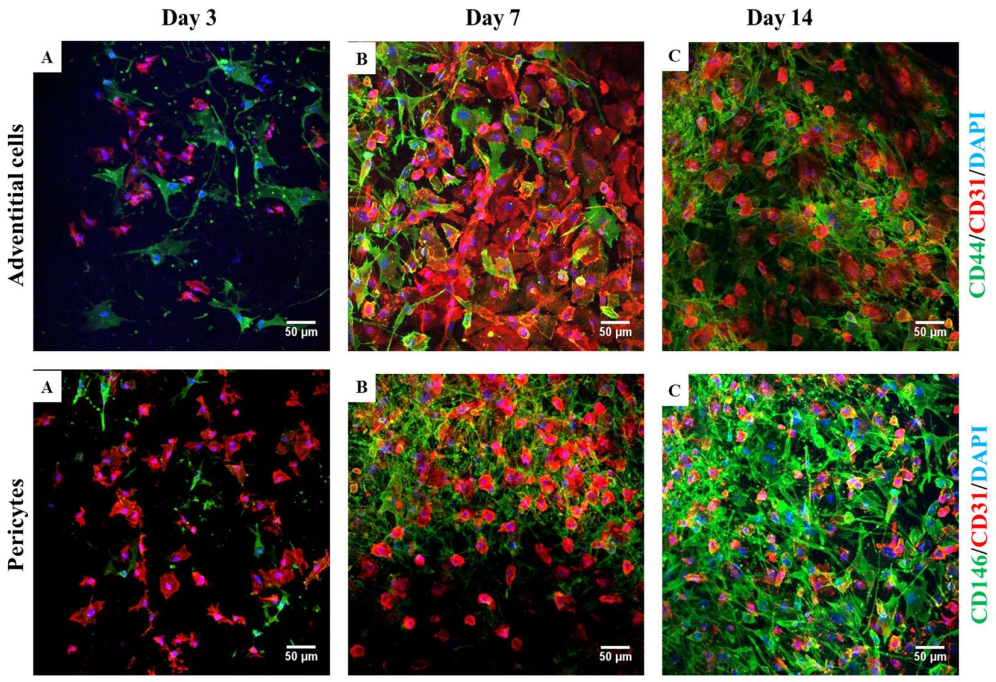


**Figure 4.31: Co-culture of perivascular stem cells with endothelial cells on 8g7 scaffold. Confocal laser scanning z-stacked images (Scale bar - 50µm).**

### 4.9.1 ANGIOGENESIS ASSAY

Angiogenesis assay was performed with the co-cultured cell supernatant (devoid of serum and supplements) in order to analyse the efficacy of co-culture system to initiate angiogenesis. The condition media collected from each co-culture system was pooled and filtered. The secretome analysis by angiogenesis proteome profiler showed that secreted angiogenesis promoting growth factors like angiogenin, platelet derived growth factor - AA/BB, vascular endothelial growth factor was highly secreted by pericyte-endothelial cell co-culture system rather than adventitial cell-endothelial cell. However, level of both epidermal growth factor and thrombospondin was less for pericyte-endothelial system compared to adventitial-endothelial system. This fairly shows that the endothelial cell maintenance was more pronounced in adventitial-endothelial system and angiogenesis was more in pericyte-endothelial system, Figure: 4.32 A, B. The study thus highlights the relevance of each cell-cell interaction on 8g7 scaffold and to conclude a tri-culture system mimicking *in vivo* conditions helps blood vessel strength and integrity.

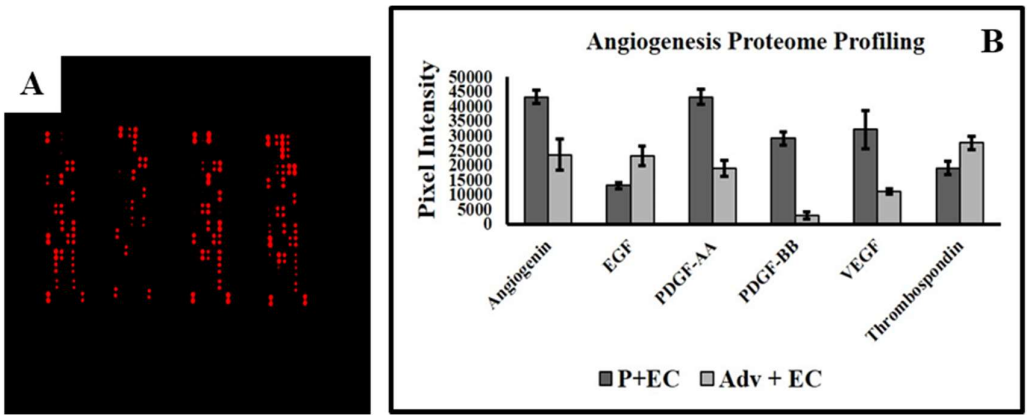


**Figure 4.32: Angiogenesis assay. (A) Angiogenesis array developed after secretome treatment (LiCOR intensity image). (B) Graft showing the pixel intensity of different growth factor in secretome of two co-culture system derived from angiogenesis array.**

# SECTION III – *IN VIVO* EVALUATION OF GELTIN-VINYL ACETATE / POLY-ε-CAPROLACTONE ELECTROSPUN SCAFFOLD, G3P1

## 4.10 PART I – *IN VIVO* EVALUATION IN RABBIT MODEL

### 4.10.1 SURGICAL REPLACEMENT OF RABBIT COMMON CAROTID ARTERY WITH G3P1 SCAFFOLD CELLULARISED WITH DIFFERENTIATED SMOOTH MUSCLE CELLS

The G3P1 – 3 mm graft with smooth muscle cells were used to as rabbit common carotid artery interposition graft. After replacement there was no blood leakage and rabbits recovered healthy post-operatively. However, the 3mm diameter graft showed a mismatch at anastomosis and it was evident during implantation. The scaffold had good handling properties and suture ability, Figure 4.33 A to C. After two weeks of the study angiograms revealed a blockage in both graft and there was no flow of dye when injected in the opposite side of graft. But there was faint flow dye in the second rabbit when injected in same side of the graft implanted. This may be either due to partial occlusion of the graft or may be dislodgement of thrombus with pressure of injection, Figure: 4.34.

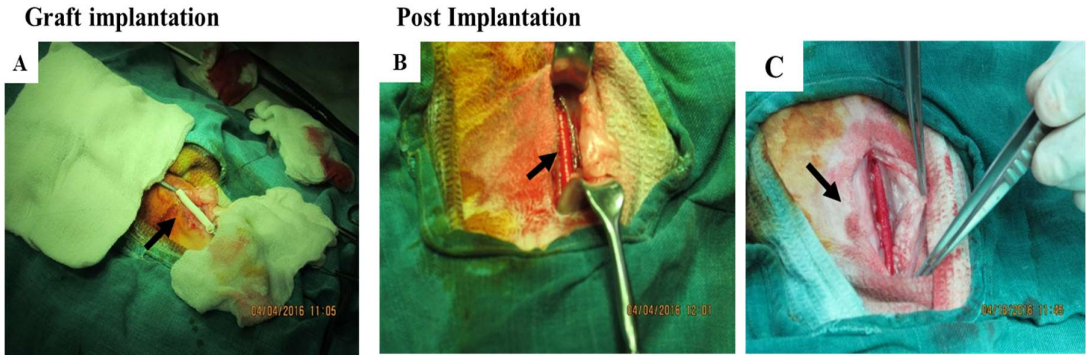


**Figure 4.33: Implantation of G3P1 – 3 mm in rabbit. (A) Graft prior to implantation. (B, C) Graft replacing carotid artery (black arrow).**

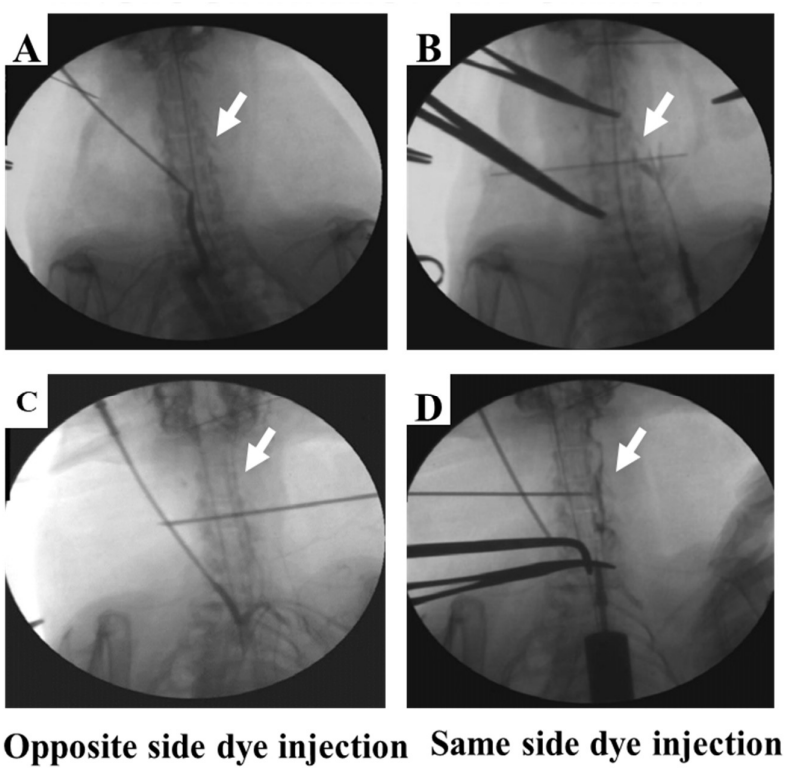


**Figure 4.34: Angiographic evaluation of implant. (A) Opposite side injection in rabbit one (B) Same side injection in rabbit one (C) Opposite side injection in rabbit two. (D) Same side injection in rabbit two (Dye flow path white arrow).**

### 4.10.2 GROSS OBSERVATION OF THE IMPLANT

The excised implant was cut open and observed after angiographic evaluation. It was seen than both the grafts were occluded at anastomosis. The mid region of graft was fairly clear indicating minimal blood flow. The size of the implant has been considerably reduced and it was surrounded by tissue, Figure: 4.35 A, B. Haematoxylin and eosin staining also confirms this, Figure: 4.34 C, D.

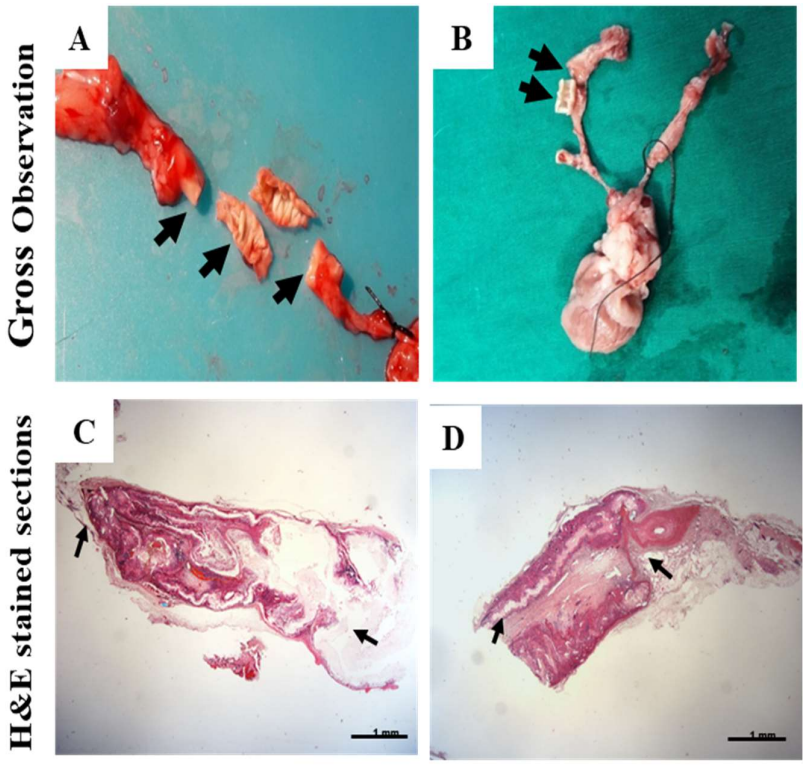


**Figure 4.35: Gross observation of graft explant. (A, B) The explanted graft with rabbit carotid artery (Black arrows shows anastomosis and lumen). (C, D) The H&E sections of graft showing occluded anastomosis and narrowed lumen (Black arrows, Scale bar – 1 mm).**

### 4.10.3 HISTOPATHOLOGICAL EVALUATIONS

The proximal and distal anastomosis contained a layer of outer connective tissue with collagen fibrils and fibroblast surrounding the graft. Lumen had fibrous tissue with fibroblasts and spindle shaped cells/Moderate granulomatous inflammation containing polymorphonuclear cells and foreign body giant cells were observed. The middle graft region remained empty with no evidence of blood flow. Moderate granulomatous inflammation was observed. The anastomoses were completely occluded. The evidence from histology also shows that there was diameter mis-match between graft of 3 mm with lesser diameter rabbit carotid artery which might have also led to anastomotic occlusion, Figure: 4.36 A to D.

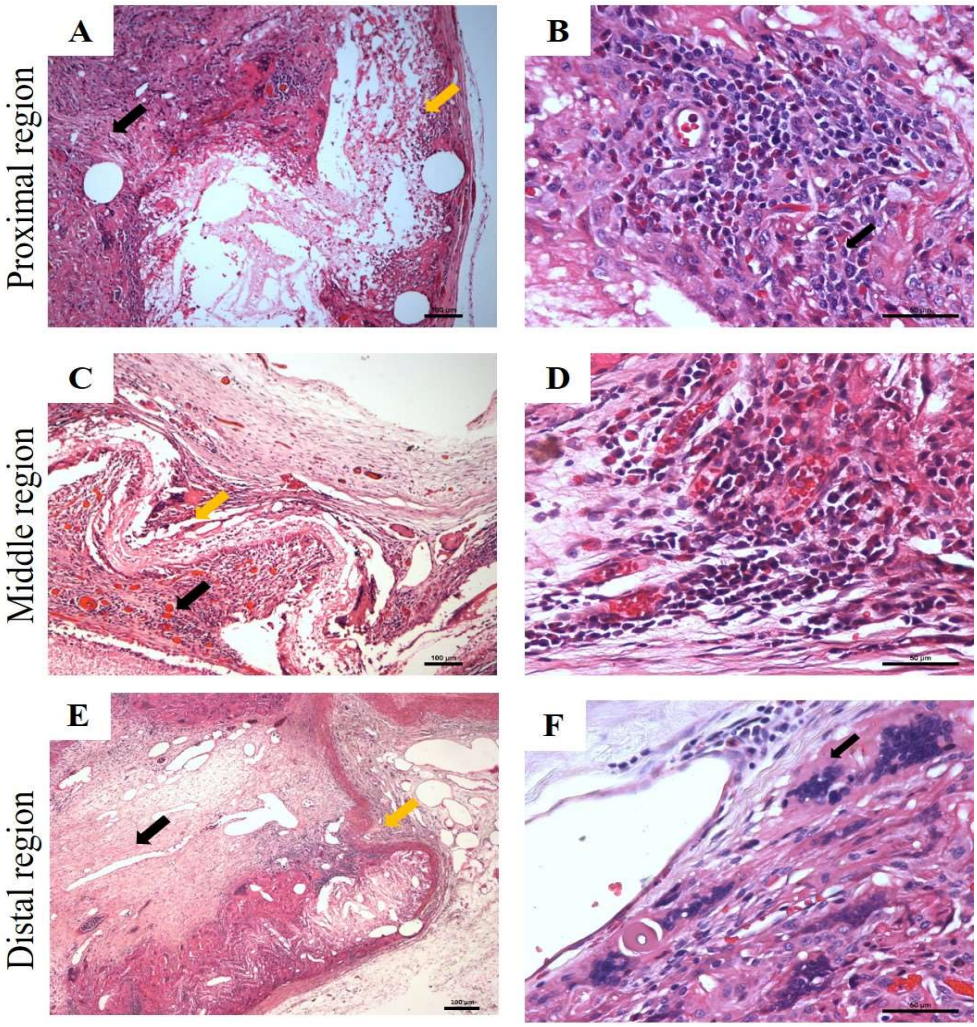


**Figure 4.36: Histopathological evaluation of implanted G3P1-3mm vascular graft explant from rabbit. (A) Proximal region graft, lumen indicated by black arrow. Anastomotic end by yellow arrow (Scale bar - 100µm, 10x). (B) Lumen of proximal region black arrow indicating poly morphonuclear cells (Scale bar - 100µm, 40x). (C) Middle region graft, lumen indicated by black arrow. Anastomotic end by yellow arrow (Scale bar - 100µm, 10x). (D) Lumen of middle region (Scale bar - 100µm, 40x). (E) Distal region graft, lumen indicated by black arrow. Anastomotic end by yellow arrow (Scale bar - 100µm, 10x). (D) Distal of middle region (Scale bar - 100µm, 40x).**

## 4.11 PART II – *IN VIVO* EVALUATION IN SHEEP MODEL

### 4.11.1 SURGICAL PROCEDURE: VASCULAR GRAFT IMPLANTATION IN SHEEP COMMON CAROTID ARTERY

The G3P1 tubular graft of 5mm internal diameter and 7 cm length cellularised with adipose derived stem cell differentiated smooth muscle cells implantation. The implanted as inter position graft in sheep common carotid artery model, Figure: 4.37 A to L. The bare grafts acted as control. The grafts were implanted on both carotid artery of the sheep. Post-operatively, sheep recovered health. The second sheep showed mild inflammation and swelling around the neck which gradually subsided after one week, Figure: 4.38 A to C. The graft handling properties were appreciable with good suturing ability. There was no blood leakage from graft after implanting and graft started pulsation when the blood flow was resumed. After 3 months the angiographic evaluation of the graft was carried out. It was observed that there was blood flow through the graft implanted and dye path was clear in both cellularised and bare grafts. The graft of sheep two was however blocked. There was also an aneurysmal bulging observed in implanted graft, Figure: 4.39 A, B Panels.

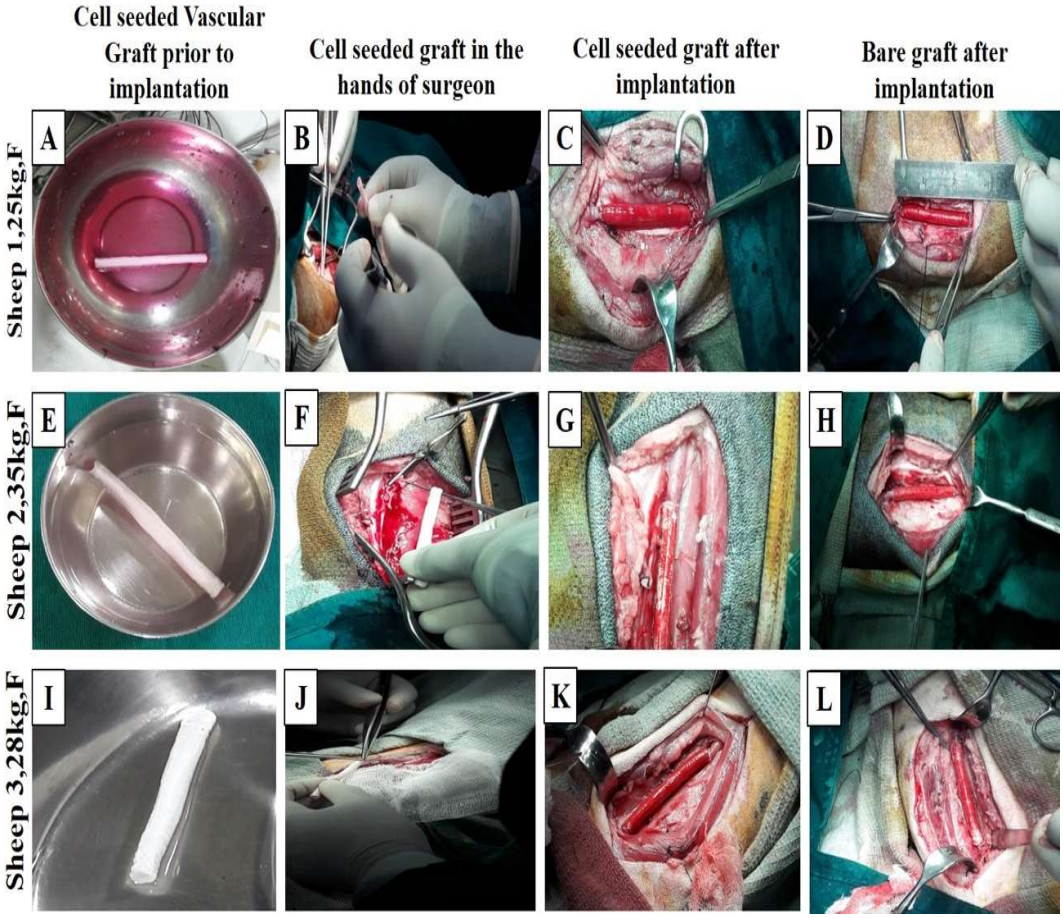


**Figure 4.37: Vascular graft G3P1 – 5 mm implantation in sheep. (A, E, I) Graft prior to implantation. (B, F, J) Graft in the hands of surgeon. (C, G, K) Implanted cell seeded graft. (D, H, L) Implanted bare graft.**

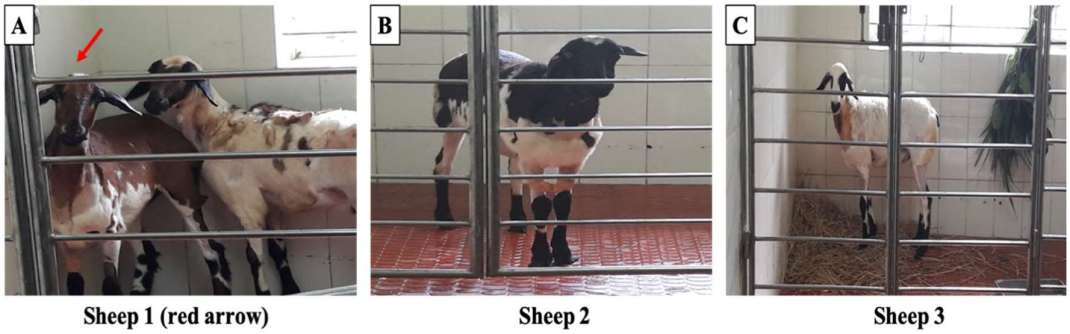


**Figure 4.38: Sheep recovered post-operatively after implantation of graft.**

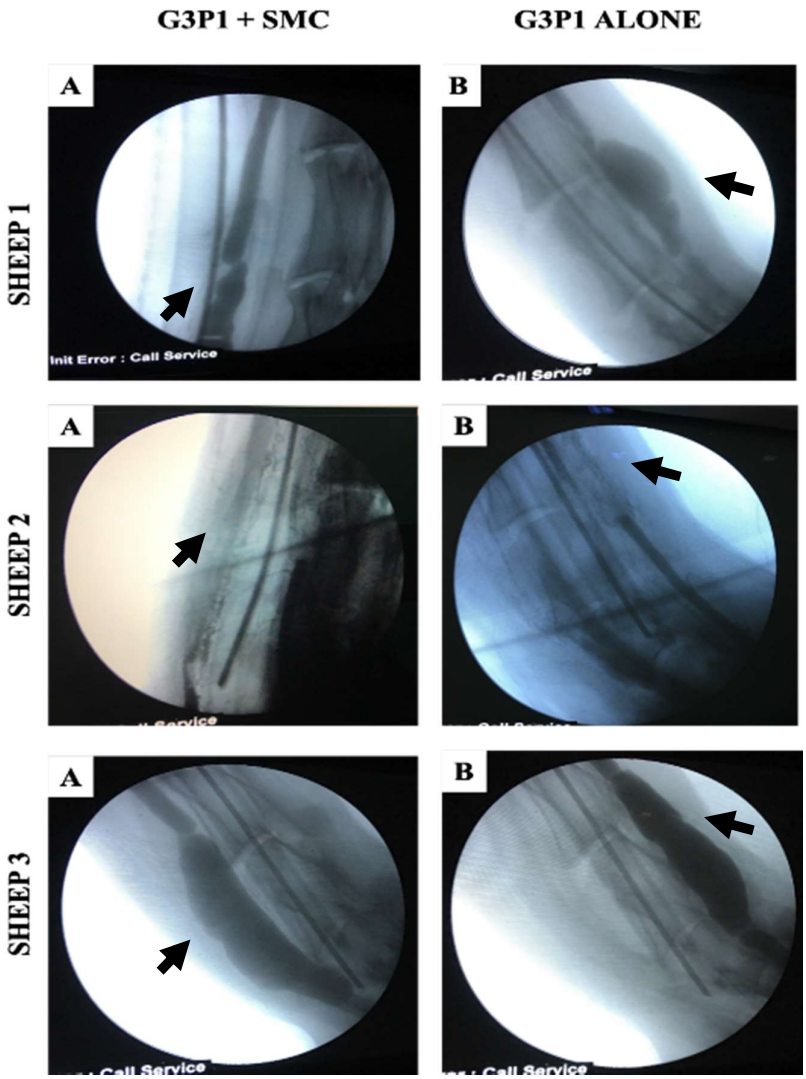


**Figure 4.39: A, B - Angiograms of G3P1 graft implanted in sheep (black arrow indicating the blood flow).**

### 4.11.2 GROSS OBSERVATION OF THE IMPLANT

For Sheep 1 and Sheep 3, in gross observation of the explanted G3P1 – 5 mm graft, the graft appeared bulged. Native intact vessel was seen on both side and non-occluded grafts. Suture material was visible at anastomosis without microthrombi. Focal discoloration of liminal area was noted. In bare graft, lumen was partially occluded 2 cm from proximal anastomosis. At distal anastomosis no visible thrombi and narrow lumen was appreciated. In sheep 2, the graft appeared bulged and lumen was completely occluded. Native vessel was seen on either side, Figure: 4.40 A, B Panels.

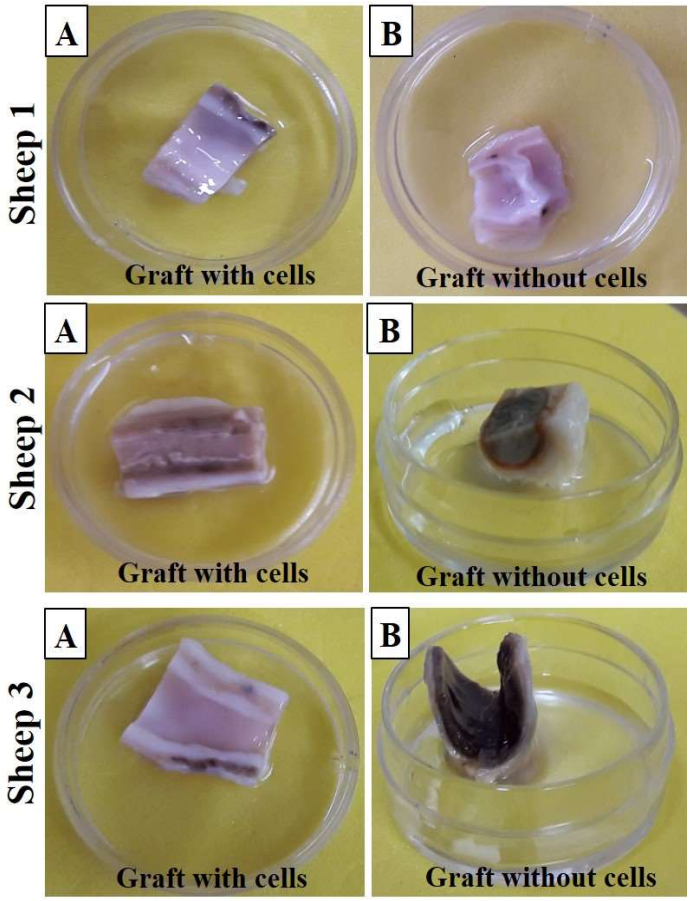


**Figure 4.40: Gross observation of graft implanted in sheep.**

### 4.11.3 ENVIRONMENTAL SCANNING ELECTRON MICROSCOPY OF THE IMPLANT

E-SEM scanning of mid region of the patent graft showed cobble-stone morphology like cells. This observation shows that there is endothelisation of implanted graft. The abluminal side showed cells of fibroblastic like appearance and it would be either smooth muscle cells or fibroblasts, Figure: 4.41 A to C.

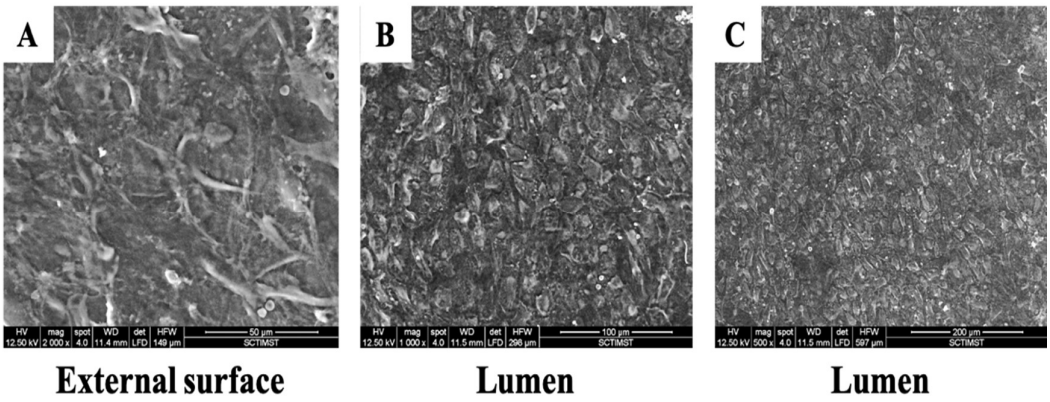


**Figure 4.41: E-SEM image of the G3P1 – 5 mm with SMCs vascular graft explant (A) External surface showing fibroblastic shape cells (Scale bar - 50µm). (B) Mid graft region of sheep 2 cobble-stone morphology like cells. (Scale bar - 100µm). (C) Mid graft region of sheep 1 cobble-stone morphology like cells (Scale bar - 200µm).**

### 4.11.4 HISTOPATHOLOGICAL EVALUATION OF THE IMPLANT

Haematoxylin and eosin staining of explanted graft, native artery, and G3P1 -5 mm scaffold was routinely done in order to analyse the cell distribution and other features. Figure: 4.42 A, shows the staining performed sheep native common carotid artery. Figure: 4.42 B shows the G3P1-5mm with SMCs prior to implantation. The middle region section of (M) of bare scaffold (Explant 1: G3P1) shows very less evidence of lumen endothelisation. The image of cell seeded scaffold (Explant 1: G3P1+ SMC) shows endothelisation (inset). After implantation of both bare and cell seeded scaffold endothelisation was pronounced in cell seeded scaffold evident from histology, Figure: 4.42 C, D. The last panel of the Figure: 4.42, E, F shows neo-vascularisation around implants. There was capillary formation around the grafts (Black arrow) with arterial and venous pattern visibly developed around cell – seeded grafts. The results suggest that regeneration of graft after implantation has occurred and it was more pronounced in graft seeded with smooth muscle cells. The stitched images representing that of cell seeded graft section showing patent lumen, Figure: 4.42 G.

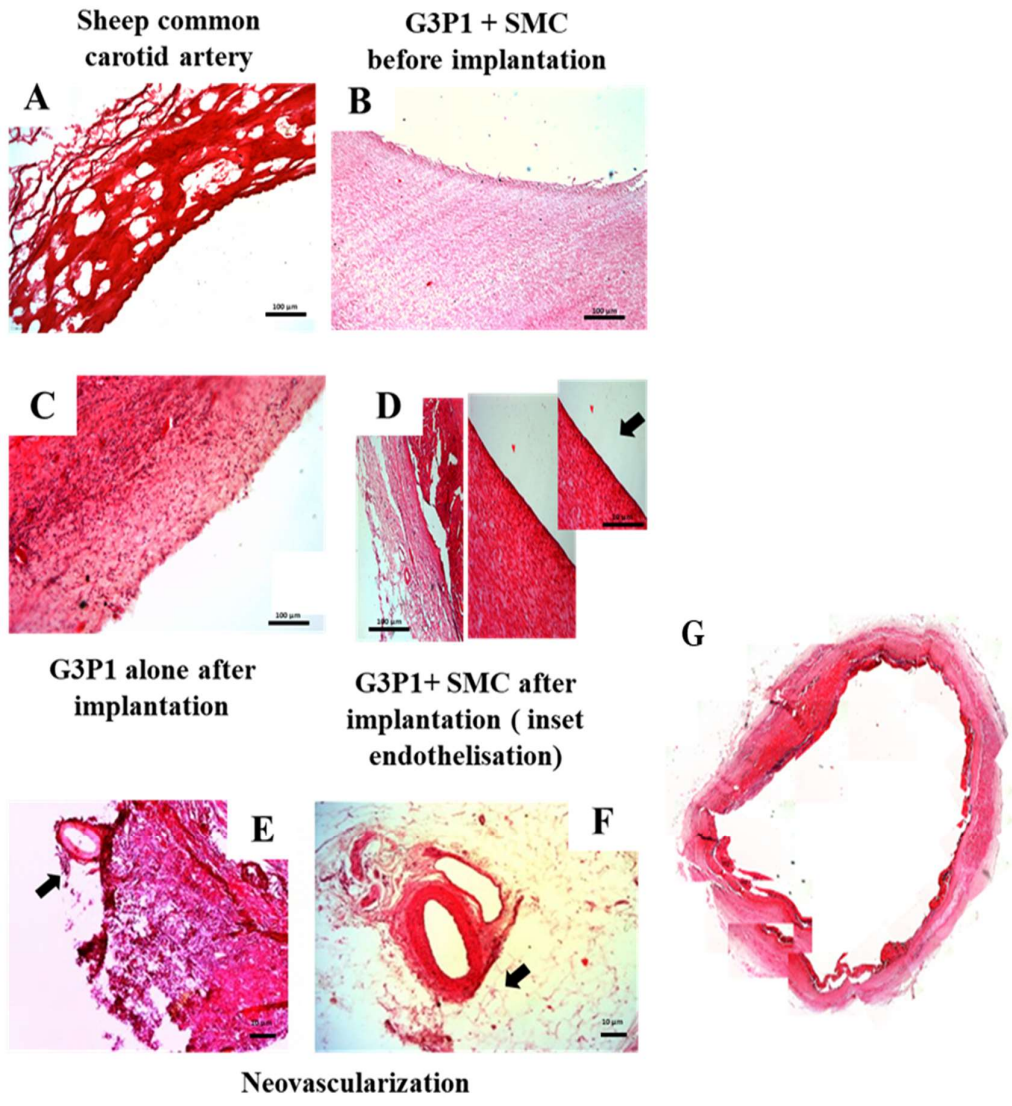


**Figure 4.42: Histological evaluation of the G3P1-5mm vascular graft. (A) Sheep common carotid artery (Scale bar - 100µm, 10x). (B) G3P1-3mm scaffold before implantation with cells (Scale bar - 100µm, 20x). (C) G3P1 graft after implantation (P, Scale bar - 100µm, 20x). (D) G3P1 + SMC after implantation (Scale bar - 100µm, 20x). (E, F) Neo-vascularisation observed (Black arrow, Scale bar - 10µm, 20x). (G) Inset showing luminal endothelisation (Scale bar - 10µm, 10x).**

Detailed histopathological evaluation, Figure: 4.43 A to L panels, of the graft explants gave the following observations. In case of sheep 1 and Sheep 3, the graft with SMCs when analysed showed no microthrombi at anastomosis of both proximal and distal regions. Endothelium like cells were present all along the graft. The mid-graft region showed thicker neointima. Graft material degradation was observed with foreign body giant cells infiltration-vascularisation was observed. Neoadventitia with connective tissue was observed all through of the graft. Distal anastomotic region showed haemorrhage over graft material and vacuolisation with varying size were also noticed.

In bare graft alone explant, the proximal and distal anastomosis had no microthrombi and there was neointima formation. Endothelisation was observed and neointima consisted of fibroblasts and ground substance. Polymorphonuclear cell infiltration was observed in neointimal region. Severe graft degradation and foreign body giant cell infiltration was observed. Hemosiderin laden macrophages and mononuclear cells were observed. Neoadventitia and neo vascularisation was observed. Vacuolisation was observed in graft walls. The mid region contained some thrombi attached to wall which contained RBC, polymorphonuclear cells, vacuolated cells and foreign body giant cells. Neoadventitia was observed. The inflammatory cells present at bare scaffold after three months which were not noticed in cell seeded grafts indicate the regeneration was much faster in cell seeded graft than in bare graft as the bare grafts were still undergoing acute inflammatory response. There was also presence of thrombus in bare graft in mid region which was absent in seeded graft. Also, thicker endothelial lining was observed in mid-graft region only in cell seeded graft.

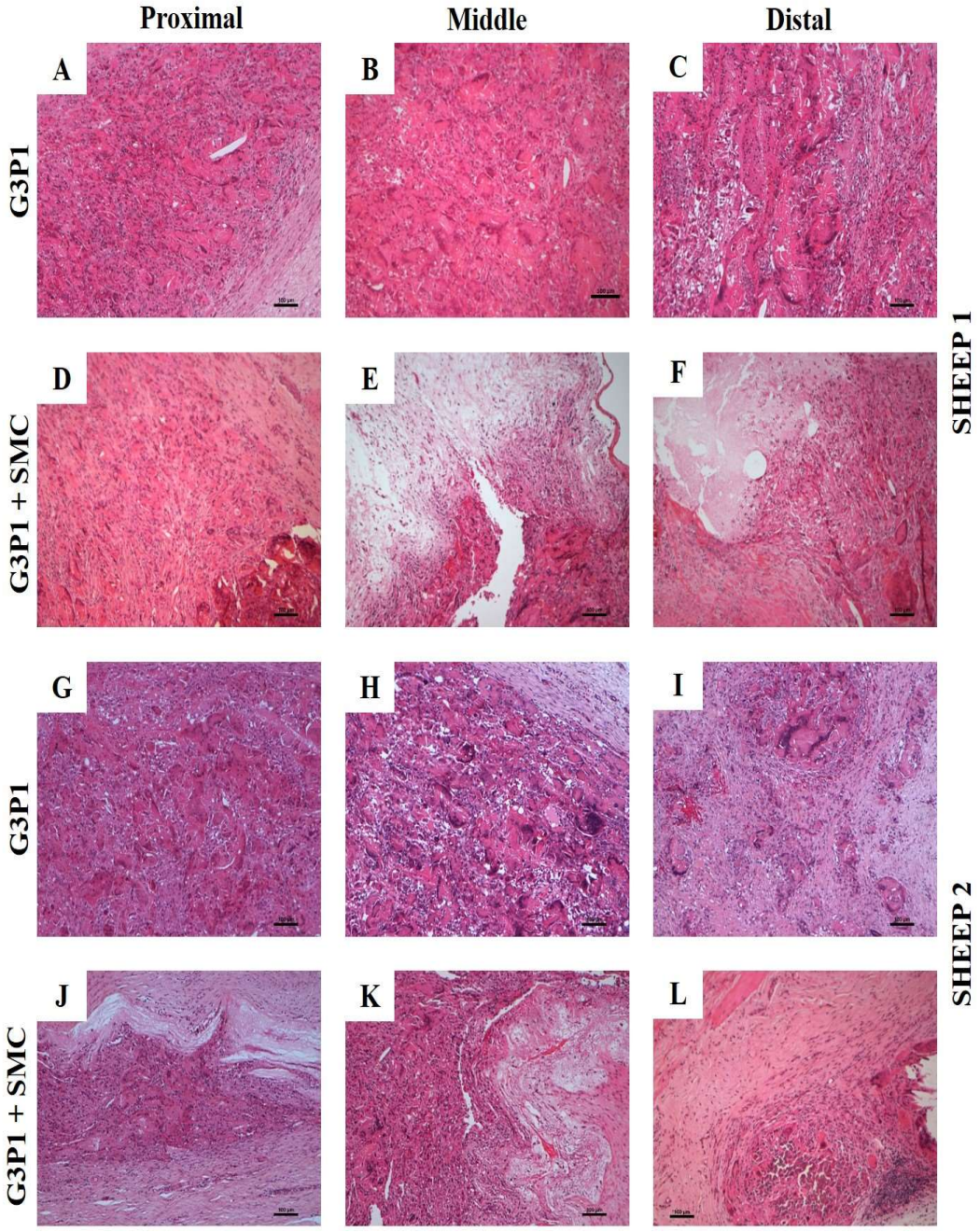


**Figure 4.43: Histopathological evaluation of implanted G3P1-3mm vascular graft explant from sheep in detail (Patent graft - Sheep 1 and 3. (A, B, C) Proximal, middle, distal regions of G3P1 alone graft of sheep 1. (D, E, F) Proximal, middle, distal regions of G3P1+SMC graft of sheep 1. (G, H, I) Proximal, middle, distal regions of G3P1 alone graft of sheep 3. (J, K, L) Proximal, middle, distal regions of G3P1+SMC graft of sheep 3. (Scale bar - 100μm, 40x).**

### 4.11.5 PICROSIRIUS RED STAINING OF COLLAGEN FIBERS

The presence of collagen fibres in the patent graft was analysed by the ability of the fibrils to bind Sircol dye. The bright field and polariser microscopic images of the graft showed excellent deposition of collagen around the graft. However, type I collagen (Orange under birefringence) was observed largely. Even though this gives an insight to the regeneration capability of graft, inflammation mediated collagen deposition cannot be ruled out. There was adequate deposition of fibrils when neo adventitia is formed, Figure: 4.44 A to H.

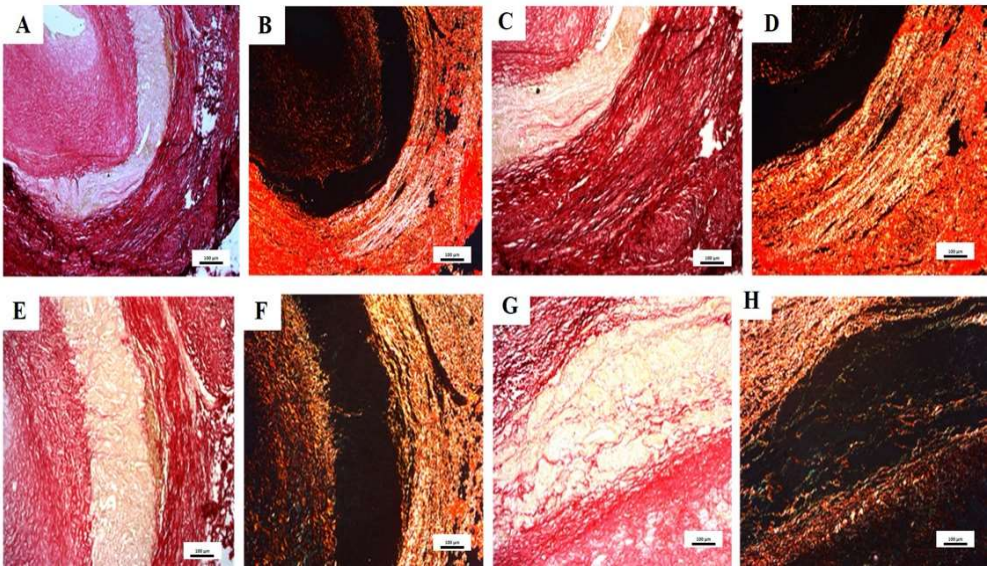


**Figure 4.44: Picrosirius red staining of collagen Sheep 1 (A) Bright field image of collagen G3P1 alone (Red fibres) (B) Bifringence of Image A (C) Bright field image of collagen G3P1 and cells (Red fibres) (D) Bifringence of Image C. Sheep 3 (E) Bright field image of collagen G3P1 alone (Red fibres) (F) Bifringence of Image E (G) Bright field image of collagen G3P1 and cells (Red fibres) (H) Bifringence of Image G (Scale bar-100µm,40x).**

### 4.11.6 VERHOEFF'S -VAN GEISON STAINING FOR ELASTIN FIBERS

The deposition of elastin was confirmed by brown coloured fibres observed by Verhoeff's staining. Elastin deposition is mainly attributed as function of smooth muscle cells, so the G3P1 – 5 mm graft with cells were stained and compared with section of native artery. It was seen that in sheep 3 explant there was clear formation of internal and external elastic lamina which was not much observed in other explants, Figure: 4.45 A to D. The brown fibres here indicate elastin and red fibres were collagen.

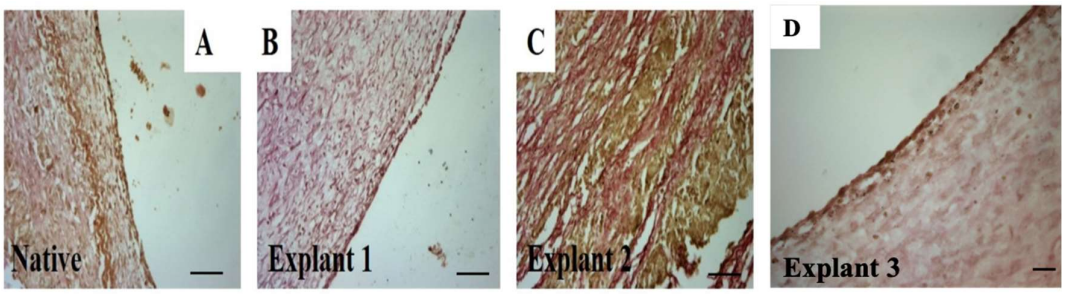


**Figure 4.45: Elastin staining (A) Native artery. (B) Sheep 1 explant. (C) Sheep 2 explant. (C) Sheep 3 explant (Scale bar - 100μm).**

### 4.11.7 IMMUNOFLUORESCENCE STAINING

The endothelisation of the mid graft region of patent explants (G3P1 – 5 mm with SMCs) were confirmed by immunofluorescence staining of CD31 specific for endothelial cells. Confocal microscopic images shown that CD31+ cells were present in the luminal lining of the patent graft. Thus, the strategy of graft fabrication showed successful regeneration and *in vivo* endothelisation potential which might have contributed to its patency. There was presence of Alpha smooth muscle actin positive cells abluminal which may be either the smooth muscle cells recruited by endothelial cells or fibroblasts, Figure: 4.46 A, B Panels.

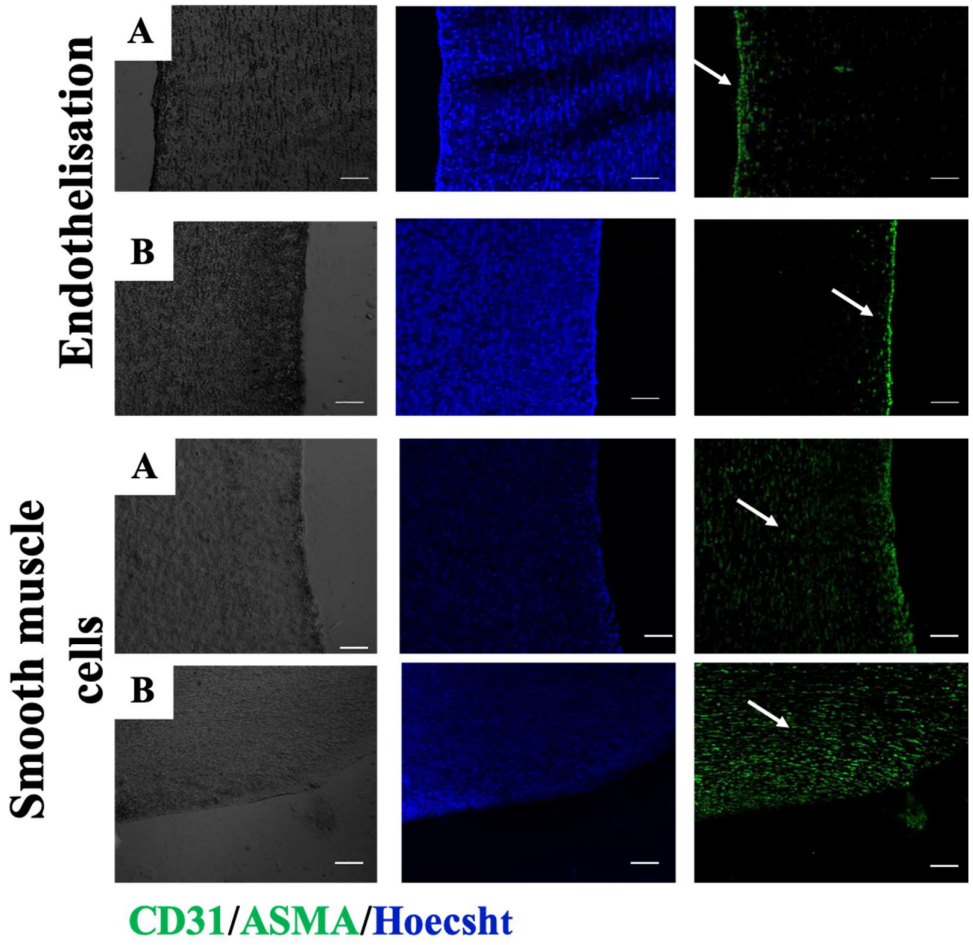


**Figure 4.46: Immunofluorescence staining of G3P1-5mm with SMCs. (A) phase contrast of scaffold section. (B) Hoechst nuclear staining (C) CD31 or ASMA staining (White arrow, Scale bar - 100µm, 10 x).**

### 4.11.8 TOTAL COLLAGEN AND ELASTIN ESTIMATION

The total collagen estimation of different explants, native artery, graft before implantation shows that there is comparable deposition of collagen, compared to native artery, graft with cells prior to implantation showed only 4 µg /mg of collagen. The occluded grafts (Explant 5, 6) showed higher deposition of collagen than not occluded grafts. Comparing between cell seeded and bare graft of not occluded grafts (explant 1 and explant 3) there is increased amount of deposition of collagen (11 µg /mg and 16 µg /mg). Native artery has 32 µg /mg of total soluble collagen, Figure: 4.47.

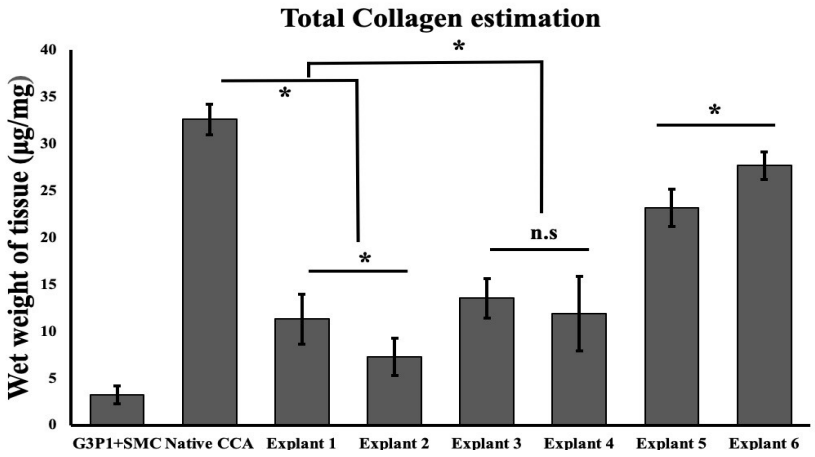


**Figure 4.47: Total collagen estimation (*p<0.001, n.s: non-significant)**

Elastin deposition was also compared in similar way as that of collagen. Here, the not occluded explants (Explant 1 and explant 4) showed more elastin deposition than any other explants, 3µg /mg and 2.3 µg /mg respectively. However, the values were lesser than native, 9.45 µg /mg. The occluded grafts showed elastin deposition than graft prior to implantation, which may be attributed by vascular cells infiltrated the graft *in vivo*, Figure: 4.48.

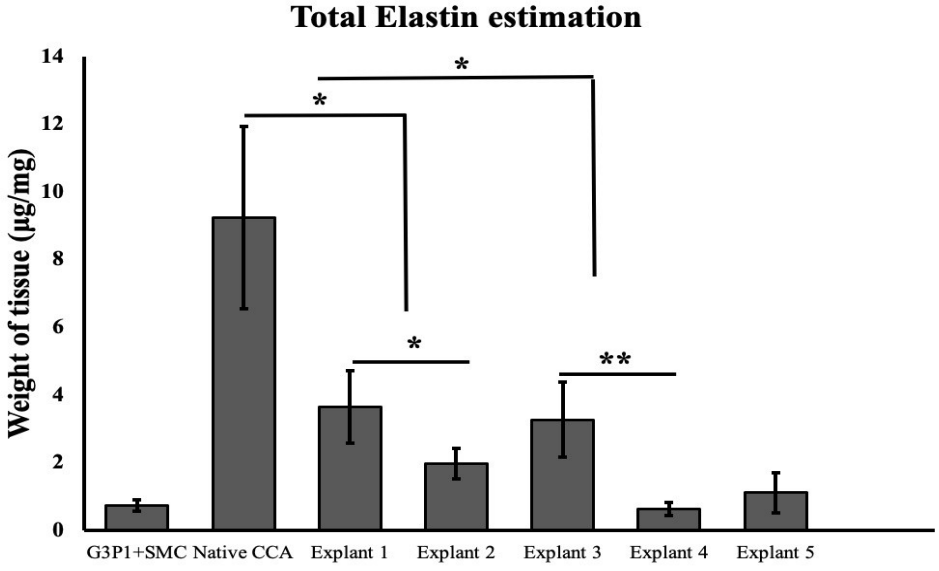


**Figure 4.48: Estimation of elastin deposition on grafts and native artery (*p<0.001, n.s: non-significant)**

# CHAPTER 5
# DISCUSSION

The major results obtained for the study which are elucidated in Chapter 4 are discussed in this chapter. The results obtained are critically analysed and co-related with recent findings available in literature. Interpretations are made and limitations are notified if any. Future perspective of the current study is noted at the end of this chapter.

The death and disability associated with cardiovascular diseases has increased the demand of vascular reconstructive or bypass surgery. In the case of small diameter vessel replacement, tissue engineered vascular grafts provides a feasible option. However, blood vessel engineering requires critical understanding of the blood vessel structure and physiological activity of the same. Taking into consideration of all factors is drawing a line in fabrication of small diameter vascular graft is a greater challenge. However, bio mimicking the native architecture and dynamics is highly conceivable. As a part of achieving this, direct scaffolding with cells, based strategy proves to be very promising as the scaffold supports the attachment, growth and differentiation of cell along with aiding the regeneration *in vivo*. A suitable scaffold and cell source that could satisfy the needed of vessel regeneration is extremely important in the success of vascular graft. Moreover, the design criteria of small diameter blood vessel engineering vary from patient to patient and is highly personal. Patient derived autologous cells or cells differentiated from autologous stem cells are one plausible cell source that can minimize the graft rejection. The scaffold provides suitable niche which is extremely important for the growth of these cells. The microenvironment provided by the scaffold solely depends on its physico-chemical properties. The present study choses a cell-scaffold based approach to fabricate small diameter vascular graft and the functional evaluation of the same provided promising results.

## 5.1 SYNTHESIS, FABRICATION AND CHARACTERISATION OF GELATIN-VINYL ACETATE/POLY-ε-CAPROLACTONE SCAFFOLD

The first line of success of personalized tissue engineered graft depends on identification of suitable biomaterial and fabricating the same into the dimensions of blood vessel intend to be replaced (Chang and Niklason, 2017b). The extracellular matrix of blood vessels consists of collagen and elastin types of proteins which contributes to biomechanical properties of vessels. The vessels experience vascular dynamics with stretch-relaxation cycles for blood flow. Thus, the scaffold material of choice should primarily contribute to physicochemical, mechanical and biological functions (Rhodes and Simons, 2007). Natural polymeric biological molecules and its derivatives like collagen (Luo et al., 2018; Parenteau-Bareil et al., 2010), elastin (Miranda-Nieves and Chaikof, 2017), tropoelastin (Coenen et al., 2018), gelatin (Aldana and Abraham, 2017; Joy et al., 2018; Shalumon et al., 2015), chitosan (Hild et al., 2015) are considered to be good choice in terms of biocompatibility however compromises has to be done regarding the mechanical strength and immunogenicity (Deepthi et al., 2018). Synthetic polymers could be tailored to perform better mechanically, but ability to enhance cell interaction and differentiation is limited (Syazana and Sukmana, 2016). A combination of natural biomolecule and synthetic polymer-based selection of material is proposed to conveniently address the limitations of individual material components (Wong et al., 2013).

Natural biomolecules exhibit optimum properties encouraging cell binding, proliferation and differentiation. Collagen forms the major extracellular component of blood vessels apart from elastin. Gelatin which is derived from collagen has promising potential for tissue engineering approaches. Chemically, the evident presence of arginine-glycine-aspartic acid (RGD) sequences in gelatin makes it conducive for cell attachment and growth (Davidenko et al., 2016; Gautam et al., 2013; Zhang et al., 2005). The solubility and lack of mechanical strength, however, makes gelatin a less attractive candidate for vascular tissue engineering which otherwise requires extensive crosslinking (Van Vlierberghe, 2016). In comparison to collagen, gelatin has added advantages as a scaffold candidate which are attributed to its inherent similarity to collagen chemistry with modifiable ability, lack of immunogenicity, excellent

cytocompatibility and low costs (Ma et al., 2005). However, the mechanical strength and solubility of unmodified gelatin remains a challenge. Our group has modified gelatin with free radical polymeric grafting of vinyl acetate moieties on to gelatin (Thomas and Nair, 2013). Though this material has added advantage of improved solubility, utilization of low percentage cross-linking agent and native vascular smooth muscle cell proliferation, the mechanical strength is less comparable to the blood vessels. Poly-ε-caprolactone (PCL) is widely used as a biodegradable and biocompatible tissue engineering scaffold and is also FDA approved material. It has a slow hydrolytic degradation profile over more than a year comparable to that of complete re-vascularization. Even though the hydrophobic nature of PCL makes it less conducive for cell growth, mechanical robustness makes it an attractive scaffold material (Wang et al., 2009).

In the present study, we fabricated a combination graft of gelatin-vinyl acetate and poly caprolactone through a dual electrospinning technique for addressing the issue of better cell adhesion and mechanical strength. We modified gelatin with vinyl acetate to enhance its properties in terms of solubility and stability by free radical mechanism according to previous protocol (Thomas and Nair, 2013). A weight ratio of 71.5:28.5 (Gelatin to vinyl acetate) has been chosen for synthesis. The grafting ratio was found to 0.49 with an efficiency of 49.7 ± 0.7%. The AT-IR FTIR of gelatin-vinyl acetate in comparison with gelatin, shows the presence peaks of amide I (1641 $cm^{-1}$) and amide II peak at (1536 $cm^{-1}$) and intense C=O stretch at 1754 $cm^{-1}$, which confirm the grafting reaction.

Gel permeation chromatography of gelatin and gelatin-vinyl acetate showed an increase in molecular weight and poly dispersity for gelatin-vinyl acetate. The weight average molecular weight was increased from 47 kDa to 95 kDa. The poly dispersity of gelatin vinyl acetate has also been increased to 2.63. The increase in molecular weight clearly indicate the vinyl acetate has been grafted on to gelatin which was further confirmed by TNBS assay using glycine as standard wherein, it was deduced that there was a reduction in percentage of amine group in synthesized gelatin-vinyl acetate. The percentage amine group of gelatin is 70 ± 1.2% while gelatin-vinyl acetate is 49 ± 2%.

Recent years has seen the advancement in electrospinning technology in manufacturing of scaffolds for tissue engineering. The major highlight of this versatile technique is the ability to produce polymeric fibres with diameter ranges of nano-and micro scale (Hasan et al., 2014b). By standardizing the spinning parameters, a wide range of natural, synthetic and combinational electrospun materials can be made (Wang et al., 2013). The scaffolds created are three dimensional and highly porous in nature with nano-architecture, making it bio mimic the native architecture of extracellular matrix (Popryadukhin et al., 2017). In the case of blood vessels, the bi- component extracellular matrix have fibrous architecture microscopically. Electrospinning has been widely used to make scaffold with dual components by modification of the basic technical set up (Agarwal et al., 2008). Dual source co-electrospinning method utilizes the ability to spin two different polymeric solution onto same fibre collector from different spinnerets resulting in a bi-component scaffold with both polymers interspersed (Du et al., 2017; Xu et al., 2012). The polymers could maintain their individual physico-chemical and biological properties in these scaffolds. Macroscopically, the overall nature of the scaffold will be the combination of its individual component (Han et al., 2011). Also, the ease of fabrication is that co-electrospinning allows the freedom to use much cheaper solvent system than used for chemically blending the polymers (Wang et al., 2015). Moreover, the concentration of each polymer component can also be altered by changing the feed rate of it (Ladd et al., 2011; Torricelli et al., 2014). Dual source co-electrospinning is expected to add advantage of natural and synthetic polymers as whole to scaffold while chemically keeping the individual identity of polymers (Nieponice et al., 2008b; Zhao et al., 2013). Incorporation of polymers using the present solvent systems leads to a much cost effective and greener fabrication strategy. More amount of gelatin vinyl acetate present in the scaffold makes the scaffold more conducive for cell-based interaction.

In the present study, gelatin-vinyl acetate and PCL polymers has been selectively incorporated in to scaffold. The scaffold obtained so is expected to have properties of both individual polymers. The amount of gelatin-vinyl acetate in the hybrid scaffold by TNBS assay showed in G3P1 combination had the highest amount (more than 70% of gelatin-vinyl acetate). Also, the water contact angle of scaffold combinations showed that the G3P1 have contact angle $74^0$. It has reported in several studies that the conducive

scaffold wettability for mesenchymal stem cells to attach and differentiate is in between $60^0$- $80^0$ (Wang et al., 2014). This is extremely important as the scaffold is intended to be used as platform for differentiation of stem cells to smooth muscle cells. The PCL polymer fibres contribute immensely to maintain the current nature of scaffold making it moderately hydrophilic than using gelatin-vinyl acetate alone. The hybrid nature of the scaffold was evident from the FT-IR spectroscopy that shows both peaks of gelatin and PCL. Crosslinking strategy of using 0.5% glutaraldehyde solution was reported to be non-cytotoxic (Azami et al., 2010; Tamimi et al., 2016). Moreover, vinyl acetate stabilization of gelatin prior to scaffold fabrication also might have decreased the need of extensive crosslinking of gelatin with increased amount of chemicals which would otherwise be the case (Hellio and Djabourov, 2006).

For cellularisation of scaffold, the ultrastructure of scaffold plays a vital role. Microscopically the scaffold showed smooth fibers and highly porous nature which is the characteristics of electrospun scaffolds. The frequency histogram by image J shows the average fibre diameter of G3P1 - 3mm was 894 nm and G3P1 – 5 mm was 729 nm. The reported collagen fibre diameter by reported ultra-structural analysis of collagen fibers in native arteries is 1800 nm (Davidenko et al., 2016). Cells on scaffold needs to perform physiological functions like proliferation. Exchange of nutrients and waste. Moreover, gaseous exchange to deeper part of the scaffold is facilitated by pores (Diban and Stamatialis, 2011). From micro CT analysis of three-dimensional analysis of scaffold section provided detailed architecture of electrospun scaffold. The pore distribution over a range of 12 - 60 μm. The average pore size 48 μm. For engineering a blood vessel, small pores limit the infiltration of smooth muscle cells, attributed to size, however endothelial cells require much smaller pore size than SMCs. Too large pore size greater than 200μm leads to hindering of cell migration as it does not provide tethering points while on traction. Also, it increases vessel permeability and blood leakage. It is reported that SMCs tend to grow well in scaffolds with [pore size range of 38 – 100 μm (Zorlutuna et al., 2009). The scaffold showed a swelling percentage increase to 160 - 172% within first 15 minutes which remain stabilized over time further. However, there was no extensive dimensional change of scaffold visibly and it is assumed that swelling is caused by wicking action of scaffold holding PBS in its extremely porous ultrastructure. This also accounts for the stability of scaffold in media with pH 7.4. The characteristic weight

loss of scaffold over time period is attributed to its *in vitro* degradation. The scaffold shows 38 - 42% weight loss over 12 weeks. Compared to PCL which show minimal weight loss (<10%), it was assumed that 70% weight loss is experienced by gelatin-vinyl acetate alone. Blood vessel regeneration aims replacing the implanted scaffold with native tissue over time. The implants are expected to degrade while cells lay down their extracellular matrix (Cui et al., 2008; Dulnik et al., 2016). PCL degrades in long term and the degradation is by hydrolysis. However, gelatin vinyl acetate can degrade both by hydrolysis and enzymatic and hence will be the first component to degrade out of scaffold. The initial mass loss of the scaffold may be hence be due to degradation of gelatin-vinyl acetate fibers which is advantageous as cells attaching to the scaffold will produce its own collagenous extracellular matrix and compensate gelatin based loss. While designing a vascular graft, the mechanical strength of the material has to be assessed thoroughly. During the *in vivo* application of graft, it will be undergoing the hemodynamic stresses and scaffold should withstand the pressure of blood flow (Gauvin et al., 2011). The average thickness of scaffold was measured to be 200 μm for G3P1-3 mm and 300 μm for G3P1 – 5 mm. The wall thickness of human saphenous vein is around 250 μm and human arteries range from 300 – 700 μm (Andel et al., 2003). A blood vessel conduit experiences stretch–relaxation cycles both longitudinally and circumferentially. Ring tensile stress of G3P1 scaffold pre wetted in PBS at $37^0$ C showed a Young's modulus of 2.9 ± 0.3 MPa (G3P1 – 3 mm) and 5.5 MPa (G3P1 – 5 mm) respectively compared to gelatin-vinyl acetate and PCL circumferential tensile strength of 0.27 ± 0.06 MPa and 1.5 ± 0.5 MPa respectively. The bi-component scaffold shows increased tensile strength compared to parent polymers. The longitudinal tensile strength was 1.2±0.2MPa for the G3P1 – 3 mm and 2.1MPa for G3P1 – 5 mm scaffold. The values also indicate that the mechanical properties of graft vary with that of its inner diameter, however in this study the parent polymer tubes are of diameter 3mm. Blood vessel is generally viscoelastic in nature. As the pressure increases the elasticity gradually decreases and vessels becomes much stiffer. The ultimate tensile strength gives direct indication of burst pressure. Theoretical estimation of burst pressure considering the wall thickness of 250 μm is 4680 mmHg for G3P1 – 3 mm and 1545 mmHg for G3P1 – 5 mm. The saphenous vein and internal mammary artery at physiological pressure has an elastic modulus of 4.5 MPa and 7.3 MPa respectively. According to ISO 7198:2016 International standards of cardiovascular implants - Tubular vascular prosthesis, a

vascular graft should possess mechanical strength at least comparable to saphenous vein. The G3P1 scaffold proves to be much more mechanically robust when compared to native vessels. The advantage of this can attributed towards scaffold's ability to with stand physiological pressure dynamics even undergoing degradation and regeneration simultaneously. Other aspect of mechanical profile of scaffold is suture ability of the scaffold. According to ISO standards 7198:2016 as mentioned above, a graft should possess minimum retention force of 2.5 N for the surgeon to handle it with ease during implantation. The suture retention force of G3P1 – 3 mm scaffold 2.3 N and 5 mm was 2.9 N

## 5.2 DIFFERENTIATION ADIPOSE DERIVED MESENCHYMAL STEM CELLS TO SMOOTH MUSCLE CELLS ON GELATIN-VINYL ACETATE/PCL (G3P1) TUBULAR SCAFFOLD

In order to differentiate mesenchymal stem cells to smooth muscle cells, the stem cells were isolated from adipose tissue of both rabbit and sheep by collagenase treatment. The isolated cells expressed mesenchymal stem cell markers - CD44, CD90, CD34/45 (negative) which was confirmed by flow cytometry and immunofluorescence staining. The data is in accordance to minimal criteria for defining multi-potent mesenchymal stem cells by International society for stem cell therapy (Dominici et al., 2006). The cells also showed differentiation to three lineages under suitable media for adipogenesis, osteogenesis and chondrogenesis.

The G3P1 scaffold was cyto-compatible and was evident from the set of cell-material interaction experiments conducted. Mouse fibroblast and mesenchymal stem cells showed no sign of cell death or change in morphology when in direct contact with sterile cross-linked scaffold. This indicate that scaffold is cell friendly. Moreover, the viability of cell when treated with scaffold extract of day 14 was more than 80% for both rabbit and sheep mesenchymal stem cells. This confirms the cytocompatibility of the scaffold. These results are agreeing with the procedures as per ISO standard for *in vitro* cell compatibility of the biomaterials. A new technique of analysing cell interaction on the scaffold was employed in this study and that is confocal Raman imaging of the cell seeded scaffold. Raman spectroscopy employs microscopic and chemo metric approach

in order to analyse the biochemical changes of cells on scaffold. Single cell imaging on scaffold is possible by this technique and our results shows that under the influence of co-electrospun G3P1 scaffold, mesenchymal stem cell shows no biochemical variation. The spectra also confirm the hybrid nature of scaffold (Baldock et al., 2019).

Blood vessel is tri-layered, and tunica media consists of smooth muscle cell layers. Presence of smooth muscle in bioengineered blood vessel is very crucial as these cells directly contribute to the mechanical strength of vessel and maintaining the vascular tone in synchronization with endothelial lining (Guo and Chen, 2012b). It is well known that TGF-β1 mediated differentiation of smooth muscle cells. The growth factor plays significant role in smooth muscle cell differentiation during embryonic development and phenotypic switching of SMCs (Gu et al., 2018). In the initial stage of differentiation, TGF-β1 activates Smad path way and leads to the expression of early marker genes like alpha smooth muscle actin (ASMA), SM22α (Transgelin), Calponin (CNN3) etc., It is well known that ASMA markers do not solely define the Smooth muscle lineage fate of stem cells as these are also expressed in other cells (Wang et al., 2010). This is in concordance with present protocol that mesenchymal stem cells seeded on G3P1 scaffold with induction medium shows 33-fold increase in ASMA expression, 55-fold increase in transgelin expression and 12-fold increase in acidic Calponin (CNN3) compared to cells on TCPS with control medium. The expression pattern of SMC genes is under the influence of induction medium on TCPS were also found to be increasing but lesser extent compared to scaffold. The panel of antibody stained for ASMA, SM22α confocal laser scanning microscope also shows the positivity of cells for early smooth muscle cells markers. Our results show that, in addition to increase in the early and mid-markers of SMCs there is an increase in the expression of late marker myosin heavy chain, MYH11 on G3P1 scaffold. While the expression of the marker is not so pronounced on TCPS which is less than baseline calibrator. SMMHC is the sole markers that is not associated with fibrotic nature of mesenchymal stem cells and expression of the same confirms the contractile nature of differentiated smooth muscle cells. The influence of TGF-β1 on differentiation of stem cells into contractile natured SMCs is highly pronounced (Kothapalli et al., 2009). The down regulation of the gene in TCPS may be due to enhanced modulus of TCPS (30GPa) as the stiffness of material directly influence the cellular behaviour (Gilbert et al., 2010). A natural biomolecule-based scaffold system

thus has an added advantage. Phenotypic modulation and proliferation of SMC can also be attributed to heparin (Gohda et al., 2001). The contractile nature of SMCs is crucial for the successful application of tissue engineered vascular bypass (Huang et al., 2016a). Compared to rabbit cell differentiation, sheep cell differentiation varies in expression of ASMA in TCPS and G3P1, here differentiated sheep cells express the ASMA in higher fold on TCPS than on G3P1. However, this data proves that cells on G3P1 is contractile in nature than proliferative SMCs, ASMA gene is also sole marker for proliferative nature of SMCs and this marker is even expressed in fibroblast cells that are highly proliferative. So, the G3P1 scaffold could also offer to decrease the synthetic phenotype of the differentiate SMCs which is an added advantage. The contractile nature of sheep SMCs was further confirmed by the fold increase in expression of SMMHC on scaffold than on TCPS.

Blood vessel extracellular matrix plays a crucial role in maintaining the overall physiological function of the vessel. The major components form collagen and its types. Blood vessel mechanical tensile strength is mainly provided by Collagen type I alpha I while endothelial basement membrane is of collagen type IV (Huang et al., 2016b). The expression and down regulation collagen type I associated gene is an important event in vessel remodelling. The degradation and turnover of collagen subunits predicts the vessel regeneration and progression of atherosclerotic inflammation (Arora and McCulloch, 1994). Smooth Muscle cells produce collagen in blood vessels apart from perivascular fibroblasts. Ascorbic acid in the differentiation media is proposed to be a positive up regulator of collagen synthesis. The collagen gene expression profile of SMCs differentiated on G3P1 scaffold shows a 147-fold increase and 42-fold increase on TCPS. This pronounce that differentiated cells produce collagen type 1and vascular graft is conducive for *in vivo* regeneration of its own. Total soluble collagen extracted from scaffold is assayed to be 150 µg/mg of wet weight of tissue by Sircol assay. Another relevant component of blood vessel extracellular matrix is elastin which functions as creep stabilizer of pulsatile blood vessel (Wong et al., 2013). Elastic fibres helps vessel recoiling with variation in pressure-flow functions of blood. Our results show appreciable up regulation of elastin gene on G3P1 scaffold while it's less than base line on TCPS. The total elastin estimation provided an amount of 15 µg/mg wet weight of

elastin deposition on scaffold. TGF-β1 is potent enhancer of elastogenesis on three-dimensional scaffold by activating Smad pathway (Davidson, 2002).

The results of the *in vitro* hemocompatibility test carried out for G3P1 scaffold according to the ISO standard indicate that the scaffold is blood compatible. The PCL component in the graft material is hydrophobic and may have tendency to adsorb more proteins which may lead to activation of blood coagulation cascade. However, there are several studies that blood compatibility of PCL based scaffold could be enhanced by the effect of other natural polymers (Correia et al., 2016). The hybrid scaffold possess minimal haemolysis and percentage change of counts of leucocytes, RBCs and platelets in the blood upon exposure to scaffold is within the prescribed limit. The thrombogenic mechanism is initiated by attachment of leucocyte on grafts which in turn recruit platelets and other inflammatory cells. The platelet adhesion assay shows the scaffold does not support platelet aggregation. Even though the results in terms of blood compatibility of G3P1 is highly promising, the exact behaviour of any blood contacting graft can be explored only through its *in vivo* evaluation in the circulation.

## 5.3 SYNTHESIS, FABRICATION AND CHARACTERISATION OF POLY (ETHYL METHACRYLATE-CO-DI ETHYL AMINO ETHYL ACRYLATE) TUBULAR SCAFFOLD BY ELECTROSPINNING AND CHARACTERISATION

Long-term patency of vascular graft determines its ultimate success. The patency is related to biocompatibility, non-thrombogenicity and non-hyperplasic nature of the vascular graft. The anti-thrombogenic and haemocompatible luminal surface of graft is majorly attributed by the presence on continuous endothelial cell lining. Thus, endothelisation vascular graft is extremely important and is an essential step (Sánchez et al., 2018). There are different strategies to endothelialize the vascular graft by functionalising vascular graft that include by attaching antibodies, peptides, oligonucleotides or magnetic molecules that intend capture circulating endothelial progenitor cells from blood stream (Melchiorri et al., 2013). These strategies require intricate fabrication procedures and lack cell specificity. A biomaterial that has inherent property to selectively bind to mature or progenitor endothelial cells has been identified from among 354 polymeric microarray and that is poly (ethyl methacrylate-co-di ethyl

amino ethyl acrylate), 8g7 (Pernagallo et al., 2012a). The present study focuses to develop this material itself into small diameter vascular graft through electrospinning which is explored for first time. Moreover, this material also exhibited minimal platelet attachment.

In another study involving poly (ethyl methacrylate-co-di ethyl amino ethyl acrylate), 8g7 this material was coated to the inner surface of decellularized carotid artery and they have proved it supported re-endothelisation of in coated artery compared to non-coated artery (López-Ruiz et al., 2017). The polymer 8g7 was thus synthesised according to the protocol (López-Ruiz et al., 2017; Pernagallo et al., 2012b). The molecular weight of the polymer was in accordance with reported weight of 110000 kDa. The FT-IR spectra of the synthesised polymer assigned the peaks at -C-H stretch at 2974 $cm^{-1}$, -C=O stretch at 1721 $cm^{-1}$, -C-N at 1141 $cm^{-1}$ confirming the polymerisation.

The process of scaffold fabrication by electrospinning offers the ability to generate three dimensional highly porous substrate that mimic the native extracellular matrix of tissues. This unique micro-architecture of scaffold provides suitable niche for cells very similar to their *in vivo* counterparts and allow them to spatially interact, replicate and remodel compared to two-dimensional culture substrates (Syazana and Sukmana, 2016). Electrospinning technique utilises high voltage electric field to generate ultra-fine polymeric fibers that ranges in its diameter from nanometres to micrometres. The resemblance of these fibres to the fibrillar morphology of extracellular matrix makes the cell more conducive to the cell - ECM interactions, adsorption of cell adhesion molecules, maintain cellular phenotype, activate appropriate signalling pathway that promotes differentiation of stem cells. The blood vessel intima is made of collagen type IV fibres on which endothelial cells attach and function.

The critical parameters to be standardised during electrospinning a polymer solution are many. Both intrinsic and extrinsic parameters should work together in order to obtain fine fibre. The electrospin-ability of a solution depends upon its viscosity and conductivity which is in turn dependent on solvent selected and concentration. 8g7 polymer was screened for its solubility in various organic solvents. Based on solubility at various concentrations, ease of electrospinning in producing a stable jet of fibres

without spraying or spitting and also considering the time required for dissolution of the polymer, a combination DMF: THF (9:1) was selected. The polymer was easily soluble in THF than in DMF, but electrospun-ability was poor compared to DMF. It may be attributed to dielectric value of DMF. But DMF alone had posed problems of producing consistent fibres. Even though at lower concentration fibres were produced, a bead less morphology was obtained at 60% concentration. Also, fibres were produced well at 10.5 kV at 0.5 ml/hour flow rate. The electrical force that drives the solution to fibres is dependent on applied voltage (Beachley and Wen, 2009). A high voltage changes the morphology of fibres and at low voltage the solution may not spin. The mandrel used to collect the fibres were 3 mm/5 mm internal diameter. However, 5 mm scaffold were further used for co-culture experiments.

The SEM images of scaffold showed smooth fibrous wall characteristic of electrospun scaffold. It showed highly porous nature. The average fibre diameter was around 4μm. It was reported that pore size increases with increase in fibre diameter (Wulkersdorfer et al., 2010). From the micro-CT images of the tubular scaffold it was deduced that the porosity was around 36 μm. The three-dimensional analysis of tubular scaffold is highly facilitated by non-destructive imaging techniques like micro-CT. Exposing the scaffold to small quantities of ionising radiation and measurement of absorption was done in this technique. The resulting grey scale image from sequential slices are reconstructed to obtain a density map of the sample and porous nature of the scaffold could be deduced from this. Cell growth, migration and interactions are modulated by spatiotemporally integrated biophysical mechanisms that are influenced both by biochemistry of ECM and intracellular signalling. Specific cell requires different pore size for optimal functioning. In case of blood vessel engineering, however the pore size has to be fine-tuned not only to satisfy cellular requirement, but also should prevent blood leakage. Studies have reported that the average pore size should be always less than 100μm for successful blood vessel engineering. For endothelial cells, micro pores (<80μm) is much pronounced, but for cells like fibroblasts or smooth muscle cells pores of range 60-150 μm is adequate (Wang et al., 2014).

Surface hydrophobicity of scaffold also plays a crucial role in governing cell response. The air-water contact angle measurement gives a fair idea regarding the surface

wettability nature of scaffold and lower the contact angle more hydrophilic the substrate. Several reports substantiate that a moderate hydrophilicity is conducive for cell growth and attachment. This is because a hydrophilic surface tends to resist protein adsorption and a hydrophobic surface adsorbs more proteins. Cell adhesion on substrate requires co-ordinated activity of series of proteins to establish stable contact site (Duband and Thiery, 1990). However extremely hydrophilic nature also facilitates adsorption of proteins that initiates coagulation cascade and thereby causes thrombotic complications in blood vessel engineering. It was reported that a hydrophobic-hydrophilic balanced domain suppresses platelet activation and make the scaffold non thrombogenic (Okano et al., 1986). This is in concordance with previous studies reported regarding the 8g7 scaffold (Pernagallo et al., 2012b). The contact angle at zero second on 8g7 scaffold was obtained as $104 \pm 8^0$and eventually water droplet was absorbed by the scaffold within one minute. This shows the scaffold moderately hydrophobic nature. A contact angle between $60^0$ and $80^0$ is were maximum adhesion was reported for fibroblasts (Chang and Wang, 2011). However, there is no clear information about the interaction of perivascular stem cells or endothelial cells with scaffold with various contact angles in the scenario of blood vessel engineering. The percentage swelling of the scaffold is more than 50% making the scaffold suitable for cell growth and exchange of natural molecules (Thaburet et al., 2004).

Blood vessel experience constant contraction and relaxation stress cycle with pressure changes. In order to withstand the physiological dynamic activity, the fabricated vascular graft should possess enough mechanical strength. The analysis of the mechanical properties showed that the modulus of the tubular scaffold was comparable with that to native vessel and scaffold showed higher theoretical burst pressure of 3000 mmHg than the native which comes around 2000 mmHg. The suture retention force of 2.3 N also indicated that tubular scaffold may have good handling properties when intended to be extrapolated for *in vivo* implantation of the scaffold.

## 5.4 CO-CULTURE STUDY

Mesenchymal stem cells have promising properties that make them attractive in regeneration of tissue, especially adipose derived cells prove to reliable autologous source of these cells. However, the cells contained in the stromal vascular fraction after adipose digest is highly heterogeneous and true nature of these cells has been obscure. Mesenchymal stem cells are virtually present in all organs and blood vessels also are associated with these cells. These mesodermal progenitors are present in tunica adventitia of blood vessels and also around the capillary. Perivascular cells- adventitial cells, pericytes, smooth muscle cell contributes to overall maintenance of healthy blood vessel by interacting either directly or indirectly with endothelial cells (Gerhardt and Betsholtz, 2003). Among the perivascular cells- adventitial and pericytes are proved to be the *in vivo* counterparts of MSCs obtained in culture from various organs. Even though these cells have similar locational origin, these cells have distinct phenotypes as well as different behaviours *in vitro* (Tarallo et al., 2012). Expression of different markers on surface of these cells makes the isolation of these cells possible and hence likely to help in exploration of these cells in regeneration of tissues. These cell unlike classic heterogeneous population of MSCs has appreciable regeneration potential and more chromosomal stability. Pericytes and adventitial cells were successfully isolated from adipose digest based on panel of markers and is evident in FACS analysis. These cells also maintain their characteristic markers on 8g7 scaffold when seeded and cultured in DMEM-HG complete media with FBS. Similarly, endothelial cells also maintain their characteristic markers on scaffold, and they were maintained on EGM-2 media (Souza et al., 2018). This gives the idea that the 8g7 scaffold helps the cells to maintain their identity on scaffold similar to that of other in vitro cell culture methods used to maintain these cells.

The cytocompatibility of the scaffold was evident from the scaffold interaction with the cells. Both perivascular cells and endothelial cells when seeded on scaffold were viable with minimal cell death. Also, on day 14 the number of cells seemed to be increasing which was evident from the live/dead cell images on this day. The viability of cells on scaffold was also confirmed by MTT assay. It was evident from the assay that

metabolic activity of the cells was not impeded by the scaffold and even in day 14, cells were active.

The co-culture of the perivascular stem cells derived from adipose tissue and endothelial cells were established in EGM-2 media. It was reported that pre-conditioning of adipose derived stem cells in EGM-2 media enhance the pro-angiogenic potential of these cells than other conventional media (Souza et al., 2018). It was observed that adventitial cells when co-cultured with endothelial cells at lower ratios of endothelial cells always overpopulated and does not support the growth of endothelial cells. This could be attributed to increased proliferation potential of these cells on scaffold as compared to endothelial counterparts. The endothelial cells however maintained its number adequately when cultured five times more in number than adventitial cells. In a previous study it was reported that human vascular adventitial cells require 1.5 days for doubling (Hoshino et al., 2008) and endothelial cells may require much longer time 44.5 hours for first 3 to 5 days and 23 hours for next 6 to 8 days (Yan et al., 1996). In the case of pericyte-endothelial co-culture however equal numbers of both cells were required in order to establish a successful system. This may be due the in vitro doubling time of pericytes which is 45 hours (Cathery et al., 2018). The functioning of endothelial layer is highly influenced by the perivascular cells. Absence of suitable perivascular-endothelial interaction leads to endothelial cell layer degradation, followed by apoptosis. Blood vessel stabilisation is a complex process in which endothelial cells interact with its perivascular components in a sequential manner. These include temporal secretion of angiogenic factors, formation of extracellular matrix, cell proliferation and migration (Merfeld-Clauss et al., 2010). Generally, for angiogenesis, either growth of endothelial cells in hypoxic environment or transfecting cells with angiogenesis promoting genes like VEGF is carried out. These indirect methods have its own limitations and are less applicable in vascular tissue engineering scenario. Establishing a co-culture system thus has its own added advantages. In our study, when cells were co-cultured and the angiogenic potential of scaffold was analysed, it was observed that pericytes are more pro-angiogenic than adventitial cells on 8g7 scaffold. It has been reported that adipose tissue derived stem cells has pro-angiogenic activity. Adipose tissue itself produce angiogenesis activators and inhibitors (Panina et al., 2018). Pericyte function in regulating the perfusion pressure, endothelial proliferation and overall maintenance of

vascular tone (Tarallo et al., 2012). Even though there are reports on advantages of adventitial cells in angiogenesis, the present co-culture data suggest that growth factors and other angiogenic factors secreted as result of co-culture of adventitial cells and endothelial cells on 8g7 scaffold was comparatively less to that of pericyte based co-culture. The pro-angiogenic factors analysed were angiogenin and VEGF-1, both these biomolecules contribute substantially in angiogenesis and blood vessel stabilisation. However, in the adventitial cell-endothelial co-cultures these factors were less. Similarly, acidic and basic platelet derived growth factor beta was secreted in increased amount by pericyte - endothelial co-culture on scaffold. The role of pericytes in physiological angiogenesis is very evident.

## 5.5 *IN VIVO* EVALUATION OF GELATIN-VINYL ACETATE / POLY-ε-CAPROLACTONE ELECTROSPUN SCAFFOLD IN LAPINE AND OVINE MODELS

For successful application of fabricated tissue engineered vascular graft require the *in vivo* evaluation of the same. Even though the in vitro characteristics of a vascular graft is appreciable, the behaviour of graft with respect to physiological stress and regeneration capability may vary. Analysing the pre-clinical outcome is thus extremely relevant for extrapolating the vascular graft to human subjects. Normally a blood vessel experiences heavy load of vascular dynamics and this in turn effect the patency of implanted graft. Also, *in vivo* blood compatibility is also important (Fukunishi et al., 2016). The efficiency of the G3P1 tubular scaffold seeded with adipose stem cell derived smooth muscle cells, to with stand functional compliance and to from well-organised neo-tissue through vascular remodelling has to be accessed.

A range of different animal models are subjected to vascular graft implantation for evaluating its functional efficiency, however no single animal model satisfies the optimal performance criteria required. Among the small animal models like rat, mice or rabbit, rabbit models have advantages of ease of handling, ability to implant 1-4mm diameter grafts, multiple implantation site like carotid artery, abdominal aorta and also has regeneration mechanism more or less similar to human being. However vascular physiology and dynamics entirely limits its application and only short-term studies are only possible (Zheng et al., 2012b). In the present study the G3P1 – 3 mm graft when

implanted in the carotid artery was occluded within two weeks. It has to infer that there was diameter mismatch between graft and vessel diameter of the rabbit. This mismatch might have led to anastomotic thrombosis of the graft as the histological analysis reveals that the vessel was occluded at both its anastomosis and there were no traces of blood flow in the graft mid region. Here, we have to conclude that rabbit model is not feasible to evaluate the properties of G3P1 scaffold both in terms of its practical applicability or regeneration potential. However, the histological analysis of the grafts provided a clear idea of the inflammatory mechanisms associated with the biomaterial. The in vivo integration and regeneration of vascular graft in to host circulatory system is a complex mechanism and is still highly not explored. Several evidences claim that the host immune cells like macrophages, monocytes and neutrophils plays a major role in graft remodelling. When G3P1 – 3 mm grafts were implanted in rabbits there was presence of moderate granulomatous inflammation containing polymorphonuclear cells, mononuclear cell and foreign body giant cells. These mechanisms are typical response of blood contacting biomaterials and this data cannot give a clear idea regarding the ultimate regeneration potential of the vascular graft. The insights from rabbit study was not enough in order to evaluate the efficiency of G3P1 grafts due to reasons stated above. Even though, the graft was not patent in rabbit, our inference is that failure rate was mostly attributed by the animal model characteristics than the graft properties. This has led to implantation of the graft in sheep carotid artery model and both SMC cellularised G3P1 – 5 mm graft and bare graft was implanted. The patency of the graft was 67%. Ovine models are attractive choice for evaluation of vascular grafts. The cardiovascular physiology, thrombogenicity and endothelisation mechanisms are similar to human beings. Also, the graft size comes in between 4 -6 mm for sheep. Human carotid artery diameter is almost 6 mm and coronary is 4 mm. Sheep model provides long necks suitable for implantation of graft in their carotid artery, also long-term studies are also possible. However, the drawback of sheep model is their tendency of hypercoagulability and cost (Pashneh-Tala et al., 2016).

The gross evaluation of the explanted G3P1 – 5 mm grafts showed that there was enlargement of vessel diameter to more than 7 mm of the graft. Aneurysmal bulging of the graft is attributed to its mechanical properties and possibility of a thinner scaffold material. Comparing the *in vitro* burst pressure of 1568 mmHg, the graft may have to be

improved for its mechanical robustness to withstand the physiological stresses. The histological analysis of the explant showed that graft showed excellent regeneration behaviour. As stated earlier, the inflammatory mechanisms may mediate the vessel regeneration. Both in cell seeded and bare scaffold graft, there was presence of inflammatory cells like mononuclear cells. Any biomaterial when implanted elicits cellular and tissue responses. The major events mediating this are inflammatory process, wound healing response, foreign body reaction and fibrous encapsulation of the implant (Sheikh et al., 2015). Histologically these initial reactions were evident in the implanted graft. However, in the due course of implantation, these inflammatory cells are the mediators of graft remodelling and regeneration. After initial inflammation mononuclear cells may recruit monocyte (Roh et al., 2010). Monocytes presence were detected in blood vessel grafts even after many weeks of implantation suggesting that these cells may participate in regeneration (Burn et al., 1994; Hoerstrup et al., 2006). Also, these cells when seeded on scaffold and implanted has shown to recruit smooth muscle cells and endothelial cells (Roh et al., 2010). The other features of graft regeneration are endothelisation, neo-vascularisation and extracellular matrix deposition. These characteristics were more pronounced in G3P1 – 5 mm graft seeded with smooth muscle cell layer. Even in the mid region of the graft there was neointima layer formation. The study proves that smooth muscle cells helps in endothelisation of vascular grafts. The extracellular matrix and other biomolecules secreted by these cells may help in creating a niche favourable for endothelial progenitor cells adhesion and maturation. Endothelisation was evident from immunostaining of CD 31 antibody and also from SEM. Grafts seeded by autologous cells may undergo moderate inflammation mechanisms which may convert to regeneration mechanisms easily than the unseeded graft. Endothelisation was observed to be complete in almost 12 weeks' time in some previous studies which is in concordance with present implantation time. There was also adequate deposition of elastin in graft with cells which indicate that implant scaffold has *in vivo* regeneration capability (Pashneh-Tala et al., 2016).

## 5.6 LIMITATIONS

The present study has certain limitations, the *in vivo* evaluation of G3P1 scaffold was carried out only for three months, so the outcome of the graft after this time point cannot be deduced. The mechanical properties and gene expression analysis of the explant were not conducted. Moreover, the inflammatory macrophages were not identified after explanting the graft. The co-culture study on 8g7 scaffold has to go further in terms of its implantation potential and in vivo angiogenesis capacity which is not addressed in the present study. However, the preliminary observations of the results of both grafts suggest that autologous perivascular cells immensely contribute to endothelisation and thereby success of the small diameter vascular graft.

# CHAPTER 6

# SUMMARY AND CONCLUSION

## 6.1 SUMMARY

The present study intended to evaluate the functional efficiency of small diameter vascular graft developed by the direct scaffolding and cell-based strategy. For this, two different polymeric grafts were prepared in order analyse the regeneration potential of each graft. One scaffold was chosen based on its ability to support growth and proliferation of smooth muscle cell (Gelatin-vinyl acetate/poly-ε-caprolactone co-electrospun scaffold, G3P1) and other based on ability to selectively bind endothelial cells (Poly-ethyl methacrylate-co-diethyl amino ethyl acrylate, 8g7). Despite of intensive *in vitro* study of both grafts and strategies applied, only one among the graft was only studied in *in vivo* conditions and that graft exhibited adequate regeneration capability.

The initial strategy of generating small diameter vascular graft was to adopt an outside in strategy were smooth muscle cells derived from patient's own adipose stem cells on scaffold is employed. The study was to investigate whether the graft generated will help in mediating the regeneration and remodelling when implanted. In order to achieve this, the fabrication of scaffold was done by dual-source electrospinning of gelatin-vinyl acetate and poly-ε-caprolactone. The gelatin-vinyl acetate was initially synthesised and characterised. The synthesised polymer was then co-electrospun with PCL. The conditions and parameters of electrospinning were standardised. Varying the flow rate different combination of hybrid scaffold was fabricated of which the 3 ml/hour flow rate of gelatin-vinyl acetate and 1 ml/hour flow rate PCL scaffold combination was selected for further graft fabrication based on its properties (G3P1). In order to fabricate tubular scaffold of internal diameter 3 mm and 5 mm, respective collecting mandrels were selected. The tubes fabricated - G3P1 – 3 mm and G3P1 – 5 mm were extensively characterised for its properties like gross morphology, micro-structure, pore nature, swelling, degradation and mechanical characteristics.

For differentiation of smooth muscle cells on scaffold, adipose tissue was isolated from rabbits and sheep. The chosen animals were further used for implantation study at the end. The mesenchymal stem cells were characterised for expression of stem cell markers and for differentiating them into various lineages. The biocompatibility of the scaffold was further checked with these cells and was found to be cyto-compatible. The cytocompatibility studies included direct contact assay, MTT assay and Raman mapping of cell seeded scaffold. Further mesenchymal stem cells were differentiated to smooth muscle lineage on scaffold (G3P1 – 3 mm for rabbit and G3P1 – 5 mm for sheep) under the influence of growth factor cocktail through TGF-β1 mediated Smad pathway. The differentiated cells were analysed for their contractile nature on the scaffold by PCR analysis of major genes and immunofluorescence. Data supported that the differentiated smooth muscle cells maintained the contractile phenotype by expressing smooth muscle heavy chain protein. The extracellular collagen and elastin secreted were also analysed. *In vitro* blood compatibility of the scaffold was performed according to ISO standard and scaffold seemed to be blood compatible. The G3P1 – 3 mm graft with differentiated autologous smooth muscle cells was implanted in rabbit common carotid artery. After two weeks terminal angiogram showed occluded graft, however this was as expected as there was diameter mismatch during implantation and thereby anastomotic occlusion of graft. Initial inflammatory response of the graft was deduced from this study. The G3P1-5 mm graft with autologous differentiated smooth muscle cells was implanted in sheep model by replacing a part of carotid artery. Both cellularised and bare scaffold alone grafts were implanted. After three months the angiographic evaluation showed 67% patency of the graft. The explant was histologically evaluated for its regeneration capability. The smooth muscle cellularised graft showed improved regeneration potential than that of bare graft, which was evident from the endothelisation, neo vascularisation and elastogenesis of the explant. The work here can be summarised as an application of outside-in strategy of vascular graft generation, were smooth muscle seeded scaffold mediates the endothelisation of graft and thereby regeneration of occluded blood vessel when replaced.

The second strategy of acrylate-based scaffold fabrication involved the synthesis and characterisation of the Poly-ethyl methacrylate-co-diethyl amino ethyl acrylate, 8g7). Here as part of inside-out strategy, an endothelial cell binding material was chosen

to pre-endothelialize the graft. However, the effect of endothelial cells on scaffold when interacted with perivascular cells like pericytes and adventitial cells were analysed through co-culturing. Electrospinning of the polymer was first reported in this study. The electrospinning of the polymer was standardised, and tubular graft was fabricated. The fabricated graft was analysed for its properties like surface wettability, swelling, porosity and mechanical properties. Adipose derived mesenchymal stem cells were isolated from human adipose tissue for conducting this study. However, the stem cell isolated was much purified version of otherwise heterogeneous population of mesenchymal stem cells. The cells isolated were perivascular in origin - Adventitial cells and pericytes. The cytocompatibility of adventitial cells, pericytes and endothelial cells were studied on 8g7 scaffold by MTT assay, live dead assay and also by analysing the expression of specific markers of each cell type on the scaffold. The electrospun scaffold was found to be cell conducive. Further co-culture of adventitial cells with endothelial cells and pericytes with endothelial cells were standardised on scaffold. The secretome of each co-culture was profiled for its ability to initiate angiogenesis and it was found that pericyte-endothelial co-culture had advantageously facilitated scaffold-based angiogenesis than the other system. Here, to summarise, the inside out strategy of seeding endothelial cells and perivascular cells also helped in endothelialisation of graft and which was more pronounced in pericyte-endothelial co-culture model.

The present study involved two scaffold system and two different strategies to approach the fabrication of tissue engineered small diameter vascular graft. The data obtained agrees with feasibility of both strategies however G3P1 scaffold-based graft definitely has an upper hand due its appreciable performance *in vivo*.

## 6.2 CONCLUSION

1. Tissue engineered small diameter vascular graft of dual source co-electrospun gelatin-vinyl acetate – Poly-ε-caprolactone scaffold with adequate biomechanical property and blood compatibility were fabricated.
2. Autologous adipose cells differentiated to smooth muscle cells on tubular scaffold showed 67% patency when implanted in sheep common carotid artery replacement model.
3. The endothelial friendly acrylate based electrospun tubular scaffold promoted attachment and functioning of perivascular stem cells and endothelial cells.
4. The co-culture of cells on scaffold concluded that pericyte –endothelial interaction is more pronounced in angiogenesis.
5. The patient specific vascular graft developed by electrospun scaffold and autologous adipose derived stem cells has the ability to perform better and may be further explored.

## 6.3 FUTURE PERSPECTIVES

The present study has immense scope of perspectives to be carried out further. The G3P1 scaffold could be improved for its mechanical robustness and should be implanted in a greater number of animals. Mechanisms of smooth muscle based endothelization of G3P1 scaffold should be elucidated. The acrylate-based scaffold should be further explored for its co-culture study of pericytes/smooth muscle cells with endothelial cells and the *in vivo* potential has to be explored. However, a combination of both gelatin based and acrylate based scaffold is considered to have a promising future which need to be further explored.

# BIBLIOGRAPHY


20.1 Structure and Function of Blood Vessels | Anatomy & Physiology, n.d. URL http://library.open.oregonstate.edu/aandp/chapter/20-1-structure-and-function-of-blood-vessels/ (accessed 6.11.19).

Agarwal, S., Wendorff, J.H., Greiner, A., 2008. Use of electrospinning technique for biomedical applications. Polymer 49, 5603–5621. https://doi.org/10.1016/j.polymer.2008.09.014

Alberts, B., Johnson, A., Lewis, J., Raff, M., Roberts, K., Walter, P., 2002. Blood Vessels and Endothelial Cells. Mol. Biol. Cell 4th Ed.

Aldana, A.A., Abraham, G.A., 2017. Current advances in electrospun gelatin-based scaffolds for tissue engineering applications. Int. J. Pharm. 523, 441–453. https://doi.org/10.1016/j.ijpharm.2016.09.044

Andel, C.J. van, Pistecky, P.V., Borst, C., 2003. Mechanical properties of porcine and human arteries: implications for coronary anastomotic connectors. Ann. Thorac. Surg. 76, 58–64. https://doi.org/10.1016/S0003-4975(03)00263-7

Ardila, D.C., Tamimi, E., Doetschman, T., Wagner, W.R., Vande Geest, J.P., 2019. Modulating smooth muscle cell response by the release of TGFβ2 from tubular scaffolds for vascular tissue engineering. J. Controlled Release 299, 44–52. https://doi.org/10.1016/j.jconrel.2019.02.024

Arora, P.D., McCulloch, C.A.G., 1994. Dependence of collagen remodelling on α-smooth muscle actin expression by fibroblasts. J. Cell. Physiol. 159, 161–175. https://doi.org/10.1002/jcp.1041590120

Avolio, E., Alvino, V.V., Ghorbel, M.T., Campagnolo, P., 2017. Perivascular cells and tissue engineering: Current applications and untapped potential. Pharmacol. Ther. 171, 83–92. https://doi.org/10.1016/j.pharmthera.2016.11.002

Azami, M., Rabiee, M., Moztarzadeh, F., 2010. Glutaraldehyde crosslinked gelatin/hydroxyapatite nanocomposite scaffold, engineered via compound techniques. Polym. Compos. 31, 2112–2120. https://doi.org/10.1002/pc.21008

Baldock, S.J., Talari, A.C.S., Smith, R., Wright, K.L., Ashton, L., 2019. Single-cell Raman microscopy of microengineered cell scaffolds. J. Raman Spectrosc. 50, 371–379. https://doi.org/10.1002/jrs.5525

Beachley, V., Wen, X., 2009. Effect of electrospinning parameters on the nanofiber diameter and length. Mater. Sci. Eng. C Mater. Biol. Appl. 29, 663–668. https://doi.org/10.1016/j.msec.2008.10.037

Bergheanu, S.C., Bodde, M.C., Jukema, J.W., 2017. Pathophysiology and treatment of atherosclerosis. Neth. Heart J. 25, 231–242. https://doi.org/10.1007/s12471-017-0959-2

Bibevski, S., Ruzmetov, M., Fortuna, R.S., Turrentine, M.W., Brown, J.W., Ohye, R.G., 2017. Performance of SynerGraft Decellularized Pulmonary Allografts Compared With Standard Cryopreserved Allografts: Results From Multiinstitutional Data. Ann. Thorac. Surg. 103, 869–874. https://doi.org/10.1016/j.athoracsur.2016.07.068

Boccafoschi, F., Rajan, N., Habermehl, J., Mantovani, D., 2007. Preparation and characterization of a scaffold for vascular tissue engineering by direct-assembling of collagen and cells in a cylindrical geometry. Macromol. Biosci. 7, 719–726. https://doi.org/10.1002/mabi.200600242

Brooke, B.S., Karnik, S.K., Li, D.Y., 2003. Extracellular matrix in vascular morphogenesis and disease: structure versus signal. Trends Cell Biol. 13, 51–56.

Brugmans, M., Serrero, A., Cox, M., Svanidze, O., Schoen, F.J., 2019. Morphology and mechanisms of a novel absorbable polymeric conduit in the pulmonary circulation of sheep. Cardiovasc. Pathol. 38, 31–38. https://doi.org/10.1016/j.carpath.2018.10.008

Burn, T.C., Petrovick, M.S., Hohaus, S., Rollins, B.J., Tenen, D.G., 1994. Monocyte chemoattractant protein-1 gene is expressed in activated neutrophils and retinoic acid-induced human myeloid cell lines. Blood 84, 2776–2783.

Campagnolo, P., Gormley, A.J., Chow, L.W., Guex, A.G., Parmar, P.A., Puetzer, J.L., Steele, J.A., Breant, A., Madeddu, P., Stevens, M.M., 2016. Pericyte seeded dual peptide scaffold with improved endothelialization for vascular graft tissue engineering. Adv. Healthc. Mater. 5, 3046–3055. https://doi.org/10.1002/adhm.201600699

Carrabba, M., Madeddu, P., 2018. Current Strategies for the Manufacture of Small Size Tissue Engineering Vascular Grafts. Front. Bioeng. Biotechnol. 6. https://doi.org/10.3389/fbioe.2018.00041

Cathery, W., Faulkner, A., Maselli, D., Madeddu, P., 2018. Concise Review: The Regenerative Journey of Pericytes Toward Clinical Translation. STEM CELLS 36, 1295–1310. https://doi.org/10.1002/stem.2846

Catto, V., Farè, S., Freddi, G., Tanzi, M.C., 2014. Vascular Tissue Engineering: Recent Advances in Small Diameter Blood Vessel Regeneration [WWW Document]. Int. Sch. Res. Not. https://doi.org/10.1155/2014/923030

Chang, H.-I., Wang, Y., 2011. Cell Responses to Surface and Architecture of Tissue Engineering Scaffolds. Regen. Med. Tissue Eng. - Cells Biomater. https://doi.org/10.5772/21983

Chang, W.G., Niklason, L.E., 2017a. A short discourse on vascular tissue engineering. NPJ Regen. Med. 2. https://doi.org/10.1038/s41536-017-0011-6

Chang, W.G., Niklason, L.E., 2017b. A short discourse on vascular tissue engineering. Npj Regen. Med. 2, 7. https://doi.org/10.1038/s41536-017-0011-6

Chen Yikuan, Wong Mei Mei, Campagnolo Paola, Simpson Russell, Winkler Bernhard, Margariti Andriani, Hu Yanhua, Xu Qingbo, 2013. Adventitial Stem Cells in Vein Grafts Display Multilineage Potential That Contributes to Neointimal Formation. Arterioscler. Thromb. Vasc. Biol. 33, 1844–1851. https://doi.org/10.1161/ATVBAHA.113.300902

Coenen, A.M.J., Bernaerts, K.V., Harings, J.A.W., Jockenhoevel, S., Ghazanfari, S., 2018. Elastic materials for tissue engineering applications: Natural, synthetic, and hybrid polymers. Acta Biomater. 79, 60–82. https://doi.org/10.1016/j.actbio.2018.08.027

Correia, T.R., Ferreira, P., Vaz, R., Alves, P., Figueiredo, M.M., Correia, I.J., Coimbra, P., 2016. Development of UV cross-linked gelatin coated electrospun poly(caprolactone) fibrous scaffolds for tissue engineering. Int. J. Biol. Macromol., Biological Macromolecules for Tissue Regeneration 93, 1539–1548. https://doi.org/10.1016/j.ijbiomac.2016.05.045

Cui, W., Li, X., Zhou, S., Weng, J., 2008. Degradation patterns and surface wettability of electrospun fibrous mats. Polym. Degrad. Stab. 93, 731–738. https://doi.org/10.1016/j.polymdegradstab.2007.12.002

Davidenko, N., Schuster, C.F., Bax, D.V., Farndale, R.W., Hamaia, S., Best, S.M., Cameron, R.E., 2016. Evaluation of cell binding to collagen and gelatin: a study of the effect of 2D and 3D architecture and surface chemistry. J. Mater. Sci. Mater. Med. 27, 148. https://doi.org/10.1007/s10856-016-5763-9

Davidson, J.M., 2002. Smad about Elastin Regulation. Am. J. Respir. Cell Mol. Biol. 26, 164–166. https://doi.org/10.1165/ajrcmb.26.2.f228

Deepthi, S., Nivedhitha Sundaram, M., Vijayan, P., Nair, S.V., Jayakumar, R., 2018. Engineering poly(hydroxy butyrate-co-hydroxy valerate) based vascular scaffolds to mimic native artery. Int. J. Biol. Macromol. 109, 85–98. https://doi.org/10.1016/j.ijbiomac.2017.12.077

Dhulekar, J., Simionescu, A., 2018. Challenges in vascular tissue engineering for diabetic patients. Acta Biomater. 70, 25–34. https://doi.org/10.1016/j.actbio.2018.01.008

Diban, N., Stamatialis, D.F., 2011. Functional Polymer Scaffolds for Blood Vessel Tissue Engineering. Macromol. Symp. 309–310, 93–99. https://doi.org/10.1002/masy.201100038

Dominici, M., Le Blanc, K., Mueller, I., Slaper-Cortenbach, I., Marini, F., Krause, D., Deans, R., Keating, A., Prockop, D., Horwitz, E., 2006. Minimal criteria for defining multipotent mesenchymal stromal cells. The International Society for

Cellular Therapy position statement. Cytotherapy 8, 315–317. https://doi.org/10.1080/14653240600855905

Du, L., Xu, H.Z., Li, T., Zhang, Y., Zou, F.Y., 2017. Fabrication of ascorbyl palmitate loaded poly(caprolactone)/silver nanoparticle embedded poly(vinyl alcohol) hybrid nanofibre mats as active wound dressings via dual-spinneret electrospinning. RSC Adv. 7, 31310–31318. https://doi.org/10.1039/C7RA03193A

Duband, J.-L., Thiery, J.P., 1990. Spatio-temporal distribution of the adherens junction-associated molecules vinculin and talin in the early avian embryo. Cell Differ. Dev. 30, 55–76. https://doi.org/10.1016/0922-3371(90)90074-7

Dulnik, J., Denis, P., Sajkiewicz, P., Kołbuk, D., Choińska, E., 2016. Biodegradation of bicomponent PCL/gelatin and PCL/collagen nanofibers electrospun from alternative solvent system. Polym. Degrad. Stab. C, 10–21. https://doi.org/10.1016/j.polymdegradstab.2016.05.022

Eble, J.A., Niland, S., 2009a. The extracellular matrix of blood vessels. Curr. Pharm. Des. 15, 1385–1400.

Eble, J.A., Niland, S., 2009b. The extracellular matrix of blood vessels. Curr. Pharm. Des. 15, 1385–1400.

Echtermeyer, F., Streit, M., Wilcox-Adelman, S., Saoncella, S., Denhez, F., Detmar, M., Goetinck, P., 2001. Delayed wound repair and impaired angiogenesis in mice lacking syndecan-4. J. Clin. Invest. 107, R9–R14. https://doi.org/10.1172/JCI10559

Elzorkany, K.M.A., Montaser, B.A.M., El-Hefnawy, S.M., 2018. Plasma von Willebrand Factor and a Disintegrin and Metalloproteinase with Eight Thrombospondin-type 1 Motif Levels in Hemodialysis Patients: Relation to Vascular Access Thrombosis. Indian J. Nephrol. 28, 278–282. https://doi.org/10.4103/ijn.IJN_184_17

Engbers-Buijtenhuijs, P., Buttafoco, L., Poot, A.A., Dijkstra, P.J., Vos, R.A.I. de, Sterk, L.M.T., Geelkerken, R.H., Vermes, I., Feijen, J., 2006. Biological characterisation of vascular grafts cultured in a bioreactor. Biomaterials 27, 2390–2397. https://doi.org/10.1016/j.biomaterials.2005.10.016

Fang, Q., Gu, T., Fan, J., Zhang, Y., Wang, Y., Zhao, Y., Zhao, P., 2019. Evaluation of a hybrid small caliber vascular graft in a rabbit model. J. Thorac. Cardiovasc. Surg. https://doi.org/10.1016/j.jtcvs.2019.02.083

Fukunishi, T., Best, C.A., Sugiura, T., Opfermann, J., Ong, C.S., Shinoka, T., Breuer, C.K., Krieger, A., Johnson, J., Hibino, N., 2017. Preclinical study of patient-specific cell-free nanofiber tissue-engineered vascular grafts using 3-dimensional printing in a sheep model. J. Thorac. Cardiovasc. Surg. 153, 924–932. https://doi.org/10.1016/j.jtcvs.2016.10.066

Fukunishi, T., Best, C.A., Sugiura, T., Shoji, T., Yi, T., Udelsman, B., Ohst, D., Ong, C.S., Zhang, H., Shinoka, T., Breuer, C.K., Johnson, J., Hibino, N., 2016. Tissue-Engineered Small Diameter Arterial Vascular Grafts from Cell-Free Nanofiber PCL/Chitosan Scaffolds in a Sheep Model. PLOS ONE 11, e0158555. https://doi.org/10.1371/journal.pone.0158555

Gautam, S., Dinda, A.K., Mishra, N.C., 2013. Fabrication and characterization of PCL/gelatin composite nanofibrous scaffold for tissue engineering applications by electrospinning method. Mater. Sci. Eng. C Mater. Biol. Appl. 33, 1228–1235. https://doi.org/10.1016/j.msec.2012.12.015

Gauvin, R., Guillemette, M., Galbraith, T., Bourget, J.-M., Larouche, D., Marcoux, H., Aubé, D., Hayward, C., Auger, F.A., Germain, L., 2011. Mechanical Properties of Tissue-Engineered Vascular Constructs Produced Using Arterial or Venous Cells. Tissue Eng. Part A 17, 2049–2059. https://doi.org/10.1089/ten.tea.2010.0613

Gerhardt, H., Betsholtz, C., 2003. Endothelial-pericyte interactions in angiogenesis. Cell Tissue Res. 314, 15–23. https://doi.org/10.1007/s00441-003-0745-x

Gilbert, P.M., Havenstrite, K.L., Magnusson, K.E.G., Sacco, A., Leonardi, N.A., Kraft, P., Nguyen, N.K., Thrun, S., Lutolf, M.P., Blau, H.M., 2010. Substrate elasticity regulates skeletal muscle stem cell self-renewal in culture. Science 329, 1078–1081. https://doi.org/10.1126/science.1191035

Gimble Jeffrey M., Katz Adam J., Bunnell Bruce A., 2007. Adipose-Derived Stem Cells for Regenerative Medicine. Circ. Res. 100, 1249–1260. https://doi.org/10.1161/01.RES.0000265074.83288.09

Gohda, M., Magoshi, T., Kato, S., Noguchi, T., Yasuda, S., Nonogi, H., Matsuda, T., 2001. Terminally Alkylated Heparin. 2. Potent Antiproliferative Agent for Vascular Smooth Muscle Cells. Biomacromolecules 2, 1178–1183. https://doi.org/10.1021/bm010097x

Grus, T., Lambert, L., Mlcek, M., Chlup, H., Honsova, E., Spacek, M., Burgetova, A., Lindner, J., 2018. In Vivo Evaluation of Short-Term Performance of New Three-Layer Collagen-Based Vascular Graft Designed for Low-Flow Peripheral Vascular Reconstructions [WWW Document]. BioMed Res. Int. https://doi.org/10.1155/2018/3519596

Gu, W., Hong, X., Le Bras, A., Nowak, W.N., Issa Bhaloo, S., Deng, J., Xie, Y., Hu, Y., Ruan, X.Z., Xu, Q., 2018. Smooth muscle cells differentiated from mesenchymal stem cells are regulated by microRNAs and suitable for vascular tissue grafts. J. Biol. Chem. 293, 8089–8102. https://doi.org/10.1074/jbc.RA118.001739

Guo, X., Chen, S.-Y., 2012a. Transforming growth factor-β and smooth muscle differentiation. World J. Biol. Chem. 3, 41–52. https://doi.org/10.4331/wjbc.v3.i3.41

Guo, X., Chen, S.-Y., 2012b. Transforming growth factor-β and smooth muscle differentiation. World J. Biol. Chem. 3, 41–52. https://doi.org/10.4331/wjbc.v3.i3.41

Han, J., Lazarovici, P., Pomerantz, C., Chen, X., Wei, Y., Lelkes, P.I., 2011. Co-electrospun blends of PLGA, gelatin, and elastin as potential nonthrombogenic scaffolds for vascular tissue engineering. Biomacromolecules 12, 399–408. https://doi.org/10.1021/bm101149r

Hansen, F., Mangell, P., Sonesson, B., Länne, T., 1995. Diameter and compliance in the human common carotid artery — variations with age and sex. Ultrasound Med. Biol. 21, 1–9. https://doi.org/10.1016/0301-5629(94)00090-5

Hasan, A., Memic, A., Annabi, N., Hossain, M., Paul, A., Dokmeci, M.R., Dehghani, F., Khademhosseini, A., 2014a. Electrospun scaffolds for tissue engineering of vascular grafts. Acta Biomater. 10, 11–25. https://doi.org/10.1016/j.actbio.2013.08.022

Hasan, A., Memic, A., Annabi, N., Hossain, M., Paul, A., Dokmeci, M.R., Dehghani, F., Khademhosseini, A., 2014b. Electrospun scaffolds for tissue engineering of vascular grafts. Acta Biomater. 10, 11–25. https://doi.org/10.1016/j.actbio.2013.08.022

He, W., Ma, Z., Teo, W.E., Dong, Y.X., Robless, P.A., Lim, T.C., Ramakrishna, S., 2009. Tubular nanofiber scaffolds for tissue engineered small-diameter vascular grafts. J. Biomed. Mater. Res. A 90, 205–216. https://doi.org/10.1002/jbm.a.32081

He, W., Nieponice, A., Soletti, L., Hong, Y., Gharaibeh, B., Crisan, M., Usas, A., Peault, B., Huard, J., Wagner, W.R., Vorp, D.A., 2010. Pericyte-based human tissue engineered vascular grafts. Biomaterials 31, 8235–8244. https://doi.org/10.1016/j.biomaterials.2010.07.034

Heart Disease and Stroke Statistics—2019 Update: A Report From the American Heart Association, n.d. 473.

Hellio, D., Djabourov, M., 2006. Physically and Chemically Crosslinked Gelatin Gels. Macromol. Symp. 241, 23–27. https://doi.org/10.1002/masy.200650904

Higashi, Y., 2015. Assessment of endothelial function. History, methodological aspects, and clinical perspectives. Int. Heart. J. 56, 125–134. https://doi.org/10.1536/ihj.14-385

Hild, M., Rez, M.F.A., Aibibu, D., Toskas, G., Cheng, T., Laourine, E., Cherif, C., 2015. Pcl/Chitosan Blended Nanofibrous Tubes Made by Dual Syringe Electrospinning. Autex Res. J. 15, 54–59. https://doi.org/10.1515/aut-2015-0016

Hiob, M.A., Crouch, G.W., Weiss, A.S., 2016. Elastomers in vascular tissue engineering. Curr. Opin. Biotechnol. 40, 149–154. https://doi.org/10.1016/j.copbio.2016.04.008

Ho, M.S.P., Böse, K., Mokkapati, S., Nischt, R., Smyth, N., 2008. Nidogens—Extracellular matrix linker molecules. Microsc. Res. Tech. 71, 387–395. https://doi.org/10.1002/jemt.20567

Hoerstrup, S.P., Cummings Mrcs, I., Lachat, M., Schoen, F.J., Jenni, R., Leschka, S., Neuenschwander, S., Schmidt, D., Mol, A., Günter, C., Gössi, M., Genoni, M., Zund, G., 2006. Functional growth in tissue-engineered living, vascular grafts: follow-up at 100 weeks in a large animal model. Circulation 114, I159-166. https://doi.org/10.1161/CIRCULATIONAHA.105.001172

Horakova, J., Mikes, P., Lukas, D., Saman, A., Jencova, V., Klapstova, A., Svarcova, T., Ackermann, M., Novotny, V., Kalab, M., Lonsky, V., Bartos, M., Rampichova, M., Litvinec, A., Kubikova, T., Tomasek, P., Tonar, Z., 2018. Electrospun vascular grafts fabricated from poly(L-lactide-co-$\upepsilon$-caprolactone) used as a bypass for the rabbit carotid artery. Biomed. Mater. 13, 065009. https://doi.org/10.1088/1748-605X/aade9d

Hoshino, A., Chiba, H., Nagai, K., Ishii, G., Ochiai, A., 2008. Human vascular adventitial fibroblasts contain mesenchymal stem/progenitor cells. Biochem. Biophys. Res. Commun. 368, 305–310. https://doi.org/10.1016/j.bbrc.2008.01.090

Huang, Y., Shen, Z., Chen, Q., Huang, P., Zhang, H., Du, S., Geng, B., Zhang, C., Li, K., Tang, C., Du, J., Jin, H., 2016a. Endogenous sulfur dioxide alleviates collagen remodeling via inhibiting TGF-β/Smad pathway in vascular smooth muscle cells. Sci. Rep. 6, 19503. https://doi.org/10.1038/srep19503

Huang, Y., Shen, Z., Chen, Q., Huang, P., Zhang, H., Du, S., Geng, B., Zhang, C., Li, K., Tang, C., Du, J., Jin, H., 2016b. Endogenous sulfur dioxide alleviates collagen remodeling via inhibiting TGF-β/Smad pathway in vascular smooth muscle cells. Sci. Rep. 6, 19503. https://doi.org/10.1038/srep19503

Jirofti, N., Mohebbi-kalhori, D., Samimi, A., Hadjizadeh, A., Kazemzadeh, G., 2018. Small-diameter vascular graft using co-electrospun of composite PCL/PU nanofibers. Biomed. Mater. 13. https://doi.org/10.1088/1748-605X/aad4b5

Johnson, R., Ding, Y., Nagiah, N., Monnet, E., Tan, W., 2019. Coaxially-structured fibres with tailored material properties for vascular graft implant. Mater. Sci. Eng. C 97, 1–11. https://doi.org/10.1016/j.msec.2018.11.036

Jordan, S.W., Haller, C.A., Sallach, R.E., Apkarian, R.P., Hanson, S.R., Chaikof, E.L., 2007. The effect of a recombinant elastin-mimetic coating of an ePTFE prosthesis on acute thrombogenicity in a baboon arteriovenous shunt. Biomaterials 28, 1191–1197. https://doi.org/10.1016/j.biomaterials.2006.09.048

Joy, J., Pereira, J., Aid-Launais, R., Pavon-Djavid, G., Ray, A.R., Letourneur, D., Meddahi-Pellé, A., Gupta, B., 2018. Gelatin - Oxidized carboxymethyl cellulose blend based tubular electrospun scaffold for vascular tissue engineering. Int. J. Biol. Macromol. 107, 1922–1935. https://doi.org/10.1016/j.ijbiomac.2017.10.071

Kabirian, F., Ditkowski, B., Zamanian, A., Hoylaerts, M.F., Mozafari, M., Heying, R., 2019. Controlled NO-Release from 3D-Printed Small-Diameter Vascular Grafts Prevents Platelet Activation and Bacterial Infectivity. ACS Biomater. Sci. Eng. 5, 2284–2296. https://doi.org/10.1021/acsbiomaterials.9b00220

Koch, S., Flanagan, T.C., Sachweh, J.S., Tanios, F., Schnoering, H., Deichmann, T., Ellä, V., Kellomäki, M., Gronloh, N., Gries, T., Tolba, R., Schmitz-Rode, T., Jockenhoevel, S., 2010. Fibrin-polylactide-based tissue-engineered vascular graft in the arterial circulation. Biomaterials 31, 4731–4739. https://doi.org/10.1016/j.biomaterials.2010.02.051

Kothapalli, C.R., Taylor, P.M., Smolenski, R.T., Yacoub, M.H., Ramamurthi, A., 2009. Transforming Growth Factor Beta 1 and Hyaluronan Oligomers Synergistically Enhance Elastin Matrix Regeneration by Vascular Smooth Muscle Cells. Tissue Eng. Part A 15, 501–511. https://doi.org/10.1089/ten.tea.2008.0040

Kühn, K., 1995. Basement membrane (type IV) collagen. Matrix Biol. J. Int. Soc. Matrix Biol. 14, 439–445.

Ladd, M.R., Lee, S.J., Stitzel, J.D., Atala, A., Yoo, J.J., 2011. Co-electrospun dual scaffolding system with potential for muscle-tendon junction tissue engineering. Biomaterials 32, 1549–1559. https://doi.org/10.1016/j.biomaterials.2010.10.038

Langer, R., Vacanti, J.P., 1993. Tissue engineering. Science 260, 920–926. https://doi.org/10.1126/science.8493529

Lerman, D.A., Alotti, N., Ume, K.L., Péault, B., 2016. Cardiac Repair and Regeneration: The Value of Cell Therapies. J. - Card. Repair Regen. Value Cell Ther.

L'Heureux, N., McAllister, T., 2008. Cytograft Tissue Engineering: a new paradigm in cardiovascular tissue engineering. Regen. Med. 3, 471–475. https://doi.org/10.2217/17460751.3.4.471

L'Heureux, N., Pâquet, S., Labbé, R., Germain, L., Auger, F.A., 1998. A completely biological tissue-engineered human blood vessel. FASEB J. Off. Publ. Fed. Am. Soc. Exp. Biol. 12, 47–56. https://doi.org/10.1096/fasebj.12.1.47

Li, W., Chen, J., Xu, P., Zhu, M., Wu, Y., Wang, Z., Zhao, T., Cheng, Q., Wang, K., Fan, G., Zhu, Y., Kong, D., 2018. Long-term evaluation of vascular grafts with circumferentially aligned microfibers in a rat abdominal aorta replacement model. J. Biomed. Mater. Res. B Appl. Biomater. 106, 2596–2604. https://doi.org/10.1002/jbm.b.34076

Libby Peter, Theroux Pierre, 2005. Pathophysiology of Coronary Artery Disease. Circulation 111, 3481–3488. https://doi.org/10.1161/CIRCULATIONAHA.105.537878

Lindsey, P., Echeverria, A., Cheung, M., Kfoury, E., Bechara, C.F., Lin, P.H., 2018. Lower Extremity Bypass Using Bovine Carotid Artery Graft (Artegraft): An Analysis of 124 Cases with Long-Term Results. World J. Surg. 42, 295–301. https://doi.org/10.1007/s00268-017-4161-x

López-Ruiz, E., Venkateswaran, S., Perán, M., Jiménez, G., Pernagallo, S., Díaz-Mochón, J.J., Tura-Ceide, O., Arrebola, F., Melchor, J., Soto, J., Rus, G., Real, P.J., Diaz-Ricart, M., Conde-González, A., Bradley, M., Marchal, J.A., 2017. Poly(ethylmethacrylate-co-diethylaminoethyl acrylate) coating improves endothelial re-population, bio-mechanical and anti-thrombogenic properties of decellularized carotid arteries for blood vessel replacement. Sci. Rep. 7, 407. https://doi.org/10.1038/s41598-017-00294-6

Lovett, M., Eng, G., Kluge, J., Cannizzaro, C., Vunjak-Novakovic, G., Kaplan, D.L., 2010. Tubular silk scaffolds for small diameter vascular grafts. Organogenesis 6, 217–224. https://doi.org/10.4161/org.6.4.13407

Luo, X., Guo, Z., He, P., Chen, T., Li, L., Ding, S., Li, H., 2018. Study on structure, mechanical property and cell cytocompatibility of electrospun collagen nanofibers crosslinked by common agents. Int. J. Biol. Macromol. 113, 476–486. https://doi.org/10.1016/j.ijbiomac.2018.01.179

Ma, Z., He, W., Yong, T., Ramakrishna, S., 2005. Grafting of gelatin on electrospun poly(caprolactone) nanofibers to improve endothelial cell spreading and proliferation and to control cell Orientation. Tissue Eng. 11, 1149–1158. https://doi.org/10.1089/ten.2005.11.1149

Madhavan, K., Elliot, W., Tan, Y., Monnet, E., Tan, W., 2018. Performance of marrow stromal cell-seeded small-caliber multilayered vascular graft in a senescent sheep model. Biomed. Mater. 13, 055004. https://doi.org/10.1088/1748-605X/aac7a6

Marneros, A.G., Olsen, B.R., 2005. Physiological role of collagen XVIII and endostatin. FASEB J. Off. Publ. Fed. Am. Soc. Exp. Biol. 19, 716–728. https://doi.org/10.1096/fj.04-2134rev

McClure, M.J., Sell, S.A., Simpson, D.G., Walpoth, B.H., Bowlin, G.L., 2010. A three-layered electrospun matrix to mimic native arterial architecture using polycaprolactone, elastin, and collagen: a preliminary study. Acta Biomater. 6, 2422–2433. https://doi.org/10.1016/j.actbio.2009.12.029

Melchiorri, A., Hibino, N., Best, C., Yi, T., Lee, Y., Kraynak, C., Kimerer, L., Krieger, A., Kim, P., Breuer, C., Fisher, J., 2016. 3D Printed Biodegradable Polymeric Vascular Grafts. Adv. Healthc. Mater. 5, 319–325. https://doi.org/10.1002/adhm.201500725

Melchiorri, A.J., Hibino, N., Fisher, J.P., 2013. Strategies and Techniques to Enhance the In Situ Endothelialization of Small-Diameter Biodegradable Polymeric Vascular Grafts. Tissue Eng. Part B Rev. 19, 292–307. https://doi.org/10.1089/ten.teb.2012.0577

Merfeld-Clauss, S., Gollahalli, N., March, K.L., Traktuev, D.O., 2010. Adipose Tissue Progenitor Cells Directly Interact with Endothelial Cells to Induce Vascular Network Formation. Tissue Eng. Part A 16, 2953–2966. https://doi.org/10.1089/ten.tea.2009.0635

Miranda-Nieves, D., Chaikof, E.L., 2017. Collagen and Elastin Biomaterials for the Fabrication of Engineered Living Tissues. ACS Biomater. Sci. Eng. 3, 694–711. https://doi.org/10.1021/acsbiomaterials.6b00250

Mithieux, S.M., Weiss, A.S., 2005. Elastin. Adv. Protein Chem. 70, 437–461. https://doi.org/10.1016/S0065-3233(05)70013-9

Myllyharju, J., Kivirikko, K.I., 2004. Collagens, modifying enzymes and their mutations in humans, flies and worms. Trends Genet. TIG 20, 33–43. https://doi.org/10.1016/j.tig.2003.11.004

Nieponice, A., Soletti, L., Guan, J., Deasy, B.M., Huard, J., Wagner, W.R., Vorp, D.A., 2008a. Development of a tissue engineered vascular graft combining a biodegradable scaffold, muscle-derived stem cells and a rotational vacuum seeding technique. Biomaterials 29, 825–833. https://doi.org/10.1016/j.biomaterials.2007.10.044

Nieponice, A., Soletti, L., Guan, J., Deasy, B.M., Huard, J., Wagner, W.R., Vorp, D.A., 2008b. Development of a tissue-engineered vascular graft combining a biodegradable scaffold, muscle-derived stem cells and a rotational vacuum seeding technique. Biomaterials 29, 825–833. https://doi.org/10.1016/j.biomaterials.2007.10.044

O'Brien, F.J., 2011. Biomaterials & scaffolds for tissue engineering. Mater. Today 14, 88–95. https://doi.org/10.1016/S1369-7021(11)70058-X

Okano, T., Aoyagi, T., Kataoka, K., Abe, K., Sakurai, Y., Shimada, M., Shinohara, I., 1986. Hydrophilic-hydrophobic microdomain surfaces having an ability to suppress platelet aggregation and their in vitro antithrombogenicity. J. Biomed. Mater. Res. 20, 919–927. https://doi.org/10.1002/jbm.820200707

Pan, Y., Zhou, X., Wei, Y., Zhang, Q., Wang, T., Zhu, M., Li, W., Huang, R., Liu, R., Chen, J., Fan, G., Wang, K., Kong, D., Zhao, Q., 2017. Small-diameter hybrid vascular grafts composed of polycaprolactone and polydioxanone fibers. Sci. Rep. 7, 3615. https://doi.org/10.1038/s41598-017-03851-1

Panina, Y.A., Yakimov, A.S., Komleva, Y.K., Morgun, A.V., Lopatina, O.L., Malinovskaya, N.A., Shuvaev, A.N., Salmin, V.V., Taranushenko, T.E., Salmina, A.B., 2018. Plasticity of Adipose Tissue-Derived Stem Cells and

Regulation of Angiogenesis. Front. Physiol. 9. https://doi.org/10.3389/fphys.2018.01656

Parenteau-Bareil, R., Gauvin, R., Berthod, F., 2010. Collagen-Based Biomaterials for Tissue Engineering Applications. Materials 3, 1863–1887. https://doi.org/10.3390/ma3031863

Pashneh-Tala, S., MacNeil, S., Claeyssens, F., 2016. The Tissue-Engineered Vascular Graft-Past, Present, and Future. Tissue Eng. Part B Rev. 22, 68–100. https://doi.org/10.1089/ten.teb.2015.0100

Patel, A., Fine, B., Sandig, M., Mequanint, K., 2006. Elastin biosynthesis: The missing link in tissue-engineered blood vessels. Cardiovasc. Res. 71, 40–49. https://doi.org/10.1016/j.cardiores.2006.02.021

Peck, M., Gebhart, D., Dusserre, N., McAllister, T.N., L'Heureux, N., 2012. The evolution of vascular tissue engineering and current state of the art. Cells Tissues Organs 195, 144–158. https://doi.org/10.1159/000331406

Pernagallo, S., Tura, O., Wu, M., Samuel, K., Diaz-Mochon, J.J., Hansen, A., Zhang, R., Jackson, M., Padfield, G.J., Hadoke, P.W.F., Mills, N.L., Turner, M.L., Iredale, J.P., Hay, D.C., Bradley, M., 2012a. Novel Biopolymers to Enhance Endothelialisation of Intra-vascular Devices. Adv. Healthc. Mater. 1, 646–656. https://doi.org/10.1002/adhm.201200130

Pernagallo, S., Tura, O., Wu, M., Samuel, K., Diaz-Mochon, J.J., Hansen, A., Zhang, R., Jackson, M., Padfield, G.J., Hadoke, P.W.F., Mills, N.L., Turner, M.L., Iredale, J.P., Hay, D.C., Bradley, M., 2012b. Novel Biopolymers to Enhance Endothelialisation of Intra-vascular Devices. Adv. Healthc. Mater. 1, 646–656. https://doi.org/10.1002/adhm.201200130

Phan, E., Ahluwalia, A., Tarnawski, A.S., 2007. Role of SPARC--matricellular protein in pathophysiology and tissue injury healing. Implications for gastritis and gastric ulcers. Med. Sci. Monit. Int. Med. J. Exp. Clin. Res. 13, RA25-30.

Popryadukhin, P.V., Popov, G.I., Yukina, G.Y., Dobrovolskaya, I.P., Ivan'kova, E.M., Vavilov, V.N., Yudin, V.E., 2017. Tissue-Engineered Vascular Graft of Small Diameter Based on Electrospun Polylactide Microfibers [WWW Document]. Int. J. Biomater. https://doi.org/10.1155/2017/9034186

Pöschl, E., Schlötzer-Schrehardt, U., Brachvogel, B., Saito, K., Ninomiya, Y., Mayer, U., 2004. Collagen IV is essential for basement membrane stability but dispensable for initiation of its assembly during early development. Dev. Camb. Engl. 131, 1619–1628. https://doi.org/10.1242/dev.01037

Prabhakaran, D., Singh, K., Roth, G.A., Banerjee, A., Pagidipati, N.J., Huffman, M.D., 2018. Cardiovascular Diseases in India Compared With the United States. J. Am. Coll. Cardiol. 72, 79–95. https://doi.org/10.1016/j.jacc.2018.04.042

Prapas, S.N., Tsakiridis, K., Zarogoulidis, P., Katsikogiannis, N., Tsiouda, T., Sakkas, A., Zarogoulidis, K., 2014. Current options for treatment of chronic coronary artery disease. J. Thorac. Dis. 6, S2–S6. https://doi.org/10.3978/j.issn.2072-1439.2013.10.25

Rhodes, J.M., Simons, M., 2007. The extracellular matrix and blood vessel formation: not just a scaffold. J. Cell. Mol. Med. 11, 176–205. https://doi.org/10.1111/j.1582-4934.2007.00031.x

Rifkin, D.B., 2005. Latent transforming growth factor-beta (TGF-beta) binding proteins: orchestrators of TGF-beta availability. J. Biol. Chem. 280, 7409–7412. https://doi.org/10.1074/jbc.R400029200

Roh, J.D., Sawh-Martinez, R., Brennan, M.P., Jay, S.M., Devine, L., Rao, D.A., Yi, T., Mirensky, T.L., Nalbandian, A., Udelsman, B., Hibino, N., Shinoka, T., Saltzman, W.M., Snyder, E., Kyriakides, T.R., Pober, J.S., Breuer, C.K., 2010. Tissue-engineered vascular grafts transform into mature blood vessels via an inflammation-mediated process of vascular remodeling. Proc. Natl. Acad. Sci. 107, 4669–4674. https://doi.org/10.1073/pnas.0911465107

Ruß, M., Werdan, K., Cremer, J., Krian, A., Meinertz, T., Zerkowski, H.-R., 2009. Different Treatment Options in Chronic Coronary Artery Disease. Dtsch. Ärztebl. Int. 106, 253–261. https://doi.org/10.3238/arztebl.2009.0253

Rzucidlo, E.M., Martin, K.A., Powell, R.J., 2007. Regulation of vascular smooth muscle cell differentiation. J. Vasc. Surg., Current Topics in Clinical and Basic Vascular Research 45, A25–A32. https://doi.org/10.1016/j.jvs.2007.03.001

Sakakura, K., Nakano, M., Otsuka, F., Ladich, E., Kolodgie, F.D., Virmani, R., 2013. Pathophysiology of Atherosclerosis Plaque Progression. Heart Lung Circ. 22, 399–411. https://doi.org/10.1016/j.hlc.2013.03.001

Sánchez, P.F., Brey, E.M., Briceño, J.C., 2018. Endothelialization mechanisms in vascular grafts. J. Tissue Eng. Regen. Med. 12, 2164–2178. https://doi.org/10.1002/term.2747

Schmidli, J., Savolainen, H., Heller, G., Widmer, M.K., Then-Schlagau, U., Baumgartner, I., Carrel, T.P., 2004. Bovine mesenteric vein graft (ProCol) in critical limb ischaemia with tissue loss and infection. Eur. J. Vasc. Endovasc. Surg. Off. J. Eur. Soc. Vasc. Surg. 27, 251–253. https://doi.org/10.1016/j.ejvs.2003.12.001

Schmittgen, T.D., Livak, K.J., 2008. Analyzing real-time PCR data by the comparative C(T) method. Nat. Protoc. 3, 1101–1108.

Scott, J., 2004. Pathophysiology and biochemistry of cardiovascular disease. Curr. Opin. Genet. Dev. 14, 271–279. https://doi.org/10.1016/j.gde.2004.04.012

Shalumon, K.T., Deepthi, S., Anupama, M.S., Nair, S.V., Jayakumar, R., Chennazhi, K.P., 2015. Fabrication of poly (l-lactic acid)/gelatin composite tubular scaffolds for vascular tissue engineering. Int. J. Biol. Macromol. 72, 1048–1055. https://doi.org/10.1016/j.ijbiomac.2014.09.058

Sheikh, Z., Brooks, P.J., Barzilay, O., Fine, N., Glogauer, M., 2015. Macrophages, Foreign Body Giant Cells and Their Response to Implantable Biomaterials. Mater. Basel Switz. 8, 5671–5701. https://doi.org/10.3390/ma8095269

Shirakigawa, N., Ijima, H., 2017. Decellularized Tissue Engineering, in: Tripathi, A., Melo, J.S. (Eds.), Advances in Biomaterials for Biomedical Applications, Advanced Structured Materials. Springer Singapore, Singapore, pp. 185–226. https://doi.org/10.1007/978-981-10-3328-5_5

Smyth, N., Vatansever, H.S., Murray, P., Meyer, M., Frie, C., Paulsson, M., Edgar, D., 1999. Absence of basement membranes after targeting the LAMC1 gene results in embryonic lethality due to failure of endoderm differentiation. J. Cell Biol. 144, 151–160. https://doi.org/10.1083/jcb.144.1.151

Song, H.-H.G., Rumma, R.T., Ozaki, C.K., Edelman, E.R., Chen, C.S., 2018a. Vascular Tissue Engineering: Progress, Challenges, and Clinical Promise. Cell Stem Cell 22, 340–354. https://doi.org/10.1016/j.stem.2018.02.009

Song, H.-H.G., Rumma, R.T., Ozaki, C.K., Edelman, E.R., Chen, C.S., 2018b. Vascular Tissue Engineering: Progress, Challenges, and Clinical Promise. Cell Stem Cell 22, 340–354. https://doi.org/10.1016/j.stem.2018.02.009

Souza, L.E.B., Beckenkamp, L.R., Sobral, L.M., Fantacini, D.M.C., Melo, F.U.F., Borges, J.S., Leopoldino, A.M., Kashima, S., Covas, D.T., 2018. Pre-culture in endothelial growth medium enhances the angiogenic properties of adipose-derived stem/stromal cells. Angiogenesis 21, 15–22. https://doi.org/10.1007/s10456-017-9579-0

Syazana, N., Sukmana, I., 2016. Electrospun-based fibrous scaffold for cardiovascular engineering applications: a review 11, 4.

Syedain, Z., Reimer, J., Lahti, M., Berry, J., Johnson, S., Tranquillo, R.T., 2016. Tissue engineering of acellular vascular grafts capable of somatic growth in young lambs. Nat. Commun. 7, 12951. https://doi.org/10.1038/ncomms12951

Syedain, Z.H., Meier, L.A., Bjork, J.W., Lee, A., Tranquillo, R.T., 2011. Implantable arterial grafts from human fibroblasts and fibrin using a multi-graft pulsed flow-stretch bioreactor with noninvasive strength monitoring. Biomaterials 32, 714–722. https://doi.org/10.1016/j.biomaterials.2010.09.019

Tamimi, E., Ardila, D.C., Haskett, D.G., Doetschman, T., Slepian, M.J., Kellar, R.S., Vande Geest, J.P., 2016. Biomechanical Comparison of Glutaraldehyde-Crosslinked Gelatin Fibrinogen Electrospun Scaffolds to Porcine Coronary Arteries. J. Biomech. Eng. 138. https://doi.org/10.1115/1.4031847

Tamimi, E.A., Ardila, D.C., Ensley, B.D., Kellar, R.S., Vande Geest, J.P., 2019. Computationally Optimizing the Compliance of Multilayered Biomimetic Tissue Engineered Vascular Grafts. J. Biomech. Eng. 141, 061003-061003–14. https://doi.org/10.1115/1.4042902

Tarallo, S., Beltramo, E., Berrone, E., Porta, M., 2012. Human pericyte-endothelial cell interactions in co-culture models mimicking the diabetic retinal microvascular environment. Acta Diabetol. 49 Suppl 1, S141-151. https://doi.org/10.1007/s00592-012-0390-5

Tennant, M., McGeachie, J.K., 1990. Blood Vessel Structure and Function: A Brief Update on Recent Advances. Aust. N. Z. J. Surg. 60, 747–753. https://doi.org/10.1111/j.1445-2197.1990.tb07468.x

Thaburet, J.-F., Mizomoto, H., Bradley, M., 2004. High-Throughput Evaluation of the Wettability of Polymer Libraries. Macromol. Rapid Commun. 25, 366–370. https://doi.org/10.1002/marc.200300234

Thomas, L.V., Nair, P.D., 2013. The effect of pulsatile loading and scaffold structure for the generation of a medial equivalent tissue engineered vascular graft. BioResearch Open Access 2, 227–239. https://doi.org/10.1089/biores.2013.0003

Thomas, L.V., Nair, P.D., 2012. Influence of mechanical stimulation in the development of a medial equivalent tissue-engineered vascular construct using a gelatin-g-vinyl acetate co-polymer scaffold. J. Biomater. Sci. Polym. Ed. 23, 2069–2087. https://doi.org/10.1163/092050611X607148

Thottappillil, N., Nair, P.D., 2015. Scaffolds in vascular regeneration: current status. Vasc. Health Risk Manag. 11, 79–91. https://doi.org/10.2147/VHRM.S50536

Torricelli, P., Gioffrè, M., Fiorani, A., Panzavolta, S., Gualandi, C., Fini, M., Focarete, M.L., Bigi, A., 2014. Co-electrospun gelatin-poly(l-lactic acid) scaffolds: Modulation of mechanical properties and chondrocyte response as a function of composition. Mater. Sci. Eng. C 36, 130–138. https://doi.org/10.1016/j.msec.2013.11.050

Tura, O., Skinner, E.M., Barclay, G.R., Samuel, K., Gallagher, R.C.J., Brittan, M., Hadoke, P.W.F., Newby, D.E., Turner, M.L., Mills, N.L., 2013. Late Outgrowth Endothelial Cells Resemble Mature Endothelial Cells and Are Not Derived from Bone Marrow. STEM CELLS 31, 338–348. https://doi.org/10.1002/stem.1280

Van Vlierberghe, S., 2016. Crosslinking strategies for porous gelatin scaffolds. J. Mater. Sci. 51, 4349–4357. https://doi.org/10.1007/s10853-016-9747-4

Vatankhah, E., P. Prabhakaran, M., Ramakrishna, S., 2017. Impact of electrospun Tecophilic/gelatin scaffold biofunctionalization on proliferation of vascular smooth muscle cells. Sci. Iran. 24, 3458–3465. https://doi.org/10.24200/sci.2017.4420

Wallez, Y., Huber, P., 2008. Endothelial adherens and tight junctions in vascular homeostasis, inflammation and angiogenesis. Biochim. Biophys. Acta 1778, 794–809. https://doi.org/10.1016/j.bbamem.2007.09.003

Wang, C., Yin, S., Cen, L., Liu, Q., Liu, W., Cao, Y., Cui, L., 2010. Differentiation of adipose-derived stem cells into contractile smooth muscle cells induced by transforming growth factor-beta1 and bone morphogenetic protein-4. Tissue Eng. Part A 16, 1201–1213. https://doi.org/10.1089/ten.TEA.2009.0303

Wang, H.,., Lopez, A.D., Murray, C.J.L., 2016. Global, regional, and national life expectancy, all-cause mortality, and cause-specific mortality for 249 causes of death, 1980–2015: a systematic analysis for the Global Burden of Disease Study 2015. The Lancet 388, 1459–1544. https://doi.org/10.1016/S0140-6736(16)31012-1

Wang, R., Wang, Z., Lin, S., Deng, C., Li, F., Chen, Z., He, H., 2015. Green fabrication of antibacterial polymer/silver nanoparticle nanohybrids by dual-spinneret electrospinning. RSC Adv. 5, 40141–40147. https://doi.org/10.1039/C5RA03288A

Wang, S., Zhang, Y., Wang, H., Yin, G., Dong, Z., 2009. Fabrication and properties of the electrospun polylactide/silk fibroin-gelatin composite tubular scaffold. Biomacromolecules 10, 2240–2244. https://doi.org/10.1021/bm900416b

Wang, X., Ding, B., Li, B., 2013. Biomimetic electrospun nanofibrous structures for tissue engineering. Mater. Today 16, 229–241. https://doi.org/10.1016/j.mattod.2013.06.005

Wang, Z., Cui, Y., Wang, J., Yang, X., Wu, Y., Wang, K., Gao, X., Li, D., Li, Y., Zheng, X.-L., Zhu, Y., Kong, D., Zhao, Q., 2014. The effect of thick fibers and large pores of electrospun poly(ε-caprolactone) vascular grafts on macrophage polarization and arterial regeneration. Biomaterials 35, 5700–5710. https://doi.org/10.1016/j.biomaterials.2014.03.078

Weinberg, C.B., Bell, E., 1986. A blood vessel model constructed from collagen and cultured vascular cells. Science 231, 397–400. https://doi.org/10.1126/science.2934816

WHO | Global atlas on cardiovascular disease prevention and control [WWW Document], n.d. . WHO. URL http://www.who.int/cardiovascular_diseases/publications/atlas_cvd/en/ (accessed 6.11.19).

Wight, T.N., Merrilees, M.J., 2004. Proteoglycans in atherosclerosis and restenosis: key roles for versican. Circ. Res. 94, 1158–1167. https://doi.org/10.1161/01.RES.0000126921.29919.51

Wong, C.S., Liu, X., Xu, Z., Lin, T., Wang, X., 2013. Elastin and collagen enhances electrospun aligned polyurethane as scaffolds for vascular graft. J. Mater. Sci. Mater. Med. 24, 1865–1874. https://doi.org/10.1007/s10856-013-4937-y

Wu, Y., Qin, Y., Wang, Z., Wang, J., Zhang, C., Li, C., Kong, D., 2018. The regeneration of macro-porous electrospun poly(ε-caprolactone) vascular graft during long-term in situ implantation. J. Biomed. Mater. Res. B Appl. Biomater. 106, 1618–1627. https://doi.org/10.1002/jbm.b.33967

Wulkersdorfer, B., Kao, K.K., Agopian, V.G., Ahn, A., Dunn, J.C., Wu, B.M., Stelzner, M., 2010. Bimodal Porous Scaffolds by Sequential Electrospinning of Poly(glycolic acid) with Sucrose Particles. Int. J. Polym. Sci. 2010, 1–9. https://doi.org/10.1155/2010/436178

Xu, F., Li, L., Cui, X., 2012. Fabrication of Aligned Side-by-Side TiO2/SnO2 Nanofibers via Dual-Opposite-Spinneret Electrospinning [WWW Document]. J. Nanomater. https://doi.org/10.1155/2012/575926

Yan, Q., Vernon, R.B., Hendrickson, A.E., Sage, E.H., 1996. Primary culture and characterization of microvascular endothelial cells from Macaca monkey retina. Invest. Ophthalmol. Vis. Sci. 37, 2185–2194.

Yao, L., Liu, J., Andreadis, S.T., 2008. Composite fibrin scaffolds increase mechanical strength and preserve contractility of tissue engineered blood vessels. Pharm. Res. 25, 1212–1221. https://doi.org/10.1007/s11095-007-9499-6

Yi, B., Shen, Y., Tang, H., Wang, X., Li, B., Zhang, Y., 2019. Stiffness of Aligned Fibers Regulates the Phenotypic Expression of Vascular Smooth Muscle Cells. ACS Appl. Mater. Interfaces 11, 6867–6880. https://doi.org/10.1021/acsami.9b00293

Yokota, T., Ichikawa, H., Matsumiya, G., Kuratani, T., Sakaguchi, T., Iwai, S., Shirakawa, Y., Torikai, K., Saito, A., Uchimura, E., Kawaguchi, N., Matsuura, N., Sawa, Y., 2008. In situ tissue regeneration using a novel tissue-engineered, small-caliber vascular graft without cell seeding. J. Thorac. Cardiovasc. Surg. 136, 900–907. https://doi.org/10.1016/j.jtcvs.2008.02.058

Zavan, B., Vindigni, V., Lepidi, S., Iacopetti, I., Avruscio, G., Abatangelo, G., Cortivo, R., 2008. Neoarteries grown in vivo using a tissue-engineered hyaluronan-based scaffold. FASEB J. Off. Publ. Fed. Am. Soc. Exp. Biol. 22, 2853–2861. https://doi.org/10.1096/fj.08-107284

Zhang, L., Ao, Q., Wang, A., Lu, G., Kong, L., Gong, Y., Zhao, N., Zhang, X., 2006. A sandwich tubular scaffold derived from chitosan for blood vessel tissue engineering. J. Biomed. Mater. Res. A 77, 277–284. https://doi.org/10.1002/jbm.a.30614

Zhang, Y., Ouyang, H., Lim, C.T., Ramakrishna, S., Huang, Z.-M., 2005. Electrospinning of gelatin fibers and gelatin/PCL composite fibrous scaffolds. J. Biomed. Mater. Res. B Appl. Biomater. 72, 156–165. https://doi.org/10.1002/jbm.b.30128

Zhao, J., Qiu, H., Chen, D., Zhang, W., Zhang, D., Li, M., 2013. Development of nanofibrous scaffolds for vascular tissue engineering. Int. J. Biol. Macromol. 56, 106–113. https://doi.org/10.1016/j.ijbiomac.2013.01.027

Zheng, W., Wang, Z., Song, L., Zhao, Q., Zhang, J., Li, D., Wang, S., Han, J., Zheng, X.-L., Yang, Z., Kong, D., 2012a. Endothelialization and patency of RGD-functionalized vascular grafts in a rabbit carotid artery model. Biomaterials 33, 2880–2891. https://doi.org/10.1016/j.biomaterials.2011.12.047

Zheng, W., Wang, Z., Song, L., Zhao, Q., Zhang, J., Li, D., Wang, S., Han, J., Zheng, X.-L., Yang, Z., Kong, D., 2012b. Endothelialization and patency of RGD-functionalized vascular grafts in a rabbit carotid artery model. Biomaterials 33, 2880–2891. https://doi.org/10.1016/j.biomaterials.2011.12.047

Zhou, Z., Wang, J., Cao, R., Morita, H., Soininen, R., Chan, K.M., Liu, B., Cao, Y., Tryggvason, K., 2004. Impaired angiogenesis, delayed wound healing and retarded tumor growth in perlecan heparan sulfate-deficient mice. Cancer Res. 64, 4699–4702. https://doi.org/10.1158/0008-5472.CAN-04-0810

Zhu, M., Wu, Y., Li, W., Dong, X., Chang, H., Wang, K., Wu, P., Zhang, J., Fan, G., Wang, L., Liu, J., Wang, H., Kong, D., 2018. Biodegradable and elastomeric vascular grafts enable vascular remodeling. Biomaterials 183, 306–318. https://doi.org/10.1016/j.biomaterials.2018.08.063

Zorlutuna, P., Elsheikh, A., Hasirci, V., 2009. Nanopatterning of collagen scaffolds improve the mechanical properties of tissue engineered vascular grafts. Biomacromolecules 10, 814–821. https://doi.org/10.1021/bm801307y

Zou, T., Fan, J., Fartash, A., Liu, H., Fan, Y., 2016. Cell-based strategies for vascular regeneration. J. Biomed. Mater. Res. A 104, 1297–1314. https://doi.org/10.1002/jbm.a.35660

# LIST OF PUBLICATIONS

## MANUSCRIPTS

I. Neelima Thottappillil, Prabha D. Nair, Dual source co-electrospun tubular scaffold generated from gelatin-vinyl acetate and poly-ε-caprolactone for smooth muscle cell mediated blood vessel engineering, Materials Science and Engineering: C, Volume 114, September 2020, 111030, ISSN 0928-4931, https://doi.org/10.1016/j.msec.2020.111030 , Impact factor: 5.88.

II. Thottappillil, N., & Nair, P. D. Scaffolds in vascular regeneration: current status. Vascular health and risk management, *11*, 79–91, 2015, https://doi.org/10.2147/VHRM.S50536 Impact factor: 2.33

III. Thottappillil N, Unnikrishnan M, Umashankar P.R, Sachin J Shenoy, Nair. P.D. *In vivo* evaluation of small diameter vascular graft in Ovine carotid artery replacement model (Under preparation).

IV. Thottappillil N, Dong H, Callanan C, Khan N, Nair PD, Peaullt B and Bradley M, Co-culture of peri-vascular cells and endothelial cells on electrospun Poly (ethyl methacrylate-co-diethyl aminoethyl acrylate) scaffold for blood vessel replacement. (Under preparation).

V. Thottappillil, Neelima & Nair, Prabha. Biomimetic scaffold with stem cell derived smooth muscle cells: A designer vascular substitute. Frontiers in Bioengineering and Biotechnology Conference abstract: 10th World Biomaterial Congress, Volume 4, January, 2016, https://doi.org/10.3389/conf.FBIOE.2016.01.02487

VI. N. Thottappillil and P. Damodaran Nair, Generation of TEVG using RAMSC derived RSMC seeded on a Biomimetic Nano fibrous scaffold, Tissue Engineering: Part A, S-248, Volume 21, Supplement 1, September, TERMIS 2015, DOI: 10.1089/ten.tea.2015.5000.abstracts.

## CONFERENCES

1) Neelima Thottappillil, Prabha D. Nair, Biomimetic Scaffold with stem cell derived smooth muscle cells: A designer vascular substitute, 10th World Biomaterial Congress, May 17-22, Montreal, Canada, 2016 (Oral presentation- DST Travel award).
2) Neelima Thottappillil, Prabha D. Nair, Differentiation of rabbit adipose derived mesenchymal stem cells to vascular smooth muscle cells on gelatin-vinyl acetate-poly-ε-caprolactone blend scaffold. Indo-Australian conference on Biomaterials, Tissue Engineering, Drug delivery & Regenerative medicine (BiTERM- 2015), February 5-7, Anna University, Chennai, India, 2015 (Oral presentation).
3) Neelima Thottappillil, Prabha D. Nair, Generation of TEVG using RAMSC derived RSMC seeded on a Biomimetic Nano fibrous scaffold, 4th TERMIS World Congress, September 8-11, Boston, USA, 2015 (Poster Presentation - DBT Travel award.
4) Thottappillil N, Dong H, N Khan, B Peault, M Bradley, Perivascular stem cell-based tissue engineered vascular graft Cardiovascular symposium, June 2017, University of Edinburgh (Poster presentation)
5) Thottappillil N, Dong H, N Khan, B Peault, M Bradley, Perivascular stem cell-based tissue engineered vascular graft, Chemistry, Stem cells and Regenerative medicine, Symposium conducted by Royal Society of Chemistry, London, September 2017 (Poster presentation - Commonwealth Travel award).
6) Neelima Thottappillil, Prabha D. Nair, Dual source electrospun scaffold facilitates differentiation of adipose stem cells to smooth muscle cells for blood vessel engineering, International Conference on Bio-materials, Bio-engineering and Bio-theranostics (BioMET 2018), July 24-28, Vellore Institute of Technology, Vellore, Tamilnadu, India,2018 (Poster presentation).

5b7293bdeaf7e5c5d2dcc61c47d9a171050e3156.docx
Jul 2, 2019
32103 words / 183187 characters

# PhD Thesis-Neelima.docx

Sources Overview

## 4% Overall Similarity

| | | |
|---|---|---|
| 1 | tulane.edu<br>INTERNET | <1% |
| 2 | www.ijp-online.com<br>INTERNET | <1% |
| 3 | circ.ahajournals.org<br>INTERNET | <1% |
| 4 | www.omicsonline.org<br>INTERNET | <1% |
| 5 | atvb.ahajournals.org<br>INTERNET | <1% |
| 6 | dro.deakin.edu.au<br>INTERNET | <1% |
| 7 | www.ncbi.nlm.nih.gov<br>INTERNET | <1% |
| 8 | link.springer.com<br>INTERNET | <1% |
| 9 | www.biologie.uni-regensburg.de<br>INTERNET | <1% |
| 10 | World Journal of Science, Technology and Sustainable Development, Volume 8, Issue 1 (2012-08-06)<br>PUBLICATION | <1% |
| 11 | www.witec-instruments.com<br>INTERNET | <1% |
| 12 | tampub.uta.fi<br>INTERNET | <1% |
| 13 | hub.hku.hk<br>INTERNET | <1% |
| 14 | www.frontiersin.org<br>INTERNET | <1% |
| 15 | tcr.amegroups.com<br>INTERNET | <1% |
| 16 | prr.hec.gov.pk<br>INTERNET | <1% |
| 17 | witec.biz<br>INTERNET | <1% |
| 18 | www.jbc.org<br>INTERNET | <1% |
| 19 | d-nb.info<br>INTERNET | <1% |
| 20 | www.biocolor.co.uk<br>INTERNET | <1% |